Heterodimeric glycolipid complexes as targets for neuropathy associated pathogenic autoantibodies and other lectins

Dr Simon Rinaldi
BSc (Hons) MBChB MRCP(UK, Neuro) MRCPSG

Thesis submitted for the degree of PhD
to the University of Glasgow,
Division of Clinical Neuroscience.

July 2011

Author's Declaration

All experiments are the work of the author unless specifically stated otherwise within the text.

Dr Simon Rinaldi, BSc (Hons) MBChB MRCP(UK, Neuro) MRCPSG

Acknowledgements

I would like to thank the following people, without whom this work would not have been possible;

Hugh Willison ushered me into his office one afternoon in May 2007, and by the time I had left some hours later had confirmed his widespread reputation as an inspirational, highly knowledgeable, approachable and brilliant authority on diverse aspects of neuroimmunology, glycobiology, and peripheral neuropathy. His interest in Munros and Bothy renovations would only become apparent in subsequent months. When I was offered the opportunity to become a Clinical Research Fellow in his lab following an interview later that day I had no hesitation in accepting the post. Hugh of course proved to be an ideal supervisor – supportive and enthusiastic without being overbearing – and I never regretted moving to Glasgow to work for him.

Carl Goodyear acted as my Advisor and provided many invaluable suggestions regarding modifications to the methods I was attempting to employ in this study – having performed many of them himself in the past, and no doubt more ably. He was also an irritatingly tireless runner in the irregular GBRC fives games, somehow always on the opposition.

Katie Brennan deserves special mention for her efforts in developing and optimising the glycoarray, also for being another clinical neurologist to gently whinge with on the other side of the bench to the bedside, but particularly for frequently proving the first to crack to the temptation of a large glass of white wine. Many other colleagues gave advice, instruction, demonstration and demystification in varying proportions. Sue Halstead set me on my way, helpfully performing initial ELISAs essentially in parallel to mine, although at still unobtainable speeds, and occasionally whilst listing to Hendrix at unfathomable volumes. Kate Townson taught me TLC, liposome manufacture and the dreaded PBMC/RNA extraction protocol, all while remaining extremely friendly and unflappable, but unfortunately suffered being the person I asked most questions of, despite being away on maternity for 9 months. Kay Greenshields unravelled the mysteries of the fluorescent microscope, and taught me the value of always taking a jumper, amongst many other things. Alistair Easton could be relied to think deeply on any question posed to him, and came up with some very

interesting answers, usually not requiring the use of the ‘deep thought’ book, as far as I know. Denggao Yao just about kept up with my escalating requests for mice, helped immensely with their genotyping and identification, and certainly kept smiling at all times. Anne Donnachie did many good things, but her dexterity in capturing the little murine fellas and in locating their tail veins, as well as her desire to always walk back from the CRF through what little sun there was wearing shades, stand out. Angie Rupp provided fuel for the internal fires with the frequent provision of home baked goodness. Rhona McGonigal constantly stole my pipettes, but made up for this with quality chat through the shelves, musical suggestions, and Thursday nights. I could have probably lived without the Buckfast, mind. ‘Chesc’ Galban (sorry mate) arrived as a breath of Catalan fresh air to re-energise my final year, even if we occasionally proved mutually incomprehensible.

Lindsay MacLellan, Susan Kitson, Ariel Arthur, Catherine Hurson, Cat Wilson, Elinor Anderson, Clive McKimmie, Kenny Pallas, Katy Malpass, and Jen Montgommery were all friendly faces about and away from the laboratory, mainly providing much needed and extremely varied distraction and japery.

Lastly, but most importantly, Kirstin Lund moved to Scotland with me, fed me, watered me, encouraged me, cajoled me, chastised me, listened to me, ignored me, talked to me, proof read for me, and did whatever else it took for me to finish this thing. I love her very much and now she is my wife.

Table of Contents

Author's Declaration 2

Acknowledgements 3

Table of Contents 5

List of Tables 11

List of Figures 12

List of Accompanying Material 15

Definitions/Abbreviations 16

Short summary 18

Summary 19

1 Introduction 22

1.1 Guillain-Barré syndrome – an acute inflammatory disorder of the peripheral nervous system 22

1.1.1 Overview 22

1.1.2 Historical aspects 23

1.1.3 Epidemiology 26

1.1.4 Clinical features and diagnosis 27

1.1.5 Disease subtypes and variants 30

1.1.6 Current treatments 32

1.1.7 Pathophysiology 33

1.1.7.1 Gangliosides and molecular mimicry 34

1.1.7.2 Host susceptibility factors 38

1.1.7.3 The pathogenic potential of anti-ganglioside antibodies 40

1.1.7.4 Clinical-serological associations 44

1.2 Ganglioside complexes 45

1.3 Aims 53

2 Methods 54

2.1 Materials and solutions 54

2.1.1 Gangliosides and other lipids 54

2.1.2 Secondary antibodies 54

2.1.2.1 Peroxidase conjugated 54
2.1.2.2 Fluorescent labelled antibodies and markers 55

2.2 Methods 55

2.2.1 Combinatorial PVDF glycoarray 55

2.2.2 Ganglioside and glycolipid complex ELISA 59

2.2.3 Ganglioside liposome ELISA 60

2.2.4 TLC immuno-overlay 61

2.2.5 Monoclonal antibody production from existing cell lines 63

2.2.6 Liposome production for immunisation 66

2.2.7 Immunisation protocol 67

2.2.8 Monoclonal antibody generation from immunised animals 67

2.2.8.1 Using liquid based media 68
2.2.8.2 Using semi-solid selection media 71

2.2.9 Ex vivo hemidiaphragm preparations 74

2.2.10 Disease modelling by passive transfer 76

2.2.11 Disease modelling by active immunisation 77

2.2.12 Behavioural testing 77

2.2.12.1 Balance bar 78
2.2.12.2 Forelimb grip strength 78
2.2.12.3 Total grip strength 78
2.2.12.4 Hindlimb reflex extension 78
2.2.12.5 Platform 79
2.2.12.6 Rotarod 79
2.2.12.7 Open field activity 80

2.2.13 Plethysmography 80

2.2.14 Diaphragm and soleus dissection and staining 81

2.2.15 Imaging and analysis of neuromuscular sections 82

3 The ganglioside complex binding properties of monoclonal antibodies 84

3.1 Introduction 84

3.2 Results 86

3.2.1 Development of ganglioside complex ELISA and initial analysis of mAb binding 86

3.2.2 The effect of premixing by sonication on GSC formation and antibody binding 89

3.2.3 Validation of the complex ELISA using neuropathy sera 92

3.2.4 Screening of existing b series monoclonal antibodies 94

3.2.5 Impetus for the development of a novel immunoassay for investigating ganglioside complex binding 96

3.2.6 Development of the combinatorial PVDF glycoarray 97

3.2.7 The effect of ganglioside mixing and complex formation on adhesion to the PVDF membrane 103

3.2.8 The differing response of two anti-GM1 antibodies to ganglioside complexes 106

3.2.9 The disparate binding of mAbs to GSCs on ELISA and PVDF 110

3.2.10 GSC Liposome ELISA 111

3.2.11 The disparate binding of mAbs to GSCs on TLC, ELISA and PVDF 112

3.2.12 Antibodies in neuropathy sera bind GM1:GD1a complexes on ELISA and PVDF glycoarray 116

3.2.13 GM1:GD1a anti-sera ex vivo binding assays 117

3.3 Discussion 120

4 The ganglioside binding properties of bacterial toxins and siglecs 129

4.1 Introduction 129

4.2 Results 131

4.2.1 Siglec-ganglioside interactions are modulated by ganglioside complexes 131

4.2.2 Certain bacterial toxin-ganglioside interactions are complex modulated 136

4.3 Discussion 138

5 Anti-ganglioside and glycoplipid complex antibodies in a cohort of Guillain Barré syndrome patients 142

5.1 Introduction 142

5.2 Results 145

5.2.1 Patient cohort 145

5.2.1.1 Patients 145
5.2.1.2 Clinical data 145

5.2.2 Target selection 148

5.2.3 Validation of intra- and inter assay variation for sera 149

5.2.4 Summary array data 149

5.2.4.1 SGPG and SGPG-series complexes 154
5.2.4.2 Sulfatide and sulfatide-series complexes 158

5.2.5 Cluster analysis of GBS array data 161

5.2.5.1 Cluster analysis data 162
5.2.5.2 Cluster analysis heatmaps 163

5.2.6 Disease associations 166

5.2.6.1 Disease subtype 166
5.2.6.2 Disease severity and requirement for ventilation 167
5.2.6.3 Preceding infection 168
5.2.6.4 Presence of cranial nerve deficits, bulbar impairment or sensory involvement 169

5.2.7 Low frequency antibodies 170

5.3 Discussion 174

6 The immune response to GSC containing liposomes 178

6.1 Introduction 178

6.2 Results 180

6.2.1 GM1:GD1a liposomes 180

6.2.1.1 ELISA analysis 181

6.2.1.2 PVDF glycoarray analysis 182
6.2.2 GD1a : GD1b liposomes 185
6.2.2.1 ELISA analysis 185
6.2.2.2 PVDF glycoarray analysis 186
6.2.3 Sphingomyelin complex response 188
6.2.3.1 GM1:GD1a immunisations 189
6.2.3.2 GD1a:GD1b immunisations 192
6.3 Discussion 195

7 Cloning and characterisation of anti-GSC antibodies 201
7.1 Introduction 201
7.2 Results 203
7.2.1 Liquid medium selection 203
7.2.2 Semi-solid medium selection 203
7.3 Discussion 207

8 An active immunisation model of GBS 209
8.1 Introduction 209
8.1.1 Background 209
8.1.2 Development of a transgenic neurofilament promoter GalNAcT / GalNAcT$^{-/-}$ mouse 212
8.2 Results 216
8.2.1 Ex vivo Model 216
8.2.1.1 Perisynaptic Schwann cell injury 223
8.2.2 Passive transfer (αGT1b) 224
8.2.2.1 Plethysmography 224
8.2.2.2 Tissue analysis 227
8.2.3 Active immunisation (GT1b) 228
8.2.3.1 Immune response 229
8.2.3.2 Plethysmography 231
8.2.3.3 Behavioural testing 232
8.2.3.4 Tissue analysis 236
8.2.4 Active immunisation (GM1:GD1a complex) 238
8.2.4.1 Immune response 238
8.3 Discussion 239

9 Conclusion 243

9.1 Summary 243

9.2 Weaknesses 245

9.3 Parallel developments 247

9.4 Future work 250

Appendices 254

1 Commonly used solutions 254

PBS 254
2%/1% BSA 254
OPD detection buffer 254
OPD stop solution 254
Orcinol 255
Resorcinol 255
0.4% PIBM 255
Ringer's medium 255
20% / 10% complete medium 255

2 Example array programme 256

Layout for 10x10 grid 256
Programme for first slide 257
Vial assignment 259

3 Antigens significantly associated with GBS using stepup correction .. 260

4 Publications arising 261

Combinatorial glycoarray. 261
Lipid arrays identify myelin-derived lipids and lipid complexes as prominent targets for oligoclonal band antibodies in MS 273
The GD1a glycan is a cellular receptor for adenoviruses causing epidemic keratoconjunctivitis 283
Transgenic rescue of ganglioside expression in the peripheral nervous system of ganglioside-null mice facilitates an active immunisation model of acute motor axonal neuropathy 291
Heteromeric glycolipid complexes as modulators of autoantibody and lectin binding. 293
Analysis of lectin binding to glycolipid complexes using combinatorial glycoarrays. 303
Detection of autoantibody and lectin binding to ganglioside complexes using a novel combinatorial glycoarray. 312
The neuropathic potential of anti-GM1 autoantibodies is regulated by the local glycolipid environment. 314
Ganglioside antibodies and neuropathies. 331

List of references 339

List of Tables

Table 1.1 - Antibody-disease associations in GBS subtypes..... 44
Table 2.1 - Scoring system for hindlimb reflex extension 78
Table 3.1 - GSC ELISA layout 86
Table 3.2 - Intra-assay variation measurement 103
Table 3.3 - Inter-assay variation calculation 103
Table 4.1 - Siglecs provided by Prof. Paul Crocker 130
Table 5.1 - GBS disability score at selected time points..... 147
Table 5.2 - Breakdown of cranial nerve deficits 147
Table 5.3 - Single glycolipids used in the 28x10 PVDF glycoarray 148
Table 5.4 - Antigens on the PVDF glycoarray significantly associated with binding by GBS as compared with control sera..... 152
Table 5.5 - GBS sera with phosphatidylserine complex attenuated SGPG binding 157
Table 5.6 - GBS sera with phosphatidylserine complex enhanced SGPG binding158
Table 5.7 - 2x2 contingency table for GA1 and sulfatide single versus complex binding..... 160
Table 5.8 – ANOVA analysis of log transformed intensity data..... 162
Table 5.9 - Disease subtype antigen associations 167
Table 5.10 - Antigens associated with disease severity 168
Table 5.11 - Antigens significantly associated with preceding diarrhoea 168
Table 5.12 - Identified infection and antigens detected..... 169
Table 5.13 - Association with cranial nerve deficit..... 169
Table 5.14 - Antigens negatively correlated with sensory disturbance..... 170
Table 5.15 - Contingency table required for significance with disease frequency of 1 in 181 175
Table 7.1 - Summary of fusion experiments using liquid selection media 205
Table 7.2 - Summary of experiments using semi-solid selection media 206
Table 8.1 - Counts of ethidium positive cell nuclei per end plate by tissue type 224
Table 9.1 - Summary of proposed future work 253

List of Figures

Figure 1.1 - Features supportive of the diagnosis of GBS 28
Figure 1.2 - Features casting doubt on the diagnosis of GBS 29
Figure 1.3 - Features that rule out the diagnosis of GBS 29
Figure 1.4 - Pathological differences between AIDP and AMAN 32
Figure 1.5 - The biosynthetic pathway and structure of gangliosides 35
Figure 1.6 - *Campylobacter jejuni* sialyltransferase activity directs neuropathy subtype 37
Figure 1.7 - Possible sites of action of anti-ganglioside antibodies 42
Figure 1.8 - The first TLC demonstration of GSC binding antibodies in GBS 47
Figure 1.9 - GSC antibodies in GBS and MFS detected by ELISA. 49
Figure 2.1 - The ATS4 autosampler and slide guide 57
Figure 3.1 - Ganglioside complex ELISA with IgM and IgG monoclonal antibodies 88
Figure 3.2 - Effect of premixing and differing ganglioside ratios on ganglioside complex formation and binding 91
Figure 3.3 - ELISA with Japanese neuropathy sera assayed against a limited panel of gangliosides 94
Figure 3.4 - The response of anti-b series mAbs to GM1:GD1a complexes 95
Figure 3.5 - Relationship between number of single gangliosides and potential number of complexes 97
Figure 3.6 - Typical layout for a 10x10 PVDF-glycoarray 98
Figure 3.7 - Development and initial validation of the PVDF glycoarray 101
Figure 3.8 - Structure of BODIPY FL C5-ganglioside GM1 104
Figure 3.9 – GD1a in a GM1:GD1a complex does not modulate the amount of GM1 binding to the PVDF membrane 105
Figure 3.10 - Reactivity of anti-GM1 mAbs DG1 and DG2 to ganglioside complexes containing GM1 in solid phase 109
Figure 3.11 - The display platform influences the binding of anti-b-series mAbs to GM1:GD1a complex 111
Figure 3.12 - GSC liposome ELISA with GM1:GD1a complex 112
Figure 3.13 - CGM2 and CGM3 bind GD1a:GD1b complex by TLC with immuno-overlay 115
Figure 3.14 - Neuropathy sera binding GM1:GD1a complex on PVDF and in ELISA 117
Figure 3.15 - Glycoarray and ELISA analysis of complex specific, independent and attenuated sera used in subsequent ex vivo assay 119
Figure 3.16 - Potential mechanisms of ganglioside complex mediated binding 122

Figure 3.17 - The disparate ex vivo binding patterns of two anti-GM1 monoclonal antibodies 124
Figure 4.1 - The binding of siglecs E and F is modulated by ganglioside complexes 132
Figure 4.2 - Siglec-7 and TeNT H_C binding is modulated by ganglioside complexes 135
Figure 4.3 - Cholera Toxin B subunit binding to GM1 is unaffected by complexes 137
Figure 4.4 - Complex attenuated, complex independent and complex enhanced binding 141
Figure 5.1 - Complex attenuated and enhanced binding in neuropathy sera ... 142
Figure 5.2 - Electrophysiological categorisation of disease subtype 146
Figure 5.3 - Receiver operator characteristics for the glycoarray 150
Figure 5.4 - Contribution of single glycolipids to antigens bound in an absolute complex dependent manner 151
Figure 5.5 - Individual value plots for the 17 antigen spots significantly associated with GBS 153
Figure 5.6 - The relationship between SGPG and SGPG:PS complex binding within the same sera 155
Figure 5.7 - The relationship between SGPG, PS and SGPG:PS complex binding within the same sera 156
Figure 5.8 - Contrast in binding patterns between GBS and control sera towards single sulfatide and GA1 as compared with sulfatide:GA1 complex 160
Figure 5.9 - Heatmap analysis of glycoarray intensity data 166
Figure 5.10 - Example of complex antigen bound by only one serum tested ... 171
Figure 5.11 - GBS sera with highly specific binding patterns 172
Figure 5.12 - GBS sera with more promiscuous binding patterns 173
Figure 6.1 - Anti-GSC antibody response following GM1:GD1a immunisation ... 182
Figure 6.2 - PVDF array analysis of sera from GM1:GD1a immunised GM2 KO mice 184
Figure 6.3 - Anti-GSC antibody response following GD1a:GD1b immunisation . 186
Figure 6.4 – The different complex response of GD1a:GD1b immunisation between GM2 KO and GD2s KO mice 187
Figure 6.5 - Differing responses of GM2 KO and GD3s KO mice to immunisation with GD1a:GD1b liposomes 188
Figure 6.6 - Layout for 7x7 grid 189
Figure 6.7 - Sphingomyelin complex IgG reactivity following GM1:GD1a immunisation 191
Figure 6.8 - Sphingomyelin complex reactivity following GD1a:GD1b immunisation 194
Figure 6.9 - A hypothetical reason for enhanced binding to GM2:GD1a on PVDF despite immunisation with GM1:GD1a 197

Figure 8.1 – The current passive transfer model of anti-ganglioside mediated neuropathy in mice 211

Figure 8.2 - Development of the GM2-neurofilament light transgenic / GM2 KO mouse 213

Figure 8.3 - Immunofluorescent staining of neuromuscular tissue from the lumbricals of transgenic, knockout and wild type mice 214

Figure 8.4 - HP-TLC using acidic glycolipid fractions extracted from transgenic, KO and WT mice brain..... 215

Figure 8.5 - Organ bath containing mouse diaphragm in Ringer's 216

Figure 8.6 - Ex vivo application demonstrates the sensitivity of transgenic NMJs to anti-ganglioside antibodies..... 221

Figure 8.7 - Quantification of *ex vivo* staining data 222

Figure 8.8 - Neurofilament loss over the NMJ following ganglioside antibody and complement administration *ex vivo*..... 223

Figure 8.9 - Baseline tidal volume..... 226

Figure 8.10 – Whole body plethysmography following passive transfer of MOG16 anti-ganglioside antibody 227

Figure 8.11 - Immunoglobulin and complement deposition following passive transfer 228

Figure 8.12 - The IgG response to GT1b immunisation in WT, KO and NFL Tg mice 230

Figure 8.13 - The IgM response to GT1b immunisation in WT, KO and NFL Tg mice 230

Figure 8.14 – Plethysmography following active immunisation 232

Figure 8.15 - Baseline behavioural and strength testing..... 233

Figure 8.16 - Open field behaviour at baseline..... 234

Figure 8.17 - Rotarod testing..... 235

Figure 8.18 - Immunoglobulin and complement deposition following active immunisation with GT1b-liposomes 237

List of Accompanying Material

Publications Arising

Combinatorial Glycoarray.
Rinaldi S, Brennan KM, Willison HJ.
Methods in Molecular Biology. 2012 ;808:413-23

Lipid arrays identify myelin-derived lipids and lipid complexes as prominent targets for oligoclonal band antibodies in multiple sclerosis.
Brennan KM, Galban-Horcajo F, Rinaldi S, O'Leary CP, Goodyear CS, Kalna G, Arthur A, Elliot C, Barnett S, Linington C, Bennett JL, Owens GP, Willison HJ.
Journal of Neuroimmonology. 2011 Sep 15;238(1-2):87-95

The GD1a glycan is a cellular receptor for adenoviruses causing epidemic keratoconjunctivitis.
Nilsson EC, Storm RJ, Bauer J, Johansson SM, Lookene A, Ångström J, Hedenström M, Eriksson TL, Frängsmyr L, Rinaldi S, Willison HJ, Pedrosa Domellöf F, Stehle T, Arnberg N.
Nature Medicine. 2011 Jan 17(1):105-9

Transgenic rescue of ganglioside expression in the peripheral nervous system of ganglioside-null mice facilitates an active immunisation model of acute motor axonal neuropathy.
Rinaldi S, Yao D, Greenshields K, McKinnon A, Fewou S, Furukawa K, Brophy PJ, Willison HJ.
Journal of Neuroimmonology. 2010 Nov 228(1-2):87 (Abstract)

Heteromeric glycolipid complexes as modulators of autoantibody and lectin binding.
Rinaldi S, Brennan KM, Willison HJ.
Progress in Lipid Research. 2010 Jan 49(1):87-95

Analysis of lectin binding to glycolipid complexes using combinatorial glycoarrays.
Rinaldi S, Brennan KM, Goodyear CS, O'Leary C, Schiavo G, Crocker PR, Willison HJ.
Glycobiology. 2009 Jul 19(7):789-96.

Detection of autoantibody and lectin binding to ganglioside complexes using a novel combinatorial glycoarray.
Rinaldi S, Brennan KM, Greenshields KN, Goodyear CS, O'Leary C, Schiavo G, Crocker PR, Willison HJ.
Journal of the Peripheral Nervous System. 2009 Jul 14(21):126 (Abstract).

The neuropathic potential of anti-GM1 autoantibodies is regulated by the local glycolipid environment.
Greenshields KN, Halstead SK, Zitman FMP, Rinaldi S, Brennan KM, O'Leary C, Chamberlain LH, Easton A, Roxburgh J, Pediani J, Furukawa K, Furukawa K, Goodyear CS, Plomp JJ and Willison HJ.
Journal of Clinical Investigation. 2009 Mar 119(3):595-610.

G*anglioside antibodies and neuropathies.*
Rinaldi S, Willison HJ.
Current Opinion in Neurology 2008 Oct 21(5):540-546.

Definitions/Abbreviations

αBTx - alpha-Bungarotoxin

AI – arbitrary intensity

AIDP – acute inflammatory demyelinating polyradiculopathy

APES - 3-aminopropyltriethoxysilane

BSA - bovine serum albumin

Cer – ceramide

CI – confidence interval

CSF - cerebrospinal fluid

CTB – cholera toxin B subunit

CTH - trihexosylceramide (ceramide trihexosides)

CV – coefficient of variation

DHFR - dihydrofolate reductase

DMEM - Dublecco's Modified Eagle's medium

DMPC - dimyristoylphosphatidylcholine

DMSO – dimethyl sulfoxide

ECL - enhanced chemiluminescence

ELISA - enzyme linked immunosorbent assay

FBS – foetal bovine serum

FITC - fluorescein isothiocyanate

GA1 – asialo-ganglioside GM1/ ceramide tetrahexoside (Cer-Glc-Gal-GalNAc-Gal)

Gal - galactose

GalC - glactocerebroside (galactosylceramide)

GalNAc - N-acetylgalactosamine

$GalNAcT^{-/-}$ - N-acetylgalactosaminyl-transferase knockout

Gb_3 - globotriaosylceramide

Gb_4 - globoside (globotetrahexosylceramide)

GBS - Guillain-Barré syndrome

GD1a - disialoganglioside GD1a (Cer-Glc-Gal(NeuAc)-GalNAc-Gal-NeuAc)

GD1b – disialoganglioside GD1b (Cer-Glc-Gal(NeuAc-NeuAc)-GalNAc-Gal)

GD2 – disialoganglioside GD2 (Cer-Glc-Gal(NeuAc-NeuAc)-GalNAc)

GD3 - disialoganglioside GD3 (Cer-Glc-Gal-NeuAc-NeuAc)

$GD3s^{-/-}$ - GD3 synthase knockout

GM1 – monosialoganglioside GM1 (Cer-Glc-Gal(NeuAc)-GalNAc-Gal)

GM2 – monosialoganglioside GM2 (Cer-Glc-Gal(NeuAc)-GalNAc)

GM3 - monosialoganglioside GM3 (Cer-Glc-Gal-NeuAc)

Glc - glucose

GQ1b – tetrasialoganglioside GQ1b (Cer-Glc-Gal(NeuAc-NeuAc)-GalNAc-Gal-NeuAc-NeuAc)

GSC – ganglioside complex

GSL – glycosphingolipid

GT1a - trisialoganglioside GT1a (Cer-Glc-Gal(NeuAc)-GalNAc-Gal-NeuAc-NeuAc)

GT1b – trisialoganglioside GT1b (Cer-Glc-Gal(NeuAc-NeuAc)-GalNAc-Gal-NeuAc)

h – hour(s)

HAT - hypoxanthine-aminopterin-thymidine selection medium

$HGPRT^{-/-}$ - hypoxanthine-guanine phosphoribosyltransferase deficient

HP-TLC – high performance thin layer chromatography

HRP - horse radish peroxidase

HT - hypoxanthine-thymidine medium

Ig - immunoglobulin

ip - intraperitoneally

iv – intravenously

LM1 - sialosyl-neolactotetraosylceramide

mAb - monoclonal antibody

MAC - membrane attack complex

min - minutes

nAChR - nicotinic acetylcholine receptor

NeuAc – sialic acid / N-acetylneuraminic acid

NFL – neurofilament light

NFL-Tg - GalNAcT GalNAcT $^{-/-}$ transgenic (Tg(Nfl-GalNAcT)GalNAcT$^{-/-}$)

NHS - normal human serum

NMJ – neuromuscular junction

OD – optical density

OPD - *o*-Phenylenediamine dihydrochloride

PBS - phosphate buffered saline

PEG - polyethylene glycol

PS – phosphatidylserine

pSC - peri-synaptic Schwann cell

PVDF - polyvinylidene difluoride

RPMI - Roswell Park Memorial Institute (tissue culture medium)

SGPG – sulfated glucuronyl paragloboside

Siglec – sialic acid binding, immunoglobulin like lectin

TLC - thin layer chromatography

TRITC - Tetramethyl Rhodamine Isothiocyanate

TV - tidal volume

WT - wild type

Short summary

There is plentiful evidence that the pathology of Guillain Barré syndrome (GBS) is driven by autoantibodies generated following infection. A number of inconsistencies with this theory remain, and in many clinical cases such antibodies are not detected. Recent descriptions of ganglioside complex (GSC) antibodies suggest a potential explanation for this. This study aimed to further investigate GSCs and associated antibodies with a particular focus on GBS. GSCs were found to modulate the binding of other lectins such as bacterial toxins, immunomodulatory receptors, and monoclonal antibodies. The development of a semi-automated array system allowed screening of a large cohort of GBS sera against multiple complexes, revealing a greater antibody detection rate (particularly in demyelinating forms) than had previously been achieved. Binding that was both enhanced and attenuated by complexes was seen, and this varied between disease and control sera. Immunisation experiments provided insights into the generation of the GSC immune response. A transgenic mouse model of GBS was also developed, demonstrating that local axonal expression of gangliosides does not induce systemic tolerance.

The work described in this thesis has thus significantly advanced knowledge in the field of glycolipid complexes, particularly with respect to anti-glycolipid complex antibodies and their association with inflammatory neuropathies such as Guillain-Barré syndrome.

Summary

Guillain Barré syndrome (GBS) is an acute, acquired peripheral neuropathy characterised clinically by ascending weakness and loss of the deep tendon reflexes. Since the index case description, various theories regarding its pathogenesis have been proposed. Following the first detection in affected patients' sera of antibodies directed against glycolipids, evidence has accumulated to suggest that such antibodies arise via a process of molecular mimicry following infection, resulting in complement mediated failure of neuromuscular transmission and structural nerve damage. However, unresolved issues regarding this disease model remain. Anti-GQ1b ganglioside antibodies are found in 90-95% of patients with the regional Miller Fisher variant of GBS, and the majority of patients with axonal variants are positive for anti-GM1, GD1a or related antibodies. However, in the more common demyelinating form of the disease (Acute Inflammatory Demyelinating Polyneuropathy, AIDP) no specific antibody has been identified. Where antibodies are found, their predilection for particular nerves types is unexplained. For example, GD1a antibodies are associated with a motor phenotype, yet GD1a is present in roughly equal proportions in motor and sensory nerves. There are also unexplained discrepancies in the apparent pathogenic potential of different anti-GM1 antibodies. Furthermore, following infections associated with GBS, the mechanism by which self tolerance is overcome in a small proportion of patients, but is preserved in the vast majority of others, is unknown.

It is on this background that the detection of anti-ganglioside complex (GSC) antibodies by Japanese researchers proved particularly intriguing. These antibodies react with pairs of gangliosides, whilst failing to bind to each

individually. It may be, therefore, that investigators have previously failed to identify GBS associated antibodies because the focus has been in assessing binding to purified, homogenous preparations of glycolipids *in vitro*, rather than considering the antigenic diversity potentially produced by glycolipid-glycolipid inter-combinations occurring *in vivo*. It can also be envisaged that if GSCs form differently on motor and sensory nerves, or fail to form in sites where immunological tolerance is generated, then this initial observation may be able to be expanded upon to answer some of the additional questions posed above.

The overall aim of the research described herein was therefore to further investigate GSCs with a particular focus on assessing the characteristics of anti-GSC antibodies associated with GBS.

Initially existing ganglioside ELISA methodology was expanded to include the combinatorial element. This revealed that anti-ganglioside monoclonal antibodies (mAbs) frequently demonstrated complex modulated binding. Even when an antibody had been generated with specificity against a single, defined, ganglioside, cross reactivity was seen towards other complexes. In addition to the complex enhanced binding previously described, certain mAbs behaved in a different way. These 'complex attenuated' antibodies bound well to single gangliosides, but were prevented from doing so when certain complex partners were additionally present. The most notable example seen was with the anti-GM1 antibodies DG1 and DG2. DG1 binding is complex attenuated, whereas DG2 remains able to bind the GM1:GD1a complex. This correlates with the pathogenic potential or otherwise of these two antibodies

The major methodological advance detailed in the thesis is the development of the combinatorial glycoarray. The glycoarray allowed screening of numerous

lectins against a large number of different glycolipids and complexes. This showed that other lectins, such as bacterial toxins and siglecs (sialic acid binding immunoglobulin like lectins), additionally display complex modulated binding. The combinatorial glycoarray was then used to look for anti-complex antibodies in a large cohort of Western European GBS patients, largely made up of the AIDP variant. The application of the array technology increased the antibody detection rate in confirmed AIDP cases from 14.3% by ELISA to 62.5% by glycoarray. Complex specific antibodies were found in 43.6% of disease associated sera, and only 4.1% of controls. When single glycolipid reactive antibodies were detected in disease and control sera, they often showed divergent patterns of binding with respect to complex enhancement or attenuation. Nine antigens showed statistically increased binding in GBS versus controls. Particular antibodies were associated with particular clinical features, including disease severity and the requirement for mechanical ventilation.

Immunisation experiments provided important insights into the generation of the anti-ganglioside and GSC immune response. This was further investigated using newly developed transgenic mice with axonal specific rescue of complex ganglioside synthesis. These studies demonstrated that restricted axonal ganglioside expression does not generate systemic tolerance, and allowed the development of a single animal, mouse model of GBS.

The work described in this thesis has thus significantly advanced knowledge in the field of glycolipid complexes, particularly with respect to anti-glycolipid complex antibodies and their association with inflammatory neuropathies such as Guillain-Barré syndrome.

1 Introduction

The overall aim of this study is to evaluate ganglioside complexes (GSC) and GSC antibodies with particular focus on their potential role in Guillain-Barré syndrome. A more detailed description of these aims is given in section 1.3 below. This introduction sets this current research in context and is not intended to be an all encompassing review of the vast amount of work already performed in the wider field.

1.1 Guillain-Barré syndrome – an acute inflammatory disorder of the peripheral nervous system

1.1.1 Overview

Guillain-Barré-syndrome (GBS) is a post infectious, monophasic, acute inflammatory neuropathy. It was first described by Guillain, Barré and Strohl in 1916, having been observed in two infantrymen (Guillain *et al.*, 1916). The syndrome is characterised by a symmetrical ascending weakness, loss of the deep tendon reflexes, and 'albuminocytological dissociation' (raised protein with normal cell count) on analysis of the cerebrospinal fluid (CSF) (Asbury, 1990). Epidemiological studies give an average annual incidence for the disease of 0.4 to 4.0 per 100,000. The lifetime incidence is around 1 in 1000 (Alter, 1990). Diagnosis is largely based on clinical history and physical examination, supported by CSF analysis (where appropriate) and neurophysiological assessment (Asbury & Cornblath, 1990). Supportive treatment is of paramount importance, and the disease course can be positively influenced by immunomodulatory therapy with intravenous immunoglobulin, plasmapheresis, or both (Raphael *et al.*,

2002;Hughes *et al.*, 2007). Most patients will make a good recovery, but will often require prolonged periods in hospital, and some weeks to months in intensive care. Most patients have long term persistent health problems (Bernsen *et al.*, 1997;Dornonville & Jakobsen, 2005), and historically 5-15% of patients died in the acute phase of the disease. Contemporary studies in countries with advanced critical care facilities suggest the mortality rate has fallen to around 2.5% (Alshekhlee *et al.*, 2008).

The current, widely accepted, pathological model for the disease is that auto-reactive antibodies arise following infection, by a process of molecular mimicry, and drive complement mediated damage to peripheral nerves (Yuki *et al.*, 1990;Yuki, 2007a;Yuki & Kuwabara, 2007;Goodyear *et al.*, 1999). There are however a number of inconsistencies with this theory, as later discussed.

1.1.2 Historical aspects

As noted, GBS takes its name from the 1916 study by Georges Guillain, Jean-Alexandre Barré, and André Strohl. An earlier case series of 'ascending paralysis' had been described by Landry in 1859 (Landry, 1879). Landry's 10 cases included a mixture of ascending paralysis with and without ascending sensory loss. CSF sampling was not performed, as the technique had not yet been developed. The location of the pathology was not identified at autopsy in the three patients that died, as the peripheral nerves were not examined.

Guillain, Barré and Strohl's paper had the advantage of coming after the development of lumbar puncture by Quincke and Wynter in 1891, included a relatively accurate speculation on the site of the pathology, and a succinct description of the key clinical features;

> "The syndrome is characterised by motor disorders, abolition of the tendon reflexes with preservation of the cutaneous reflexes, paraesthesias with slight disturbance of objective sensation, pain on pressure of the muscle masses, marked modifications in the electrical reactions of the nerves and muscles, and remarkable hyperalbuminosis of the cerebrospinal fluid with absence of cytological reaction (albuminocytological dissociation).This syndrome seemed to us to depend on a concomitant injury of the spinal roots, the nerves, and the muscles, probably of infectious or toxic nature."

There then followed a long lasting debate about the exact nature and boundaries of the disorder. Guillain in particular resisted suggestions that GBS was similar to Landry's ascending paralysis, citing the respiratory failure occasionally seen in the latter, along with the absence of CSF analysis and suggested that the pathology in Landry's cases was instead bulbar (Guillain, 1936). Three years after Guillain, Barré and Strohl's paper, Bradford, Bashford and Wilson described 30 further cases under the heading 'Acute Infective Polyneuritis' and briefly claimed to have indentified an infective pathogen. (Bradford *et al.*, 1919) Thereafter, there was a tendency to label any acute lower motor neuron paralytic illness GBS or acute infective polyneuritis with the terms seemingly being used interchangeably. There was additionally frequent speculation of an infective or toxic mechanism.

In 1949 an attempt was made to define the disease not in terms of the presence or absence of specific clinical features, but by the underlying pathological process (Haymaker & Kernohan, 1949). Haymaker and Kernohan preformed autopsy studies on 50 cases of 'Landry-Guillain-Barré syndrome,' some of whom had died shortly after the onset of their illness. By comparing tissue obtained at different stages of the disease process they hoped to be able to reconstruct the temporal sequence of events. Two principle findings were highlighted by the authors. The first was that presentations which would previously have been variously termed Landry's ascending paralysis, GBS, or acute (infective)

polyneuritis all shared pathological features, and were therefore best considered as one disorder. The second was that the initial pathological change was swelling of peripheral nerve myelin, before later infiltration of inflammatory cells. The authors concluded that neurological dysfunction occurred before lymphocytes and macrophages appeared, and speculated that the cells might instead be involved in the reparative process. This led others to begin to search for a humoral factor in blood or CSF which might be the key pathogenic agent.

In 1955, rabbits injected with an homogenised preparation of sciatic nerve and/or spinal roots and ganglia were observed to develop a flaccid paralysis after a two week interval (Waksman & Adams, 1955). Lymphocytic infiltration and myelin degradation of the nerve roots, spinal ganglia, and peripheral nerves was noted, along with an increase in the total protein content of the spinal fluid while cell counts remained normal. This disease model was termed experimental allergic neuritis (EAN), and the many similarities to GBS were discussed. Refinements to the technique revealed that EAN could be induced by immunisation with specific myelin proteins, and that disease activity could be transferred along with myelin protein autoreactive T cells (Rostami *et al.*, 1985;Heininger *et al.*, 1986). Research was therefore focussed along such lines, notwithstanding the observations that antibodies to the immunogen were also induced and that transfer of such humoral factors also exacerbated disease (Archelos *et al.*, 1993;Hahn *et al.*, 1993).

In the 1980s it was established that in paraproteinaemic neuropathy the protein band detected was often autoreactive against myelin associated glycoprotein (MAG) or nerve associated glycolipids (Braun *et al.*, 1982). This, coupled with the observation that plasma exchange was effective in GBS, reignited interest in

circulating, humoral components of the immune system in the disease (Gruener *et al.*, 1987;Zerbi *et al.*, 1981;The Guillain-Barré Syndrome Study Group, 1985;Willison & Yuki, 2002). In 1988, antibodies to gangliosides and related glycolipids were first detected in 5 patients with GBS (Ilyas *et al.*, 1988). The disease associations, induction and pathogenic effects of anti-ganglioside antibodies in GBS have been extensively studied in the intervening period, as discussed below (1.1.7).

1.1.3 Epidemiology

The incidence of GBS is estimated to be between 0.4 and 4.0 cases per 100,000 people per year (Alter, 1990;Hughes & Rees, 1997). In Western Europe the exact figure is likely to be around 1.3 to 1.8/100,000 per year (Rees *et al.*, 1998). Almost all series show an excess of male over female cases, unusual for a presumed autoimmune disease. The annual incidence increases with increasing age – from 0.8/100,000 in people less than 18, to 3.2/100,000 in those over 60 in one study (Beghi *et al.*, 1985). As this study also highlighted, in GBS, around 60-70% of patients will have experienced an infection in the previous month. Respiratory and gastro-intestinal symptoms have been shown to be statistically more common in suffers in the month preceding onset of GBS. A more recent prospective case-control study has confirmed this association (Sinha *et al.*, 2007). In this Indian series, antecedent infection was reported by 49% of patients and 4% of controls, with positive serology in 50% and 8% respectively, both highly statistically significant differences. On serological testing, *Campylobacter jejuni* is the most frequently identified pathogen, although other infections are sometimes identified (Winer *et al.*, 1988;Hadden *et al.*, 2001;van Koningsveld *et al.*, 2000). Cases generally have a uniform incidence throughout the year, save

for certain GBS variants in Northern China which display seasonal variation (see 1.1.5 below for further details).

1.1.4 Clinical features and diagnosis

Guillain, Barré and Strohl's 1916 description succinctly captures the key features of a typical GBS case. Following the possible link between an increase in GBS cases and the 1976/1977 swine flu vaccine, formal diagnostic criteria were devised at the behest of the then National Institute of Neurological and Communicative Disorders and Stroke (NINCDS) (Asbury, 1978). These were essentially reaffirmed in 1990, with further refinement of the electrodiagnostic criteria (Asbury & Cornblath, 1990). Two features are required for the diagnosis, namely progressive motor weakness of more than one limb and areflexia. The former ranges from mild weakness of the legs to total paralysis of all 4 limbs, and of the facial, bulbar, and respiratory muscles with complete external ophthalmoplegia. The areflexia is usually absolute but suppression without total absence of proximal reflexes is stated as acceptable if other features are in keeping. By definition, the weakness progresses over a maximum of 4 weeks, whereas recovery almost always occurs over a much longer period. In around a quarter of those affected, involvement of the respiratory muscles leads to the requirement for mechanical ventilation on the intensive care unit. Between 4% and 15% of patients die, although this may be improving, and up to 20% have not fully recovered after 1 year and may never do so (Rees *et al.*, 1998;Hughes *et al.*, 2005;Alshekhlee *et al.*, 2008). Clearly, this represents a significant burden on both the acute medical and rehabilitation services.

Complementary to the core criteria, further features in keeping with the diagnosis are provided, in addition to features casting doubt and features excluding the diagnosis. These are summarised below (Figure 1.1, Figure 1.2 and Figure 1.3).

- **A. Clinical features (ranked in order of importance)**
  - 1. Progression. Symptoms and signs of motor weakness develop rapidly but cease to progress by four weeks into the illness. Approximately 50% will reach the nadir by two weeks, *80%* by three weeks, and more than 90% by four weeks.
  - 2. Relative symmetry. Symmetry is seldom absolute, but usually, if one limb is affected, the opposite is as well.
  - 3. Mild sensory symptoms or signs.
  - *4.* Cranial nerve involvement. Facial weakness occurs in approximately 50% and is frequently bilateral. Other cranial nerves may be involved, particularly those innervating the tongue and muscles of deglutition, and sometimes the extraocular motor nerves. On occasion (less than *5%),* the neuropathy may begin in the nerves to the extraocular muscles or other cranial nerves.
  - *5.* Recovery. It usually begins two to four weeks after progression stops. Recovery may be delayed for months. Most patients recover functionally.
  - 6. Autonomic dysfunction. Tachycardia and other arrhythmias, postural hypotension, hypertension,and vasomotor symptoms, when present, support the diagnosis. These findings may fluctuate. Care must be exercised to exclude other bases for these symptoms, such as pulmonary embolism.
  - 7. Absence of fever at the onset of neuritic symptoms.
- **B. Cerebrospinal fluid features strongly supportive of the diagnosis**
  - 1. CSF protein. After the first week of symptoms, CSF protein is elevated or has been shown to rise on serial lumbar punctures.
  - 2. CSF cells. Counts of 10 or fewer mononuclear leukocytes/mm^3 in CSF.
- **C. Electrodiagnostic features strongly supportive of the diagnosis**
  - Approximately 80% will have evidence of nerve conduction slowing or block at some point during the illness. Conduction velocity is usually less than 60% of normal, but the process is patchy and not all nerves are affected. Distal latencies may be increased to as much as three times normal. Use of F-wave responses often gives good indication of slowing over proximal portions of nerve trunks and roots. Up to 20% of patients will have normal conduction studies. Conduction studies may not become abnormal until several weeks into the illness.

Figure 1.1 - Features supportive of the diagnosis of GBS

From Asbury AK, Cornblath DR. Assessment of current diagnostic criteria for Guillain-Barré syndrome. Ann Neurol 1990; 27 (suppl): S21–24.

- 1. Marked, persistent asymmetry of weakness.
- 2. Persistent bladder or bowel dysfunction.
- *3.* Bladder or bowel dysfunction at onset.
- *4.* More than 50 mononuclear leukocytes/mm^3 in CSF.
- *5.* Presence of polymorphonuclear leukocytes in CSF.
- 6. Sharp sensory level.

Figure 1.2 - Features casting doubt on the diagnosis of GBS

From Asbury AK, Cornblath DR. Assessment of current diagnostic criteria for Guillain-Barré syndrome. Ann Neurol 1990; 27 (suppl): S21–24.

- 1. A current history of hexacarbon abuse (volatile solvents; n-hexane and methyl n-butyl ketone). This includes huffing of paint lacquer vapors or addictive glue sniffing.
- 2. Abnormal porphyrin metabolism indicating a diagnosis of acute intermittent porphyria. This would manifest as increased excretion of porphobilinogen and 6-aminolevulinic acid in the urine.
- *3.* A history or finding of recent diphtheritic infection, either faucial or wound, with or without myocarditis.
- *4.* Features clinically consistent with lead neuropathy (upper limb weakness with prominent wrist drop; may be asymmetrical) and evidence of lead intoxication.
- *5.* The occurrence of a purely sensory syndrome.
- 6. A definite diagnosis of a condition such as poliomyelitis, botulism, hysterical paralysis, or toxic neuropathy (e.g., from nitrofurantoin, dapsone, or organophosphorus compounds), which occasionally may be confused with Guillain-Barre syndrome.

Figure 1.3 - Features that rule out the diagnosis of GBS

From Asbury AK, Cornblath DR. Assessment of current diagnostic criteria for Guillain-Barré syndrome. Ann Neurol 1990; 27 (suppl): S21–24.

Although the above clinical criteria are widely accepted, the electrodiagnostic parameters are more problematic. There are a number of reasons for this. As noted above, such studies may remain normal for several weeks following the onset of disease. Furthermore, later in the disease course axonal degeneration can complicate an initial demyelinating process, thus altering the electrophysiological abnormalities seen. The description of axonal variants of GBS in the early to mid-1990s (Acute Motor Axonal Neuropathy, AMAN, and Acute Motor-Sensory Axonal Neuropathy, AMSAN) (McKhann *et al.*, 1993), with an

entirely separate set of nerve conduction study changes, additionally compounds the situation. Essentially, nerve conduction studies can be used to confirm that the disease process is due to a peripheral neuropathy and additionally categorise this into demyelinating or axonal subtypes. More recent revisions to the diagnostic criteria in general, taking into account these variants, have been proposed (van der Meche *et al.*, 2001).

1.1.5 Disease subtypes and variants

Both axonal and regional variants of GBS exist. The most well known regional variant is Miller Fisher syndrome (MFS). First reported in 1956, the striking clinical features are ophthalmoplegia, ataxia, and areflexia (Fisher, 1956). Formes fruste, with isolated ataxia or ophthalmoplegia, are additionally recognised. The Pharyngeal-Cervical-Brachial (PCB) subtype predominantly involves the oropharyngeal, neck and shoulder muscles with facial palsy and ptosis but with much less pronounced (or entirely absent) lower limb weakness. Likewise, although areflexia is seen in the upper limbs the lower limb reflexes may be preserved. Sensory impairment is uncommon. Initially this syndrome was speculated to be a GBS variant on the basis of the presence of albuminocytological dissociation in the CSF along with electrophysiological changes in keeping with the diagnosis and a typical disease course (Ropper, 1986). More recently, larger case series have further supported the suspicion that PCB is part of a spectrum of GBS with clinical features overlapping with all of MFS, typical GBS and Bickerstaff's Brainstem Encephalitis (BBE). BBE itself was initially speculated to be similar to 'infective polyneuritis' in the Birmingham Neurologist's 1957 paper (Bickerstaff, 1957). This was due to;

> "the mode of onset and progression, the stationary state at maximal disability, and the rapid recovery of gross paralysis with slower final extinction of all abnormality. Indeed, several patients had lost all tendon reflexes even at a time when neither hypotonia nor paralysis of the limbs was marked."

Again, further, larger case series in recent years support the concept the BBE also lies at one end of a spectrum of GBS and, in particular, MFS, given the prominent ophthalmoplegia and ataxia in addition to disturbances of consciousness (Ito *et al.*, 2008).

Historically, the eponym GBS was held widely to be synonymous with the more pathologically descriptive term Acute Inflammatory Demyelinating Polyradiculoneuropathy (AIDP). However, from the early 1990s onwards, it has been increasingly recognised that there are subtypes of the disease which appear clinically similar but have a different underlying epidemiology, pathology, and presumably aetiology. In a study of patients in China, who mainly came form the rural north, it was shown that a syndrome previously diagnosed clinically as GBS had a number of unusual features (McKhann *et al.*, 1993). For example, seasonal peaks of acute paralysis were observed and the average age of patients was 19 years, younger than for AIDP. Furthermore, the progression of weakness was somewhat more rapid than for 'classical' GBS, with a nadir being reached in just under 6 days on average. Bulbar muscles were more commonly involved and sensory symptoms rare. However, it was the electrophysiological findings and pathology which really set this disease apart as a distinct subtype. Nerve conduction studies demonstrated reduced amplitude of action potentials, consistent with axonal injury. Pathological studies confirmed the presence of motor axonal damage (Figure 1.4) and Wallerian degeneration, and this disease was termed Acute Motor Axonal Neuropathy (AMAN), and proposed to be a variant of GBS (McKhann *et al.*, 1993). Soon after, another axonal variant, Acute

Motor and Sensory Axonal Neuropathy (AMSAN), was described (Griffin *et al.*, 1996).

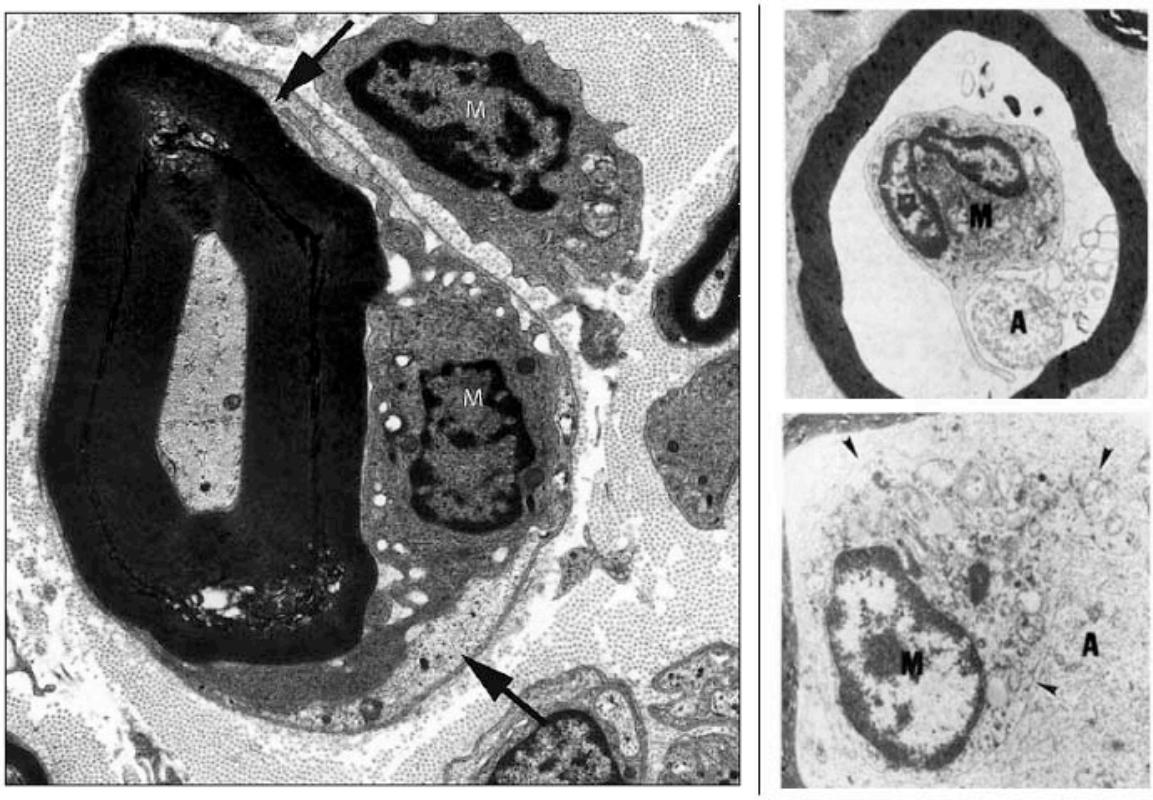

Figure 1.4 - Pathological differences between AIDP and AMAN

Electron micrographs from AIDP (left panel, taken from (Hughes & Cornblath, 2005)) and AMAN (right two panels, taken from (Griffin *et al.*, 1996)) are compared. In the former, a macrophage (M) can be seen invading the Schwann cell and has stripped myelin from around some of the axons (arrows). In contrast, in the AMAN specimens in the right-hand panels, macrophages within an intact myelin sheath can be seen to surround the axon (upper panel) and cause axonal granular degeneration (lower panel).

1.1.6 Current treatments

The only treatment shown to be beneficial as compared to supportive treatment alone in GBS is plasma exchange (Zerbi *et al.*, 1981;The Guillain-Barre Syndrome Study Group, 1985;McKhann, 1990;Gruener *et al.*, 1987). This technique is expensive, requires specialist machinery and intra-venous access, and is only partially effective. With treatment, the proportion of patients requiring

mechanical ventilation is nearly halved (but still remains at around 14%), whereas the percentage who have regained full muscle strength by one year is only improved from 55% to 68% (Raphael *et al.*, 2002). Intravenous immunoglobulin has been compared to plasma exchange, and found to be equivalent (van der Meche & Schmitz, 1992;Hughes *et al.*, 2004). Perhaps surprisingly, the effect of corticosteroids in the inflammatory neuropathies is variable; deleterious in multifocal motor neuropathy (MMN) (Slee *et al.*, 2007), harmful (oral) or equivalent to placebo (intravenous) in GBS (Hughes *et al.*, 2007), and sometimes beneficial in Chronic Inflammatory Demyelinating Polyneuropathy (CIDP) (Toothaker & Brannagan, III, 2007). It is therefore hypothesised that steroids might in some cases interfere with the scavenging of nerve debris following injury, and hence delay regeneration and recovery, or in some other way adversely affect nerve conduction (Hughes *et al.*, 2004;Hughes *et al.*, 2006). A range of other immunosuppressants have been investigated in the treatment of the GBS and related neuropathies, ranging from long established drugs such as azathioprine, methotrexate and ciclosporin, to more recently developed monoclonal antibodies such as rituximab and alemtuzumab (which deplete B and T lymphocytes respectively). Despite a theoretical basis for efficacy, and in some cases supportive data from animal models such as EAN (experimental autoimmune neuritis), these approaches lack convincing evidence of benefit in humans (zu Horste *et al.*, 2007).

1.1.7 Pathophysiology

Pathological studies in GBS typically show an inflammatory, cellular infiltrate with macrophages damaging myelin or axons as pictured above (Figure 1.4). It was initially thought that macrophages were targeted to myelin antigens by

activated T-cells, based on studies of EAN. However, some pathological studies demonstrated myelin swelling apparently preceding cellular infiltration (Haymaker & Kernohan, 1949). Furthermore, immunological studies showed that antibodies directed against gangliosides and related molecules were found in the sera of patients with GBS (Ilyas *et al.*, 1988). Both of these studies therefore suggest that autoreactive antibodies might first attach to myelin or axolemmal antigens, fix complement, and secondarily attract a cellular infiltrate.

1.1.7.1 Gangliosides and molecular mimicry

Gangliosides themselves were originally described by Klenk in 1935, who isolated what he initially termed 'substance x' from the spleens of patients with Niemann-Pick and Tay Sachs diseases (Klenk , 1935). He later established that this substance was much more enriched in the nervous system, and as the nature of this substance was further unravelled the term ganglioside was coined. It is now known that gangliosides are membrane incorporated glycosphingolipids (GSLs). They are amphipathic molecules, with a long, hydrophobic, lipid tail (ceramide) and a much more variable, hydrophilic, charged, sialic-acid-containing, oligosaccharide head group (Sonnino *et al.*, 2007). It is this oligosaccharide head group which gives gangliosides their variability (Figure 1.5) and which acts as a target for anti-ganglioside antibodies.

The widely accepted, abbreviated, ganglioside nomenclature and classification was first proposed by Svennerholm, based on the migration pattern of the different subtypes on TLC. The initial capital letter (M, D, T, Q) refers to the number of sialic acid molecules present (1, 2, 3, 4). The number gives the oligosaccharide chain length (1=4, 2=3, 3=2, 4=1). The final lowercase letter (a,

b, c) denotes the different isometric arrangements of sialic acid possible.

(IUPAC-IUB Commission on Biochemical Nomenclature, 1978)

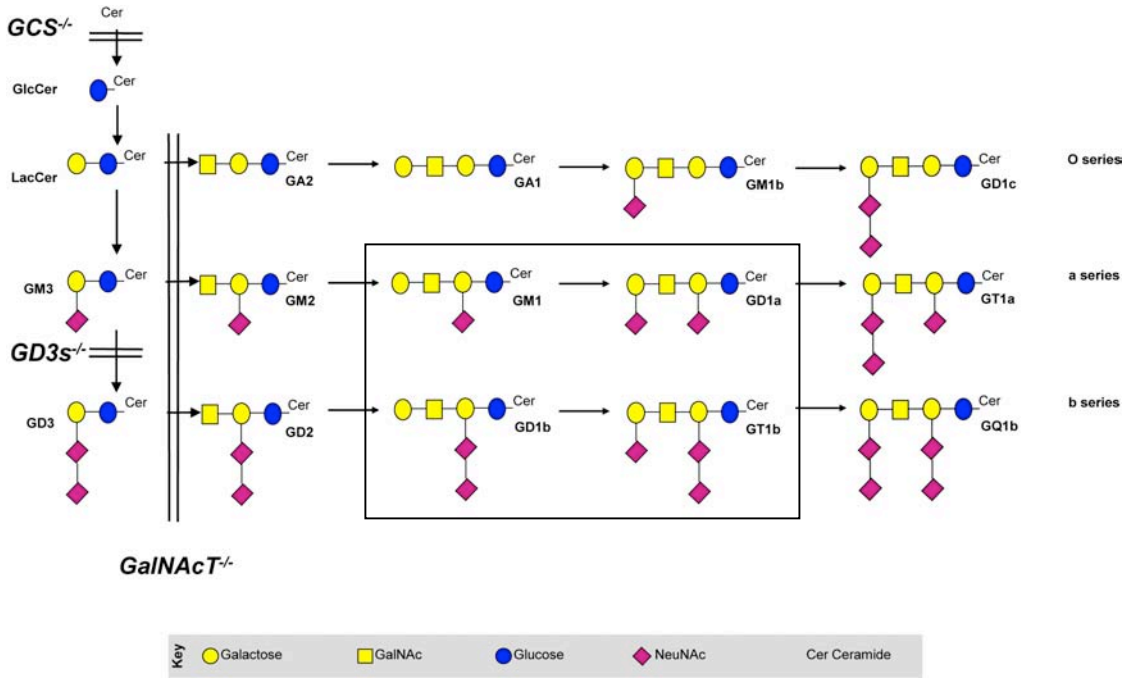

Figure 1.5 - The biosynthetic pathway and structure of gangliosides

The gangliosides are synthesised by sequential addition of monosaccharide groups and sialic acid onto the ceramide tail, producing a large variety of different headgroups, as shown. The first step is the addition of glucose, which occurs in the endoplasmic reticulum and is driven by glucosylcermaide synthase (GCS). N-acetylgalactosaminyl-transferase knockout (GalNAcT-/-) mice lack the GalNAc-transferase (GM2 synthase) enzyme, and hence do not express and are intolerant of all gangliosides right of the double vertical line. GD3-/- mice lack the GD3 synthase enzyme, and do not express b-series gangliosides (those below the double horizontal line in the above diagram). Both of these mutants have previously been used by the Willison group to generate anti-ganglioside monoclonal antibodies. The box encloses those gangliosides most enriched in the nervous system.

In keeping with the suggestion that prior infection and molecular mimicry is a key pathogenic event in GBS, a number of micro-organisms, including *C.jejuni*, have been shown to express ganglioside-like epitopes on their cell surface (Aspinall *et al.*, 1994). In addition, extracts of this lipopolysaccharide (LPS) have been shown to induce anti-ganglioside antibody production in immunisation studies (Goodyear *et al.*, 1999). Evidence supporting the concept that the immune response directed against bacterial oligosaccharides can cross react with neural self antigens is strongest for the axonal variants of GBS associated

with *Campylobacter jejuni* infection. Contemporary studies have led some to brand this disease induction pathway a 'true case of molecular mimicry' (Yuki, 2007b). By knocking out the *waaF* gene from *C.jejuni*, resulting in the production of truncated cell surface lipo-oligosaccharide (LOS), Perera et al demonstrated that these ganglioside mimicking molecules, and not other cell surface components (such as capsular polysaccharide or flagella), are required for the production of anti-ganglioside antibodies in the mouse (Perera *et al.*, 2007).

Furthermore, analysis of LOS from strains isolated from GBS patients using a combination of mass spectrometry and genetic analysis showed that the majority bear ganglioside mimics (Godschalk *et al.*, 2007a). However, 6/26 did not; whether this indicates that other mechanisms are involved, that antibodies directed against non-sialylated oligosaccharides (such as asialo-GM1) may sometimes cross react with their sialylated homologues, or merely that there was co-infection with two strains or a subsequent mutation in the bacterial genes governing LOS synthesis, remains to be seen.

Strong evidence exists to demonstrate that variability in the activity of the *C.jejuni* sialyltransferase enzyme cstII directs development of the particular neuropathy subtype. CstII with α2,3- activity alone results in LOS with GM1 and GD1a like mimics, inducing the acute motor axonal neuropathy (AMAN) variant of GBS, whereas bifunctional α2,3- and α2,8- cstII activity generates disialosyl mimics and leads to Miller Fisher syndrome (MFS) (Figure 1.6) (Koga & Yuki, 2007;Yuki, 2007a;Yuki & Kuwabara, 2007). Similarly, analysis of a strain of *Haemophilus influenza* from a patient with MFS revealed an homologous bifunctional sialyltransferase (Lic3B) producing a disialosyl group linked to the

terminal galactose of the LOS (Houliston *et al.*, 2007a). One mechanism by which cross reactivity can occur between gangliosides which share such groups, such as bacterial GD1c and host GQ1b, GT1a and/or GD3, has been demonstrated by epitope mapping using saturation transfer difference NMR spectroscopy (Houliston *et al.*, 2007b). For one monoclonal antibody (mAb), only a tightly confined area on the terminal sialic acid, common to all the above molecules, was required for binding.

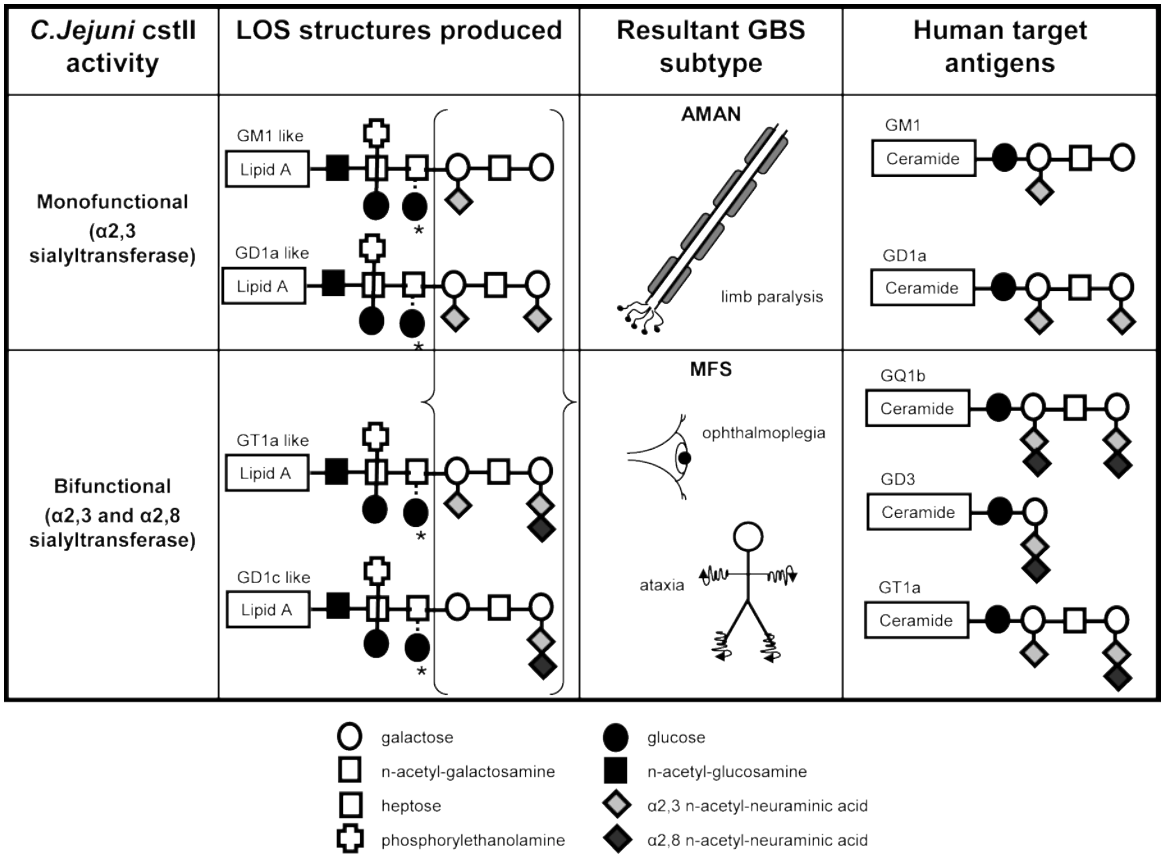

Figure 1.6 - *Campylobacter jejuni* sialyltransferase activity directs neuropathy subtype

C.jejuni with the cstII allele Thr51 have α2,3 activity alone and produce GM1 and GD1a like LOS, resulting in AMAN via the induction of anti-GM1 and anti-GD1a antibodies. Those possessing the Asn51 allele have bifunctional enzyme activity. GT1a and GD1c LOS with terminal disialosyl groups induce anti-GQ1b, GD3 and GT1a antibodies. (Chen *et al.*, 2009) = ganglioside mimicking structure of LOS. *presence of second glucose on core LOS structure is serotype dependent. (Diagram from Rinaldi and Willison, Anti-ganglioside Antibodies and Neuropathy, Current Opinion in Neurology, 2008)

Despite these observations, the bacterial factors governing whether infection simply results in uncomplicated enteritis or precipitates GBS are largely unknown

(if they indeed exist). Taboada and colleagues analysed 1712 genes in 56 neuropathogenic strains and 56 from cases of uncomplicated enteritis (Taboada *et al.*, 2007). Despite the finding of differing absence rates for 6 genes, 4 involved in LOS biosynthesis and sialylation, the neuropathogenic and enteritis groups were remarkably similar. In a PCR-restriction fragment length polymorphism approach, only one gene was found to be statistically associated with neuropathogenic strains, yet was also present in 39% of enteritis controls (Godschalk *et al.*, 2007b), highlighting the crucial importance of other contributing factors.

1.1.7.2 Host susceptibility factors

As discussed, it can be seen that the genetic diversity of the infective organism does not seem to adequately explain why only a small proportion of infected individuals go on to develop neuropathy (Tam *et al.*, 2007). Likewise, investigation of a number of factors which might explain this response, such as HLA associations, T-cell receptor, CD14 and Toll-like receptor 4 typing, has failed to reveal any consistent pattern (Geleijns *et al.*, 2004;Ma *et al.*, 1998). Particular polymorphisms in CD1 genes have been associated with an increase risk of developing GBS (Caporale *et al.*, 2006). This study revealed that those with the CD1E*01/01 genotype are 2.5 times more likely to develop GBS, whereas those with CD1A*01/02 or CD1E*01/02 genotypes have a reduced risk. This makes some theoretical sense, as these molecules are thought to be involved in glycolipid antigen presentation to T cells, which could then induce a pro-inflammatory response or provide help to auto-reactive, anti-glycolipid B cells. (Caporale *et al.*, 2006;De Libero *et al.*, 2002;Shamshiev *et al.*, 2000). Anti-glycolipid antibody responses were previously felt to be T-cell independent,

however, and no such association has been found for chronic inflammatory demyelinating polyneuropathy (CIDP) or multifocal motor neuropathy (MMN) (De Angelis *et al.*, 2007), suggesting differences in the immune dysregulation distinguish acute versus chronic inflammatory neuropathies. Contrary to this, IgG1 and IgG3 are the predominant subclasses of GM1 and GQ1b antibodies found in MFS and AMAN. These subclasses are capable of complement fixation, and generally felt to be T-cell dependent and to arise following class switching from IgM (Willison & Veitch, 1994;Ogino *et al.*, 1995). Furthermore, it has been shown that only CD1d molecules can bind bacterial LOS, yet CD1d knockout mice produced identical concentrations of each subclass of IgG anti-ganglioside antibody, as compared with their wild-type equivalents, suggesting T cell help is not required in this model (or occurs via another pathway) (Matsumoto *et al.*, 2008). Differing from the initial observation in GBS patients, a follow up study did not find differences in single nucleotide polymorphisms (SNPs) of CD1A and CD1E genes in GBS patients versus controls (Kuijf *et al.*, 2008). The description of MFS and positive anti-GQ1b antibodies in a patient with advanced AIDS further highlights the uncertainty over the relative involvement and interactions of T and B-lymphocytes in the different inflammatory neuropathies, and the exact immunological pathways involved in these diseases have clearly not been fully characterised. (Hiraga *et al.*, 2007)

There is recent case report of severe GBS complicating Charcot-Marie-Tooth disease, and inherited motor and sensory neuropathy with numerous subtypes. In this instance the association was with type 1A (CMT1A) which is caused by a 17p11.2-12 chromosomal duplication, resulting in an overproduction of PMP22 protein, early excess myelin production and subsequent loss of myelinated fibres. The later development of GBS described in the case report suggests that

genes out with the immune system might also modulate the risk of developing inflammatory neuropathy (Munch *et al.*, 2008). This genetic abnormality, along with the MPZ mutation which causes a different subtype of CMT also associated with co-existing inflammatory neuropathy (Ginsberg *et al.*, 2004), affects myelin proteins. It is possible that the resultant deranged myelin production exposes otherwise sequestered antigen, be this protein or glycolipid, to immune surveillance and attack. As yet unrecognised variability in the way in which gangliosides are displayed on the surface of neuronal cells in patients without additional inherited neuropathies may similarly modify the risk of developing inflammatory neuropathy.

Recent immunization experiments with GM1 ganglioside in rats, attempting to model motor axonal neuropathy, failed to produce any clinical disease or pathological nerve injury, despite inducing anti-GM1 IgM antibodies (Ilyas & Chen, 2007). In contrast, similar studies in rabbits did induce axonal GBS (Yuki, 2007a). This might be explained by differences in the fine specificity, titre, class, affinity or pro-inflammatory characteristics of the antibodies, as discussed in the following section. Alternatively, species variability in the potency of local complement inhibitors, involvement of a concurrent process that affects blood nerve barrier permeability, or some other discrepancy in antigen accessibility, could be influential.

1.1.7.3 The pathogenic potential of anti-ganglioside antibodies

In the simplest model of neuronal injury by anti-ganglioside antibodies, antibodies bind to their target antigen, fix complement, and cause cell death via the formation of MAC (membrane attack complex) pores. However, several observations indicate that the pathological process is not so straight forward. In

some cases of AMAN, recovery of neurophysiological abnormalities occurs much more rapidly than could be explained by regenerating nerve fibres (Tamura *et al.*, 2007). Likewise, pathological studies in affected subjects sometimes fail to demonstrate any evidence of nerve fibre degeneration (Buchwald *et al.*, 2007). A recent small case series also showed a similar prompt recovery in patients with acute sensory ataxic neuropathy and anti-GD1b antibodies. Sensory nerve action potentials improved from undetectable to normal within 3 months, having shown initial signs of recovery as early as week one (Notturno *et al.*, 2008).

The Willison group has previously demonstrated that anti-GQ1b antibodies bind to motor nerve terminals in *ex vivo* preparations of mouse hemi-diaphragm, and subsequently activate complement. MAC pore formation leads to unregulated calcium influx, which induces massive acetylcholine release followed by neuromuscular transmission block (Halstead *et al.*, 2004b;Plomp *et al.*, 1999;Roberts *et al.*, 1994). This has been dubbed an α-latrotoxin like effect, in recognition of the similarity of this process to the paralytic pathology induced by the neurotoxin of the black widow spider (genus *Latrodectus*). A recent study of seven patients positive for anti-GQ1b antibody alone (but without limb weakness) found no evidence of endplate transmission block by single fibre electromyography of limb muscles (Kuwabara *et al.*, 2007). This apparent difference might represent species-type or regional differences in the distribution of GQ1b or the effects of its antibody, but clearly it would be most informative to see whether neuromuscular conduction is impaired in muscles primarily affected in MFS.

Returning to the rabbit model of AMAN, Susuki *et al* demonstrated absent F-waves, and lengthening of nodes at the ventral roots with complement

deposition, suggesting a more proximal site of injury (Susuki *et al.*, 2007). A progressive disruption of the nodal architecture was observed, with the clusters of voltage gated sodium channels being dispersed and disruption of cell adhesion molecules critical to the axoglial junction as the inflammatory lesion extended towards the juxtaparanodal region. These early changes demonstrate how nerve function can be impaired without axonal degeneration. They also suggest that multiple sites along the neural axis can be disturbed by anti-ganglioside antibodies (Figure 1.7), echoing the speculation in the seminal 1916 paper (Guillain *et al.*, 1916).

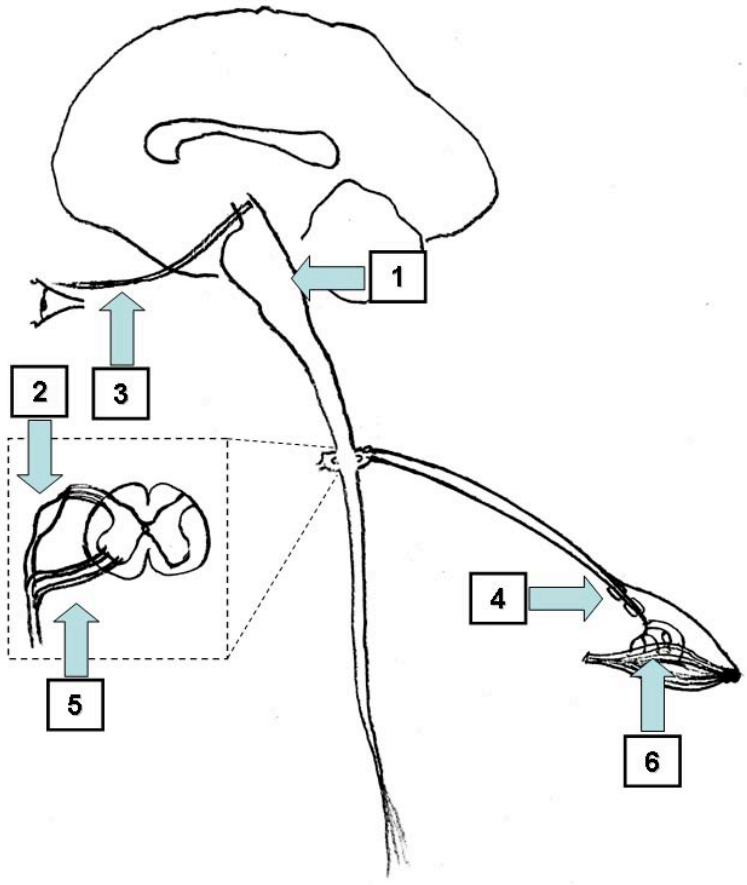

Figure 1.7 - Possible sites of action of anti-ganglioside antibodies

[1] Brainstem. **[2]** Dorsal root ganglion. **[3]** Oculomotor nerve. **[4]** Node of Ranvier. **[5]** Spinal nerve roots. **[6]** Neuromuscular junction.

Recently, other investigators have assessed the effects of different anti-ganglioside antibodies on neuromuscular transmission in the mouse hemi-diaphragm. Anti-GM1 and anti-GD1a antibodies, associated with AMAN, were able to suppress pre-synaptic evoked quantal release in the absence of complement. This was correlated with the ability of the same antibodies to reduce calcium influx in a model of depolarization in neuronal cell cultures (Buchwald *et al.*, 2007). Once again, these observations provide a mechanism by which a functional impairment in nerve activity can occur in the absence of structural damage.

Interestingly, significant variability has been described in the ability of anti-ganglioside antibodies to induce inflammation. In rabbits immunized with GM1 from whom anti-GM1 antibodies were isolated, only the antibodies from subjects who developed paralysis were able to cause leukocyte degranulation and activate complement. This difference was independent of antibody titre, suggesting that this characteristic is essential to induce disease (van Sorge *et al.*, 2007). Conversely, in the rabbit model of GD1b induced sensory ataxic neuropathy, apoptotic neurons were observed in the dorsal root ganglia without any cellular infiltration (Takada *et al.*, 2008).

It seems likely that the severity of injury induced by anti-ganglioside antibodies can vary from reversible functional impairment, through partial axonal injury, to complete axonal transection with subsequent Wallerian degeneration. The degree (and pattern) of damage sustained is presumably reflected in the variability of disease severity and in the tempo of the subsequent recovery. It has also been demonstrated that some anti-ganglioside antibodies can impair axonal regeneration (Lehmann *et al.*, 2007). An anti-GD1a antibody caused

dystrophic nerve sprouting and appearances consistent with stalled growth cones. This effect was not observed in mice lacking longer chain gangliosides, and was at most partially dependent on complement. This suggests direct binding of the antibody to membrane associated gangliosides as the likely mechanism, and suggests one explanation for the poor prognosis associated with anti-GD1a antibodies.

1.1.7.4 Clinical-serological associations

As can be partly inferred from the prior introduction, the spectrum of antibodies associated with GBS has expanded since their initial detection. Furthermore, particular antibodies have been found to map onto specific disease subtypes (Table 1.1).

Disease subtype	Antibodies
AIDP	Unknown
AMSAN	GM1, GM1b, GD1a
AMAN	GM1, GM1b, GD1a, GalNAc-GD1a
Acute sensory neuronopathy	GD1b
Acute pandysautonomia	nAChR (nicotinic acetylcholine receptor)
Regional variants	
MFS	GQ1b, GT1a
Oropharyngeal	GT1a
Overlap	
MFS/GBS overlap	GQ1b, GM1, GM1b, GD1a, GalNAc-GD1a

Table 1.1 - Antibody-disease associations in GBS subtypes
From (Hughes & Cornblath, 2005)

It is in the MFS variant of GBS that the association with anti-ganglioside antibodies holds most strong. Over 90% of patients will have anti-GQ1b antibodies, which are absent from control groups (Yuki *et al.*, 1993;Willison *et al.*, 1993;Chiba *et al.*, 1992). In the axonal subtypes between 30 and 70% of cases are positive for antibodies to a number of different gangliosides. However, the associations are not absolute. In AIDP, the most common subtype of GBS in the Western world, no clear sero-pathological connection exists, although

galactocerebroside, sulphated-glucuronyl-paragloboside, and LM1 are occasionally recognised as antigens (Willison & Yuki, 2002;Hughes & Cornblath, 2005). Considerable effort continues to be focused on identifying other antibody markers directed towards myelin or Schwann cell membrane antigens (Willison & Yuki, 2002;Hughes & Cornblath, 2005). There is an expectation, based on epidemiological and treatment-related data, that such antibodies are present and are likely to be directed towards unknown membrane glycans. Other problems are unresolved: for example, it is not understood why the clinical phenotype associated with anti-GM1 antibodies can be purely motor, when GM1 antigen is also present in sensory nerves; the implication being that GM1 is not always 'visible' to pathogenic autoantibodies. Likewise, although GQ1b is relatively enriched in the nerves affected in MFS, its distribution is much more widespread than might be suspected from the restricted clinical features usually seen (Svennerholm *et al.*, 1994;Chiba *et al.*, 1997).

1.2 Ganglioside complexes

It is in light of these unresolved issues in the pathogenesis of GBS that the description of ganglioside complexes (GSC) and related antibodies proves particularly intriguing. Previously, as discussed, research has focused on assessing purified, single glycosphingolipids as potential antigenic targets. These more recent observations cast doubt on the validity of this as the sole approach.

The concepts that there may be some lateral order to glycolipid distribution in the living membrane, and that carbohydrate-carbohydrate interactions occur, are not new. Originally, however, the fluid mosaic hypothesis proposed that the function of lipids in the membrane was as a relatively inert solvent in which

proteins were randomly distributed and free to move (Singer & Nicolson, 1972). Much evidence now exists to suggest that clusters of cholesterol and glycosphingolipids form, which act as platforms for proteins, and are involved in signal transduction (Simons & Ikonen, 1997). It was hypothesised previously that oligosaccharides from different glycans might form a 'clustered saccharide patch' which could act as a distinct epitope for lectin binding (Varki, 1994).

Furthermore, the chemical structure of GSLs, containing hydroxyl and acetamide groups, allows these molecules to act as both hydrogen bond donors and acceptors, and is postulated as the explanation behind their ability to form clusters (Todeschini & Hakomori, 2008). *Trans* carbohydrate-carbohydrate interactions (i.e. between two neighbouring cells) were initially described over 20 years ago, having been shown to be of critical importance in compaction of the early mouse embryo (Eggens *et al.*, 1989;Fenderson *et al.*, 1984). There is now an increasing realisation that *cis* interactions (i.e. 'side to side' within the same membrane) may also be functionally important, as recently shown for the gangliosides GM2 and GM3 in the anti-metastasis factor CD82 mediated control of cell motility (Todeschini *et al.*, 2008). Furthermore, the ability of anti-ganglioside monoclonal antibodies to bind to their targets has previously been shown to be inhibited by the presence of other ganglioside species. In different melanoma cell lines, anti-GM3 antibodies were only able to bind when GM3 was the sole surface ganglioside. Even in cells expressing 50% GM3, if a longer chain ganglioside, such as GM2, was also present, anti-GM3 binding was abolished (Lloyd *et al.*, 1992).

More recently, interactions between pairs of gangliosides have been shown to be of importance in determining antibody binding in GBS associated sera.

Researchers found that, in a proportion of GBS patients, antibodies exist which bind to pairs of gangliosides, but fail to bind either component ganglioside in isolation. These have been termed anti-ganglioside complex (GSC) antibodies (Kaida *et al.*, 2004;Kaida *et al.*, 2006;Kaida *et al.*, 2007). In the initial study, it was noted that on a crude preparation of bovine brain ganglioside run on a thin layer chromatography plate that one neuropathy serum demonstrated binding just below the level of GD1a ganglioside following immuno-overlay. This appeared to correspond to the overlapping portion between GD1a and GD1b. By additionally running lanes of GD1a, GD1b and both GD1a and GD1b, this speculation was confirmed (Figure 1.8).

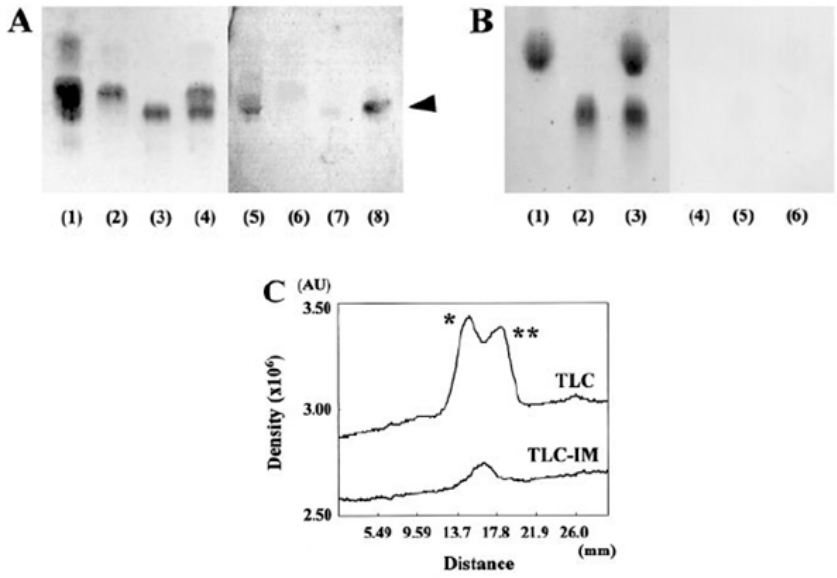

Figure 1.8 - The first TLC demonstration of GSC binding antibodies in GBS

From (Kaida *et al.*, 2004). In (**A**), the left hand panels (1-4) are stained with orcinol to reveal the location of the ganglioside, and the right hand panels (5-8) have been overlain with sera then an IgG secondary antibody. Lane A1 is whole brain ganglioside, A2 GD1a, A3 GD1b, and A4 GD1a and GD1b. As can be seen from the overlay, the antibody only binds when both GD1a and GD1b are present, and then only to the overlapping, incompletely separated portion. Likewise, if the TLC running buffer is changed (**B**), so that the gangliosides are further separated when applied together (lane B3), binding is again abolished (lane B6). (**C**) confirms the impression drawn from (**A**), demonstrating that the band seen on immuno-overlay (TLC-IM, lower line) corresponds to the region between the two peaks of GD1a and GD1b on TLC-orcinol (TLC, upper line)

Subsequent ELISA analysis backed up these observations, whereby binding was only detected in wells coated with a mixture of GD1a and GD1b, and not in wells in which one or other of GD1a or GD1b was coated alone. Using this technique, 8 of 100 consecutive GBS patients were found to have similar antibodies in their sera, albeit with lesser degrees of binding to the individual gangliosides in some cases.

Subsequently, a lager series of 234 GBS patients was analysed looking for reactivity to 1:1 complexes formed by the different combinations of GM1, GD1b, GD1b and GT1b. αGSC antibodies were detected by ELISA in 39 (17%) of these patients by ELISA (Figure 1.9A). The presence of anti-GD1a:GD1b or GD1b:GT1b antibodies was found to be associated with more severe disease and the requirement for mechanical ventilation (Kaida *et al.*, 2007). In 12 patients with MFS, GM1:GQ1b complex antibodies were found in the sera of 5, and GD1a:GQ1b in 2 (Figure 1.9B) (Kaida *et al.*, 2006).

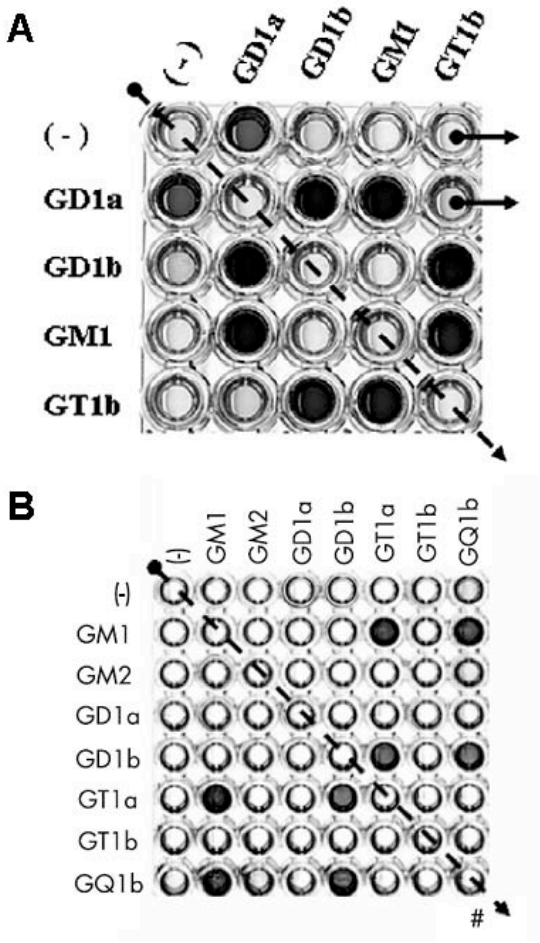

Figure 1.9 - GSC antibodies in GBS and MFS detected by ELISA.

From (Kaida *et al.*, 2007) and (Kaida *et al.*, 2006). (**A**) GBS. (**B**) MFS. In the above examples, single gangliosides are coated in the leftmost column and uppermost row of the plates. The 1:1 complexes are to the right and below, the complex at each location derived by combining the column and row labels. A line of methanol only coated wells runs from top left to bottom right (dotted line) and acts as a negative control. The GBS serum in (**A**) binds to single GD1a, but also to complexes of GT1b:GD1b and GT1b:GM1, yet not GD1a:GT1b. The MFS serum (**B**) does not bind any gangliosides in isolation, yet there is a strong signal with GM1:GT1a, GM1:GQ1b, GD1b:GT1a and GD1b:GQ1b.

These findings have implications for all aspects of the pathogenic process in GBS, and potentially for the wider field of membrane glycobiology and cell signalling. Existing studies of GSC antibodies come from Japan, where axonal forms of GBS are more common. It is intriguing to speculate that the presumed elusive antibody specificity in AIDP, the predominant GBS subtype in the Western world, will be directed against a complex. This would potentially have major diagnostic as well as pathologic importance.

While such conjecture is exciting, this is blunted somewhat by realisation that the level of complexity of any investigation is dramatically increased by these combinatorial possibilities. From 20 individual glycosphingolipids, 190 distinct pairs can be formed. Furthermore, significant technical concerns are raised, and it is unclear how GSL interactions in the artificial systems of enzyme linked immunosorbent assay (ELISA) and thin layer chromatography (TLC) relate to their behaviour in the dynamic membrane environment.

The relationship between the presence of anti-GSC antibodies and clinical features suggests a pathological potential for these antibodies, but this has yet to be demonstrated experimentally. It remains possible that anti-ganglioside and anti-GSC antibodies are merely epiphenomena and not key players in the pathological process. Similarly, it is at present uncertain whether gangliosides form complexes in the living membrane, and if so whether these are transient or more longer lasting structures. It has been suggested that micro-organisms such as *C.jejuni* might also display complexes of gangliosides on their cell surface, which would then induce anti-GSC antibody production in the host. There are, however, two other possibilities. It could equally be argued that bacterial cell surfaces coated with complexes might more effectively evade immune detection by more exactly mimicking self. Conversely, given the difference in size between the lipid a tail of *C.jejuni* LPS and the ceramide tail of gangliosides, if complexes are formed in the bacterial membrane they may be dissimilar to those of the infected host – the ability to distinguish between self and non-self complexes could thus be viewed as an advantage in the host/pathogen ‘arms race’.

The only existing study into the origin of anti-GSC antibodies could be potentially interpreted to support any of these views. Only a small proportion of those infected with *Campylobacter jejuni* bearing multiple gangliosides developed anti-complex antibodies, and in two cases such antibodies were detected in subjects who had been infected by a *C.jejuni* strain expressing only a single ganglioside species (Kuijf *et al.*, 2007).

The existence of ganglioside complexes might also be evoked in an attempt to explain the apparent nerve type specificity of certain anti-ganglioside antibodies, despite the presence of significant proportions of target antigen in unaffected nerves. It may be that a particular interaction with neighbouring GSLs is required for the target ganglioside to become accessible to antibody. As such, the relative amounts of membrane bound molecules, together with the way these interact, may be more important than the crude percentage composition in determining antigenicity.

A conceptually similar observation was also recently made by the Willison group. Two anti-GM1 antibodies (designated DG1 and DG2) with essentially identical binding to isolated GM1 on ELISA showed entirely different patterns of reactivity in the living membrane. In these *ex vivo* studies, DG2 bound and caused compliment activation, whereas DG1 did not. This difference was abolished by pre-treatment with neuraminidase, which strips sialic acid groups from more complex gangliosides and converts them to GM1. The conclusion was that another ganglioside, felt to be GD1a, was normally in complex with GM1. In this situation, DG1 was unable to bind. This may help to explain why not all anti-GM1 antibodies appear to be neuropathogenic. (This observation was further

expanded by a portion of the following work, and has since been published) (Greenshields *et al.*, 2009).

A greater understanding of anti-GSC antibodies might also impact on current attempts to develop novel therapeutic techniques. Glycan conjugated Sepharose columns have been developed in an attempt to specifically immuno-adsorb pathogenic anti-ganglioside antibodies (Townson *et al.*, 2007). These contain highly pure, synthetic ganglioside-GM1, and bind monospecific, monoclonal antibodies strongly. However, anti-GM1 antibodies from human serum are not as effectively captured (Townson, personal communication). This raises the possibility that the antibodies in human sera bind poorly because no complexes are formed by the synthetic ganglioside in the column. In contrast, the impurities found in extracted preparations used for ELISA may enhance binding, perhaps via the formation of ganglioside-ganglioside complexes. Alternatively, as previously discussed, it may be that the orientation or accessibility of the target antigen in such solid phase detection systems is not consistent with, and not representative of, the situation *in vivo*.

1.3 Aims

The aim of this thesis is therefore to further investigate glycolipid complexes, building on the work already described, and focusing on anti-complex antibodies in inflammatory neuropathies typified by Guillain-Barré syndrome. This overarching aim can be expanded into five sub-aims, as listed;

1. To develop a robust system for assessing anti-GSC binding.

2. To use this system to investigate the potential importance of GSCs on the binding of other lectins including anti-ganglioside monoclonal antibodies.

3. To investigate the sera from Western European case series of GBS, predominantly comprising the AIDP variant, for anti-GSC antibodies.

4. To assess the immune response to GSCs.

5. To establish the pathogenic potential of anti-GSC antibodies in *ex vivo* and *in vivo* systems.

2 Methods

2.1 Materials and solutions

2.1.1 Gangliosides and other lipids

GM1, asialo-GM1, GM2, GM3, GD1a, GD1b, GD2, GD3, and GT1b gangliosides were bovine brain derived products obtained from Sigma, Poole, UK. GT1a and GQ1b bovine brain derived gangliosides were obtained from Accurate Chemical & Scientific, Westbury, USA. Sulfatides, sphingomyelin, cholesterol, dicetylphosphate, phosphatidylserine, and dimyristoylphosphatidylcholine (DMPC) were also obtained from Sigma. Glactocerebroside (galactosylceramide), globoside (Gb_4; globotetrahexosylceramide), and trihexosylceramide (CTH, ceramide trihexosides, Gb_3, globotriaosylceramide) were obtained from Matreya, Pleasant Gap, USA. GalNAc-GD1a was prepared and analysed by Professor Sandro Sonnino, University of Milan, Italy. LM1 (sialosyl-neolactotetraosylceramide) and SGPG (sulfated glucuronyl paragloboside) were gifts from Dr. Robert K. Yu (Institute of Molecular Medicine and Genetics, Medical College of Georgia, Augusta, USA).

2.1.2 Secondary antibodies

2.1.2.1 Peroxidase conjugated

Anti-mouse IgM (μ chain specific), anti-mouse IgG (heavy and light chain), and anti-human IgG (F_c specific), horse radish peroxidase conjugated secondary antibodies, all raised in goats, were obtained from Sigma. Rabbit anti-human IgG and IgM were obtained from Dako, Glostrup, Denmark.

2.1.2.2 Fluorescent labelled antibodies and markers

Alpha-Bungarotoxin conjugated to Tetramethyl Rhodamine Iso-Thiocyanate fluorophore (αBTx-TRITC) was obtained from Molecular Probes, Oregon. Fluorescein isothiocyanate (FITC) conjugated anti-mouse IgG (total), and anti-mouse IgM subclass specific (1, 2b and 3), as well as anti-human IgG(total) secondary antibodies were all obtained from Southern Biotech, Alabama, USA. FITC–goat anti-rabbit IgG came from the same supplier. FITC–goat anti–human C3 came from Dako, Glostrup, Denmark. The neurofilament 1211 antibody was purchased from Affinity BioReagents, Colorado, USA.

2.2 Methods

2.2.1 Combinatorial PVDF glycoarray

Single gangliosides and lipids were purchased or obtained as detailed above. Stock solutions of each of were prepared in a 50:50 (v/v) chloroform:methanol mixture, at 1 to 10mg/ml. Working solutions were made by further dilution in methanol to 0.1mg/ml. For single samples, 200µl of the working solution was added to a 300µl capacity micro-sampling vial (Chromacol, UK). To create complexes, 100µl of each constituent glycosphingolipid (GSL), glycolipid or phospholipid was added to a vial. For the larger 28 by 10 grid used to screen the Dutch Guillain-Barré syndrome (GBS) sera, the final volume of each sample was reduced to 80µl. A test print run using methylene blue demonstrated that the needle of the thin layer chromatography (TLC) autosampler was able to reach down below 20µl, giving 60µl effective volume (sufficient for up to 300 slides) for use in subsequent print runs. Vials were sealed using caps with a rubber

insert (Chromacol, UK), allowing puncture by the autosampler needle. All samples were then sonicated for 3 minutes prior to use.

Sheets of polyvinylidene difluoride (PVDF) membrane (Sigma, UK) were cut into 20x25mm (65x25mm for the larger array) squares using a scalpel. These were then affixed 12mm from the left hand edge of a plain glass slide (VWR International, UK) using UHU glue (UHU GmbH, Germany), and allowed to air dry for 10 minutes. A metal grid was used to hold 12 slides in predefined and consistent positions on the application plate of a Camag Automatic TLC Sampler 4 (Figure 2.1, ATS4, Camag, Switzerland). The winCATS planer chromatography management software (Camag, Switzerland) was used to write programmes which result in the application of duplicate spots of 0.1µl of 100µg/ml glycolipid or glycolipid complex over a predefined 0.4µm^2 area. The programmes used and the arrays they produced are shown in appendix. Printed membranes were outlined with an hydrophobic barrier pen (Vector Laboratories, UK) and allowed to air dry for 20 minutes. They were then stored overnight at 4ºC before use.

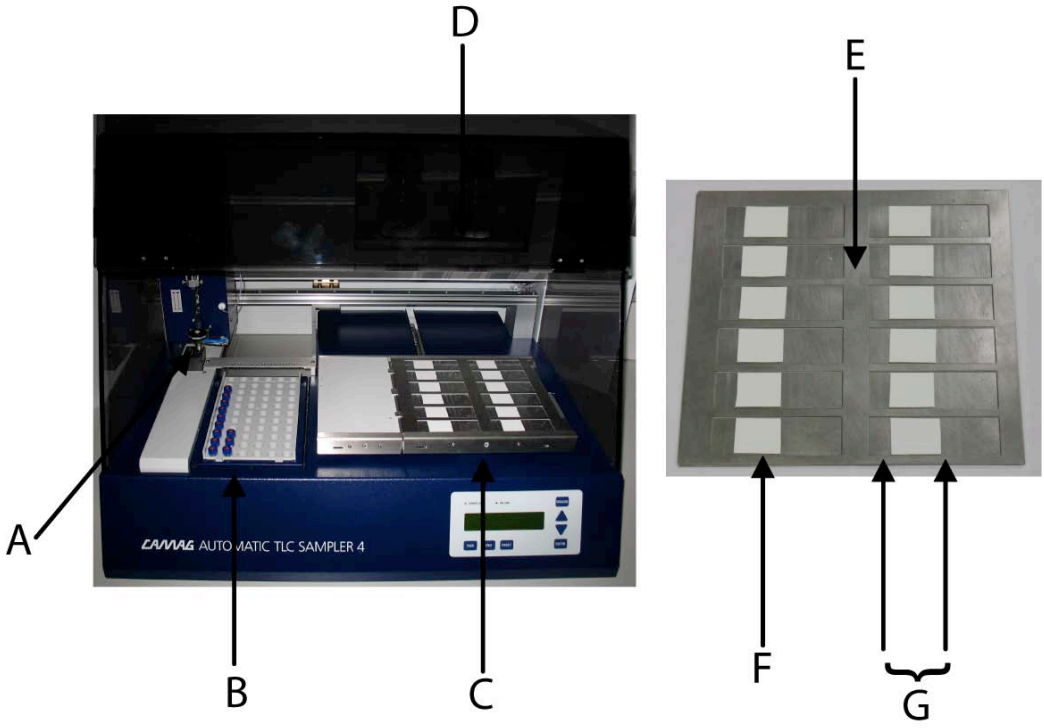

Figure 2.1 - The ATS4 autosampler and slide guide

(**A**) Dosing syringe and application needle. (**B**) Sample rack and microvials. (**C**) Application platform with bespoke slide guide loaded with 12 slides. (**D**) Wash and rinse bottles. (**E**) Close up of slide guide and slides. (**F**) PVDF membrane affixed to glass slide. (**G**) Membrane outlined with hydrophobic pen.

Membranes were blocked by immersion in 20-60ml/cm^2 of 2% bovine serum albumin/phosphate buffered saline (BSA/PBS) for 1h at 4ºC. Serum samples, cerebrospinal fluid (CSF), monoclonal antibodies (mAbs), siglec-Fc fusion proteins (preconjugated to horse radish peroxidase (HRP) linked anti-Fc antibody), or HRP-bacterial toxin conjugates were diluted in 1% BSA/PBS. 250µl / 500µl / 1ml (depending on membrane size) of this diluted sample was then applied to a pre-printed membrane and incubated at 4ºC. After 2h, the sample was tipped form the membrane and the slides were briefly placed back in the 2% BSA/PBS blocking solution. Probes requiring a secondary antibody underwent a primary wash phase. These membranes were transferred to 20-60ml/cm^2 of 1% BSA/PBS for 15 minutes of washing on a shaker set at 100rpm. This process was repeated once. These membranes were tapped dry, 250µl / 500µl / 1ml of the

appropriate HRP linked secondary antibody was applied (diluted in 1% BSA/PBS, typically to 1 in 30k), and incubated for 30min at 4ºC. All membranes then entered a wash phase. For probes not requiring a secondary antibody (siglecs and HRP-conjugated bacterial toxins) this immediately followed the primary incubation.

This wash phase consisted of two changes of 1% BSA and three changes of PBS, again each of at least 20-60ml/ cm^2. BSA washes were of 30min duration, PBS for 5min, both on a shaker set at 100rpm. Slides were then briefly dipped in two changes of distilled water (20-60ml/cm^2). A chemiluminescent detection reaction was then performed using ECL plus (Enhanced chemiluminescence, Amersham/GE Healthcare, UK), made up according to manufacturer's instructions. 450µl / 1ml of this detection solution was then applied to the membranes and left for 3 minutes at room temperature. The solution was tipped from the membranes and signal was detected on radiographic film. Exposure time was 15s for siglecs, mAbs, and bacterial toxins. For sera, a range of different exposure times were used, typically 5s, 15s, 1min, 5min and 10min. Films were digitised by flatbed scanning and the images analysed and quantified by the array analysis component of ImageQuant TL software (Amersham Biosciences, UK). Raw intensity readings were corrected for background in a two step process. Firstly, the spot edge average function of the software was used to correct for the local background level around the edges of the defined spot. Secondly, the average value for the negative control spots (methanol only) was subtracted from all other spots. When comparing the relative binding of one lectin to gangliosides and GSCs, a relative intensity reading created by normalising all other spots to the value of the most intense (set as 100), was

used in subsequent analysis. When comparing between different lectins, the non normalised corrected arbitrary intensity value was used.

2.2.2 Ganglioside and glycolipid complex ELISA

Working solutions for ELISA (enzyme linked immunosorbent assay) were made by further dilution of stock gangliosides and glycolipids in methanol to 2µg/ml. For complexes, equal volumes of the two component gangliosides were combined in a glass vial and sonicated for 3 minutes prior to use. As a negative control, 100µl of methanol only was added to a number of wells per ELISA plate. Immunolon 2HB plates were used for all ELISA assays. Subsequently, 100µl of the single or complex ganglioside solution was added per well, and allowed to air dry for 40 hours (h) in the fume hood. Although the plates were visibly dry at 16h or less, the longer drying time seemed to improve the consistency of the assay. Typically, single gangliosides and complexes were applied in a grid like pattern, with a line of methanol only coated wells running from top left to bottom right, and acting as a line of symmetry for duplicate spots within the same plate. Plates were kept at 4ºC for at least 1h prior to further use.

Plates were blocked with 200µl/well of 2% BSA/PBS for 1h at 4ºC. Primary samples were diluted as for PVDF glycoarray. 100µl of the diluted solution was then applied to each coated well of the ELISA plate. Incubation was for 2h (mAbs, siglecs, sera) or 2 minutes (cholera toxin B-subunit) at 4ºC.

The primary solution was tipped and shaken off, and the plates plunged into cold PBS then emptied five times. For bacterial toxins and siglecs, the next step was to apply detection buffer. For mAbs and sera, 100µl of the appropriate secondary antibody, diluted 1:3000 in 1% BSA, was applied to the wells and

incubated for 1h at 4ºC. The plates then underwent the same wash protocol as for the primary. Detection was performed with 50µl/well of an *o*-Phenylenediamine dihydrochloride solution (see appendix). The reaction was terminated with 25µl of 4M H_2SO_4. Optical density at 492nm was detected by an automated plate reader (Ascent Multiscan, Labsystems, GMI, USA).

2.2.3 Ganglioside liposome ELISA

Dimyristoylphosphatidylcholine (DMPC, 200µl of a 5mg/ml solution) and 10µl of ganglioside from 1mg/ml stock in 1:1 (v:v) chloroform:methanol solvent were mixed in a 15ml tube. To make ganglioside complex liposomes for ELISA, 10µg of each constituent ganglioside was added. Blank liposomes containing no ganglioside were also produced. The mixture was then briefly vortexed and sonicated for 3 minutes. This solution was dried under a steady stream of N_2 in the fume hood to leave a thin film on the inside of the tube. Subsequently, 1ml of PBS was added and the tube alternately vortexed and sonicated for 15 minutes, until all of the dried lipid was removed from the walls of the tube and the solution had turned a uniformly milky colour. This mixture was then freeze-thawed 5 times by immersion in liquid N_2 followed by thawing in a water bath set to 37ºC. Unilamellar liposomes were then created by repeated extrusion (11 times) through a 0.4µm-pore size membrane using a hand driven extruder. This was followed by 1h of ultra-centrifugation using a Ti70 rotor (Beckman Coulter, Brea, California, USA) at 38500rpm and 22ºC. The resulting pellet was resuspended in 5ml of PBS to give a final ganglioside concentration of 2µg/ml. These liposomes were added at 100µl/well to an Immunolon 2HB ELISA plate and incubated overnight at 4ºC. The liposome solution was then discarded and the plate patted dry.

From this point, blocking, primary and secondary incubation, washes, and the detection reaction were performed as for Ganglioside and Glycolipid Complex ELISA above (2.2.2).

2.2.4 TLC immuno-overlay

Thin layer chromatography (TLC) with immuno-overlay was used to assess the binding of antibodies to the overlapping and non-overlapping portions of different gangliosides migrated by organic solvents. Silica backed TLC plates, previously dried by gentle heating on a hot plate to 100ºC, were first cut in half, before 3 to 5µl of 1mg/ml ganglioside solution was applied in 0.5cm wide bands 1cm apart using the ATS4 autosampler. In lanes where two different gangliosides were applied, their starting positions were adjusted empirically to alter the degree of overlap produced when the plate was run. The pattern of ganglioside application was repeated at least once across each plate. This allows the migration of glycolipids on one half to be assessed using an orcinol solution, which can then be compared with the pattern of immuno-staining seen on the other. While the plate was allowed to dry, a running solution of chloroform:methanol:0.2% $CaCl_2$ was prepared. For standard development, a 50:45:10 (v/v/v) mixture of the above was made. To achieve greater separation of the individual glycolipids, the ratio was altered to 30:65:10, the greater excess of methanol over chloroform producing a more polar solvent.

One half length and one full length strip of blotting paper were then placed reclining against opposite inside walls of a glass TLC tank. The running solution was poured down either wall of tank, soaking the blotting paper. The lid was

replaced, sealed with petroleum jelly, and weighted down. The tank was then left overnight to allow the internal atmosphere to become saturated.

The following day, the prepared TLC plate was quickly placed inside the tank, leaning against the wall above the half height blotting paper. The lid was replaced and resealed, and the solvent allowed to migrate along the silica coated face of the plate until it was around 1cm from the topmost edge. This typically took around 25 to 30 minutes. At this point, the plate was removed from the tank and allowed to dry in the hood for 1h.

The plate was then divided further into strips containing identical patterns of applied ganglioside. One half was sprayed with orcinol or resorcinol solution (see appendix), before being heated to 150ºC for 5 minutes on a hot plate, to allow visualisation of the ganglioside migration pattern. The other half was then used for the immuno-overlay.

The half plate to be used for immuno-overlay was first coated with 0.4% polyisobutlymethacrylate (PIBM). This was made up by first dissolving PIBM granules in chloroform to 2.5%, before further dilution to 0.4% in n-hexane (see appendix). The plate was then dipped into the 0.4% solution for 1 minute, and allowed to subsequently air dry for a further 30 minutes in the fume hood. Immuno-overlay using TLC plates then followed similar steps to those used in the ganglioside ELISA. To compensate for the increased background staining seen using this technique, however, blocking with 2% BSA/PBS was performed for at least 16h overnight at 4ºC. Following this, 3ml of appropriately diluted mAb or serum was applied for 2 h, also at 4ºC. To keep the reagent on the plate, the plate was placed face up on a surface covered with a hydrophobic film (Parafilm, Alcan Packaging, USA). The diluted primary antibody solution was

then tipped from the plate, and a wash cycle performed. This consisted of 3 changes of 1% BSA/PBS, followed by 3 changes of PBS, with gentle agitation on a slow shaker for 5 minutes between each change. The appropriate secondary antibody, diluted as per the ELISA to 1:3000 in 1% BSA/PBS, was then applied for 1h at 4ºC before the wash cycle was repeated. Detection was performed by using the ECL+ system, as for the PVDF glycoarray, with the ECL solution applied for 3 minutes before 15s to 1 minute exposure on x-ray film.

2.2.5 Monoclonal antibody production and purification from existing cell lines

All cell culture procedures were carried out in sterile conditions, as maintained by a Class II hood, using standard sterile practice. All incubations were performed in a Class II incubator, set to 37ºc and 5% CO_2. Media for culture were prepared several days in advance, with a 10ml aliquot being retained and incubated separately to confirm sterility. Culture media were warmed to 37ºC in a water bath prior to use.

Frozen aliquots from previously generated hybridoma cell lines were retrieved from liquid nitrogen storage and quickly thawed at room temperature. The cells were then suspended in 50ml of RPMI and spun down for 5 minutes at 200g (1000rpm) in a Centaur 2 bench-top centrifuge (MSE, London, UK). The supernatant was discarded and cells resuspended in 14ml of 20% complete medium (see appendix) in a T25 (25cm^2 surface area) tissue culture flask (Corning, Amsterdam, The Netherlands).

The cells were incubated at 37ºC and their growth assessed regularly. Initially the cell lines were expanded into progressively larger flasks, having been spun

down and resuspended in a volume of 10% complete medium suitable for the particular flask used. Cells were then split between several different T175 flasks as appropriate. The supernatant was collected at regular intervals and replaced with fresh 10% complete medium. The supernatant was periodically checked in a standard ganglioside ELISA, as above, to ensure continued antibody production. Aliquots of supernatant were stored at 4ºC prior to purification.

When the required volume of supernatant had been collected, the monoclonal antibodies were purified by passage over a HiTrap Protein A affinity column (for IgG3 subclass antibodies) or a HiTrap Protein G column (for IgG1 and Ig2b). Initially, the supernatants were defrosted, centrifuged for 30mins at 10000rpm, and filtered through the 0.22µm membrane of a bottle top filter under vacuum. The supernatants were then dialysed overnight against 1:10 (v/v) binding buffer (see appendix) using size 2 (14.3mm), 12-14000 Dalton molecular weight cut-off dialysis tubing (Medicell International, London, UK).

The following day, peristaltic pump tubing was filled with binding buffer (maintained on ice), and then the tubing attached to the affinity column. Ten column volumes of binding buffer were then applied to the column at a rate of 1 column volume per minute, using the peristaltic pump. A fraction of binding buffer was retained to act as a blank for subsequent spectrophotometry using a Biophotometer (Eppendorf, Hamburg, Germany). Filtered supernatant (again maintained on ice) was then passed over the column at the same rate, followed by binding buffer, until the optical density of the flow through at 280nm returned to within 0.05 units of the binding buffer blank. The entire volume of flow through was retained and stored at 4ºC for subsequent testing by ELISA.

Next, 10 1.5ml collection tubes were prepared with between 200 and 450µl of 1M Tris-HCl, pH 9. The exact volume used per tube was determined by adding gradually an increasing amount of Tris-HCl to 1ml of the appropriate elution buffer, until the solution was neutralised (pH 7), as checked with pH strips. The peristaltic tubing was then emptied of binding buffer and filled with elution buffer. For protein A columns this was 0.1M citric acid, pH 3. For protein G, 0.1M glycine, pH 2.7, was used. The elution buffer was then applied to the column at 1 column volume per minute, and 1ml fractions collected in the pre-prepared tubes. Again an aliquot of elution buffer was preserved to act as a blank for spectrophotometric analysis. Fractions were collected until 3 consecutive samples returned optical densities (ODs) within 0.05 of the blank. The column was then washed with 10 column volumes of binding buffer, collected as the wash fraction, followed by 10 column volumes of 20% ethanol. The tubing was washed with 0.5mM NaOCl in 0.5M NaOH and rinsed with distilled water before use with another antibody. Each affinity column was retained for use only with a specific monoclonal antibody to prevent cross contamination.

The starting material (supernatant), flow through, elution fractions and washes were all tested on ganglioside ELISA (as above, 2.2.2) against the single ganglioside previously identified as being the major target of the monoclonal antibody in question. Elution fractions showing binding, defined as a corrected OD of >0.1, were pooled, desalted using a Sephadex PD-10 column (Amersham Biosciences, Uppsala, Sweden), and returned to PBS. Concentration was calculated from OD at 280nm (A_{280}) using the formula;

$$\text{antibody concentration (mg/ml)} = A_{280} / 1.43$$

If required, the final concentration of the antibody was adjusted by centrifugal filtration using an Amicon Ultra tube filter device (Millipore Corporation, Bedford, USA). Antibodies were aliquoted and stored at -80ºC prior to use.

2.2.6 Liposome production for immunisation

Liposomes for immunisation were manufactured using a sequential sonication, freeze-thaw, extrusion method, similar to that used for liposomes produced for ELISA. Cholesterol, sphingomyelin, dicetylphosphate and gangliosides were dissolved in a 1:1 mixture of chloroform:methanol to 10µg/ml. These lipids were mixed in a 5:4:1:1 molar ratio respectively, or 5:4:1:1:1 where a second ganglioside was included. The lipid mixture was dried down under a steady stream of nitrogen to form a film on the wall of a 15ml tube. The lipids were then resuspended in 1ml of PBS (containing ova at 5mg/ml) by vortexing and sonication alternately for at least 15 minutes. The mixture was subjected to a freeze thaw cycle by plunging into liquid nitrogen then thawing in a water bath at 37ºC. This process was repeated 5 times. The resulting suspension of multi-lamellar liposomes was clarified by centrifugation at 600g (1800rpm in a B4 centrifuge, Jouan, Saint-Herblain, France). Unilamellar liposomes were then created by repeated extrusion (11 times) through a 0.4µm-pore size membrane using a hand driven extruder. This was again followed by 1h of ultra-centrifugation using a Ti70 rotor (Beckman Coulter, Brea, California, USA) at 38500rpm and 22ºC. The resultant pellet was resuspended in sterile Dulbecco's phosphate buffered saline (Invitrogen, Paisley, UK) to give a final ganglioside concentration of 1mg/ml for ip injections.

2.2.7 Immunisation protocol

The immunisation protocol used was based on that previously employed in the Willison laboratory (Bowes *et al.*, 2002). N-acetylgalactosaminyl-transferase knockout (GalNAcT$^{-/-}$), neurofilament light-GalNAcT GalNAcT $^{-/-}$ transgenic (Tg(Nfl-GalNAcT)GalNAcT$^{-/-}$, subsequently abbreviated to NFL-Tg), GD3 synthase knockout (GD3s$^{-/-}$) and wild type (WT) mice were housed under standard conditions with food and water provided *ad libitum*. Mice aged 6 to 10 weeks were used in immunisation experiments.

On day 0, mice were injected intraperitoneally (ip) with 100µl of ova-alum (6mg/ml, 60mg of ova in 100ml of 2% aluminium hydroxide gel, Sigma, UK). This was to prime them to react against the ova-ganglioside containing liposomes. On days 7, 14 and 21 mice were injected ip with 100µl of 1mg/ml ganglioside containing liposomes prepared as above. On days 25, 26 and 27 mice were injected intravenously (iv) via the tail vein with 50µl of the same liposomes diluted to 200µg/ml (i.e. to give 10µg ganglioside per injection). Blood samples were taken from superficial tail veins on days 0, 14, 21 and 28 initially. When preliminary experiments revealed that anti-ganglioside antibodies were only being detected at day 21 and beyond, the blood sampling point at day 14 was omitted.

2.2.8 Monoclonal antibody generation from immunised animals

The blood sampled at day 28 from immunised animals was used to confirm a serum response to the immunogen and to select animals from which to create monoclonal antibody secreting hybridomas. In view of problems obtaining a stable clone using traditional fusion, expansion and selection in liquid based

media, an alternative technique whereby hybridomas were cloned immediately after fusion using a selective semi-solid medium (Stemcell Technologies, Vancouver, Canada) was subsequently employed. The traditional method is described first, before variations to the method as a result of using a semi-solid selection media are detailed.

2.2.8.1 Using liquid based media

Mouse myeloma cells (P3X63Ag8.653, subsequently referred to as '653s') were defrosted and maintained as for the existing monoclonal cell lines above. The day before the planned fusion, the 653s were spun down, counted, and resuspended at a density of between 2 and 10 x 10^5 cells/ml. For each spleen to be fused, 4 T175 flasks each containing 40ml of 653 cells were prepared.

On the day of the fusion (day 0), the 653s were spun down twice at 300g (1200rpm), pooled, and resuspended in a final 10ml volume of RPMI-1640 cell culture medium without additional supplements (0% RPMI, Sigma). This, and all other media unless otherwise stated, was prewarmed to 37ºC in a water bath. While the 653s were being prepared, the animal selected for use in the fusion was killed with a rising concentration of CO_2, as per Home Office guidelines. The spleen was removed from the alcohol soaked mouse under aseptic conditions, and blood simultaneously collected for testing later. The spleen was then transferred into 5-10ml of 20% RPMI-complete medium (see appendix) and homogenised using a 2 part glass homogeniser. The liberated splenocytes were then passed through a Falcon 70µm cell strainer (BD Biosciences, Mississauga, Ontario, Canada). The homogeniser was then rinsed with a further 20ml of 0% RPMI which was then also passed through the strainer. Like the 653s, the splenocytes were spun down twice at 300g (1200rpm), pooled, and resuspended

in a final 10ml volume of 0% RPMI. Both the 653s and splenocytes were counted using a haemocytometer and a light microscope set at 10x magnification. The volumes of resuspended cells which would yield $1x10^8$ splenocytes and $1x10^7$ 653s (i.e. a ratio of 10 spleen :1 myeloma) were calculated and these volumes were mixed together in a single 50ml vial. The mixed cells were then spun down as before and every last drop of media removed.

A water bath filled with sterile distilled water was placed in the tissue culture hood and used to maintain the cells and media at 37ºC during the fusion. 1ml of polyethylene glycol solution (PEG, 50% w/v, Sigma) was then added carefully over 1 minute using a 1ml pipette, which was also used to gently stir the cells during this process. Stirring was continued for a further 90s after all of the PEG had been added. Next, 2ml of 0% RPMI was added over 2 minutes, running the medium down the side of the tube while gently shaking the mixture. A further 20ml of 0% RPMI was then added in an identical fashion over 5 minutes. The resulting cell suspension was spun down for 15 minutes at 900rpm, then resuspended in 60ml of 20% RPMI containing 1x hypoxanthine-aminopterin-thymidine mixture (HAT, Sigma, final working concentration: 100μM hypoxanthine, 0.4μM aminopterin, 16μM thymidine). The unfused myeloma cells are hypoxanthine-guanine phosphoribosyltransferase deficient ($HGPRT^{-/-}$) and hence cannot survive the aminopterin induced blockage of the purine synthesis pathway driven by dihydrofolate reductase (DHFR). In contrast, fused cells will have regained the HGPRT enzyme from the splenocytes, and can use this salvage pathway to synthesise purines. This media therefore selects out only the successfully fused cells for survival. The cell suspension was plated out at 150μl / well over 8x96 well plates. The outer wells were filled with 0% RPMI only (to

prevent drying out of the cell containing wells) and the last two rows were filled with unfused splenocytes and 653s as negative controls.

After 7 days a further 100µl of 20% RPMI/1x HAT was added to each well. After 14 days the supernatant was aspirated from each well and replaced with 150µl of 20% RPMI with 1x hypoxanthine-thymidine supplement (HT, Sigma, final working concentration: 100µM hypoxanthine, 16µM thymidine). The aspirated supernatant was screened using the ganglioside complex ELISA technique, as described above. Positive wells were expanded by transferring ⅔ of the total volume into 2 further wells of a 96 well plate, using tips with the ends cut off to prevent fragmentation of the colonies. A further 100µl of 20% RPMI was added to all 3 wells of each expansion. On day 21 the cells were fed with a further 100µl of 20% RPMI per well. The supernatants from the expanded wells were again screened by ganglioside complex ELISA, and the positives cloned by limiting dilution. To achieve this, the cells were aspirated, spun down at 300g (1200rpm), and resuspended at 2000 cells/ml in 20% RPMI. This cell suspension was added to two rows of a 96 well plate (avoiding the outside columns) at 250µl/well, giving 500 cells/well. Aliquots of the remaining cell suspension were diluted 1 in 10 and 1 in 100, and plated out as before, giving two rows with 50 cells/well and two rows with 5 cells/well. The remaining cell suspension was added to a 24 well plate. This was grown until confluent and the cells frozen down, at -80ºC overnight in 10% dimethyl sulfoxide / foetal bovine serum (DMSO/FBS) with $2x10^6$ cells per vial, before storage in liquid nitrogen. These polyclonal fused cells could then be returned to at a later date if required.

Wells were screened at interval using ganglioside complex ELISA and positives iteratively subjected to the limiting dilution process until positive monoclonal

wells were produced. These were sequentially expanded into larger wells then flasks, with antibody being produced and purified as for existing cell lines above. In addition, aliquots of cells were preserved by freezing down in 10% dimethyl sulfoxide / foetal bovine serum (DMSO/FBS) at $2x10^6$ cells per vial and storing in liquid nitrogen.

2.2.8.2 Using semi-solid selection media

Using this variation, animals were prepared, and 653s defrosted, as for the traditional technique. All media were obtained from Stemcell Technologies. For one week prior to fusion, 653s were grown in the supplied 'medium A,' containing Dulbecco's Modified Eagle's Medium (DMEM), pre-selected serum, gentamicin, and additional supplements. Cell density was maintained at between 1 and 8 x 10^5 cells/ml. If cells grew beyond this density they were passaged at least twice to return them to the early-mid log phase of growth. The target density at the time of fusion was 2 x 10^5 / ml, and 100ml of medium containing 2 x 10^7 cells was required per fusion. On the day of fusion the myeloma 653 cells were harvested by centrifugation in 2 x 50 ml tubes. They were then washed 3 times in 30ml of serum free 'medium B' (containing DMEM and gentamicin only). Simultaneously, the spleen from the immunised animal was harvested and prepared as before. The liberated splenocytes were then themselves washed 3 times in 30ml of medium B, before both the splenocytes and the 653s were resuspended in a final volume of 25ml. The myeloma 653s were then stained with trypan blue, and the number and percentage of viable cells calculated. Similarly, a diluted sample of splenocytes 1 in 10 with 3% acetic acid and methylene blue was also prepared (resulting in lysis of the red cells and staining of the remainder) and the number of cells again calculated using a

haemocytometer. The volume of media than contained 1 x 10^8 splenocytes and 2 x 10^7 653s was then calculated and added to a fresh 50ml conical tube.

The cell mixture was spun down at 400g for 10 minutes, and every last drop of supernatant aspirated off, to ensure the greatest fusion efficiency. The resultant pellet was disrupted by gentle tapping of the tube, before 1ml of PEG solution was slowly added over 1 minute, without stirring. The cells were then gently stirred with the pipette tip for a further minute. Next, 4ml of medium B was added over 4 minutes, then a further 10ml over 4 minutes. The tube was topped up with 30ml of medium A and spun for 7 minutes at 400g. The supernatant was discarded, and cells washed in a further 40ml of medium A to ensure complete removal of the PEG. They were then slowly resuspended in 10ml of 'medium C' ('recovery medium' - containing DMEM, serum, gentamicin and supplements) and added to a T75 tissue culture flask already containing 20ml of medium C. This was incubated overnight at 37ºC, 5% CO_2.

The semi-solid, methylcellulose based, selection medium ('D') was removed from storage at -20ºC and defrosted overnight. The following day, the fused cells were transferred to a 50ml tube, spun down at 400g, and resuspended to a total volume of 10ml in medium C. This was then added in to 90ml of medium D, and mixed by gentle inversion. The mixture was allowed to rest for 15 minutes until the introduced bubbles had risen to the top. Using a 10ml syringe and 16g blunt end needles, 9.5ml of the cell suspension was added into ten 100mm diameter, sterile, petri dishes (Cornig) and the plates tilted to distribute the medium evenly. The petri dishes were then placed in a sealed, plastic container, along with an open petri dish containing 10ml of sterile, distilled water to maintain

moisture content, and incubated at 37ºC, 5% CO_2, without disruption, for 10-14 days.

After 10-14 days, then plates were examined for the presence of colonies visible to the naked eye. Around 500 to 1000 were expected over 10 plates. Several 96 well tissue culture plates were prepared, with 200µl of recovery 'medium E' (DMEM, serum, gentamicin and supplements) added per well to sufficient wells to accept all of the colonies to be harvested. Using a pipette set to 10µl and sterile tips, individual colonies were plucked form the semi-solid medium and added to separate wells of the prepared 96 well plate. Once all colonies had been transferred, they were resuspended using a multi-channel pipette set to 150µl. A separate sterile tip was used for each well to maintain clonality.

Following 4-7 days incubation, by which time the cell density had increased and the medium had begun to turn yellow, 150µl of supernatant was aspirated and tested for antibody production using the ganglioside complex ELISA technique. The supernatant was replaced with a further 150µl of fresh medium E. The hybridomas which showed a positive response on ELISA were then expanded by transferring 100µl to each of 2 wells of a 24 well tissue culture plate, each already containing 1ml of medium E. When the cell density had improved to around 4 x 10^5/ml, the cells from one well were frozen down as before, and the other expanded in a T75 flask with 5ml each of media A and E. The cells were then progressively expanded and transferred to 100% medium A, with further aliquots frozen down as required.

2.2.9 Ex vivo hemidiaphragm preparations

Diaphragms from NFL-Tg, GalNAcT$^{-/-}$ and WT mice with attached phrenic nerves were dissected out (as described in 2.2.14 below) and pinned under tension in Sylgard (silicone) lined dishes containing oxygenated Ringer's medium (see appendix). Whole diaphragms were excised along with the surrounding ribcage, by cutting away from spine as posteriorly as possible. Excess tissue was trimmed and the diaphragm pinned out through a small remaining portion of the ribcage and the central tendon to an underlying medallion of Sylgard. The diaphragms were then divided in half, each half retaining its supplying phrenic nerve. A small dorsal portion was removed from each resulting hemi-diaphragm and quickly snap-frozen. These were later used for baseline immunohistological measurements. The remainder of the hemidiaphragms were placed in a 25ml tube, still attached under tension to their semi-circular base of Sylgard, before being incubated with either Ringer's (as a control) or mAbs (100μg/ml, diluted in Ringer's) for 2h at 32°C, followed by 30 minutes at 4°C and 10 minutes at room temperature. The mAb solutions were then removed and retained for subsequent testing on ELISA.

NHS (normal human serum) diluted to 40% in Ringer's was then added as a source of complement. After 1h at room temperature, the NHS was rinsed off. The hemi-diaphragm was further divided, with the section of tissue attached to the phrenic nerve snap-frozen before being later processed for analysis of immunoglobulin binding, C3-complement, membrane attack complex (MAC) deposition and neurofilament loss.

The remaining portion of hemi-diaphragm was incubated in 2μM ethidium homodimer, as a marker of peri-synaptic Schwann cell (pSC) death, for 1h at room temperature in the dark. The tissue was then rinsed in Ringer's solution before and after fixation in 0.1% parafomaldehyde in Ringer's, applied for a further hour at room temperature. This fraction of hemi-diaphragm was cryo-sectioned at 25μm and transferred onto 3-aminopropyltriethoxysilane (APES)-coated slides. Fluorescein isothiocyanate conjugated alpha-Bungarotoxin (FITC-αBTx, Molecular Probes, Oregon, USA) was then applied for 1h at room temperature, to counter stain the post-synaptic neuromuscular junction (NMJ), before sections were rinsed in PBS and mounted in Citifluor (Citifluor Ltd, London, UK).

For immunoglobulin (Ig), C3-complement, MAC, and neurofilament staining, the previously snap-frozen diaphragm tissue was cryostat cut at 8 and 20μm thickness and transferred onto APES-coated slides (thicker sections were designated for neurofilament staining). All solutions were made up in PBS and incubations performed at 4°C. For each incubation, alpha-Bungarotoxin conjugated to Tetramethyl Rhodamine Iso-Thiocyanate fluorophore (αBTx-TRITC, Molecular Probes, Oregon, USA), was included at 1.3μg/ml (1:1000) to locate and outline the NMJs in each section, as αBTx binds to the post-synaptic acetylcholine receptor. To detect mAb binding, Fluorescein isothiocyanate (FITC) conjugated subtype-specific anti-immunoglobulin antibody of the required species, class and subtype (Southern Biotech, Alabama, USA) was applied at 3.3μg/ml (1:300) for 3h For detection of the activated complement component C3, slides were incubated in FITC–goat anti–human C3 (33μg/ml, 1:200; Dako, Glostrup, Denmark) for 2h. Mouse anti–human C5b-9 (363μg/ml, 1in 50; Dako), applied for 3.5h, was used to detect membrane attack complex (MAC)

deposition. This procedure required a separate fluorophore labelled secondary antibody, and after rinsing in PBS, FITC–goat anti-mouse IgG2a (Southern Biotech) applied at 5µg/ml (1:300) for 3.5h. For neurofilament analysis, sectioned tissue was stained for 1h with αBTx-TRITC, rinsed in PBS, and then kept for 20 minutes in freezing ethanol (–20°C) prior to incubation overnight with 1211 antibody (Affinity BioReagents, Colorado, USA) at 1:750. Slides were rinsed and incubated in FITC–goat anti-rabbit IgG (Southern Biotech, 3.3 µg/ml, 1:300) for 3.5h. In advance of assessment by confocal microscopy (2.2.15), slides were rinsed and mounted under a coverslip in Citifluor (Citifluor Ltd, London, UK).

2.2.10 Disease modelling by passive transfer

GalNAcT$^{-/-}$, NFL-Tg, and wild type (WT) mice were used at 6 to 10 weeks of age (15-30g). Baseline respiratory and neurological function was assessed using the plethysmography and behavioural testing protocols detailed below. Purified monoclonal antibody (mAb) was prepared as previously detailed, and the concentration adjusted to 1mg/ml. Each animal was then injected with 1ml of the mAb intraperitoneally (ip). After 16h, 1ml of normal human serum (NHS), as a source of complement, was injected ip. The animals were then returned to the plethysmography chambers for a further 3h of continuous monitoring of respiratory function. Following this, the behavioural tests were repeated, and the animals briefly returned to the plethysmography chambers to measure maximal tidal volume.

Following completion of the tests, the animals were killed with a rising concentration of CO_2, as per Home Office guidelines. The diaphragm and soleus

muscles were quickly dissected out and snap frozen on dry ice, before storage at -80ºC and later immunohistochemical analysis, as described below.

2.2.11 Disease modelling by active immunisation

This experiment also employed NFL-Tg mice, with GalNAcT$^{-/-}$ and WT as controls, aged 6-8 weeks at the start of the procedure. The immunisation protocol was as previously described. On day 0, mice were injected intraperitoneally (ip) with 100µl of ova-alum (6mg/ml), and baseline respiratory and neurological function data was obtained. On days 7, 14 and 21 mice were injected ip with 100µl of 1mg/ml ganglioside containing liposomes prepared as above. On days 25, 26 and 27 mice were injected intravenously via the tail vein with 50µl of the same liposomes diluted to 200µg/ml (i.e. to give 10µg ganglioside per injection).

The mice were bled via the tail vein on day 28, and the serum obtained used to check the antibody response and titre on ganglioside ELISA. Once this had been established, the mice were retested by plethysmography and behavioural testing on day 32-36, both pre- and post- 1ml of NHS injected ip. Following this, the mice were killed with a rising concentration of CO_2, and their diaphragm and soleus muscles harvested as before, and processed and analysed as described below. In addition, a terminal blood sample was taken to confirm the anti-ganglioside antibody titre at this time.

2.2.12 Behavioural testing

This involved a battery of different tests of strength, balance, co-ordination and stamina.

2.2.12.1 Balance bar

Each mouse was lowered onto the centre of a wooden bar (60-cm length, 2-cm diameter) suspended 60 cm above a foam pillow. The platforms at either end were blocked off. The latency to fall (up to 120s) was recorded for three consecutive trials.

2.2.12.2 Forelimb grip strength

A thin, triangular, metal bar was attached to a force meter (Ugo Basil, Italy). The meter was secured to the table and set to record the maximum tensile force generated. Each mouse, suspended by the tail, was allowed to grip onto the longest aspect of the metal bar. The mouse was then gently pulled back, parallel to the force meter's plane of recording, until its grip on the bar was released. This process was repeated three times and the mean force generated calculated.

2.2.12.3 Total grip strength

This was recorded as for forelimb grip strength above. The only difference was that the metal bar was replaced by a metal grid (10 x 5cm) which allowed the mouse to grip on with all 4 limbs simultaneously.

2.2.12.4 Hindlimb reflex extension

Mice were suspended by the tail for 10s, a score given as per the table below.

Score	Reflex
0	one or both hindlimbs paralysed
1	loss of reflex and hindlimbs and paws held close to the body with clasping toes
2	loss of reflex with flexion of hindlimbs
3	hindlimbs extended to form <90° angle
4	hindlimbs extended to form >90° angle

Table 2.1 - Scoring system for hindlimb reflex extension

2.2.12.5 Platform

Each mouse was lowered onto the centre of a wooden bar (60-cm length, 2-cm diameter) suspended 60cm above a foam pillow and facing one of the platforms at either end. The time to reach either platform with four paws (up to 60s) was registered in three consecutive trials. In each trial the mouse faced alternate platforms and a score of 60s was given to the animal that did not reach either platform or fell from the bar.

2.2.12.6 Rotarod

A rotarod (Ugo Basil, Italy) was used in both a fixed speed and accelerating modes.

Fixed speed

Each mouse was placed on a separate portion of the rotating cylinder (5 cm diameter) set at 5rpm.

Accelerating mode

The mouse was placed on a stopped rod. Rotation was commenced at 5rpm and increased in increments of 0.2rpm every second.

For each mode, the latency to fall from the rod was recorded (to a maximum of 300s) by a timer stopped automatically by the weight of the mouse triggering a break in the circuit when falling onto a lever under the rod. Each mouse was tested three times with each mode and a mean time taken.

2.2.12.7 Open field activity

Each mouse was placed in the middle of a walled off area (1m^2) with the floor divided into 42 squares. The latency to leave the central area, frequency of locomotion (number of squares entered with all four paws), rearing (number of times the mouse stood on its hindlimbs), and grooming (face or body grooming) were recorded over 300s. The floor of the arena was washed with 70% ethanol between mice.

2.2.13 Plethysmography

Non-invasive whole body plethysmography using a four-chamber system (EMMS, Hants, UK), set up and calibrated according to manufacturer's instructions, was used to assess respiration in the passive transfer and active immunisation experiments detailed above. Mice were initially acclimatised to the apparatus over a 30 minute period. The supplied eDacq software was then used to continuously monitor respiratory rate and tidal volume (TV) over the next 3h. The software records time stamped data in a spreadsheet, averaging 25 accepted breaths for each time point and reporting a mean. If the TV falls below 0.1ml or the inspiratory to expiratory ratio exceeds 60%, the breath is either not detected or rejected. The respiratory parameters were recorded every 30 minutes by taking the next 25 readings from each time point and calculating the mean. If individual animals showed respiratory embarrassment to such an extent that their tidal volume was persistently below the threshold detectable by the apparatus, resulting in fewer than 25 readings over the 30 minute period, the TV was recorded as being at the threshold of detection (0.1ml). Furthermore, representative flow rate traces were also collected. In recording runs where NHS

was to be injected, baseline data was recorded for 30 minutes before this source of complement was injected.

2.2.14 Diaphragm and soleus dissection and staining

Mice from active or passive immunisation experiments, or previously unused animals, were killed by a rising concentration of CO_2 as per Home Office guidelines. Once death was confirmed, a small window was made into the thoracic cavity and the internal organs removed. Subsequently, the abdominal cavity was opened and the liver, stomach and bowels pulled away from the diaphragm, leaving it free on both sides. Whilst holding the central tendon with forceps, the diaphragm was cut away from the overlying ribcage in one piece, placed in a 1.5ml tube, and snap frozen on dry ice. To dissect out the soleus, the animal was turned prone, and the right foot pinned in plantar flexion. Overlying fur and skin was dissected away, following soaking with 70% ethanol, to reveal the underlying calf muscles and Achilles' tendon (calcaneal tendon). The Achilles' was then cut through just proximal to the calcaneus, and the proximal portion remaining attached to the gastrocnemius grabbed with forceps. Whilst maintaining upward lift on the tendon, the gastrocnemius was freed from the underlying tissue by dissection along its medial and lateral aspects, before being removed entirely by cutting across the proximal aspect. The muscle was then removed from the animal and flipped over, to reveal the underlying, more darkly coloured soleus. This was then carefully dissected away from the overlying muscle bulk and likewise snap frozen in a 0.5ml tube.

The muscles were subsequently processed, sectioned and stained as per the methodology described in 2.2.9 above. When the animals were used to assess

serum or mAb binding *ex vivo*, having not previously been exposed to a passive transfer or active immunisation protocol, serum or mAb was applied first, prior to detection of binding with a FITC-conjugated subtype-specific anti-immunoglobulin antibody and αBTx-TRITC double stain.

2.2.15 Imaging and analysis of neuromuscular sections

Stained sections were imaged using an upright, scanning, confocal microscope (Carl Ziess, UK). To assess antibody binding, C3 complement and MAC deposition, numerous NMJs in each section were sequentially centred in the field of view at 40x magnification using an oil immersion lens and the red (TRITC) channel. For each NMJ digitised pictures from both the red (TRITC) and green (FITC) channels were taken for use in later analysis. The microscope operator was blinded as to the identity of the tissue. Between 60 and 90 images were typically obtained for each experimental condition. When images had been collected from all sections, they were analysed using ImageJ software (NIH, USA, obtained from http://rsb.info.nih.gov/ij/). Using an analysis 'plugin' (written in house by Dr Peter Humphreys) the number of green pixels (of antibody, C3 or MAC) overlapping the red, TRITC-αBTx stained NMJ was counted for each image. As the data generated followed a non-parametric distribution, the Mann-Whitney test was used to make statistical comparisons between the different experimental conditions.

The procedure for analysing peri-synaptic Schwann cell (pSC) death was slightly different, and could only be performed with *ex vivo* living tissue and not on frozen section. NMJs stained with FITC-αBTx were located using the green channel, and, for each NMJ, the number of nuclei stained red with ethidium

were counted. This stain is only able to penetrate the cell membrane following cell death. The number of dead pSCs per NMJ ranged from zero to four, and the frequency counts were recorded in a contingency table, typically 6x5, as shown later. Statistical analysis was performed using the Chi-squared test.

3 The ganglioside complex binding properties of monoclonal antibodies

3.1 Introduction

As already discussed, the concept of ganglioside complexes (GSCs) and antibodies targeted against these structures has the potential to address many of the as yet unanswered questions regarding the pathogenesis of Guillain Barré syndrome (GBS). In particular, the incomplete nature of serological-pathological relationships, the variability in pathogenic potential between apparently similar antibodies, questions of tolerance, and the incongruous nerve type specificity of certain antibodies, could all be theoretically resolved by considering the further level of complexity introduced by GSCs. For example, the incomplete serological-pathological relationships, exemplified by the acute inflammatory demyelinating polyradiculoneuropathy (AIDP) variant of GBS, where no dominant antibody association is found, could be addressed by the idea that antibodies have not been previously detected because investigators have historically focussed on detecting binding towards purified, homogenous preparations of glycosphingolipid (GSL) antigens, rather than considering the potentially unique epitopes formed in vivo by interactions between different molecules. Likewise, differential expression of GSCs in the peripheral nervous system as compared with the immune system, where tolerance is initially controlled, might partly explain the breakdown in self-tolerance required for the generation of pathogenic auto-antibodies. Additionally, sensory and motor nerves contain almost identical proportions of the gangliosides GM1, GD1a, and GD1b, yet antibodies specifically directed against these antigens, as assessed by solid

phase in vitro assays, will often bind exclusively to their target antigen in motor nerve, whilst failing to bind sensory nerves, or vice versa. It can be envisaged that differing interactions in the two nerve types between the apparent target ganglioside and its partnering glycolipids could either facilitate or block antibody binding.

To begin to address and investigate these hypotheses, a number of preliminary steps are required to be taken. First of all, a reliable, reproducible system for assessing binding to GSCs is obligatory. As the initial descriptions of αGSC antibodies used thin layer chromatography (TLC) and enzyme linked immunosorbent assay (ELISA) techniques, these were employed for first round investigations. Secondly, reagents which bound preferentially, or ideally exclusively, to GSCs would be required to investigate the pathogenic potential of αGSC antibodies, and the tissue distribution of GSCs. The Willison laboratory holds an extensive library of previously generated anti-ganglioside monoclonal antibodies (mAbs). These were widely employed in this research, both as tools for developing αGSC assays, as well as being investigated as potential reagents for in vivo pathogenesis and antigen distribution studies.

3.2 Results

3.2.1 Development of ganglioside complex ELISA and initial analysis of mAb binding

The initial reports detailing the presence of αGSC antibodies in neuropathy sera relied largely on an ELISA based detection protocol, in addition to TLC with immuno-overlay. An established protocol for anti-ganglioside antibody detection was already in use in the laboratory. These together provided a starting point for the detection of GSC binding, and the existing protocol was subtly modified to include GSCs, as detailed in the methods section. Instead of rows of different antigens being plated out a grid based layout was used, with single gangliosides applied in the first rows and columns, and the resulting 1:1 complexes to the right and below, as shown (Table 3.1).

x	GM1	GM2	GD1a	GD1b	GA1	GT1b	GQ1b
GM1	x						GM1: GQ1b
GM2		x					
GD1a			x	GD1a: GD1b			
GD1b			GD1a: GD1b	x			
GA1					x		
GT1b						x	
GQ1b	GM1: GQ1b						x

Table 3.1 - GSC ELISA layout

Single ganglioside antigens were applied in the first row and column (shaded green in the example above). The resulting 1:1 complexes were applied to the plate in the wells to the right of and below the single antigens (shaded white). The complex applied at each location is determined by combining the column and row headings. The location of GD1a:GD1b and GM1:GQ1b complexes are shown above as an example. A line of negative control wells were included, running from top left to bottom right, shaded orange above. These also act as a line of symmetry for duplicate wells within the same plate.

In order to develop the technique, and also to screen for hitherto unsuspected anti-ganglioside complex reactivity, existing monoclonal anti-ganglioside antibodies were assessed using this ELISA technique. Initially, these were examined on 8x8 grids against 7 single gangliosides and their 21 associated two species complexes.

There was at first no indication which of the existing mAbs might display complex reactivity and so the initial selection of mAbs to screen was based mainly on availability and familiarity with the antibodies in the laboratory. CGM3 is an IgM mouse monoclonal generated previously by immunisation of C3H/HeN mice with LPS extracted from the OH4382 isolate of *Campylobacter jejuni* (*C.jejuni*). Its single ganglioside reactivity had already been established, showing CGM3 to be an anti-terminal-disialosyl antibody (binding GD3, GQ1b and GT1a). (Goodyear and others 1999) It has been extensively used in the generation of a mouse model of Miller Fisher syndrome (MFS), where it binds to the neuromuscular junction, fixes complement, induces massive quantal release of acetylcholine and block neuromuscular conduction. (Plomp and others 1999; Halstead S.K. and others 2008) The initial mAb concentration used in these GSC assays was chosen by reference to the previously established half-maximal binding concentrations with respect to the single ganglioside antigen. Figure 3.1A demonstrates that the binding of this monoclonal to gangliosides on ELISA is influenced by complex formation. At a concentration of 1.5µg/ml, the average optical density reading (OD) for GQ1b alone was 0.51, whereas that seen for complexes containing GQ1b ranged from 1.06 to 1.47, although higher levels of non-specific background binding were seen with complexes, as later discussed. Furthermore, for the complexes GD1a:GT1b and GD1b:GT1b reactivity was equivalent to that seen for GQ1b if the differing background signal was

discounted, and returning about half the OD reading following background correction. Never the less, this suggests that a neo-epitope had been formed by these complexes and was a novel target for CGM3 binding.

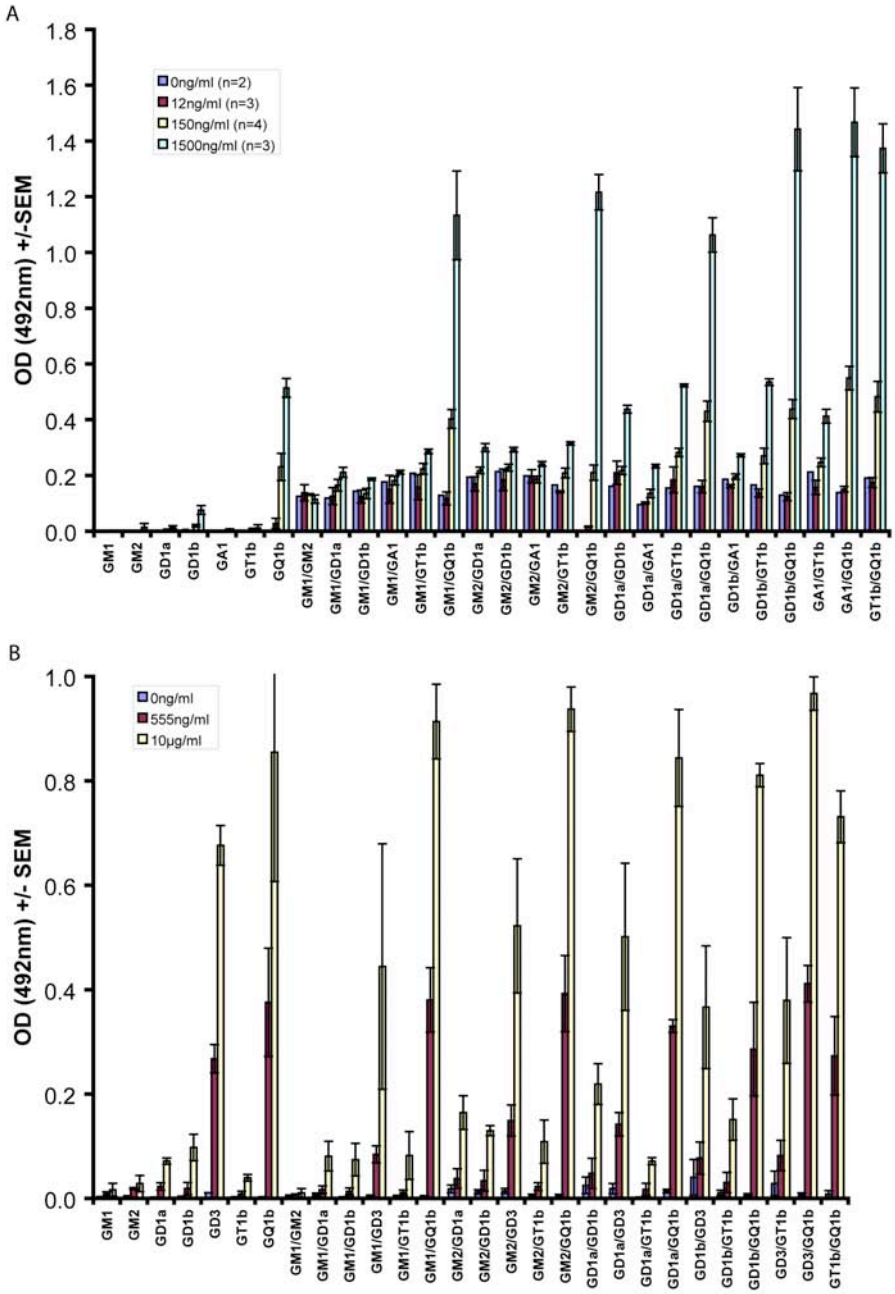

Figure 3.1 - Ganglioside complex ELISA with IgM and IgG monoclonal antibodies

Histogram of mAb CGM3 (**A**, IgM) and EG1 (**B**, IgG) binding intensity against a limited panel of seven gangliosides and their potential two-component complexes. EG1 results are derived from the average of three independent experiments.

Unfortunately, as discussed, this interpretation is somewhat confounded by the increased background signal to GSCs seen with the anti-mouse IgM secondary antibody – which appears to react to most GSCs included in the panel (Figure 3.1A, blue bars, secondary antibody only applied). As such, a monoclonal IgG antibody with similar single ganglioside reactivity, EG1, was also investigated. Whilst this demonstrated (Figure 3.1B) that the background signal was much reduced with the anti-mouse IgG secondary antibody, ganglioside complexes did not enhance or attenuate the binding of this monoclonal. A similar observation was seen with the anti-GD1a monoclonal MOG35, which retained its ability to bind GD1a in complex with other gangliosides without any attenuation or enhancement of signal.

3.2.2 The effect of premixing by sonication on GSC formation and antibody binding

One of the first IgG mAbs to be indentified which displayed GSC binding was TBG2. This antibody was previously generated by the immunisation of GalNAcT$^{-/-}$ mice with lipopolysaccharide (LPS) extracted from the O4 strain of *Campylobacter jejuni*. The predominant target of the antibody is the GD1a ganglioside, with minor reactivity towards GM1 and GT1b also having been noted previously. Initial GSC ELISA screening of this antibody revealed enhanced reactivity towards the GM1:GT1b complex as compared with the individual gangliosides in isolation. This allowed some of the underlying concepts of GSC reactivity to be addressed. It could be envisaged that the reactivity seen towards GSCs might simply reflect a summation of lesser degrees of interaction with each constituent ganglioside. Likewise, given that each GSC contains only half of the mass amount of each of the single gangliosides, it could be argued

that this difference alone accounts for modulated binding seen with GSCs. Similarly, it may be that the presence of a second ganglioside simply enhances the binding of the first to the ELISA plate, resulting in more antigen being available for binding and thus an increased signal.

To begin to tackle some of these issues, a simple experiment was envisaged. Focussing on the TBG2 antibody and GM1 and GT1b, these single gangliosides were applied to an ELISA plate both at the standard single ganglioside concentration (100µl of 2µg/ml, giving 0.2µg/well) and at the concentration obtained when the gangliosides were present in a 1:1 GSC (by 50:50 dilution with methanol to 1µg/ml, giving 0.1µg/well). Furthermore, 50µl of each ganglioside at the standard concentration were applied sequentially in both orders (GM1 then GT1b, GT1b then GM1). Finally, GSCs were created and applied in the usual way by premixing equal volumes of 2µg/ml single ganglioside solutions and then sonicating for 3 minutes. As the initial reported protocol employed premixing for 30 minutes, this was also included. (Kaida *et al.*, 2004)

As can be seen (Figure 3.2A), the binding to gangliosides which had been premixed by sonication was significantly increased in comparison with that seen to the individual gangliosides, or when these were added sequentially (General Linear Model ANOVA with Bonferroni correction, $n=4$, $p<0.0001$ for each comparison).

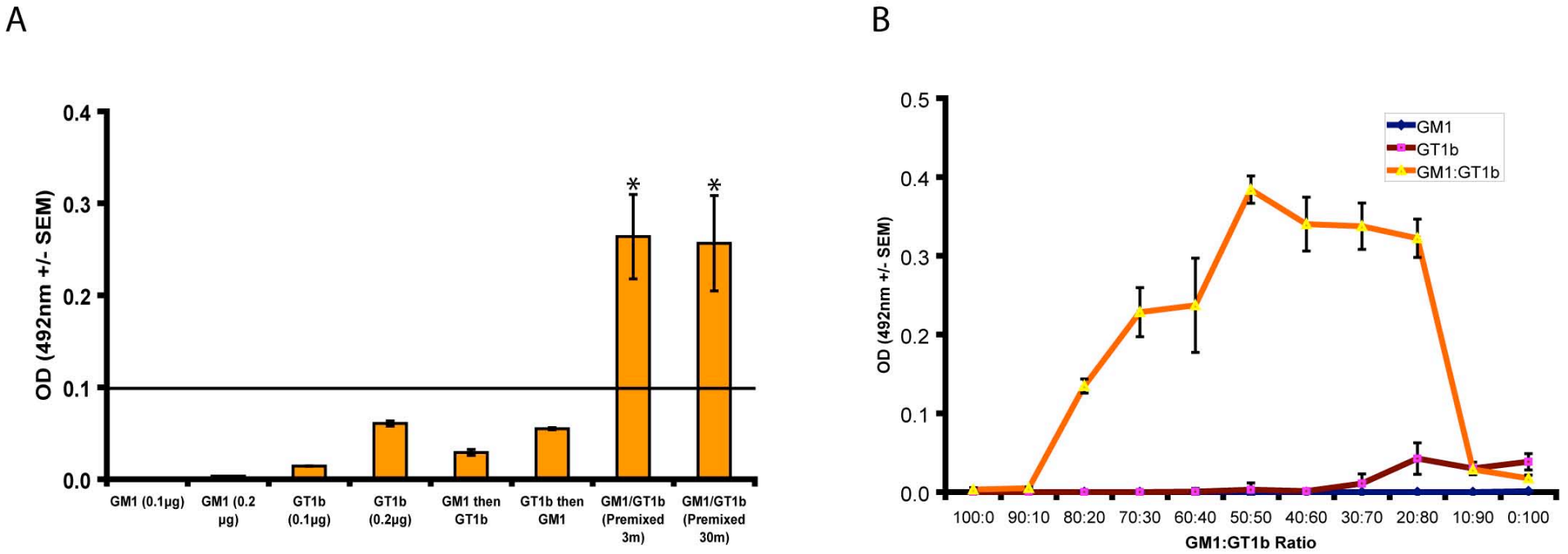

Figure 3.2 - Effect of premixing and differing ganglioside ratios on ganglioside complex formation and binding

(**A**) Comparison of TBG2 ELISA binding intensity towards non-premixed, premixed GM1 and GT1b and to each ganglioside alone. The solid horizontal line reflects the conventional OD value used to define positive binding. * = significant difference in OD compared with all non-premixed wells. (**B**) Variation in TBG2 ELISA binding intensity with differing ratios of GM1:GT1b in the complex mixture..

There was no significant difference when comparing premixing for 3 or 30 minutes, and the shorter time was subsequently adopted as standard. Minor increases in OD were observed between 0.2µg and 0.1µg of single ganglioside per well. The absolute ODs here fell below the traditional threshold to define positivity, although the ODs for GT1b (0.2µg), GM1 then GT1b, and GT1b then GM1, are all significantly above zero. In either case, the change in OD does not explain the differences seen between single and complex binding, as for GSCs the lesser amounts of single ganglioside are combined. Similar issues are returned to later, in light of the observation of complex attenuated binding and the development of a new immunoassay.

Binding to GSCs has previously been observed to be most intense when these are created by mixing a 50:50 ratio (w:w) of component gangliosides (Kaida *et al.*, 2004). A similar pattern was seen when testing TBG2 against varying ratios of GM1 and GT1b (Figure 3.2B). Working solutions of both gangliosides were prepared at 2µg/ml, and then mixed in the varying proportions shown. For the control wells containing GM1 or GT1b alone, the second ganglioside was replaced with an equal volume of methanol, such that the amount and concentration of the first ganglioside was equal to that found in the two ganglioside mixture.

3.2.3 Validation of the ganglioside complex ELISA using neuropathy sera

These initial experiments highlighted a number of issues. It was apparent that the binding of mAbs could be modified by GSCs, based on the ELISA assay, but the amount of data generated even in screening a small number of gangliosides and their associated 1:1 complexes was overwhelming. Furthermore, as these

antibodies had been previously cloned based on their ability to bind single ganglioside antigens, it was extremely unlikely that we would detect GSC exclusive binding. The opportunity to test some of the sera provided by Professor Kusunoki (Kinki University, Osaka, Japan), as detailed in the original report into αGSC antibodies (Kaida *et al.*, 2004), not only provided a chance to validate our GSC ELISA assay, but also suggested an approach to these other problems.

These sera had been selected for their ability to preferentially bind the GM1:GD1a complex, and as such, a more limited ELISA panel, consisting of GM1, GD1a, GD1b and their associated GSCs was created. As can been seen (Figure 3.3), both sera (coded 192 and 194) bound preferentially to GM1:GD1a complex, as advertised, with ODs of 2.07 and 2.34 at the same 1 in 40 dilution used in the original report. Serum 194 showed a greater degree of 'complex enhanced' binding as compared to serum 192. The sums of the individual GM1 and GD1a ODs for each serum were 1.67 and 0.66, respectively. Furthermore, these results were consistent with both of the different criteria stated for establishing GSC reactivity as initially defined, namely a corrected absolute OD>0.1 (Kaida *et al.*, 2004), and an OD for the GSC greater than the sum of the ODs for the two constituent gangliosides. (Kaida *et al.*, 2007)

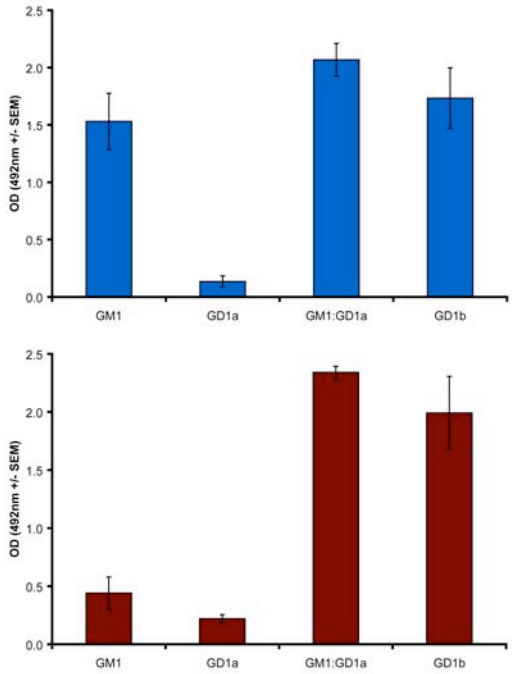

Figure 3.3 - ELISA with Japanese neuropathy sera assayed against a limited panel of gangliosides

Sera 192 (upper panel) and 194 (lower panel) were provided as examples of GM1:GD1a binding. As can be seen, this was confirmed on our assay, and lesser degrees of binding were also detected directed towards the constituent gangliosides, most notably with serum 192 and GM1. In addition, both sera bound isolated GD1b with similar ODs to that seen for the GM1:GD1a complex.

Interestingly, it was also noted that these sera bound to the single ganglioside GD1b. Whether this represented a single antibody clone binding to both GD1b and the GM1:GD1a GSC, or different antibodies with distinct specificities in a polyclonal response, was not determined. Nevertheless, this result suggested that the existing stock of in house 'b-series' mAbs (i.e. anti-GD1b, GT1b and GQ1b) might usefully be investigated for binding to a-series complexes.

3.2.4 Screening of existing b series monoclonal antibodies

If such an antibody could be identified, which bound a-series ganglioside complexes but only b-series gangliosides in isolation, this would be a suitable reagent for the investigation of GSC distribution, and for the assessment of the pathogenic potential of αGSC antibodies, in GD3s$^{-/-}$ mice. As these mice lack b-

series gangliosides, binding to these species *in vitro* could be ignored as a potential confounding factor *in vivo*, and any binding seen in vivo attributed to interactions with a-series complexes. As such, five mAbs previously generated by immunisation with GD1b containing liposomes (MOG1-4 and EG7), and four mAbs generated by immunisation with GQ1b-liposomes (MOG26-28 and MOG31), which also showed varying degrees of reactivity to isolated GD1b, were investigated. Instead of assaying against multiple ganglioside complexes, only those which might form in the membrane of a GD3s$^{-/-}$ mice were prepared. Of the five GD1b induced mAbs, two showed equivalent or greater reactivity to the neo-epitope formed by GM1:GD1a, as did one from the GQ1b group (Figure 3.4).

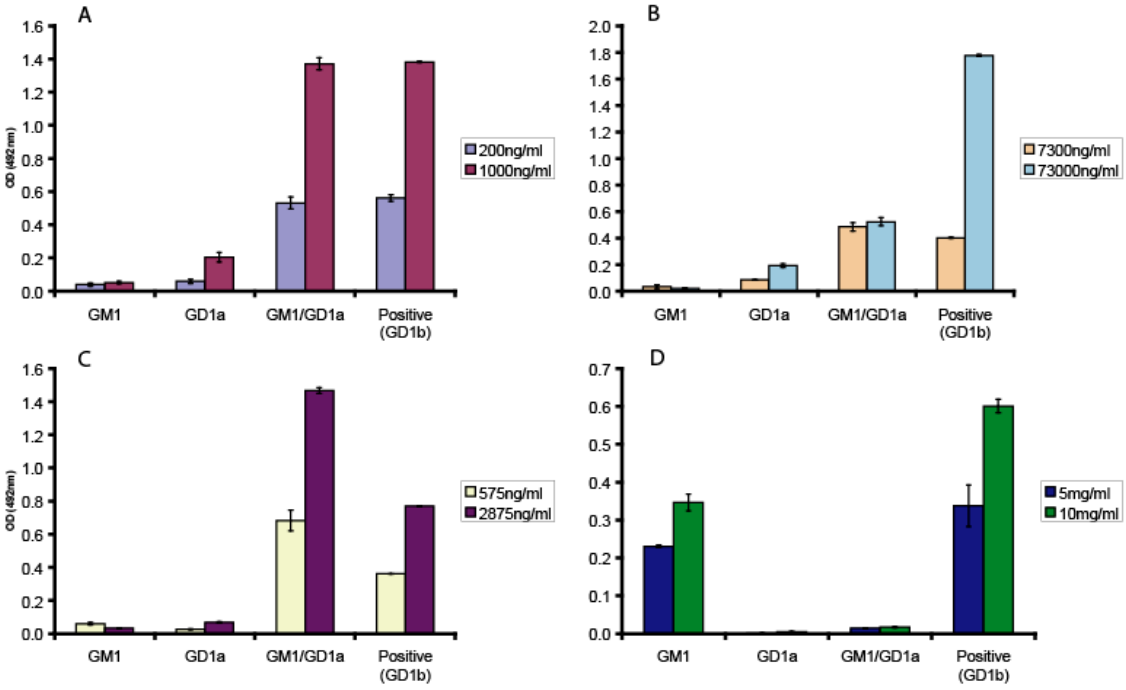

Figure 3.4 - The response of anti-b series mAbs to GM1:GD1a complexes

Average optical density results from two independent experiments performed in duplicate are shown for 4 different mAbs, +/-SEM. **(A)** MOG1 and **(B)** MOG4, both raised against GD1b containing liposomes, also bind the complex of GM1:GD1a, although in the latter binding to the complex appears to plateau at a lower concentration than for the single, positive control ganglioside. **(C)** MOG26 and **(D)** MOG27 were both raised in GalNAcT$^{-/-}$ mice immunised with GQ1b, yet display markedly different behaviours with respect to the ganglioside complex GM1:GD1a, as shown. Here, MOG26 **(C)** binds more strongly to the complex at both concentrations tested, whilst showing essentially no binding to either GM1 or GD1a alone. Conversely, MOG27 **(D)** shows some reactivity to isolated GM1, but does not recognise the complex GM1:GD1a, and is in effect inhibited from binding GM1 in the presence of GD1a.

Despite this *in vitro* ELISA data, none of these antibodies bound in *ex vivo* neuromuscular preparations taken from GD3s$^{-/-}$ mice, and they all also failed to bind to the GM1:GD1a complex when presented in the newly developed PVDF-glycoarray assay system, as discussed below.

3.2.5 Impetus for the development of a novel immunoassay for investigating ganglioside complex binding

The results obtained from the investigation of the Japanese neuropathy sera had suggested one approach to investigating GSC-lectin interactions – namely focussing on a limited panel of gangliosides and their complexes *in vitro* as a prelude to further experimentation in a biological system expressing a similar, limited panel of gangliosides. However, it was also felt desirable to be able to more efficiently screen for binding against a larger number of GSCs simultaneously, for example, when screening collections of disease associated serum samples for hitherto unidentified antibody-antigen interactions. It was apparent that the use of ELISA for this purpose had several limitations. As the number of single gangliosides is increased, the number of unique ganglioside complexes increases exponentially (Figure 3.5). When three or four component complexes are considered, this problem is further magnified. As can be seen, these numbers of complexes would quickly overwhelm the capacity of a single, 96 well ELISA plate.

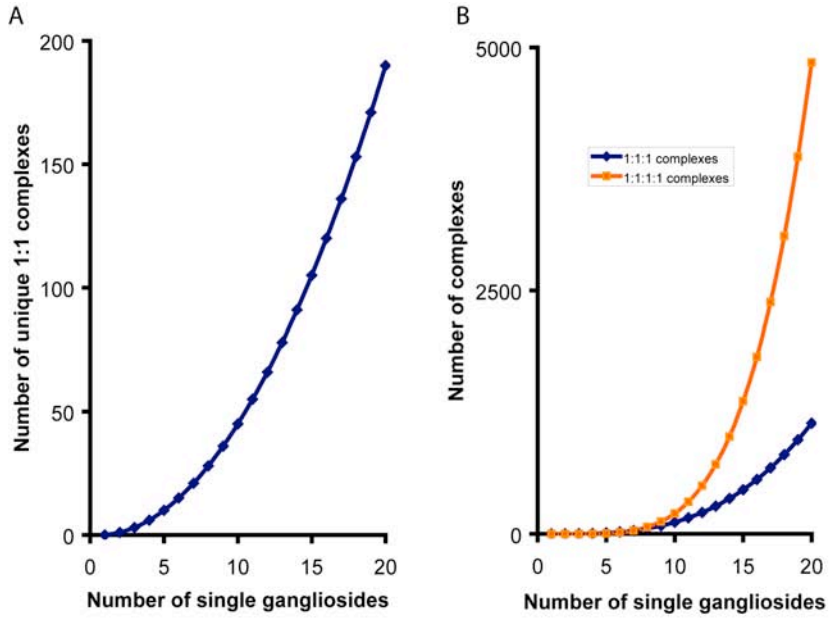

Figure 3.5 - Relationship between number of single gangliosides and potential number of complexes

(**A**) Heterodimeric complexes, (**B**) three and four species complexes. As can be seen, the number of potential complexes rises sharply as the number of single gangliosides or glycosphingolipids is increased, particularly when larger multimeric structures are considered.

Furthermore, when dealing with these numbers of potential antigens, the low-throughput ELISA becomes increasingly impractical, both in terms of the time required to prepare and plate out the potential targets, and in its consumption of large quantities of scarce reagents. As such, a miniaturised, polyvinylidene (PVDF) based, combinatorial glycoarray was developed based on a synthesis of previously published methods. (Kaida *et al.*, 2004;Kanter *et al.*, 2006).

3.2.6 Development of the combinatorial PVDF glycoarray

A detailed description of the methodology employed in investigating lipid autoantibodies in cerebrospinal fluid (CSF) and serum using PVDF membranes and an automated TLC spotter was kindly provided by Professor Bill Robinson

(Stanford University, USA). By adapting this method it was possible to include a combinatorial, GSC component and adopt layout similar to that used in the GSC ELISA (Table 3.1 and Figure 3.6).

x	GM1	GM2	GM3	GD1a	GD1b	GD3	GT1a	GT1b	GQ1b
GM1	x	GM2/GM1	GM3/GM1	GD1a/GM1	GD1b/GM1	GD3/GM1	GT1a/GM1	GT1b/GM1	GQ1b/GM1
GM2	GM1/GM2	x	GM3/GM2	GD1a/GM2	GD1b/GM2	GD3/GM2	GT1a/GM2	GT1b/GM2	GQ1b/GM2
GM3	GM1/GM3	GM2/GM3	x	GD1a/GM3	GD1b/GM3	GD3/GM3	GT1a/GM3	GT1b/GM3	GQ1b/GM3
GD1a	GM1/GD1a	GM2/GD1a	GM3/GD1a	x	GD1b/GD1a	GD3/GD1a	GT1a/GD1a	GT1b/GD1a	GQ1b/GD1a
GD1b	GM1/GD1b	GM2/GD1b	GM3/GD1b	GD1a/GD1b	x	GD3/GD1b	GT1a/GD1b	GT1b/GD1b	GQ1b/GD1b
GD3	GM1/GD3	GM2/GD3	GM3/GD3	GD1a/GD3	GD1b/GD3	x	GT1a/GD3	GT1b/GD3	GQ1b/GD3
GT1a	GM1/GT1a	GM2/GT1a	GM3/GT1a	GD1a/GT1a	GD1b/GT1a	GD3/GT1a	x	GT1b/GT1a	GQ1b/GT1a
GT1b	GM1/GT1b	GM2/GT1b	GM3/GT1b	GD1a/GT1b	GD1b/GT1b	GD3/GT1b	GT1a/GT1b	x	GQ1b/GT1b
GQ1b	GM1/GQ1b	GM2/GQ1b	GM3/GQ1b	GD1a/GQ1b	GD1b/GQ1b	GD3/GQ1b	GT1a/GQ1b	GT1b/GQ1b	x

Figure 3.6 - Typical layout for a 10x10 PVDF-glycoarray

Similarly to the ganglioside complex ELISA, single ganglioside antigens can be found in the leftmost column and uppermost row, with complexes spotted in the internal positions. The line of 'x' running top left to bottom right represents negative control spots of methanol only, and also acts as a line of symmetry for duplicate antigens within the same membrane.

Rather than using the software included with the ATS4 TLC-autospotter to write new programmes, as had been done previously, new layouts and protocols could be much more quickly established using the 'fill series' and formulae functionality of Microsoft Excel. This allowed subtle (or indeed major) alteration to the layout, spacing and dimensions of the individual spots to be rapidly made and investigated.

Many of the early technical problems with the assay had been addressed by Dr Kathryn Brennan, who had investigated different membrane surfaces, secondary antibodies and detection systems, and solved the problem of membrane detachment from the slide during the wash phase, whilst she was developing a

similar assay for further investigation of complex lipid antigens in multiple sclerosis.

Further development involved honing the secondary antibody used and the detection system employed, assessing the inter- and intra-assay variability, and addressing issues raised by the use of ganglioside complexes. Trials of fluorescent secondary antibodies were undertaken in an attempt to utilise the apparent greater dynamic range of these agents and employ automated scanning and detection systems (such as the Storm chemifluorescence imager, GE Healthcare, UK). However, shorter wavelength fluorophores, such as an anti-mouse IgG-FITC conjugate (Southern Biotech, USA), generated a high background signal with difficulty differentiating between the presence and absence of binding (Figure 3.7A). It was speculated that auto-fluorescence of both the PVDF membrane and the gangliosides themselves might be contributing to this, and that the issue could be overcome by using longer wavelength probes and filters. Unfortunately, use of a TRITC conjugate failed to address the problem, and an AlexaFluor-647 conjugated IgG secondary (Molecular Probes, USA) bound non-specifically to a spectrum of GSCs even in the absence of a primary antibody (Figure 3.7B). Neither of these problems could be overcome by altering the secondary antibody concentration, incubation period, excitation wavelength and voltage, and/or the emission filter settings. Horse-radish peroxidase (HRP) conjugated secondaries proved more successful, giving a clear distinction between positive and negative spots. Furthermore, reducing the secondary antibody concentration from 1:3000 to 1:30000 allowed clearer, individual spot definition and reduced non-specific background staining (Figure 3.7C). At concentrations below this, binding to some previously positive GSCs was lost.

Concerns about the dynamic range of an HRP-ECL (Enhanced chemiluminescence, Amersham/GE Healthcare, UK) radiographic detection system were addressed by spotting varying concentrations of secondary antibody direct onto the PVDF membrane and then processing the slides as normal. This revealed a broadly linear signal intensity response across the five secondary antibody dilutions used, and demonstrated the signal had not become saturated up to the 140000 arbitrary units level obtained by a 1:2000 dilution and 5 minutes exposure on radiographic film (Figure 3.7D). In the GBS sera series screen detailed later, this value was only exceeded on 2 occasions from 288 assays run, when maximum values of 145000 and 178000 were obtained, using 1 in 100 serum dilution, secondary antibody at 1:30k, and 1 minute exposure time.

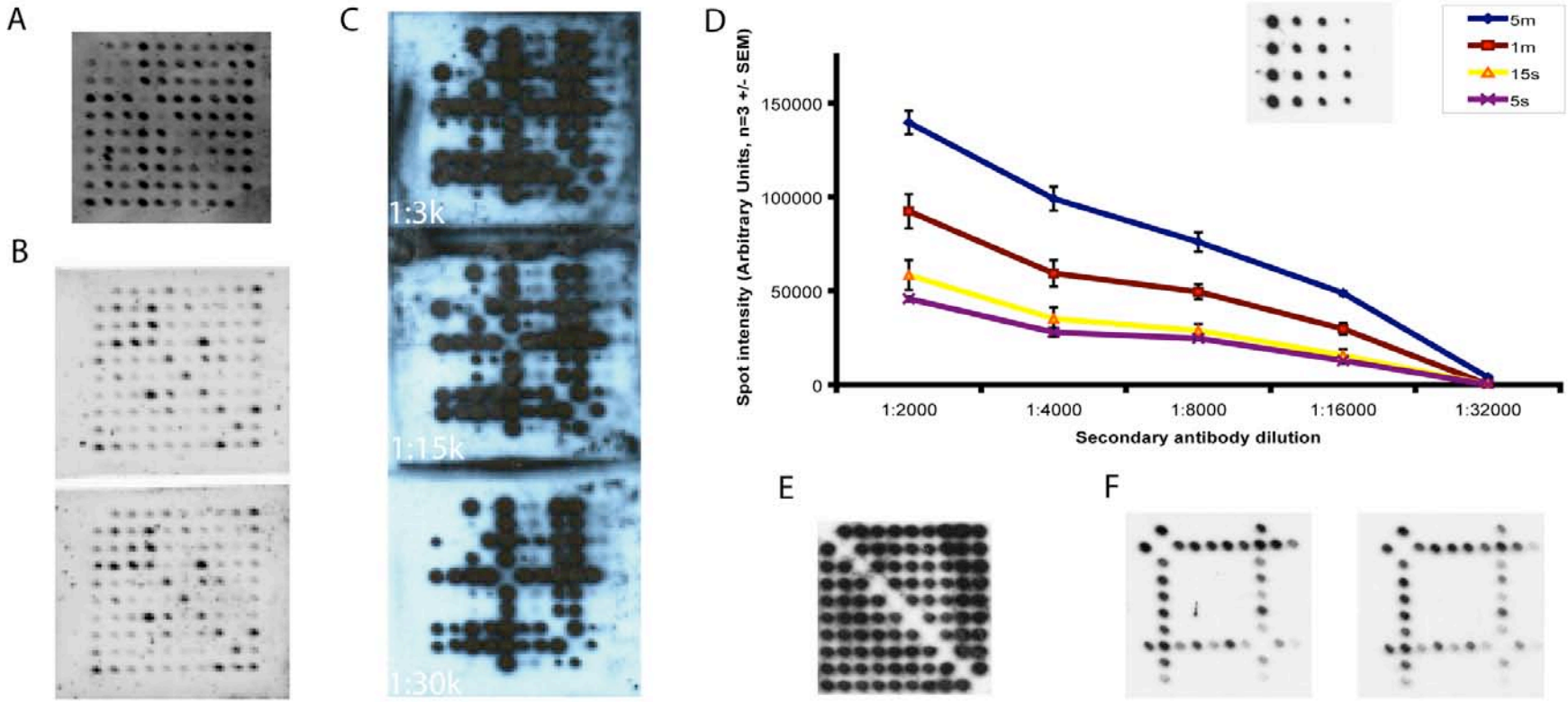

Figure 3.7 - Development and initial validation of the PVDF glycoarray

Use of a FITC conjugated secondary antibody resulted in high auto-fluorescence of the PVDF membrane and a low signal to noise ratio (**A**). Using the longer wavelength AlexaFluor-647 fluorophore, auto-fluorescence of the membrane was reduced, but non-specific binding was seen, as demonstrated by the fact that an identical binding pattern was seen with (**B**, upper panel) and without (**B**, lower panel) any primary antibody being applied. Furthermore, binding to the negative control spots of methanol only was seen with this secondary. Using an HRP-conjugated secondary, the difference between positive and negative spots was distinct, and background staining could be reduced by reducing the secondary antibody concentration from 1:3000 to 1:30,000 (**C**). Plotting a standard curve for this antibody and the ECL-radiographic detection system revealed a broadly linear response with no evidence of signal saturation over the range measured. An example of the range of intensities rendered on radiographic film following a 15s exposure is shown (**D**). Example processed grids from the intra- (**E**) and inter- (**F**) assay variation experiments are also shown.

The intra-assay variability was assessed and optimised by applying nine independently prepared samples of GM1 ganglioside to the edges of a PVDF array in duplicate. Spots around the perimeter of the arrays were chosen as these would be expected to show the greatest variability due to edge effects. Using the anti-GM1 mAb DG2, the incubation period and volume of secondary antibody applied were adjusted and co-efficient of variation (CV, mean of SD of duplicates/grand mean of duplicates x100) measured in each case (Figure 3.7E). A CV of 8.6% was measured using 500µl of antibody with a 2h incubation period (Table 3.2), and this was subsequently used in the standard protocol. Lower volumes of antibody had a negative effect on the CV, presumed to be due to incomplete covering of the membrane and/or evaporation of the reagent. Despite the prior prediction, the intra-assay co-efficient of variation of the 27 non-edge spots under the same protocol was similar, although slightly higher, at 9.2%. Following this, five repeats of the assay were run on different days, again using DG2 along with the optimum secondary antibody parameters as established in the intra-assay experiment. Inter-assay variation was calculated by dividing the SD of the individual means by the grand mean, and multiplying by 100 to give a percentage. This gave a value of 4.1% (Table 3.3). CVs less than 10% are usually considered representative of good reproducibility (Considine *et al.*, 1986) and the values obtained for the PVDF array are comparable to the standard, ganglioside ELISA (Willison *et al.*, 1999).

Antibody volume (µl)	Incubation Time (h)	Intra-assay CV (%)
100	1	83.4
250	1	14.3
500	1	13.7
500	2	8.6
500	4	9.7
500	16	13.2

Table 3.2 - Intra-assay variation measurement

Group mean	92.38
SD of mean	3.77
CV	4.1%

Table 3.3 - Inter-assay variation calculation

3.2.7 The effect of ganglioside mixing and complex formation on adhesion to the PVDF membrane

As noted for the GSC ELISA above, one potential confounding explanation for the modulated binding seen with GSCs as compared with single gangliosides is that the presence of the second ganglioside alters the amount of the first which binds (or remains bound) to the ELISA plate (or PVDF membrane). The ability to measure spot fluorescence using the Storm imager suggested a potential experiment to address this. Boron-dipyrromethene (BODIPY-FL) labelled GM1 was available commercially (Invitrogen, UK). In this preparation, the BODIPY fluorophore is attached to a truncated C5-fatty acid chain, but the sphingosine chain length and carbohydrate head groups are unaltered (Figure 3.8).

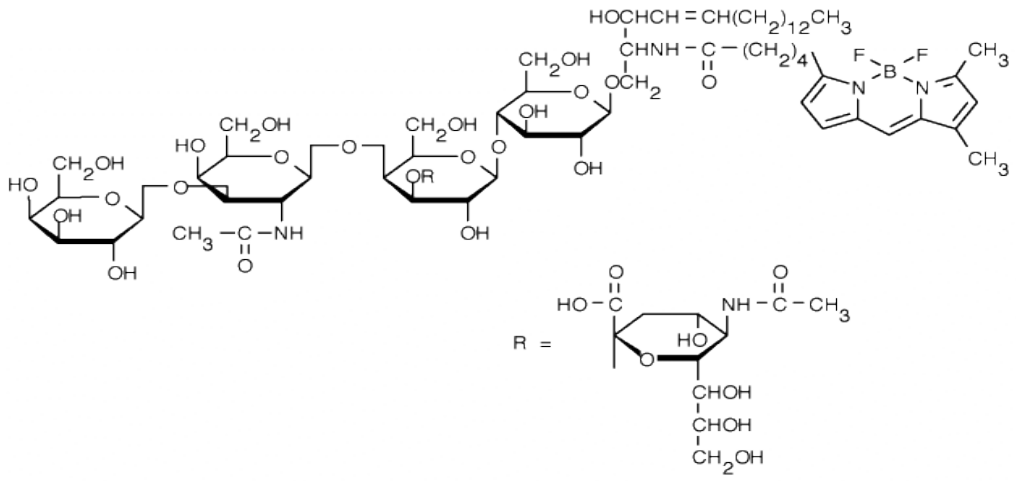

Figure 3.8 - Structure of BODIPY FL C5-ganglioside GM1

The fluorophore is present in (and partially replaces) the fatty acid component of the ceramide tail, leaving the antibody target formed by the carbohydrate headgroup chemically unaltered.

(Image taken from manufacturer's information sheet)

Using this fluorescent ganglioside, it was first established that differing amounts of GM1 per spot could be detected by applying varying concentrations of BODIPY-C5-GM1 and measuring the fluorescent intensity using the Storm imager. Six concentrations were prepared, to give expected applications of 0, 0.1, 0.2, 0.5, 1 and 2ng per spot, assuming all of the fluorescent ganglioside became attached to the PVDF membrane. These membranes underwent a standard wash cycle before spot intensity was measured. As can be seen, the spot intensity measured in relative fluorescent units (RFU) was linearly related to the amount of fluorescent ganglioside per spot (Figure 3.9A). Regression analysis with a fitted line plot gave a formula of:

Mean RFU = 1.05 + 1.52 (ng of FL-ganglioside applied per spot)

with an S value of 0.18 (a measure of how far measured points are away from the regression line) and an R2 value of 98% (a measure of the proportion of the

variation in the observed RFU response explained by the predictor – fluorescent ganglioside applied per spot). The Pearson correlation co-efficient was 0.968 ($p<0.001$), indicating a good correlation. Furthermore, there were significant differences between average RFU for 1ng and 0.5ng (n=6, estimated difference 1.19, $p<0.0001$) and between 1ng and 2ng (n=6, estimated difference 1.12, p=0.0001, both General Linear Model ANOVA with Bonferroni correction).

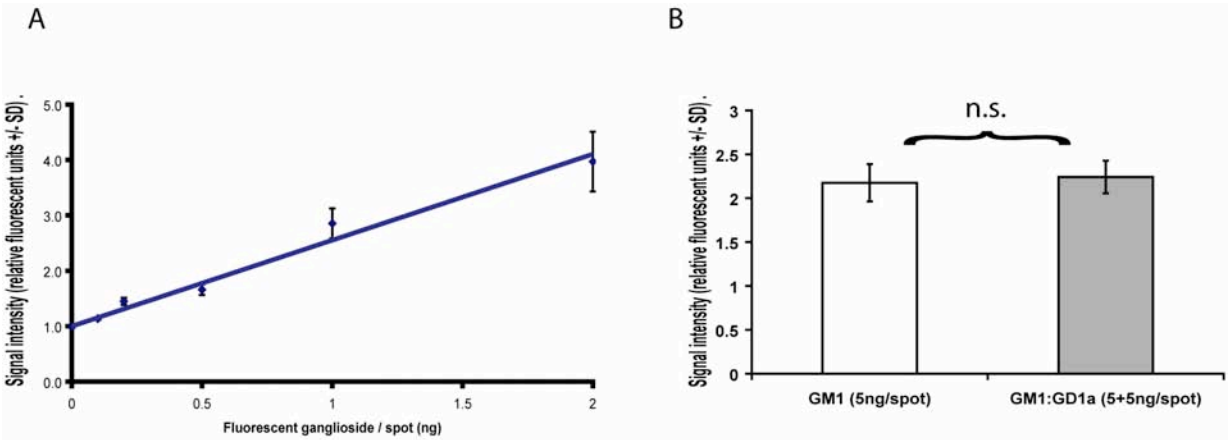

Figure 3.9 – GD1a in a GM1:GD1a complex does not modulate the amount of GM1 binding to the PVDF membrane

A linear relationship between the amount of BODIPY-C5 GM1-ganglioside spotted and fluorescent intensity is shown (**A**). No difference between the amount of GM1 binding to the membrane was observed when comparing a 1:1 mixture of GM1:methanol with a 1:1 mixture of GM1:GD1a (**B**).

The second step of the experiment involved comparing the amount of GM1-ganglioside binding to the membrane in the presence or absence of GD1a. A 100µg/ml solution of GM1, containing 20% BODIPY FL C5-GM1, was prepared. This was then mixed 1:1 (v:v) with either a 100µg/ml solution of GD1a or methanol. These two mixtures were then used to apply either GM1 alone, or the GM1:GD1a complex, to the same PVDF membrane in duplicate. Assuming GD1a made no difference to GM1 binding to the membrane, each 0.1µl spot would be expected to contain 5ng of GM1 in total, and 1ng of FL-GM1, with no difference in RFU measurement between the two. This was indeed the case, and mean observed intensities were 2.18 (GM1 alone) and 2.24 (GM1:GD1a), which was not

significantly different (n=6, estimate for difference (95% CI) 0.07 (-0.3 to 0.17), two sample T-test, p=0.55, Figure 3.9B). Power calculations based on the observed standard deviation of 0.18 revealed that the sample size of 6 would be sufficient to detect a 0.4 unit difference in RFU with 95% power, should such a difference exist. Using the previously determined standard curve regression formula, this equates to a difference of 0.26ng of fluorescent ganglioside.

3.2.8 The differing response of two anti-GM1 antibodies to ganglioside complexes

The anti-GM1 mAb DG2 was used extensively in the development and validation of the PVDF glycoarray, as has been discussed. This antibody, along with another superficially similar anti-GM1 mAb generated in-house (DG1), had also been comprehensively investigated by a previous PhD student (Dr Kay Greenshields). This was with a view to gaining a greater understanding of the pathogenic potential and mechanism of GM1 antibodies, and generating a murine model of anti-GM1 mediated acute motor axonal neuropathy (AMAN). GM1 antibodies have long been noted to have apparently inconsistent or contradictory binding patterns and effects in biological membranes, which cannot be explained simply by the presence, absence or variations in density of the putative target antigen, leading some to question their pathological importance.

Likewise, both of the in-house anti-GM1 monoclonal antibodies DG1 and DG2 were noted to bind isolated GM1 in solid phase ELISA assays, with very similar half maximal binding values of 0.5mg/ml and 0.4mg/ml respectively. (Townson *et al.*, 2007) However, when these were investigated by Dr Greenshields in *ex vivo* preparations of mouse neuromuscular tissue, disparate binding patterns

were noted. In the live motor nerve terminal of GD3s$^{-/-}$ mice, lacking b-series gangliosides but enriched in a-series gangliosides such as GM1 and GD1a, the DG2 antibody binds to the post-synaptic apparatus of the NMJ and supplying axon and fixes complement, leading to the deposition of membrane attack complex (MAC) pores and cytoskeletal disruption as evidenced by neurofilament loss. In contrast, DG1 fails to bind in such situations and does not fix complement or cause tissue damage. (Greenshields *et al.*, 2009)

It was speculated that DG1 was being prevented from interacting with GM1 in the live membrane due to an inhibitory *cis* interaction with another ganglioside, most likely GD1a in the context of the GD3s$^{-/-}$ mouse. It is of course possible that other gangliosides (e.g. GM2, GM3) could mediate similar blocking functions, particularly in membranes with other ganglioside compositions.

Ganglioside complex ELISA and the PVDF glycoarray were used to demonstrate that an inhibitory interaction between GM1 and GD1a formed *in vitro*. In ELISA, DG1 was significantly inhibited and DG2 only partially inhibited from binding GM1 in the presence of GD1a (Figure 3.10A). The mAbs were used at their GM1 half-maximal binding concentrations of 0.5μg/ml and 0.4μg/ml. This inhibitory effect was not unique to GD1a, and also occurred to a significant extent with GM1:GM2 and to a lesser extent (not significant) with GM1:GD1b. In marked contrast, complexes of GM1:GM3 and GM1:GD3 did not produce any inhibitory effects on DG1 or DG2 binding. This suggests that nonspecific displacement of GM1 by a second, nonreactive ganglioside, or simply the further dilution of GM1 by methanol, does not account for the lower signal seen with the inhibitory GM1:ganglioside complexes on ELISA.

When isolated GM1 was displayed on PVDF membranes in the PVDF glycoarray, there was no significant difference in the binding of DG1 and DG2 (Figure 3.10B). Paired assays were run, with DG1 and DG2 probed membranes processed and developed simultaneously, and binding normalised to the most intense spot across both membranes, to allow this comparison to be made. When GM1 was complexed with a range of other gangliosides, DG1 was almost completely inhibited from binding GM1. In contrast, DG2 binding to GM1 was minimally affected, although the difference in binding did reach significance for GM1:GM2 and GM1:GD1a complexes (Figure 3.10B). Two separate statistical tests were used to analyse this data. For comparisons between binding to GM1 alone and to GM1 complexes, general linear model analysis of variance (ANOVA), with Dunnett's correction to maintain the family error rate at 0.05 for multiple comparisons to the control level, was employed. Differences between DG1 and DG2 binding to each complex were assessed by the 2-tailed 2-sample t test. Bonferroni's correction was applied in view of the multiple comparisons being made, again to maintain a family error rate of less than 0.05.

Throughout these PVDF studies, the reduction in complex binding for DG1 was substantially and significantly greater than that for DG2. This figure formed part of the paper "The neuropathic potential of anti-GM1 autoantibodies is regulated by the local glycolipid environment in mice" published in the Journal of Clinical Investigation. (Greenshields *et al.*, 2009)

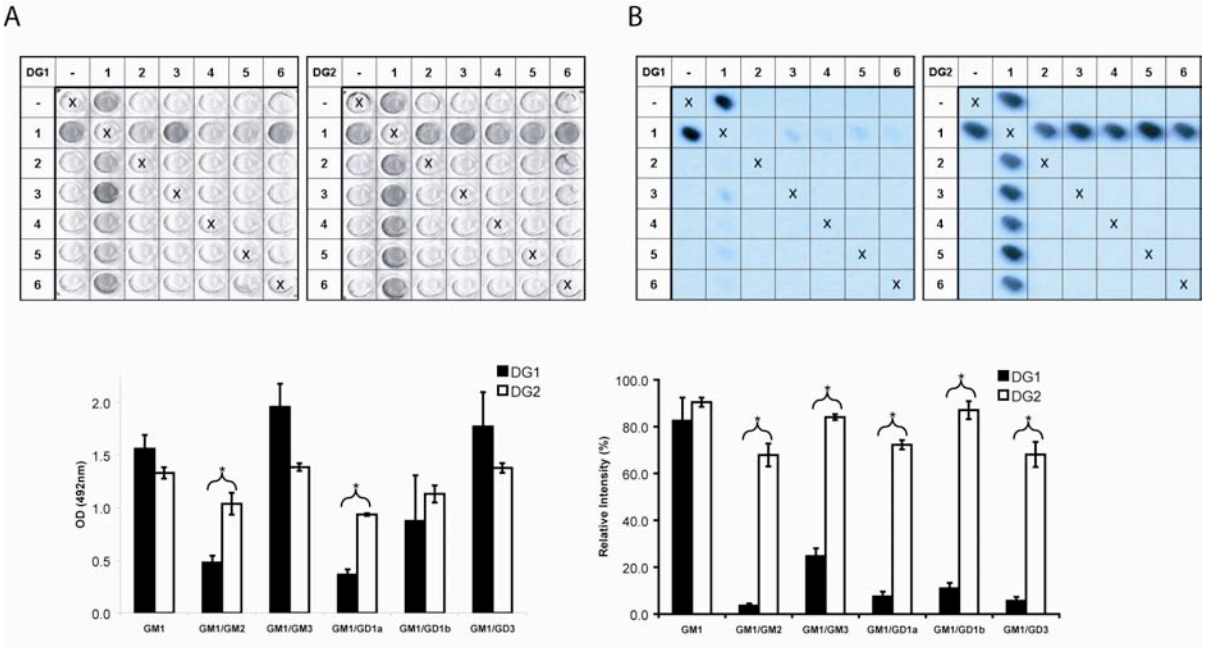

Figure 3.10 - Reactivity of anti-GM1 mAbs DG1 and DG2 to ganglioside complexes containing GM1 in solid phase

The ganglioside complex at each location is established by combining the row and column labels. Thus, coordinates 1,4 and 4,1 represent GM1:GD1a complex. Wells labelled X are negative controls (methanol only). (**A**) ELISA. DG1 (left) and DG2 (right) both bind GM1 alone, with no difference in average OD. DG1 binding to complexes GM1:GM2 and GM1:GD1a was less than that of DG2 (*=statistically significant difference in average OD for DG1 versus DG2).The binding of both antibodies to complexes of GM1 and GM2 or GD1a is reduced as compared with GM1 alone. For clarity, the statistical significance of these comparisons is not marked on the graph. No difference was observed with other combinations investigated (GM1:GM3, GM1:GD1b, and GM1:GD3). Mean results ± SEM from 3 experiments are shown.

(**B**) PVDF glycoarrays. DG1 was the primary antibody on the left membrane, DG2 on the right.. No significant difference in GM1 binding was observed for the 2 antibodies. DG1 binding to GM1 complexes was significantly reduced compared with GM1 alone ($P < 0.05$, significance level for these comparisons again not indicated in graph). DG2 binding GM1 complexes was marginally different compared with GM1 alone but statistically significant for GM1:GM2 and GM1:GD1a (not marked on graph). The inhibitory effect of complexes on antibody binding is greater for DG1 than for DG2. The average absolute reduction in signal intensity for GM1:GD1a complex, compared with GM1 alone, is 75.1% for DG1 and 18.2% for DG2 ($P < 0.05$). Mean results ± SEM for 3 experiments are shown *$P < 0.05$, **$P < 0.01$.

Key : 1, GM1; 2, GM2; 3, GM3;4, GD1a; 5, GD1b; 6, GD3.

3.2.9 The disparate binding of mAbs to GSCs on ELISA and PVDF

The results obtained with DG1 and DG2, above, demonstrated that the binding of lectins to GSCs on different surfaces can vary. For example, DG1 was significantly inhibited from binding GM1 in the GM1:GM3 complex on the PVDF glycoarray, but not by ELISA. In addition to this different inhibitory effect, it was also hypothesised that there might be a variation in the enhanced binding to complexes between the various assays. The most obvious reagents to test first were the anti-b-series mAbs which had displayed GM1:GD1a complex binding on ELISA (MOG1, MOG4, and MOG26), but failed to bind to GD3s-/- neuromuscular tissue, where such complexes might be expected to be found.

On PVDF glycoarray, all three of these mAbs failed to display enhanced binding to the GM1:GD1a complex, even when they were applied at concentrations 10 times greater than that used on ELISA. Furthermore, at the 1μg/ml and 7.3μg/ml concentrations used in the ELISAs respectively, MOG1 (Figure 3.11A) and MOG4 (Figure 3.11B) still bound strongly to GD1b (average arbitrary intensities (AI) 88300 and 72900) in a complex independent fashion. No GSC binding was demonstrated by MOG1. MOG4 bound weakly to GD1a (average AI 5500, n=3) but this was not enhanced by the GM1:GD1a complex (average AI 1400, n=3). MOG26 (Figure 3.11C) bound GQ1b, but failed to bind even isolated GD1b, as it had done in the ELISA. Additionally, no reactivity was demonstrated towards GM1:GD1a complex, although a weak signal was observed with complexes of GD1b with GM3, and to a lesser extent with GD1b:GD1a and GD1b:GT1a.

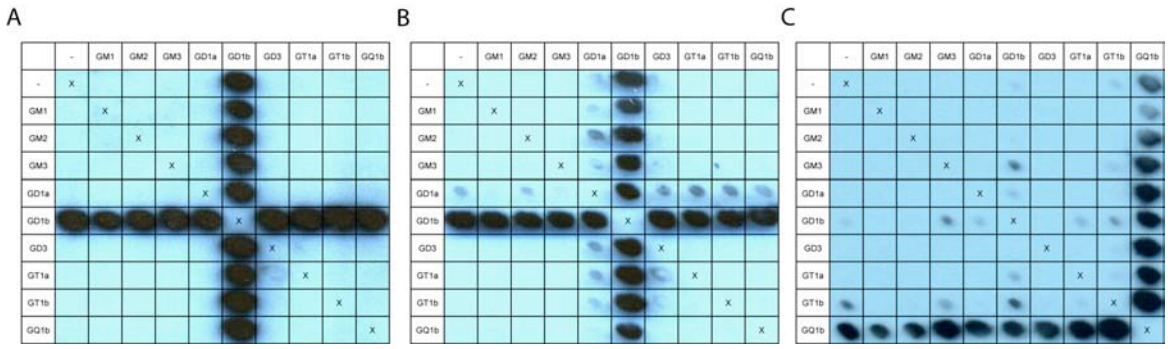

Figure 3.11 - The display platform influences the binding of anti-b-series mAbs to GM1:GD1a complex

MOG1 (**A**) and MOG4 (**B**) remain able to bind GD1b on the PVDF glycoarray, but in comparison with the ELISA assay (Figure 3.4, above) do not demonstrate binding to the GM1:GD1a complex. MOG26 (**C**) binds GQ1b, but fails to bind even isolated GD1b, as it had done in the ELISA. Additionally, no reactivity was demonstrated towards GM1:GD1a complex, although a weak signal was observed with complexes of GD1b with GM3, and to a lesser extent with GD1b:GD1a and GD1b:GT1a.

3.2.10 GSC Liposome ELISA

The disparate results seen between ELISA and PVDF prompted further testing in a third assay, a ganglioside complex liposome ELISA. As gangliosides are presented in association with a number of accessory lipids in a bilayer, this was felt to more accurately represent the living membrane. The GM1 antibodies DG1 and DG2 were examined, as was MOG4 which binds GM1:GD1a on standard ELISA but not on PVDF. The anti-GD1a mAb MOG35 was included as a positive control for GD1a containing liposomes. As can be seen, DG1 and DG2 both bound isolated GM1 as expected, with no significant difference in OD noted (n=3, 2 tailed, 2 sample T-test, p=0.19). Both antibodies bound less well to liposomes containing the GM1:GD1a complex, but once again DG1 bound significantly less well than DG2 to this antigen (n=3, 2 tailed, 2 sample T-test, p=0.01). As expected, and as previously seen on standard ELISA, MOG35 recognised GD1a and no significant difference in binding was observed as compared with GM1:GD1a complex (n=3, 2 tailed, 2 sample T-test, p=0.23). In contrast to the standard

ELISA, but in keeping with the PVDF array, MOG4 entirely failed to bind the GM1:GD1a complex in liposomes (Figure 3.12).

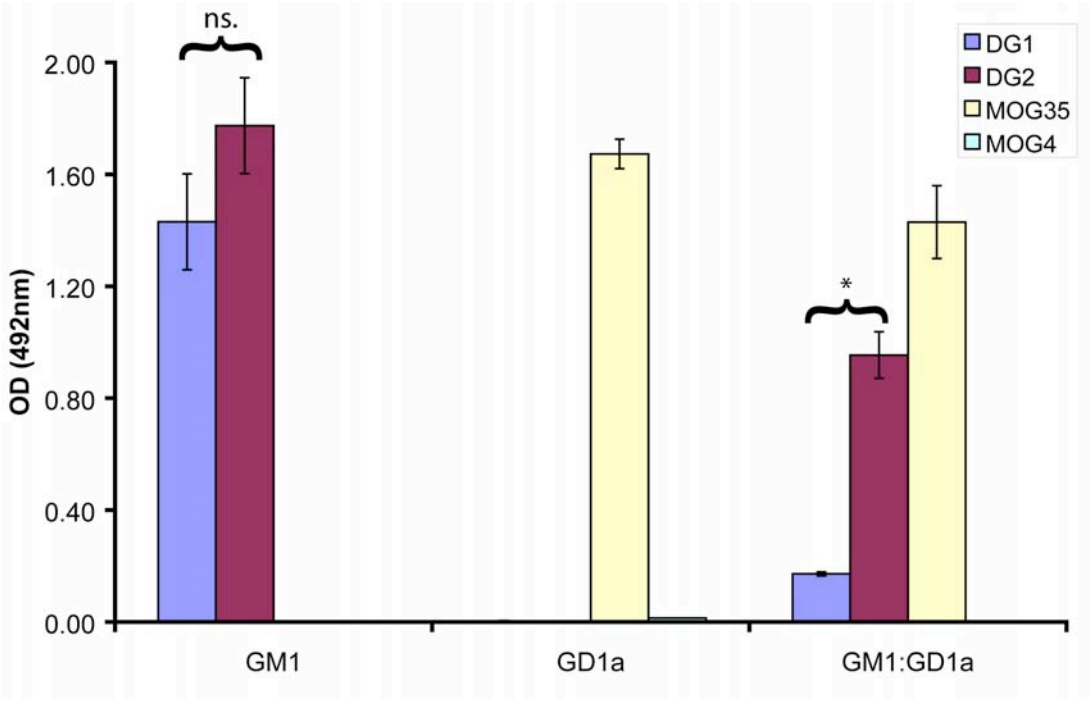

Figure 3.12 - GSC liposome ELISA with GM1:GD1a complex

Both of the GM1 antibodies DG1 and DG2 bind isolated GM1 liposomes with similar ODs. The binding of DG1 to GM1:GD1a containing liposomes is significantly poorer than that seen with DG2. MOG35 binds GD1a in GD1a and GM1:GD1a liposomes. MOG4 fails to bind GM1:GD1a complex liposomes, in contrast to the pattern seen using standard ELISA, but in keeping with that obtained using the PVDF array. (Average OD for 3 independent experiments, +/-SEM, is shown. mAbs were used at the same concentrations used in the standard ELISA. Statistical comparisons were made using a two-sample two-tailed T-test).

3.2.11 The disparate binding of mAbs to GSCs on TLC, ELISA and PVDF

On reviewing the previous work of the Willison laboratory in generating anti-ganglioside mAbs, an intriguing observation was noted. When Dr Carl Goodyear generated mAbs by immunising mice with GBS associated *Campylobacter jejuni* lipopolysaccharide, these were tested for reactivity against gangliosides by thin

layer chromatography (Goodyear *et al.*, 1999). For some of the antibodies generated, reactivity was;

> "observed with GD1b and an unidentified ganglioside(s) migrating between GD1a and GD1b."

This has distinct echoes of the comment made in Kaida's paper (Kaida *et al.*, 2004) detailing the first description of ganglioside complex antibodies in neuropathy sera;

> "an unidentified immunoreactive band [was identified] in the position just below GD1a on TLC of a crude ganglioside fraction"

strongly suggesting that these mAbs might also recognise the GD1a:GD1b complex. In fact, looking at the TLC blots themselves suggests most of these antibodies do not recognise GD1b alone, with binding corresponding only to the overlapping portion with GD1a felt to represent GD1a:GD1b complex. However, CGM2, 3, and 5 failed to bind this GSC on the PVDF glycoarray, and only CGM3 demonstrated some weak binding towards the complex on ELISA (see Figure 3.1 above). To address the hypothesis that these antibodies were indeed binding to the overlapping portion of GD1a and GD1b in the original TLC assessment, an experiment involving three lanes of ganglioside (GD1a, GD1b and both GD1a and GD1b), developed by TLC, and then overlaid with the different mAbs, was performed. Initially, ganglioside application, the solvent system used, and the development time, were optimised to result in a partial overlap of gangliosides GD1a and GD1b in lane 3 (Figure 3.13A). Subsequently, sets of these three lane panels were applied in triplicate to one TLC plate. After this had been developed in solvent and air dried, the left most panel was cut away and the distribution of ganglioside revealed by the orcinol reagent. The remaining two panels were split, and each probed with a separate mAb according to the

protocol already described. By lining up the immunoreactive bands with the orcinol processed panel, the ganglioside binding profile can be determined. As can be seen, CGM2 binds only to the overlapping portion of GD1a and GD1b in lane 3. CGM3 binds very weakly to both individual GD1a and GD1b, but a much stronger band is seen again corresponding to the overlapping portion of GD1a and GD1b. In fact, in the GD1a only lane it may be that binding is again towards GD1a:GD1b complex formed by contaminating GD1b, giving that the immunoreactive band corresponds only to the overlapping portion of GD1a and GD1b in lane three, rather than the whole extent of GD1a revealed by orcinol. In contrast, MOG35 binds GD1a in lane 1, and also recognises the same ganglioside in lane 3, with the immunoreactivity appearing to extend into the overlapping zone with GD1b (Figure 3.13B).

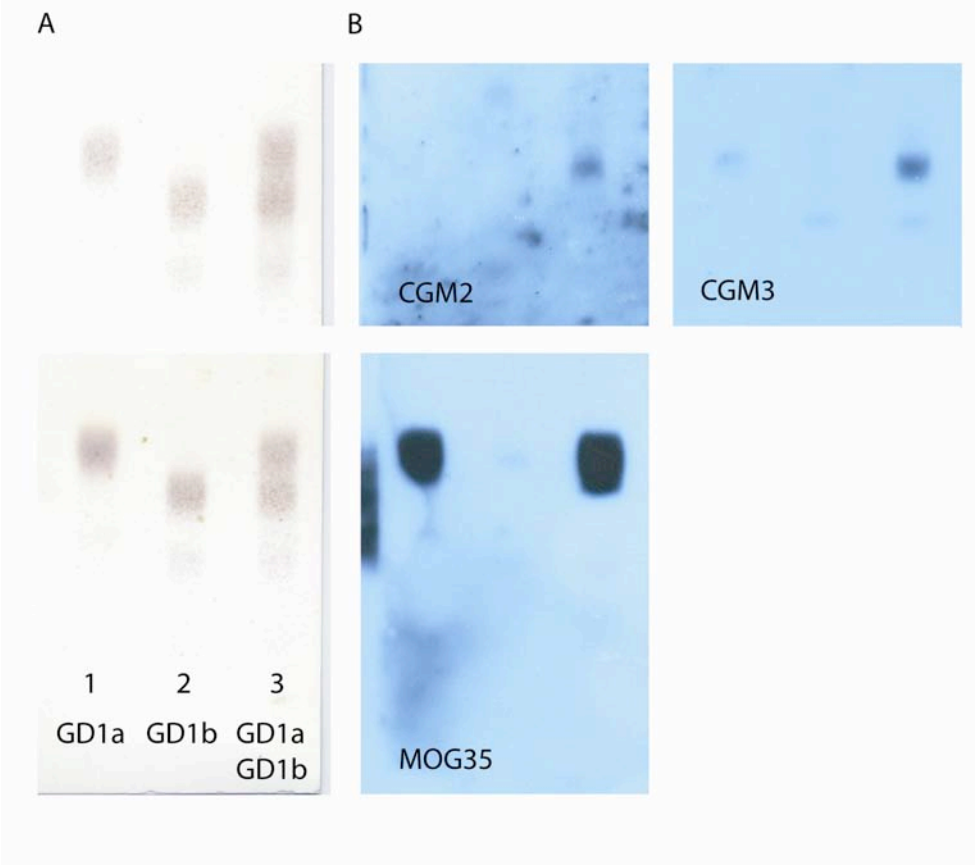

Figure 3.13 - CGM2 and CGM3 bind GD1a:GD1b complex by TLC with immuno-overlay

Three lane panels of GD1a, GD1b and both GD1a and GD1b were run in triplicate on silica coated TLC plates. These were then divided, and the left most panel developed with the orcinol reagent to reveal the distribution of the gangliosides (**A**). Overlay with CGM2 or CGM3 (**B**, both at 50µg/ml, anti-mouse IgM-HRP secondary at 1:6000, 15s exposure) revealed binding to the overlapping portion of GD1a:GD1b in lane 3. In contrast, MOG35 (30µg/ml, secondary at 1:3000, 5s exposure) shows binding to GD1a in lane 1, as well as in lane 3, where the immunoreactivity also appears to extend into the overlapping region with GD1b. A very faint band in lane 2 at the GD1a level may indicate minor contamination of GD1b with GD1a.

3.2.12 Antibodies in neuropathy sera bind GM1:GD1a complexes on ELISA and PVDF glycoarray

Provision of further sera containing antibodies purported to bind GM1:GD1a complex (again by Professor Susumu Kusunoki of Kinki University, Osaka, Japan) allowed binding to be assessed on both ELISA and PVDF glycoarray. Due to the limited volumes of sera available, the ELISA assay was limited to GM1, GD1a and GM1:GD1a in duplicate. In contrast, a full 10x10 PVDF array was able to be processed. Distinct from the disparate GM1:GD1a complex binding seen with the b-series mAbs above, both sera 444/17 and 470/23 bound the complex on PVDF (Figure 3.14A+B) and in ELISA (Figure 3.14C). Furthermore, the sera remained able to bind the complexes on PVDF even when their concentration was reduced fivefold (to 1 in 200) as compared with ELISA. Some other discrepancies were noted between the two assay systems, however, particularly for serum 470/23. On ELISA, this serum bound to GD1a (with a mean OD of 1.55 at 1 in 40 dilution) in addition to the GM1:GD1a complex. On PVDF, although binding to this complex remained, reactivity to isolated GD1a was not seen. Additionally, binding to other complexes of GM1 or GM2 with GD1a, GT1b or GQ1b was also noted (Figure 3.14B). There was insufficient 470/23 serum available to additionally assess binding on ELISA to these other complexes.

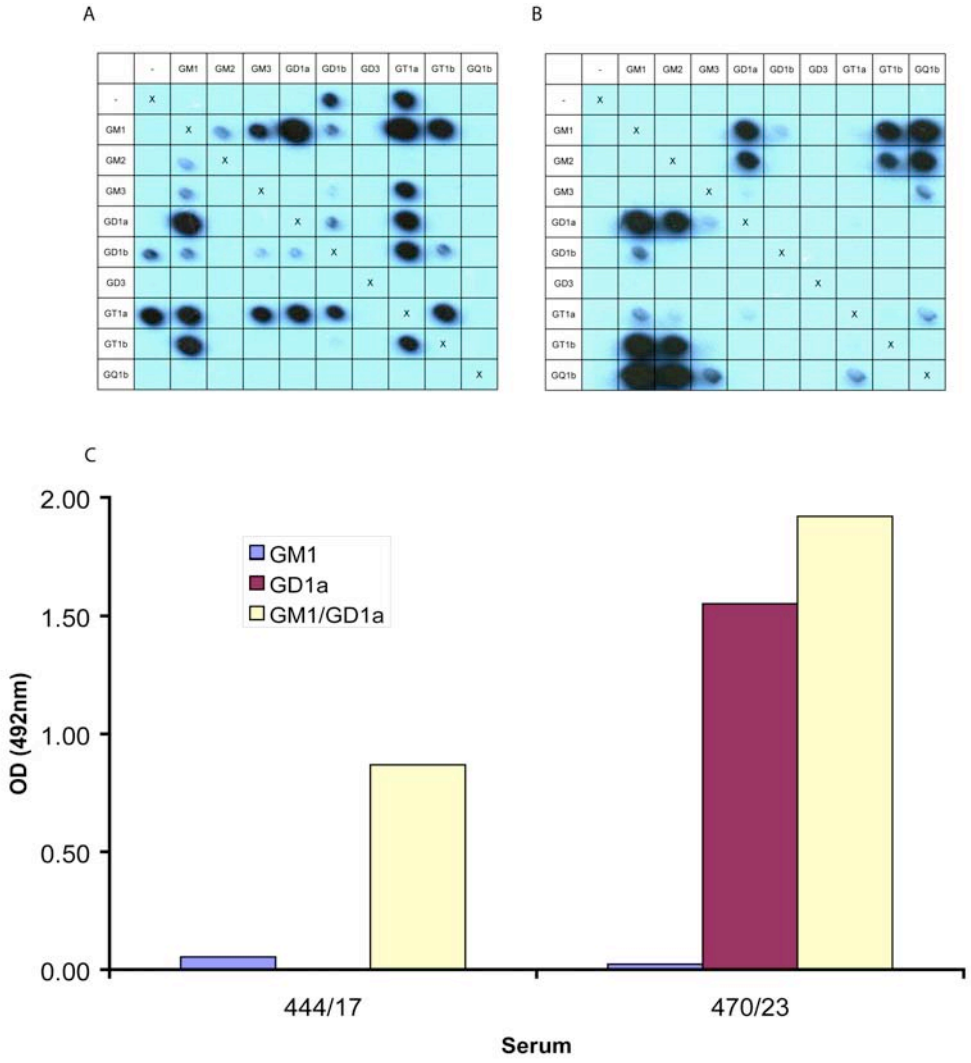

Figure 3.14 - Neuropathy sera binding GM1:GD1a complex on PVDF and in ELISA

In contrast to the findings with the b-series monoclonal antibodies, above, two GM1:GD1a binding sera remained able to bind this complex both on PVDF glycoarray (**A**) and ELISA (**B**). Binding by serum 470/23 to GD1a in isolation, as demonstrated by ELISA, was not replicated on PVDF glycoarray, which also demonstrated interaction with a range of other complexes.

3.2.13 GM1:GD1a anti-sera ex vivo binding assays

A small number of GBS associated sera were additionally kindly provided by Professor Nobuhiro Yuki (Yong Loo Lin School of Medicine, National University of Singapore). Two groups had been selected. The first contained 4 sera binding GM1:GD1a complex, the second contained 6 sera binding GM1, but not GM1:GD1a complex. Unfortunately, these were provided as lyophilised samples and only 2 sera from each group were adequately reconstituted. The remainder could only

be returned to a gelatinous, semi-solid state unsuitable for use in any sort of immunoassay. Nevertheless, 3 of the successfully reconstituted sera showed diverse IgG binding patterns on PVDF glycoarray and ELISA, and were selected for further study in *ex vivo* preparations.

As shown (Figure 3.15), serum A binds most strongly to GM1:GD1a complex, with no (on PVDF) or much reduced (ELISA) binding to GM1 and no GD1a reactivity. Complex specific binding is also seen towards GA1:GD1a, and to a lesser extent GD1a:GD1b. The other two sera would act as near ideal controls in the subsequent *ex vivo* assay. Thus, the faint GA1 binding seen with serum A is controlled for by serum B, which binds this single antigen more strongly. Serum C shows complex attenuated binding, its interaction with GM1 being blocked by other gangliosides including GD1a, but, curiously, only slightly attenuated by GalNAc-GD1a.

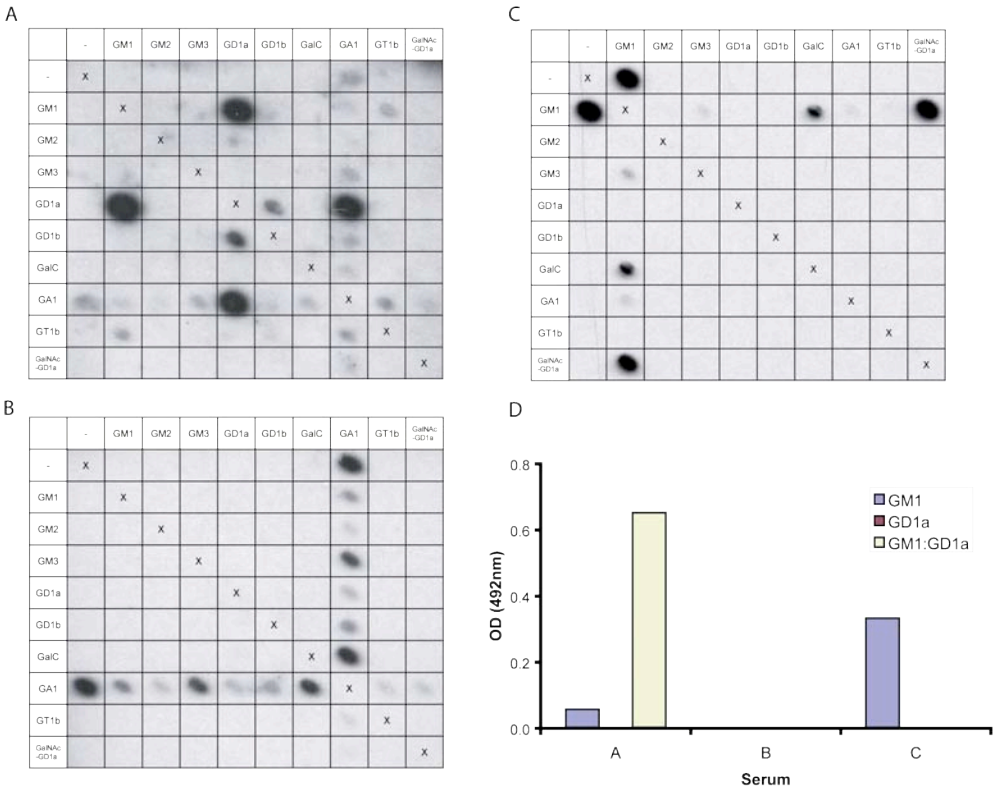

Figure 3.15 - Glycoarray and ELISA analysis of complex specific, independent and attenuated sera used in subsequent ex vivo assay

PDVF array: (**A**) serum A, (**B**) serum B, (**C**) serum C. All at 1 in 100 dilutions, 5 minutes exposure time. (**D**) Comparative ELISA data (1 in 40 dilution).

These three sera were then taken forwards for use in an *ex vivo* assay using hemidiaphragm tissue harvested from GD3s$^{-/-}$ mice. As only 100 to 200µl of each serum were available, the *ex vivo* assay with live hemidiaphragm tissue described in 2.2.9 could not be performed. This requires at least 3ml of serum at a 1:1 dilution. Instead the harvested diaphragm was snap frozen and processed as described (2.2.14), and the sera incubated directly on the frozen sections. In this protocol, only 100µl of diluted serum is required per slide. Following incubation for 4hrs at 4ºC, the slides were rinsed and an anti-IgG FITC secondary antibody applied as previously described. At serum dilution of 1 in 2, 1 in 8, and 1 in 16, no detectable binding was seen with any of the three sera assayed (results not shown).

3.3 Discussion

The results described in this chapter contribute to the understanding of antibody-ganglioside complex interactions in a number of ways. The most apparent observation is that the effect of ganglioside complexes on antibody binding has now been extended from the setting of neuropathy sera to include monoclonal antibodies. Whilst suggesting a wider importance for such interactions, this data also allows a number of other conclusions to be drawn. For example, data from polyclonal sera where binding is observed directed towards both single gangliosides and GSCs does not allow easy ascertainment of whether one antibody is able to bind both single gangliosides and complexes, or whether the range of binding seen represents a number of distinct antibodies.

Data from GSC ELISA and TLC-immuno-overlay demonstrates clearly that monoclonal antibodies raised against and reactive towards single gangliosides can additionally bind GSCs not containing this particular ganglioside, at least in certain circumstances. For example, the anti-GD1a antibody TBG2 also recognises an epitope formed by GM1:GT1b on ELISA, and the anti-disialosyl antibody CGM3 additionally binds GD1a:GD1b on TLC, and to a lesser extent on ELISA. This is intriguing but also somewhat disconcerting. It can be easily envisaged how, in a family of molecules with different but very much related structures, a recognition site on one ganglioside could be replicated by component sites on two other gangliosides. For example, a binding site created by the terminal Gal-GalNAc disaccharide and internal (attached to the inner galactose) disialosyl groups of GD1b might be recreated by the same terminal Gal-GalNAc disaccharide present on GM1, plus one internal sialic acid each from both GM1 and GD1a. Clearly, however, this is not the only potential

explanation. The presence of the second ganglioside may alter the orientation, or flexion of the oligosaccharide headgroup with respect to the lipid tail, of the first. This may then expose previously cryptic binding sites. Similarly, the presence of an additional ganglioside might simply alter the spacing of the first. For example, the terminal Gal-GalNAc disaccharide of GD1b would be expected to be spaced further apart, both in vitro and in vivo, by the greater volume occupied by its two internal sialic acids and hydration water. The terminal Gal-GalNAc disaccharide of GM1, alternatively, would pack closer together as this ganglioside has only one internal sialic acid. (Sonnino *et al.*, 2007) GD1a added to GM1 might then act as a spacer, pushing the headgroups of GM1 further apart and thus mimicking GD1b (Figure 3.16).

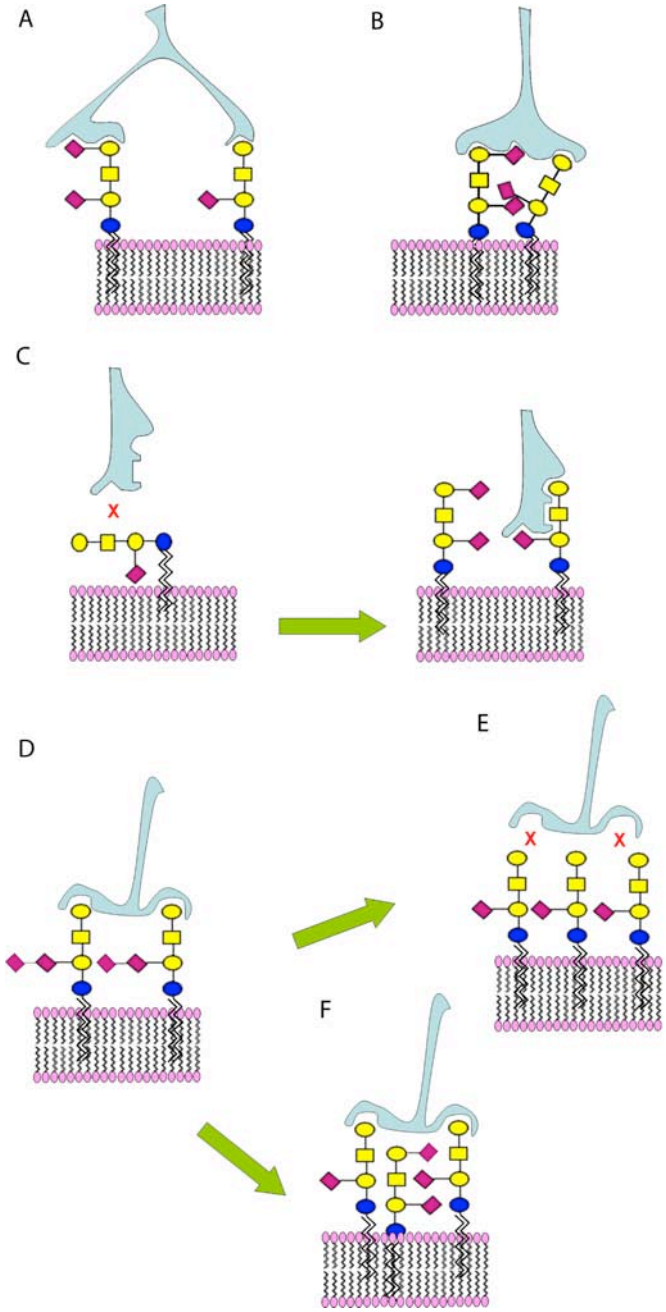

Figure 3.16 - Potential mechanisms of ganglioside complex mediated binding

Four different potential mechanisms by which the presence of a second ganglioside might enhance the binding of a lectin are illustrated, using GM1 and GD1a as an example. In the first (**A**) the proximity of two different glycolipids in the membrane allows them to occupy two discrete binding sites of a lectin, thus synergistically increasing the avidity of the interaction through the combined effect of two lower affinity bonds. In this example, the two gangliosides themselves do not chemically interact. This model could not be applied to antibodies, but may apply to other lectins with multiple glycan binding sites, such as bacterial toxins. In (**B**), GM1 and GD1a form a heterodimer, perhaps via the formation of hydrogen bonds, generating a neo-epitope with increased affinity for the lectin in comparison with either solitary ganglioside. In this example, monosaccharides from both component gangliosides are involved in the binding site. In (**C**), the binding site of one ganglioside is inaccessible until an interaction with a second ganglioside alters the orientation of the first. Only saccharide groups from one ganglioside contribute to the binding site. In (**D**), the spacing between two GD1b molecules is optimum to occupy a binding site. When GM1 is present alone (**E**), the closer packing of the headgroups no longer facilitates binding. When GD1a is also present (**F**), its interdigitation with GM1 alters the spacing of the latter ganglioside to resemble that of GD1b, and binding can occur.

However, given these thoughts and observations, it is not readily apparent whether the antigen established by *in vitro* techniques is the true target *in vivo*. In the case where multiple targets are suggested by solid phase assays, whether the antibody recognises one or more of these in the living membrane cannot seemingly be easily predicted.

The other significant finding with respect to ganglioside complexes and antibody interactions is the observation of the second ganglioside inhibiting binding of antibody to the first. This had been previously speculated to be the reason why anti-GM3 antibodies bound well to melanoma cells containing GM3 alone, but not to cells also containing more complex gangliosides such as GD2 and GD3, even when GM3 formed up to 50% of the total ganglioside content. (Lloyd *et al.*, 1992) A similar observation was made in vitro with the anti-DG1 mAb, which binds GM1 in isolation but not in the presence of GD1a. The fact that an apparently similar antibody (DG2) remains able to bind GM1 in such circumstances suggests a hitherto unsuspected mechanism whereby the fine specificity of anti-GM1 antibodies might prove critical to their pathogenic potential. This was born out by the elegant series of experiments performed by Dr Greenshields. The initial observation was that DG1 failed to bind, whereas DG2 bound strongly, to ex vivo neuromuscular preparations from GD3s$^{-/-}$ mice (Figure 3.17).

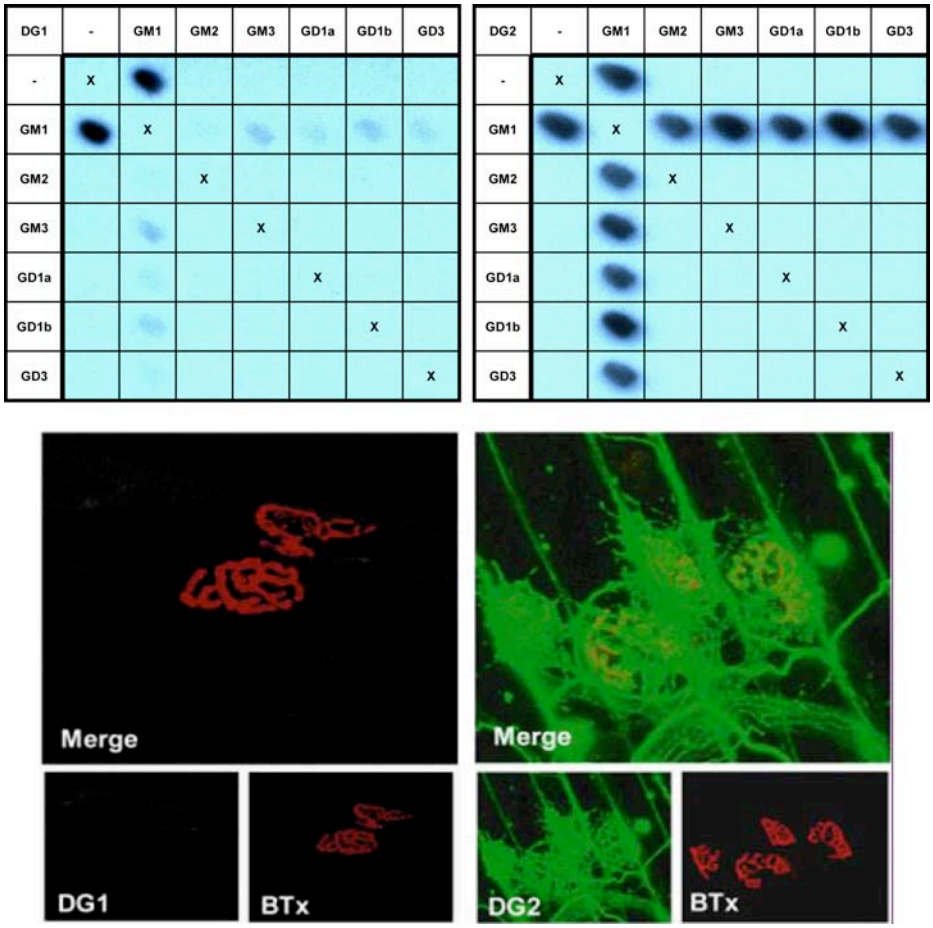

Figure 3.17 - The disparate ex vivo binding patterns of two anti-GM1 monoclonal antibodies

DG2 binds to the presynaptic apparatus of the NMJ in GD3s$^{-/-}$ mice, whereas DG1 does not (lower panels, kindly supplied by Dr Kay Greenshields). This is compared with the inhibition of DG1 binding to GM1 by other gangliosides seen on the PVDF glycoarray and the ability of DG2 to bind GM1 regardless of the presence or absence of a second ganglioside (upper panels).

After neuraminidase treatment to unmask GM1 by converting GD1a to GM1, binding of DG1 was observed to occur. Of course, in this situation, DG1 might simply be binding to *de novo* GM1 produced by the enzymatic cleavage of the terminal sialic acid of GD1a. Pre-blocking native GM1 with cholera toxin B subunit (CTB) prior to neuraminidase treatment, however, substantially reduced the binding of DG1, indicating only a proportion of the binding seen was to *de novo* GM1. Examination of IgM GM1-antibodies (SM1 and DO1, (Willison *et al.*, 1994;Paterson *et al.*, 1995)) cloned from patients with multifocal motor neuropathy (MMN) showed that they also displayed the same properties as DG1, attesting to the clinical importance of these observations (Greenshields *et al.*,

2009). It is apparent that the interaction of anti-GM1 antibodies with their target in solid phase assays does not necessarily imply that they will bind GM1 in the living membrane. Such antibodies could become important if the membrane is disturbed, for example by neuraminidase or during regeneration, when GM1 is then exposed for binding. Additionally, it was shown that the 'non-pathogenic' DG1 mAb was able to interact with the LOS GM1 mimic on the surface of both live and dead *C.jejuni* even when this was co-expressed in a 50:50 ratio with the GD1a mimic. (Greenshields *et al.*, 2009) This implies that certain GM1 antibodies might be protective against infection, without compromising self tolerance, at least under normal circumstances. Furthermore, such studies underscore the importance of the fine specificity of anti-GM1 antibodies with respect to their pathological effects, and provide a potential explanation for the previous discrepant results obtained with such antibodies.

The identification of mAbs with ganglioside complex modulated binding has allowed the assessment of factors potentially confounding the hypothesis that the interacting presence of the second ganglioside itself is critical. The TBG2 and DG1 ELISAs demonstrate that simple dilutional effects do not account for complex enhanced or attenuated binding. The idea that a straightforward summation of affinities towards each single ganglioside is responsible is countered by the observation that prior sonication of the two ganglioside mixture is required to demonstrate a modulatory effect, at least in some cases. It may be that the energy supplied by sonication breaks apart micelles containing each single ganglioside and allows them to reform as complex mixtures. There is now both direct and indirect evidence that the presence of one ganglioside does not significantly enhance or impair binding of the other to the assay surface. For example, as binding to GM1:GD1a has been observed to be

both enhanced and attenuated (as well as unaltered) as compared to GM1 alone by ELISA, it is difficult to consistently support the argument that the amount of GM1 binding to the plate is either increased or decreased. Furthermore, direct evidence from the PVDF array shows that the amount of GM1 attached to the membrane is not significantly different in the presence or absence of GD1a.

The above results also expand the concept that lectin-glycolipid interactions can be dependent on the surface used for the assay, the presence of accessory lipids, and whether or not the glycolipids are applied in aqueous phase. Similar observations have been made previously with regard to neuropathy sera binding single gangliosides. Here temperature, and whether or not liposomes were employed to present the ganglioside, both had profound, but not universal, effects on such interactions (Willison & Veitch, 1994). The data presented above also highlights the difficulty in predicting the consistency of binding patterns across different surfaces and assays, and in confirming the binding observed *in vitro* correlates with that which may or may not occur in the living membrane. Differences seen between the TLC, ELISA and PVDF array might simply be due to differences in antigen density. However, an estimation involving the well versus spot area, and concentrations and volumes of ganglioside applied suggests this should be similar between ELISA and PVDF – as was intended when developing the new assay- albeit making a number of assumptions, such as total binding of all of the applied ganglioside to the surface and no spreading of the solvent beyond the contact area on PVDF.

Another potential explanation is that the interaction of the gangliosides with the surface used for the assay (silica for TLC, polystyrene for ELISA, or PVDF) is affected by how hydrophilic each material is, and/or by differences in surface

charge. This might change the orientation of ganglioside attachment, cause different flexion of the headgroup with respect to the lipid tail, and variously facilitate or inhibit ganglioside-ganglioside interactions. In an extreme example, a positively charged surface might bind directly to the negative charge of the oligosaccharide headgroup, in which case the ganglioside might be presented 'upside down' as compared with a hydrophobic membrane in which the lipid tail would be buried and the headgroup protrude above. As has been discussed, all of these factors could potentially modulate antibody accessibility and interaction.

It is also apparent that there is a further level of fine specificity even within the concept of anti-ganglioside complex antibodies defined by ELISA, as demonstrated by the observations made with GM1:GD1a. Certain mAbs are able to bind this complex on ELISA, but not PVDF, whereas different sera remain able to bind in both settings. It may be that some antibodies are more sensitive than others to changes in target antigen spacing or orientation. It is therefore possible that some mAbs developed for use in *in vivo* assays are not fully representative of the fine specificities of the immunoglobulin found in disease associated sera, even when their binding pattern on ELISA appears identical.

The idea that complex specific, independent and attenuated antibodies have different pathological effects *in vivo* is intriguing. The experiment detailed in 3.2.13 highlights the pitfalls in attempting to use human sera to address this hypothesis. First of all, one cannot be sure that a single monoclonal antibody is being investigated, as each sample could potentially contain numerous antibodies of differing specificities from multiple expanded antibody producing clones of greater or lesser importance. Furthermore, the limited volumes most usually available permit only a restricted analysis of the complex binding pattern

in solid phase assays. A similar problem is posed by neuromuscular tissue studies. Ideally, organ bath preparations with live membranes would be performed, but these require more serum than is routinely obtainable. Despite the prior hypothesis that ganglioside complexes are disturbed in frozen sections, this was the only tissue based assay which could be practicably performed. In this context the lack of detectable binding seen with all of the three sera is difficult to interpret, and certainly no firm conclusions can be drawn from this, very limited, data. The fact that even the complex independent GA1 specific and complex attenuated GM1 specific sera (B and C) failed to bind suggests the possibility that the assay itself was flawed. The lack of an adequate positive control for this assay unfortunately means that even this assertion remains speculative.

The final contribution detailed in this chapter is the newly developed, combinatorial, PVDF glycoarray. This has been shown to be a suitable method for screening large numbers of lectins for complex modulated binding. The assay variability falls within acceptable limits, and is comparable with ganglioside ELISA. Furthermore, it is considerably more efficient than the existing techniques when considering the antigenic diversity generated by a combinatorial approach. This has utility not only in the setting of testing clinical series of neuropathy sera, but also in examining other families of lectins, as detailed in the subsequent chapter.

4 The ganglioside binding properties of bacterial toxins and siglecs

4.1 Introduction

Gangliosides are not only important as auto-antibody targets in immune neuropathies, as previously discussed. Protein-carbohydrate interactions are also involved in a wide variety of other biological processes, including cell-cell interactions and signalling, immune system modulation, bacterial toxin binding and microbial adherence. It was therefore speculated that ganglioside complex (GSC) formation might also influence lectin binding in these other systems. If such modulation was found to occur, this would have a profound impact on the understanding of all of these processes, potentially forcing a revaluation of protein-carbohydrate interactions in a more general sense. The newly developed PVDF glycoarray allowed screening of various lectins for binding against a range of gangliosides and their 1:1 complexes.

Recombinant chimeras containing the extracellular region of siglecs fused to the Fc domain of human IgG1 were kindly provided by Professor Paul Crocker (Dundee, Table 4.1). A horseradish peroxidase conjugated binding fragment of tetanus neurotoxin (TENT-HC-HRP) was prepared and provided by Professor Giampietro Schiavo (London). This neurotoxin has previously been demonstrated to bind GD1b ganglioside (Deinhardt *et al.*, 2006). Cholera toxin B subunit linked to HRP is available commercially (Calbiochem, USA) and is known to avidly bind GM1 (Lencer *et al.*, 1999).

Siglec	Concentration	Previously reported binding pattern
Sialoadhesin-Fc	0.3mg/ml	GQ1bα>>GD1a=GT1b>>GM3=GM4
MAG-Fc	0.1mg/ml	GD1a, GT1b
Siglec-7-Fc	0.6mg/ml	GD3, GQ1b, GT1b
Siglec-E-Fc	1.5mg/ml	GM3, GD3, GT1b, GQ1b
Siglec-F-Fc	0.8mg/ml	GQ1b>GT1b
Siglec-9-Fc	4.5µg/ml	
MAG-Fc	2.9mg/ml	GD1a, GT1b
Sialoadhesin-1-3-Fc	8.1mg/ml	

Table 4.1 - Siglecs provided by Prof. Paul Crocker

The first 5 siglecs in the list were provided as purified proteins. The last three were provided in a second batch as tissue culture supernatants. Sialoadhesin-1-3-Fc is a truncated mouse siaoladhesin construct. Siglec-E is a mouse siglec showing overlapping function with human siglecs 7 and 9.

4.2 Results

4.2.1 Siglec-ganglioside interactions are modulated by ganglioside complexes

Of the provided siglecs, binding to any gangliosides by ELISA and PVDF array was only detected for siglecs 7, E and F. Nevertheless, all three of these lectins exhibited binding which was modulated by GSCs. Once again, different patterns were sometimes seen when ELISA was compared with PVDF.

Siglec-E-Fc binds to GM2:GT1b on PVDF, while showing no signal for GM2 alone and only very weak binding to GT1b. Furthermore, this pattern is repeated on ELISA. In contrast, siglec-F-Fc reacts with GM2 alone as assessed by the PVDF array, remains able to bind this target in the presence of GT1b (i.e. binds to the GM2:GT1b complex), but is inhibited from GM2 binding in the presence of GM1 (fails to bind to GM1:GM2). On ELISA, siglec-F binding to GM2, GT1b and GM2:GT1b is not significantly elevated above background (Figure 4.1). Both of these siglecs also bound GD1a and GD1a series complexes to a variable extent.

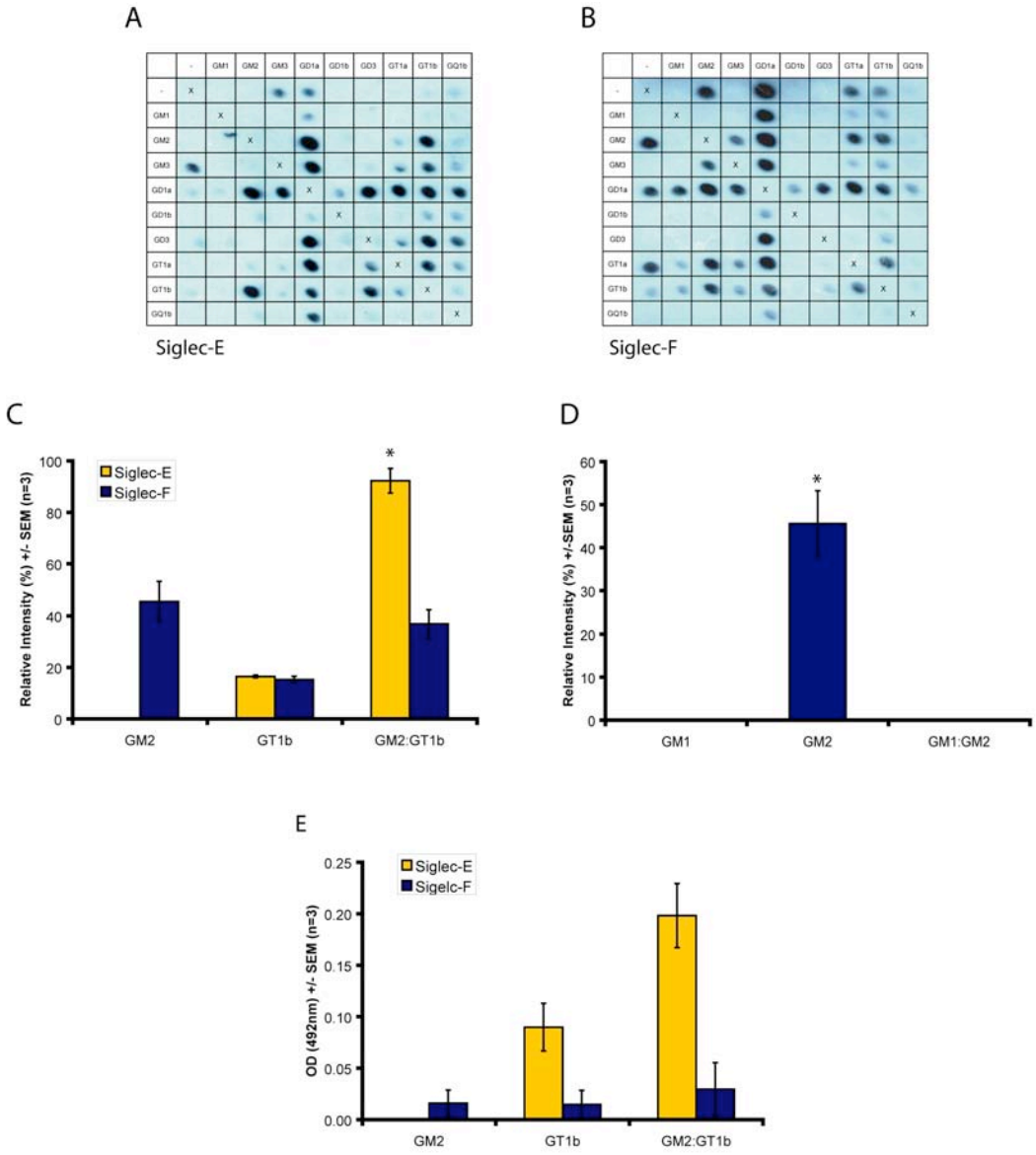

Figure 4.1 - The binding of siglecs E and F is modulated by ganglioside complexes

Example processed PVDF grids of siglec-E-Fc (**A**) and siglec-F-Fc (**B**) are shown. By this method, the binding of siglec-E to GM2:GT1b (**C**) is significantly increased as compared to sum of the intensities for GM2 and GT1b alone (an absolute binding intensity increase of 75%, p=0.004). Siglec-F Binds to GM2, and to a lesser extent GT1b, but binding to GM2:GT1b is not significantly different to the sum of these. In contrast, binding of this siglec to GM2 is significantly impaired by the GM1:GM2 complex (**D**, an average intensity reduction of 45%, p=0.027). On ELISA (**E**), the enhanced binding of siglec-E to GM2:GT1b is also seen, but just fails to reach significance (p=0.068). All statistical comparisons used a two-sample, two-tailed T-test, with an α-level of 0.05.

Siglec-7 is a human cell surface receptor present on natural killer cells and monocytes. It has previously been established to bind disialylated gangliosides such as GD3, GT1b and GQ1b.

This binding pattern was confirmed by PVDF glycoarray, but a further level of complexity was revealed. Most strikingly, the interaction of siglec-7 with GD3 is very significantly attenuated by certain complexes. The interaction with GD3 in isolation yields a mean relative signal intensity of 70.3%, yet the intensity seen with complexes of GD3 and any of GM1, GM2, GD1a, GD1b and GT1a is reduced at between 0.62% and 14.7% ($p<0.0001$, GLM ANOVA with Dunnett correction, family error rate 0.05, $n=3$). Furthermore, siglec-7 binding was modulated by a number of other complexes as compared to the component gangliosides in isolation (Figure 4.2A). The inhibitory effect of GM1 on GD3 binding was also observed to occur by ganglioside complex ELISA and liposome ELISA (Figure 4.2B).

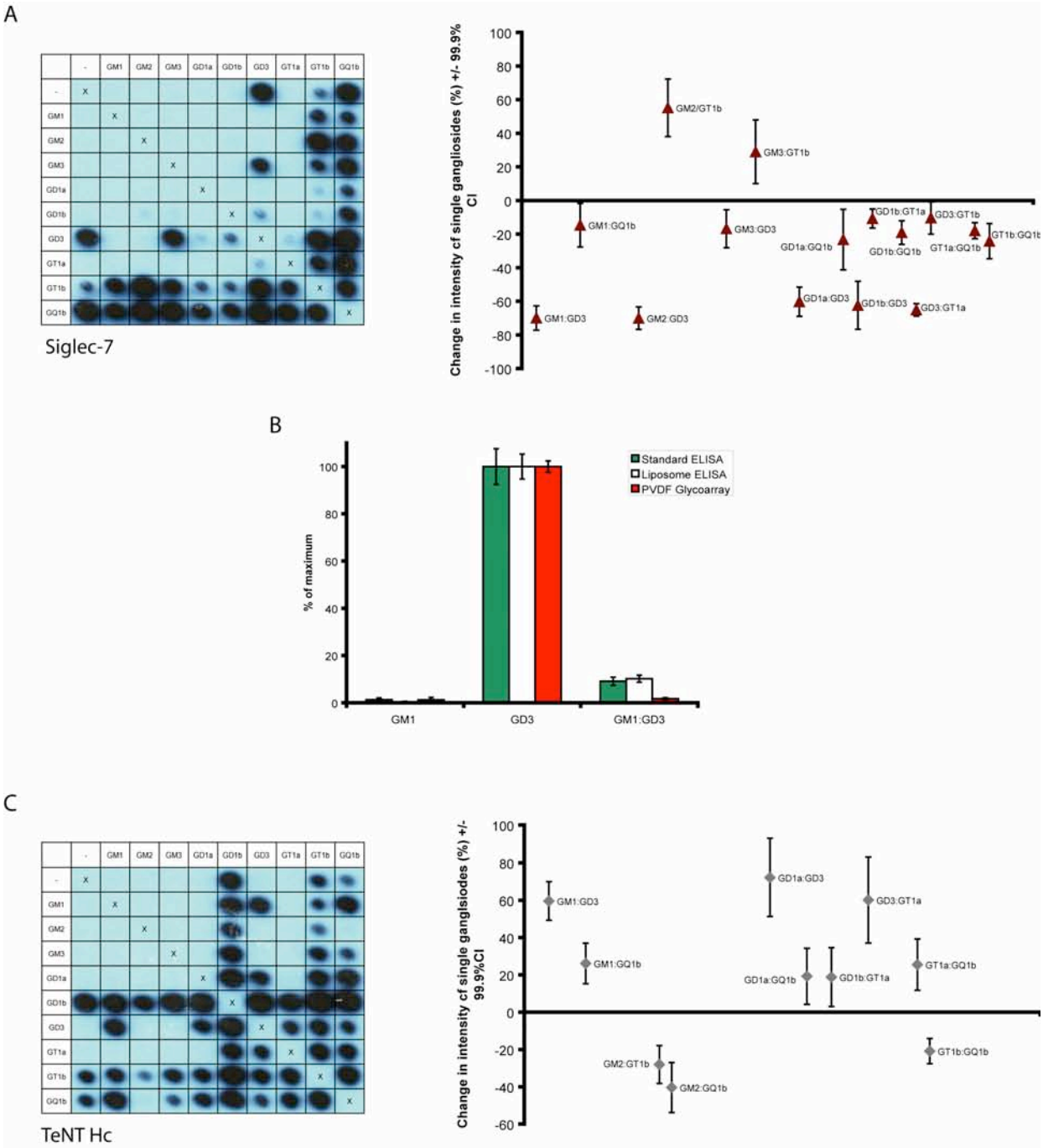
A
Siglec-7
Change in intensity cf single gangliosides (%) +/- 99.9% CI
GM2/GT1b
GM3:GT1b
GM1:GQ1b
GM3:GD3
GD1a:GQ1b
GD1b:GT1a
GD3:GT1b
GD1b:GQ1b
GT1a:GQ1b
GT1b:GQ1b
GD1a:GD3
GD1b:GD3
GD3:GT1a
GM1:GD3
GM2:GD3
B
% of maximum
Standard ELISA
Liposome ELISA
PVDF Glycoarray
GM1
GD3
GM1:GD3
C
TeNT Hc
Change in intensity cf single ganglsiodes (%) +/- 99.9%CI
GM1:GD3
GD1a:GD3
GD3:GT1a
GM1:GQ1b
GD1a:GQ1b
GD1b:GT1a
GT1a:GQ1b
GM2:GT1b
GT1b:GQ1b
GM2:GQ1b
D
Realtive Intensity (%)
Siglec-7
TeNT Hc
GD3
GD1b
GT1b
GQ1b
GD3/GM1
GD3/GM2
GD3/GM3
GD3/GD1a
GD3/GD1b
GD3/GT1a
GD3/GT1b
GD3/GQ1b

Figure 4.2 - Siglec-7 and TeNT H_C binding is modulated by ganglioside complexes

(**A**) Complex mediated binding of siglec -7 to gangliosides as demonstrated by PVDF glycoarray. The accompanying graph shows the complex reactivity which significantly differs from the sum of the binding intensities of the two component gangliosides, and the magnitude and direction of the change. The inhibitory effect of GM1 on siglec-7 interaction with GD3 is also seen on standard and liposome ELISA (**B**). The average absolute values from each set of three independent experiments have been normalised to 100% to allow comparison in the same histogram. Uncorrected maximum binding values were 0.34, 1.14 and 70.3% for standard ELISA, liposome ELISA and PVDF glycoarray respectively. Tetanus toxin (**C**) also displays complex mediated binding on PVDF. The accompanying graph again shows the complex reactivity which significantly differs from the sum of the binding intensities of the two component gangliosides, and the magnitude and direction of the change. When compared with siglec-7, the opposite effect is seen with respect to GD3 and GM1:GD3, with siglec-7 binding being inhibited and TeNT H_C enhanced by the complex (**D**). Asterisks denote complexes showing binding levels significantly different from the sum of the two individual components. Although some of the non-asterisk marked complex binding intensities are significantly different to one or other of the component gangliosides, they are not different to the sum of intensities of the component gangliosides.

4.2.2 Certain bacterial toxin-ganglioside interactions are complex modulated

Analogous to siglec-7 and GD3, the sialic acid binding fragment of tetanus toxin (TeNT H_C) is strongly inhibited from binding GQ1b in the presence of GM2 (Figure 4.2C, p=0.002, GLM ANOVA with Dunnett correction, family error rate 0.05, n=3). The interaction of TeNT H_C with GD3 series complexes is in marked contrast to siglec-7, however (Figure 4.2D). The toxin does not bind the single gangliosides GD3, GM1, GD1a or GT1a, yet reacts strongly with complexes of these gangliosides containing GD3. As previously discussed, a confounding factor in attributing this effect to the formation of a neo-epitope is that lower degrees of binding to individual glycolipids could simply summate. To take into account this possibility, the previous ELISA definition (that for true complex reactivity, the optical density - OD - for the complex must exceed the sum of the individual ODs) (Kaida et al. 2007b) has been expanded to include an additional degree of statistical rigor. Complex modulated binding is defined as the state in which the signal intensity of the complex minus the sum of the signal intensities of the isolated glycolipids (to a maximum of 100%) is significantly different from zero. Interactions meeting this definition are marked with an asterisk on the histogram (Figure 4.2D). The magnitude of the effect along with confidence intervals is depicted in the graphs of Figure 4.2A+C.

Unlike TeNT H_C, cholera toxin B subunit (CTB) binding was not complex modulated. There was no significant difference in CTB binding to GM1 as compared with any of the GM1 containing complexes at a 1:20,000 dilution (GLM ANOVA with Dunnett correction, family error rate 0.05, n=3). Furthermore, to demonstrate that the apparent uniformity of CTB binding in this situation was

not simply a result of saturation, a higher concentration of 1:10,000 was also assayed. The absolute intensity for each complex with the higher concentration was increased, showing that the signal is not saturated at the lower concentration, and again there was no significant difference in binding to GM1 as compared with any of the GM1 containing complexes. Results for the 1:20,000 dilution have been normalised to the most intense spot at 1:10,000 to reflect this (Figure 4.3).

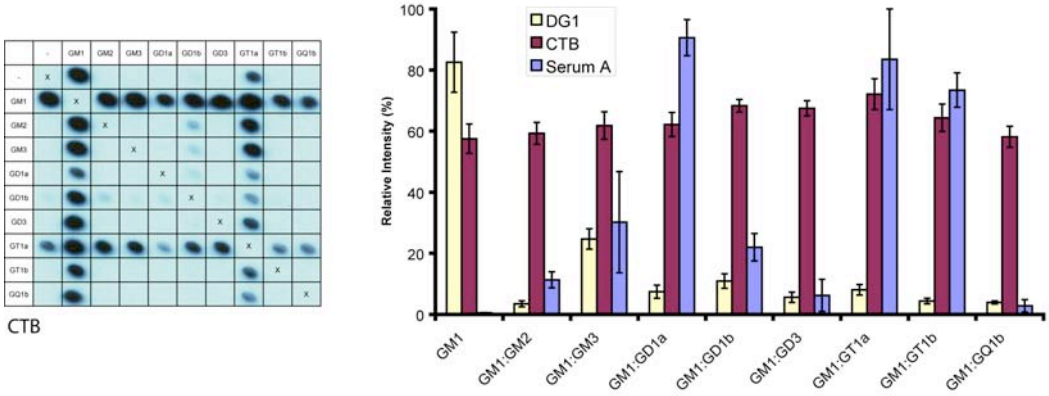

Figure 4.3 - Cholera Toxin B subunit binding to GM1 is unaffected by complexes

Unlike TeNT H_C, CTB's interaction with GM1 is unaffected by the presence or absence of partnering gangliosides. An example membrane following the application of CTB at 1:20000 dilution for 2 minutes is shown. The accompanying graph shows the signal intensity for GM1 complexes is not significantly different to that of GM1 alone. The relative intensity for CTB at 1:20000 has been normalised to the most intense spot on a separate array probed with CTB at 1:10000, demonstrating the signal seen at 1:20000 is not saturated. The complex independent binding of CTB is contrasted with the complex attenuated binding of DG1 and complex enhanced binding of serum A. Note that, on this graph, comparisons between the signal intensity obtained for the different lectins are not valid, as they have been normalised within their own set of experiments. Instead, these other lectins are included merely to compare the different patterns of complex binding seen.

4.3 Discussion

These results demonstrate that the implications of ligand-enhancing and -attenuating complexes are wide ranging as illustrated in by the following examples. Siglec-7 is a CD33 related human natural killer cell receptor (Avril et al. 2006a), and siglecs E and F are mouse lectins found on neutrophils, monocytes, dendritic cells, and eosinophils, respectively. Siglecs are involved in self/non-self recognition, yet their ligands are present on host cells an as well as on many pathogens (Crocker et al. 2007). The further level of complexity introduced by *cis* interacting glycolipids could allow fine-tuning of siglec-dependent recognition relevant to host immunity (Avril et al. 2006b).

TeNT H_C initially binds to GD1b on the axonal surface, yet when the toxin is internalised, the ganglioside remains on the plasma membrane.(Deinhardt et al. 2006) During the internalisation at the plasma membrane, GD1b might be sequestered by a different complex, reducing its affinity for TeNT H_C, and allowing the dissociation of the toxin from the ganglioside prior to internalisation. Although we have not demonstrated a dramatic on-off effect for TeNT H_C binding to GD1b series complexes, the statistically significant differences in signal intensity between a number of different GD1b complexes may have biological relevance. Alternatively, other GD1b-complexes not studied in the current array format may prove important *in vivo*. Conversely, CTB displays complex independent binding to GM1 and enters cells bound to GM1 (Lencer et al. 1999; Lencer 2004), reinforcing the notion that glycolipid complexes cannot modulate dissociation of CTB from GM1 prior to internalisation. These examples highlight the subtle ways in which differing glycolipid interactions could modify lectin binding and thereby modulate any

subsequent functional or pathological effects. Furthermore, many membrane proteins are glycosylated, and these oligosaccharides interact with other protein and carbohydrate molecules, with functional importance in processes such as cell-cell interaction (Hakomori 2002). It is possible that the heterogeneous clustering of oligosaccharides in this paradigm might also influence such processes. To date, the only direct evidence for the existence of ganglioside complexes in nature is detailed in the studies already discussed (Greenshields et al. 2009; Todeschini et al. 2008; Todeschini and Hakomori 2008). In light of the observations detailed in this chapter, however, it would seem that looking for other potentially pathophysiologically relevant glycolipid complexes and assessing their modulatory effects *in vivo* will prove to be a fruitful area of future research.

Although current considerations of the modulatory effects of ganglioside complexes, including this one, have dealt with only heterodimers, it is possible that even more intricate interactions, involving three or more glycolipids, might prove equally as important. Investigating such situations becomes increasingly more difficult as the number of component glycolipids increases, making the ability to automatically array ligands described here even more valuable.

At present, there is a conceptual mismatch between assessing lectin interactions *in vivo*, where many accessory factors in plasma membranes will influence binding, and *in vitro*, where investigations have almost exclusively focussed on assessing reactivity to isolated, purified oligosaccharides in artificial systems (for example Blixt et al. 2004; Byres et al. 2008). This concept, and its practical demonstration, reveals new horizons in the study of diverse processes including cell-cell recognition, toxin binding, autoimmunity and microbial invasion.

The results detailed in this chapter also further reinforce that concept of three distinct patterns of lectin binding with respect to glycolipid complexes. For both GM1 and GD3 series complexes in particular, complex enhanced, complex independent and complex attenuated binding has been demonstrated (Figure 4.4). Furthermore, these results also provide further evidence that the attenuation and enhancement of lectin binding seen is not simply a result of dilution of one lipid, glycolipid or ganglioside by another. For example, for tetanus toxin, simply diluting the GD3 with GM2 or GM3 has no effect on binding, whereas GD3 plus GM1 leads to a significantly enhanced signal. The same argument can be made for serum A reactivity with GM1:GD1a complex. If GM1 is instead 'diluted' with GD3 or GQ1b, or GD1a with GM3, GM3, GD3, GT1b or GQ1b, no binding results. Likewise, the inhibitory effect of GM1 on GD3 binding by siglec-7 is not replicated by dilution of GD3 with GM3.

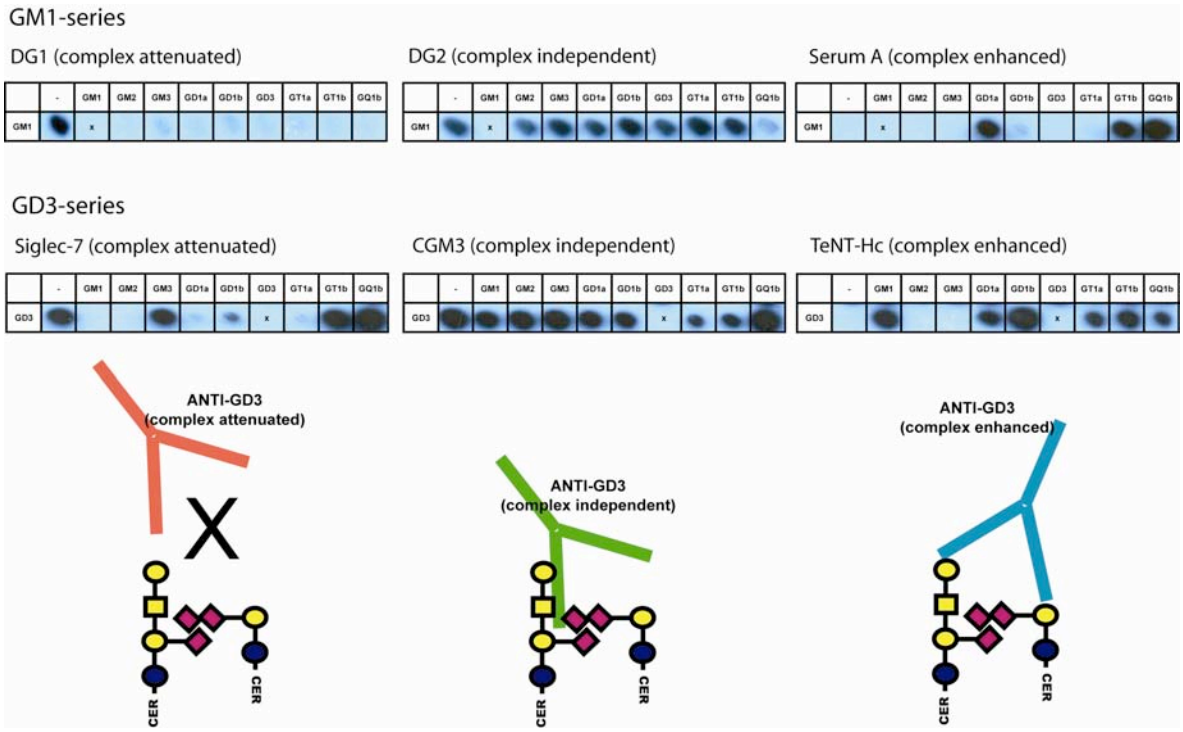

Figure 4.4 - Complex attenuated, complex independent and complex enhanced binding

Three distinct patterns of lectin-carbohydrate interaction have been demonstrated, both for GM1-series and GD3-series complexes. With complex attenuated binding, the lectin is able to interact with either GM1 or GD3 in isolation, but when a GM1:GD3 or GM1:GD1a complex is formed binding is prevented, possibly because the binding site is now cryptic. In complex independent binding, the lectin-carbohydrate interaction is unaffected by the presence or absence of a second partnering glycolipid. For complex enhanced binding, the GM1:GD3 or GM1:GD1a complex is bound, with no significant reactivity seen for either component ganglioside in isolation.

5 Anti-ganglioside and glycoplipid complex antibodies in a cohort of Guillain Barré syndrome patients

5.1 Introduction

The previously described observations provided the background and extra impetus to screen a large cohort of sera from GBS patients against a spectrum of ganglioside complex antigens using the PVDF glycoarray. Opportunistic studies using locally obtained samples on an ad hoc basis had further demonstrated that both complex enhanced and attenuated patterns of binding could be seen (Figure 5.1).

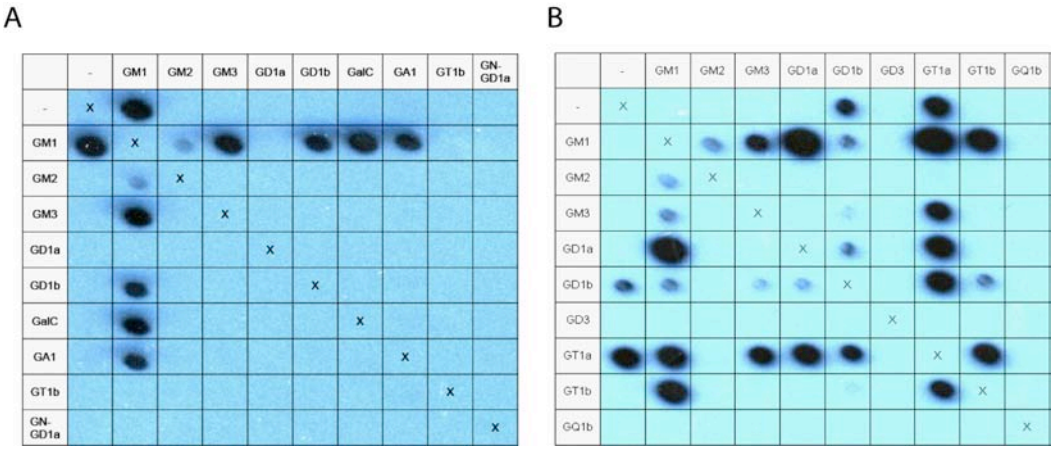

Figure 5.1 - Complex attenuated and enhanced binding in neuropathy sera

Binding of IgM antibodies in sera from a patient with multifocal motor neuropathy (MMN, **A**) follows a complex attenuated pattern. Binding is detected towards GM1 in isolation, but is not seen with GM1:GD1a complex, similar to the pattern of binding described for the monoclonal antibody DG1 in chapter 1. In contrast, sera from a patient with acute motor axonal neuropathy (AMAN, **B**) demonstrates enhanced binding to the GM1:GD1a complex by IgG as compared with GM1 and GD1a in isolation.

A large cohort of GBS associated sera, with parallel clinical data, were available via collaboration with the research group of Dr Bart Jacobs in Rotterdam.

Combined with the PVDF glycoarray, this provided the opportunity to screen a large number of sera against a large number of complex antigens. In the simplest terms, this allowed us to address the hypothesis that potential antigenic targets in GBS had been previously overlooked because the combinatorial aspect had either been overlooked entirely, or, more recently, only addressed for a limited number of complexes (Kaida *et al.*, 2004;Kaida *et al.*, 2006;Kaida *et al.*, 2007), given the constraints of the ELISA system used. In addition to addressing many of the apparent serological-pathological inconsistencies as detailed in the introduction and further highlighted in chapter 3 above, this part of the study also has the capability to further develop some of the potential clinical applications of GBS immunology.

As mentioned, the diagnosis of GBS is largely a clinical one, supported by cerebrospinal fluid analysis and nerve conduction studies, both of which may also be normal, especially early in the disease course (Asbury & Cornblath, 1990;van der Meche *et al.*, 2001). Likewise, current immunological assays in clinical use for the detection of anti-ganglioside antibodies are more often negative than positive in the disease. Therefore, if a more sensitive and specific immunological test could be derived, based on the PVDF glycoarray, this has the potential to refine and improve the diagnostic process. Furthermore, predicting prognosis and severity of GBS early in the disease can be difficult, although a recently derived clinical scoring system has been shown to be accurate predictor of the requirement for mechanical ventilation, one of the most feared complications (Walgaard *et al.*, 2010). In addition, previous analysis of GSC antibodies using ELISA has demonstrated a significant association between the presence of GD1a:GD1b and/or GD1b:GT1b complex antibodies and severe disability and the requirement for mechanical ventilation (Kaida *et al.*, 2007). It

was postulated that the fine specificity and more distinct patterns of antibody response revealed by the PVDF array might be better correlated with such important clinical parameters.

5.2 Results

5.2.1 Patient cohort

5.2.1.1 Patients

The patients in this cohort had previously participated in a clinical trial investigating methylprednisolone as an add-on to IVIg treatment in 225 GBS patients. (van Koningsveld *et al.*, 2004) Inclusion criteria were fulfilment of the NINDS diagnostic criteria for GBS, (Asbury & Cornblath, 1990) being unable to walk unaided ten metres across an open space (GBS disability score 3 or more) and onset of weakness within two weeks before randomization. Exclusion criteria were age below six years, previous GBS, known severe allergic reaction to properly matched blood products, pregnancy, known selective IgA deficiency, previous steroid therapy, severe concurrent disease, inability to attend follow-up, or contraindications for corticosteroid treatment. Approval was granted by an ethical standards committee on human experimentation for the study mentioned above. Written informed consent was received from all patients. To be included in the current study sufficient amounts of pre-treatment serum had to be available to perform the combinatorial glycoarray. Twenty samples were obtained from healthy controls in parallel with collection of the GBS associated sera, and a further 54 from healthy controls at the University of Glasgow and Southern General Hospital, Glasgow.

5.2.1.2 Clinical data

Baseline characteristics (age, gender), preceding diarrhoea or symptoms of an upper respiratory tract infection, cranial nerve dysfunction, motor function, GBS

disability score, and sensory deficit at study entry were collected prospectively. The GBS disability score is a widely accepted scale to assess functional status of GBS patients, ranging from zero (normal) to six (death). (Hughes *et al.*, 1978) Serological screening was performed to determine recent infections with *Campylobacter jejuni*, cytomegalovirus (CMV), Epstein-Barr virus (EBV), and *Mycoplasma pneumonia*. The serum samples used were obtained within four weeks from onset of weakness and before start of treatment.

Clinical data was available for 180 of 181 patients (99.4%). 103 were male (57.2%) and 77 female (42.8%). The mean age of patients was 52.6 years (range 7 to 89). Electrophysiological data was available for 149 out of 181 patients (82.3%). The majority were classified either as AIDP (56, 37.6%) or equivocal (85, 57.0%). Only 4 patients had electrophysiology consistent with the axonal variant AMAN (Figure 5.2).

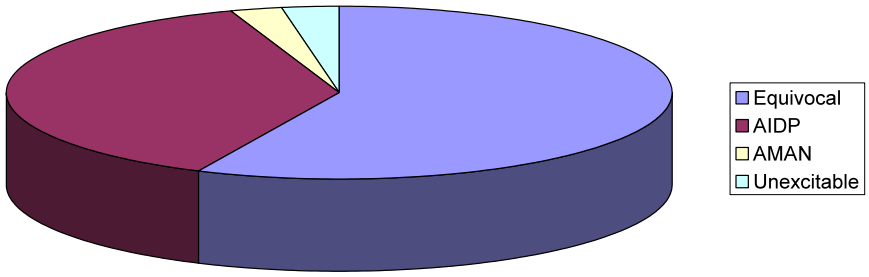

Figure 5.2 - Electrophysiological categorisation of disease subtype

Electrophysiological data was available for 149 patients in the cohort. The majority were classified as equivocal on this basis. 56, or 37.6%, were electrically confirmed as AIDP, with only 4 (2.7%) classified as AMAN.

Severity scores were recorded at a number of time points, using the GBS disability score. Data is shown for the severity score at randomisation (day 0), day 9, week 4, week 8, week 26 (Table 5.1).

GBS Disability Score		Day 0	Day 9	Week 4	Week 8	Week 26
0	healthy	0	0	2	11	40
1	minor symptoms, capable of running	0	3	32	59	79
2	able to walk 10 m unassisted, but unable to run	0	18	60	45	26
3	able to walk 10m over open space with help	46	45	16	20	11
4	bedridden or chair bound	126	81	47	29	10
5	needs ventilator at least for part of day	8	33	21	10	0
6	dead	0	0	2	2	5

Table 5.1 - GBS disability score at selected time points

Over the course of their disease, 41 patients (22.8%) required mechanical ventilation at some point. There were 5 deaths (2.8%).

There was a preceding history of upper respiratory tract infection (URTI) in 65 patients (36.1%), and diarrhoea in 49(27.2%). Campylobacter jejuni, cytomegalovirus and *Mycoplasma pneumoniae* serology was positive in 50, 24 and 11 patients (27.8, 13.3 and 6.1%) respectively. 93 (51.7%) had cranial nerve deficits during follow up, and 17 (9.4%) had bulbar involvement. A further breakdown of the cranial nerves affected is given in Table 5.2.

Cranial Nerve	Number Affected	Percentage
Optic	0	0.0
Oculomotor	6	3.3
Trochlear	3	1.7
Abducens	5	2.8
Trigeminal	9	5.0
Facial	53	29.4
Glossopharyngeal / Vagus	16	8.9
Accessory	9	5.0
Hypoglossal	4	2.2

Table 5.2 - Breakdown of cranial nerve deficits

5.2.2 Target selection

The choice of glycolipids to use in this assay was directed by three parameters; the detection of the molecule in peripheral nervous system (PNS) myelin or axonal extracts, previous reports of neuropathy sera reactivity against the glycolipid, and the availability of the glycolipid, either commercially or via collaboration with other investigators. An initial screen using a 10x10 array consisting of sulfatide, galactocerebroside, GM1, LM1, GD3, GD1a, GD1b, GT1a, GT1b, and GQ1b and the resulting 45 1:1 complexes was performed by Dr Kathryn Brennan. Following the success of this initial screen, a larger, 28x10 array composed of the single glycolipids listed below (Table 5.3), and the 1:1 complexes of these not already tested, was performed by me. The results of these two screens were then combined before the final analysis was performed. Overall, 19 single glycolipids and 162 1:1 complexes were investigated, giving 181 different target antigens in total

1	Sphingomyelin
2	Phosphatidylserine
3	Gb4Cer / globoside
4	ceramide trihexoside (CTH)
5	Sulfated glucuronyl paragloboside (SGPG)
6	GM2
7	GM3
8	GD2
9	Asialo-GM1
10	Galactocerebroside
11	LM1
12	GM1
13	GD1a
14	GD1b
15	GD3
16	GQ1b
17	GT1b
18	Sulfatide

Table 5.3 - Single glycolipids used in the 28x10 PVDF glycoarray

GT1a was additionally included in the 10x10 array.

5.2.3 Validation of intra- and inter assay variation for sera

The inter- and intra-assay coefficients of variation for a 10x10 PVDF glycoarray were previously calculated at 4.1% and 8.6% respectively, using an anti-GM1 monoclonal antibody. Using serum positive for GA1 and GA1:sulfatide complex, the intra-assay coefficients of variation using the larger grid and neuropathy sera were calculated as 12.3% and 14.1% for these two antigens, from nine 28x10 arrays produced and processed over a 3 month period, representative of the time taken to process the 255 serum samples.

5.2.4 Summary array data

Overall, serum from 113 GBS patients (62.4%) versus 11 controls (14.9%) showed IgG binding to one or more target antigen ($p<0.001$, X^2), defined as a visible spot, in a location corresponding to applied antigen, with a corrected arbitrary intensity greater than zero following background subtraction. There are theoretical reasons for suspecting IgG to be the pathogenic entity in GBS and other subclass reactivities were not sought. Only 39 of the 181 sera were positive on a standard, contemporaneous GM1, GD1a, and GQ1b ELISA (Kuijf *et al.*, 2005), and all but one of these samples was also positive on the array.

This gives a sensitivity of 62.4% and a specificity of 85.1% for the test as a whole. The global likelihood ratios for the test are therefore calculated to be 4.2 (positive) and 0.4 (negative). Reactivity towards 176 different single antigens and complexes was seen with serum from GBS patients (97.2%), whereas control sera was only seen to bind to 31 (17.1%) of the 181 different antigens across both arrays ($p<0.0001$, Binomial Analysis of Means).

By this definition (a visible spot with a corrected arbitrary intensity greater than zero following background subtraction), the glycolipid complex element of the array increased the number of positive GBS sera by 14.2% of the total (from 97 to 113). If the cut off for definition of a positive spot is increased, the contribution of complex-only positive sera to the total increases. At a cut-off of 8000 arbitrary units, complex-only positive GBS sera form 48.9% of the 88 positives. With this cut off, sensitivity is reduced to 48.6%, while specificity is improved at 91.9%. The positive and negative likelihood ratios with this threshold are therefore 6.0 and 0.6 respectively. The receiver operating characteristic for the test is improved when complexes antigens are also included, assessed across a range of threshold intensity values (Figure 5.3).

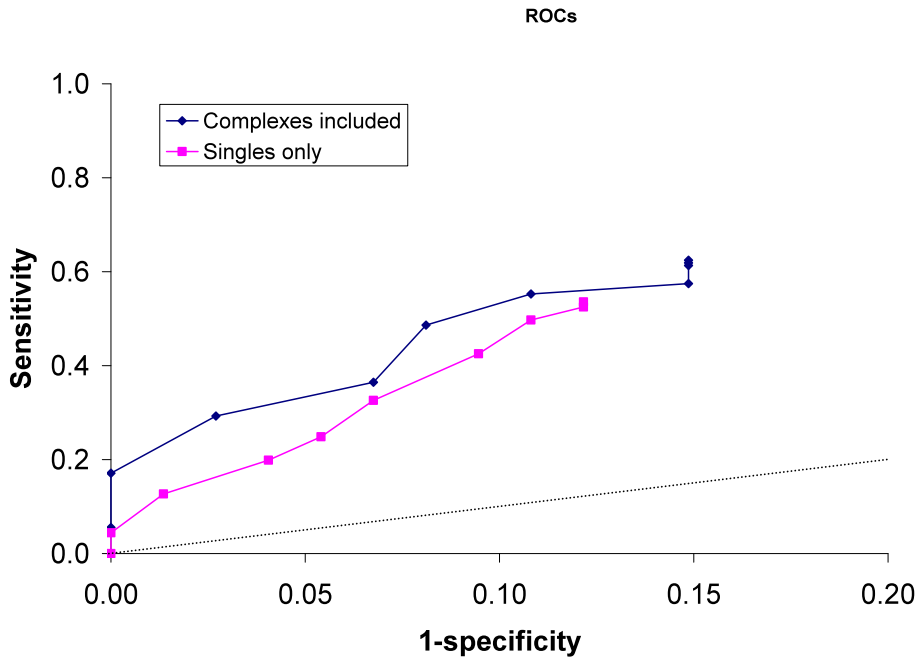

Figure 5.3 - Receiver operator characteristics for the glycoarray

The receiver operator curve demonstrates the performance of the test as a specific criterion is altered. In this example, the criterion varied for each curve is the intensity cut off used to define a positive spot, which was assessed over a range for 0 to 128,000 arbitrary units. The further the curve extends from the diagonal dashed line (representing a test no better than random guessing), and the closer towards the ideal test of 100% sensitivity and specificity represented by the point a the leftmost and top most corner of the graph (0,1), the better. As can be seen, including complexes on the array (blue line) means the test outperforms an array with single glycolipids only (pink line) across the whole range of threshold values assessed.

Furthermore, even when disease associated sera were positive for binding to one or more single glycolipid, they often bound to complexes consisting of two separate glycolipids, neither of which they bound in isolation (absolute complex dependent binding). Some 79 (43.6%) of the disease associated sera showed this pattern, as compared to only 3 (4.1%) of the control sera ($p<0.0001$, Fisher's Exact Test), adding a further level of complexity to the fine specificity of these antibodies. Phosphatidylserine and sulfatide most often contributed to complexes bound in this way, yet examples were seen with all of the different glycolipids across the array (Figure 5.4).

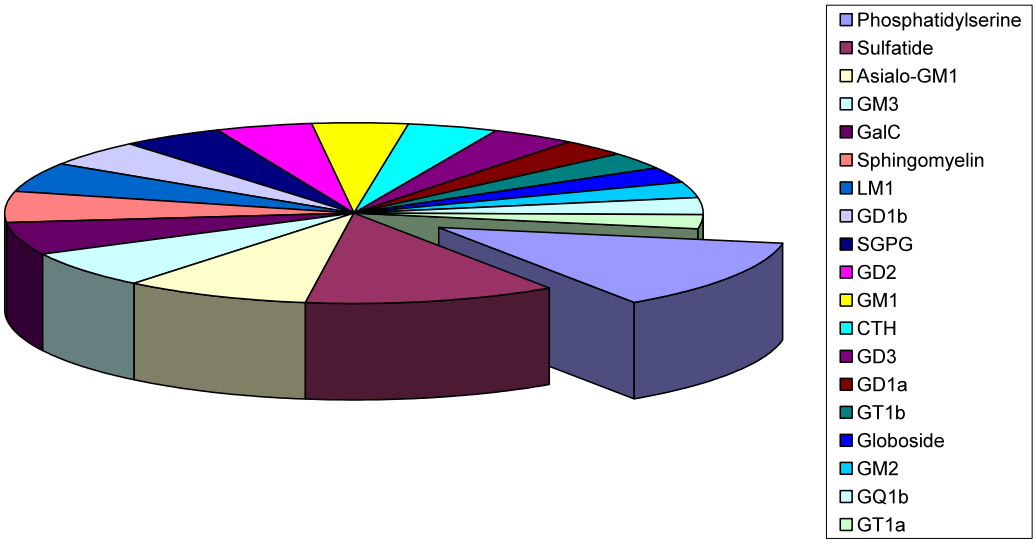

Figure 5.4 - Contribution of single glycolipids to antigens bound in an absolute complex dependent manner

Across the 181 different disease associated sera screened on the array, binding to 1:1 heterodimeric complexes in the absolute absence of binding to the component glycolipids in isolation was observed 828 times (as some sera demonstrated multiple examples of this phenomenon). All glycolipids were seen to contribute to the complexes in such circumstances, with phosphatidylserine (pulled out slice) and sulfatide performing this role most often.

Using multiple Fisher's Exact tests without correction for multiple comparisons initially, 92 spots were significantly associated with disease compared with

controls (Fisher's Exact Test, α=0.05, uncorrected). When Bonferroni's correction was applied to account for multiple comparisons, and the family error rate maintained at 0.05, 17 spots (Table 5.4 below) remained significantly associated with GBS versus controls (corrected individual α<0.0003).

Antigen	GBS+	GBS-	CON+	CON-	Sensitivity(%)	Specificity(%)	LR+	LR-
PS:Sulfatide	67	114	5	69	37.02	93.24	5.48	0.68
SM:Sulfatide	62	119	5	69	34.25	93.24	5.07	0.71
SGPG:Sulfatide	57	124	2	72	31.49	97.30	11.65	0.70
Sulfatide	55	126	5	69	30.39	93.24	4.50	0.75
PS:SGPG	52	129	5	69	28.73	93.24	4.25	0.76
CTH :Sulfatide	49	132	3	71	27.07	95.95	6.68	0.76
SGPG	45	136	3	71	24.86	95.95	6.13	0.78
GD2:Sulfatide	36	145	2	72	19.89	97.30	7.36	0.82
GA1:Sulfatide	32	149	0	74	17.68	100.00		0.82
Sulfatide :GT1a	32	149	0	74	17.68	100.00		0.82
PS:GM1	26	155	0	74	14.36	100.00		0.86
Sulfatide :GalC	26	155	0	74	14.36	100.00		0.86
Sulfatide :GD1b	26	155	0	74	14.36	100.00		0.86
PS:Asialo-GM1	25	156	0	74	13.81	100.00		0.86
Sulfatide :GM1	25	156	0	74	13.81	100.00		0.86
PS:GD1b	24	157	0	74	13.26	100.00		0.87
SGPG:GM1	24	157	0	74	13.26	100.00		0.87

Table 5.4 - Antigens on the PVDF glycoarray significantly associated with binding by GBS as compared with control sera

GBS+ : Number of GBS sera exhibiting binding to the antigen. GBS- : Number of GBS sera not binding to the antigen. CON+ : Number of control sera exhibiting binding to the antigen. CON- : Number of control sera not binding to the antigen. LR+ : Likelihood ratio positive. LR- : Likelihood ratio negative. PS : phosphatidylserine. SM – sphingomyelin. GA1 – asialo-GM1.

The data above does not make use of the intensity readings, merely whether a particular spot was present or absent on each membrane assayed. Further analysis, taken into account the intensity data, was performed subsequently, as part of the cluster analysis process, and is described in greater detail in subsequent sections. Figure 5.5 shows individual value plots for the 17 statistically significant antigen associations listed in Table 5.4. As can be seen, all of these antigens contain one or more of SGPG, phosphatidylserine (PS) or sulfatide.

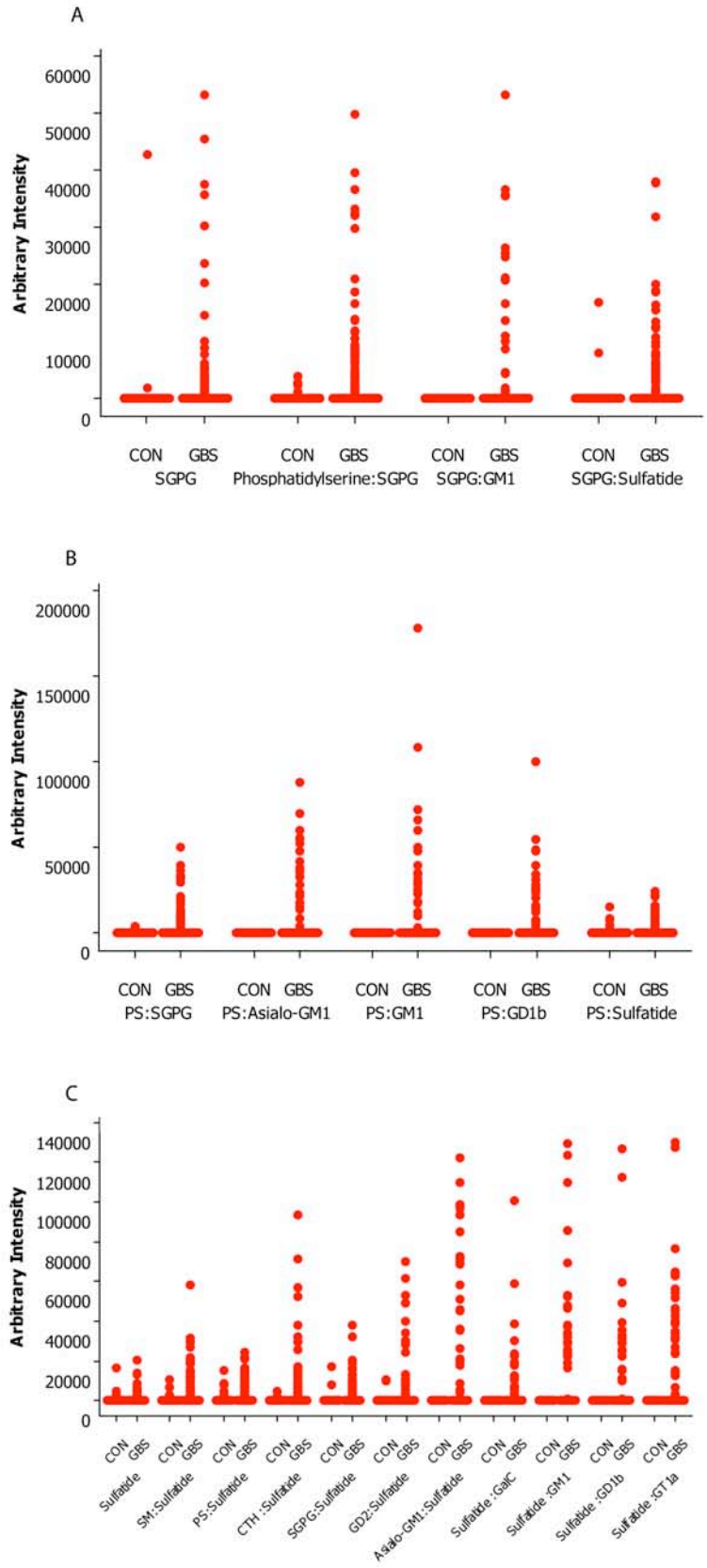

Figure 5.5 - Individual value plots for the 17 antigen spots significantly associated with GBS

(**A**) SGPG series complexes. (**B**) Phosphatidylserine series complexes. (**C**) Sulfatide series complexes.

5.2.4.1 SGPG and SGPG-series complexes

Analysis of the different patterns of SGPG and SGPG: phosphatidylserine (PS) binding between patients and controls reveals an interesting difference. When comparing the intensity values for SGPG with those for SGPG:PS, the majority of GBS patients have antibodies which bind to the former at least as well as the latter, and some show an increment. In contrast, the one control with high intensity binding towards SGPG alone (AI=42943) is strongly inhibited from binding SGPG in the SGPG:PS complex (AI=3946). Changes of this magnitude, in this direction, were not seen with patient samples (Figure 5.6), and these different patterns are maintained when the sum of individual binding intensities to PS and SGPG is used as the baseline for comparison with PS:SGPG complex binding (Figure 5.7).

Nevertheless, of the 60 GBS sera which demonstrated binding to either SGPG, PS:SGPG or both, 28 showed PS complex attenuated binding for SGPG, and 32 showed a complex enhanced binding pattern. Of the 'complex attenuated' sera, 4 had complex binding intensities within the margin of error of the assay (<14.1% different, as compared with the sum of PS and SGPG intensities) as did 5 of the 'complex enhanced sera'. These should probably be labelled complex independent on this basis.

The magnitude of this change ranged from absolute (8 sera with binding only detected to SGPG in isolation, 13 binding PS:SGPG but not SGPG or PS alone) to minimal, as below (Table 5.5 and Table 5.6).

Similar to the patterns of binding seen with siglecs, monoclonal antibodies and bacterial toxins, these observations suggest that there are (at least) three

different types of SGPG binding patterns within the sera of GBS patients and controls, namely complex attenuated, complex independent, and complex enhanced. As sera were only assessed in duplicate in one experiment statistical methods were not able to be applied to define these patterns. Instead, as above, the reproducibility/variability in the PVDF array was used to define the margin of difference chosen to define complex attenuation, enhancement and independence.

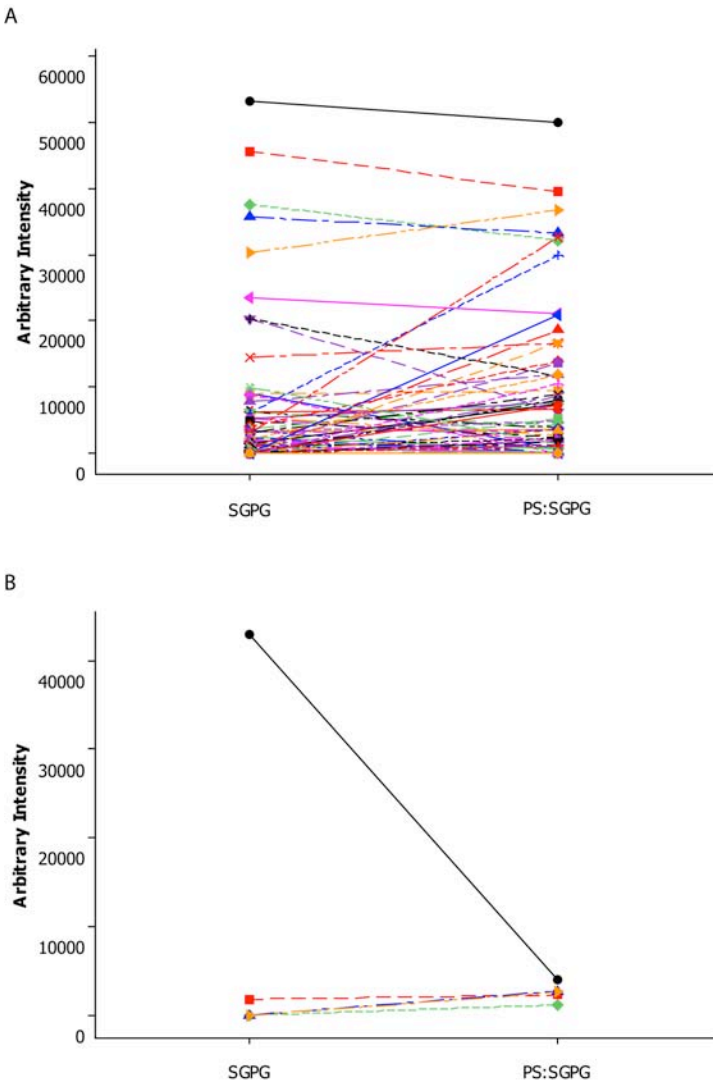

Figure 5.6 - The relationship between SGPG and PS:SGPG complex binding within the same sera

In GBS associated sera (**A**), the majority of sera bind SGPG and PS:SGPG with similar intensity values, or show a 'complex enhanced' effect for PS:SGPG over SGPG alone. In contrast, the only serum in the control group with high intensity binding to SGPG demonstrates a dramatic 'complex attenuated' fall in signal with PS:SGPG (**B**, black line).

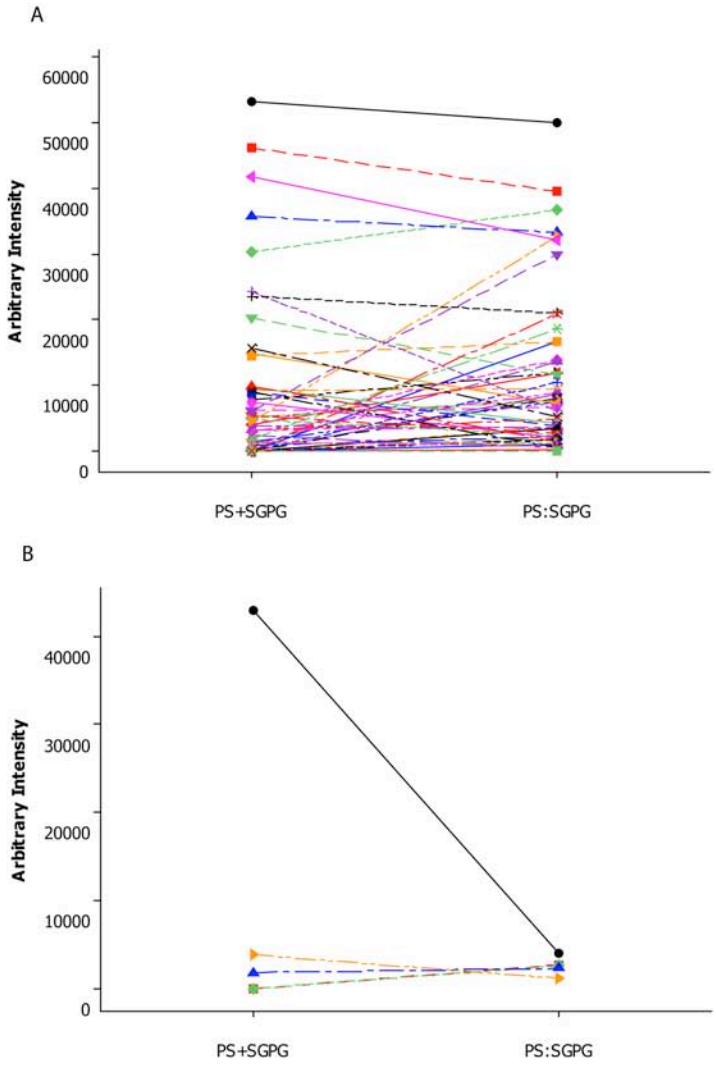

Figure 5.7 - The relationship between SGPG, PS and PS:SGPG complex binding within the same sera

When the sum of the individual phosphatidylserine and SGPG binding intensities is used as the baseline for comparison with binding to PS:SGPG complex, little difference is seen as compared with using an SGPG only baseline.

Arbitrary Intensity					
SGPG	PS	PS+SGPG	PS:SGPG	Absolute attenuation	Relative attenuation (%)
8849	0	8849	0	8849	0.0
3362	0	3362	0	3362	0.0
2317	0	2317	0	2317	0.0
2051	1188	3239	0	3239	0.0
1850	0	1850	0	1850	0.0
1084	0	1084	0	1084	0.0
1031	0	1031	0	1031	0.0
618	0	618	0	618	0.0
8970	0	8970	546	8424	6.1
9951	0	9951	1472	8479	14.8
2331	0	2331	559	1772	24.0
20332	3966	24298	6250	18048	25.7
5214	2190	7404	1943	5461	26.2
0	15623	15623	5159	10464	33.0
6217	2729	8946	3861	5085	43.2
6158	3419	9577	4214	5363	44.0
0	14836	14836	7189	7647	48.5
4834	0	4834	2416	2418	50.0
5362	0	5362	2691	2671	50.2
1383	0	1383	768	615	55.5
20290	0	20290	11673	8617	57.5
1398	0	1398	852	546	60.9
37591	4179	41770	32216	9554	77.1
45682	484	46166	39539	6627	85.6
23608	0	23608	21012	2596	89.0
3217	608	3825	3485	340	91.1
35727	0	35727	33278	2449	93.1
53313	0	53313	50009	3304	93.8

Table 5.5 - GBS sera with phosphatidylserine complex attenuated SGPG binding

The 28 SGPG binding sera showing lower binding intensities for PS:SGPG, arranged in descending order by degree of attenuation. Relative attenuation is defined as the binding intensity for PS:SGPG expressed as a percentage of the sum of SGPG and PS binding intensity (PS+SGPG). Serum results in orange fall within the margin of error for the test.

Arbitrary Intensity					
SGPG	PS	PS+SGPG	PS:SGPG	Absolute enhancement	Relative enhancement (%)
0	0	0	20869	20869	INF
0	0	0	16617	16617	INF
0	0	0	10417	10417	INF
0	0	0	8578	8578	INF
0	0	0	8117	8117	INF
0	0	0	3661	3661	INF
0	0	0	3478	3478	INF
0	0	0	2119	2119	INF
0	0	0	1805	1805	INF
0	0	0	1751	1751	INF
0	0	0	1104	1104	INF
0	0	0	227	227	INF
0	0	0	95	95	INF
876	0	876	13581	12705	1550.3
644	1177	1821	18657	16836	1024.5
3051	1517	4568	32675	28107	715.3
1402	0	1402	7544	6142	538.1
6119	0	6119	29911	23792	488.8
4006	0	4006	13891	9885	346.8
2194	1765	3959	11793	7834	297.9
3113	0	3113	8786	5673	282.2
845	0	845	2217	1372	262.4
7770	0	7770	11911	4141	153.3
3704	1415	5119	7798	2679	152.3
3210	0	3210	4822	1612	150.2
5188	0	5188	7738	2550	149.2
30352	0	30352	36754	6402	121.1
14512	0	14512	16614	2102	114.5
1174	0	1174	1314	140	111.9
3261	0	3261	3642	381	111.7
6182	0	6182	6618	436	107.1
8949	351	9300	9407	107	101.2

Table 5.6 - GBS sera with phosphatidylserine complex enhanced SGPG binding

The 32 SGPG binding sera showing higher binding intensities for PS:SGPG, arranged in descending order by degree of enhancement. Relative enhancement is defined as the binding intensity for PS:SGPG expressed as a percentage of the sum of SGPG binding intensity. Serum results in orange fall within the margin of error for the test. (INF = infinite)

5.2.4.2 Sulfatide and sulfatide-series complexes

Anti-sulfatide and sulfatide containing complex antibodies form the largest group of antibodies found to be statistically associated with GBS, making up 11

of the 17 in total. By studying the graph above (Figure 5.5C), it can be appreciated that for a number of sulfatide complexes (with asialo-GM1(GA1), galactocerebroside(GalC), GM1, GD1b and GT1a) no binding at all is observed in controls, whereas a range of intensity readings are seen with patient's sera, some approaching the highest values recorded across the whole of the array and sample series. For complexes of sulfatide with GD2 and CTH, a range of intensity readings were returned following assay with GBS sera, and 2 or 3 control sera exhibited binding towards the lower end of the intensity range. In contrast, non-complexed sulfatide and sulfatide:PS complexes returned generally lower intensity readings, and each were also bound by 5 negative control sera, the joint highest number for any of the spots on the array. Sulfatide complexes with sphingomyelin and SGPG fall somewhere between these two extremes.

Looking at sulfatide:GA1 in more detail, of the 32 GBS sera which bound this complex, 17 also bound non-complexed GA1, 22 bound non-complexed sulfatide, and 13 bound both GA1 and sulfatide outwith complexes. However, in 28 out of 32 cases binding to the complex was enhanced as compared with the sum of intensities of the two component glycolipids. When the 33 further sera which bound sulfatide but not sulfatide:GA1 are also included (and are therefore by definition complex attenuated), 28/65 which bind sulfatide and/or GA1 individually display complex enhanced binding to GA1:sulfatide. None of the sera bind GA1 alone without either also binding sulfatide or sulfatide:GA1. Once again, the binding pattern in control sera is different. Binding to sulfatide was observed in 5 control sera, 2 of which also bound GA1. No control sera bound GA1 without also binding sulfatide. Of the five, none we also able to recognise the sulfatide:GA1 complex, and hence all five showed absolute complex attenuated binding in this respect (Figure 5.8). This difference just fails to reach

statistical significance (p=0.07, Fisher's Exact test for 2x2 contingency table, Table 5.7), largely because of the small numbers of control sera binding any of GA1, sulfatide, or the GA1:sulfatide GSC.

	GA1+sulfatide v. GA1:sulfatide	
	Enhanced	Attenuated
GBS	28	37
Controls	0	5

Table 5.7 - 2x2 contingency table for GA1 and sulfatide single versus complex binding

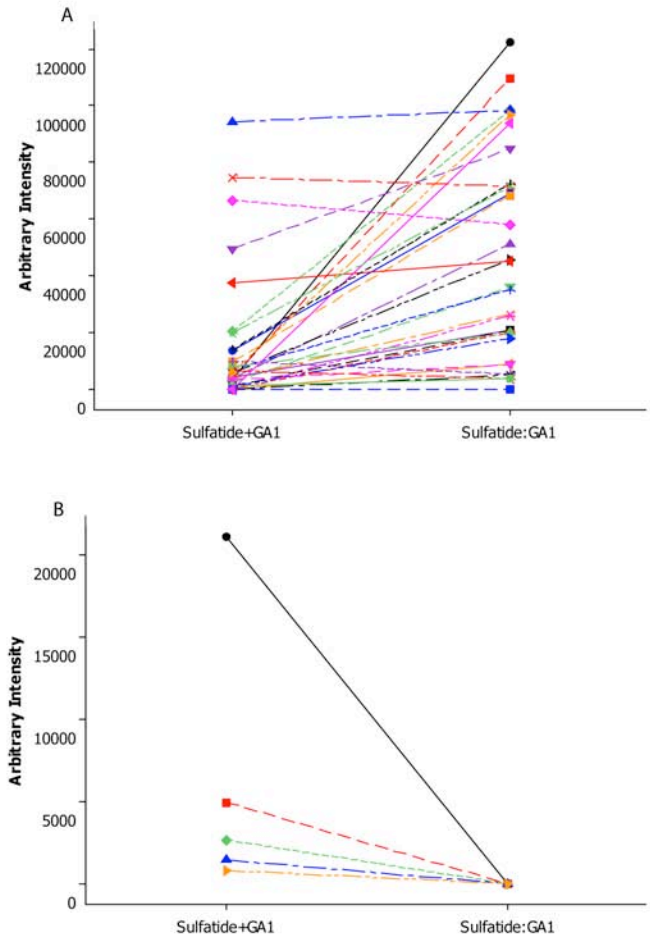

Figure 5.8 - Contrast in binding patterns between GBS and control sera towards single sulfatide and GA1 as compared with sulfatide:GA1 complex

In GBS (**A**), many of the sera show impressively enhanced binding towards sulfatide:GA1 complex as compared with the sum of intensities for sulfatide and GA1 in isolation (sulfatide+GA1 above). In the two most extreme cases the intensity is seen to increment from 3000 and 4000 to over 100000 (black circle and red square). In contrast, all 5 of the control sera (**B**), show an absolute complex attenuated pattern with respect to the same targets. The most marked example here (black circle) falls from an arbitrary intensity of over 20000 to 0.

5.2.5 Cluster analysis of GBS array data

Cluster analysis was performed using a variety of approaches by Dr Gabriella Kalna, a biomedical statistician with a specialist interest in microarray analysis, based at the Beatson Institute, Garscube Estate, Glasgow. In addition, she employed ANOVA analysis of log transformed intensity data including testing for independence and Bonferroni correction for multiple comparisons. This approach yielded 9 glycolipid and glycolipid complex antigens with significantly increased binding intensities for GBS as compared to control sera. These 9 are a subset of the 17 significantly associated antigens identified by the binary analysis described in section 5.2.4 above. Furthermore, this subset of 9 includes all 4 of the antibody targets discussed in further detail, namely SGPG and SGPG:PS (5.2.4.1), and sulfatide and sulfatide:GA1(5.2.4.2). Output from this statistical analysis for these nine targets is shown in Table 5.8.

5.2.5.1 Cluster analysis data

Table 5.8 – ANOVA analysis of log transformed intensity data

ANOVA analysis of log transformed intensity data from the PDVF glycoarray analysis of 181 GBS associated sera and 74 control sera revealed 9 glycolipid and glycolipid complex array antigens significantly associated with disease versus controls, following Bonferroni correction for multiple comparisons.

Antigen	Uncorrected p-value (GBS vs. controls)	Bonferroni (p-value) (GBS vs. controls)	stepup (p-value) (GBS vs. controls)	Fold-Change (GBS vs. controls)	GBS			Controls		
					Mean Spot Intensity	SD	Maximum Spot Intensity	Mean Spot Intensity	SD	Maximum Spot Intensity
SGPG:Sulfatide	$1.26x10^{-06}$	$2.28x10^{-04}$	$1.70x10^{-04}$	10.23	3.72	5.63	15.21	0.37	2.21	14.04
PS:Sulfatide	$1.88x10^{-06}$	$3.41x10^{-04}$	$1.70x10^{-04}$	11.36	4.36	5.83	14.57	0.86	3.21	13.88
Sphingomyelin:Sulfatide	$7.48x10^{-06}$	$1.35x10^{-03}$	$4.51x10^{-04}$	9.17	3.98	5.70	15.82	0.79	2.96	13.39
CTH :Sulfatide	$2.82x10^{-05}$	$5.11x10^{-03}$	$1.28x10^{-03}$	7.03	3.25	5.50	16.51	0.44	2.17	12.15
SGPG	$5.54x10^{-05}$	$1.00x10^{-02}$	$2.01x10^{-03}$	6.21	3.02	5.34	15.70	0.39	2.19	15.39
PS:SGPG	$7.95x10^{-05}$	$1.44x10^{-02}$	$2.24x10^{-03}$	6.95	3.56	5.71	15.61	0.76	2.84	11.95
Sulfatide	$8.66x10^{-05}$	$1.57x10^{-02}$	$2.24x10^{-03}$	5.78	3.31	5.12	14.32	0.78	2.93	13.98
Sulfatide :GT1a	$1.08x10^{-04}$	$1.96x10^{-02}$	$2.45x10^{-03}$	6.11	2.61	5.70	16.99	0	0	0
Asialo-GM1:Sulfatide	$1.24x10^{-04}$	$2.24x10^{-02}$	$2.49x10^{-03}$	6.00	2.58	5.70	16.90	0	0	0

5.2.5.2 Cluster analysis heatmaps

The intensity values generated were then used to produce heatmaps. Prior to any clustering it can be appreciated that the frequency and distribution of positive spots, and intensity of binding, is greater in the disease sera as compared with controls (Figure 5.9A). In advance of clustering, sera with no detectable binding were excluded. These were membranes where none of the antigen spots generated a signal intensity greater than zero following background correction. Both GBS and control sera were included in the clustering process. Several techniques, including covariance as shown, were then used for cluster analysis. This revealed a number of distinct populations of sera (Figure 5.9B). The vertical tramlines enclose sulfatide and 5 sulfatide containing complexes, demonstrating the high prevalence, and frequent co-existence in the same serum, of binding to all of these antigens in positive sera. Lesser numbers of sera can be seen to bind to a number of LM1, SGPG, GA1, GM1, GD1a and GT1b containing complexes, as labelled on the heatmap. A proportion of these sera also bind promiscuously to antigens in the other groups (Figure 5.9B).

A

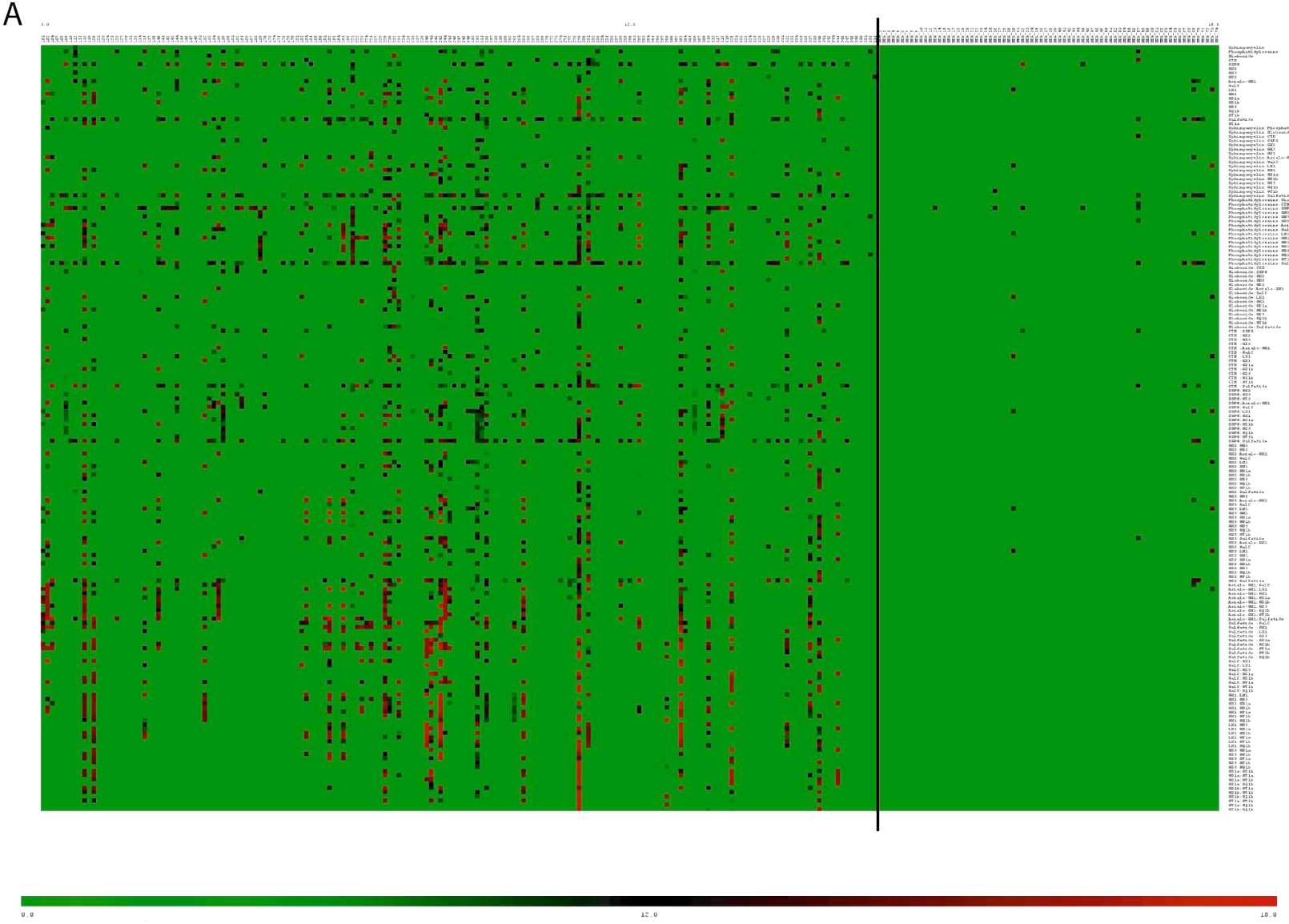

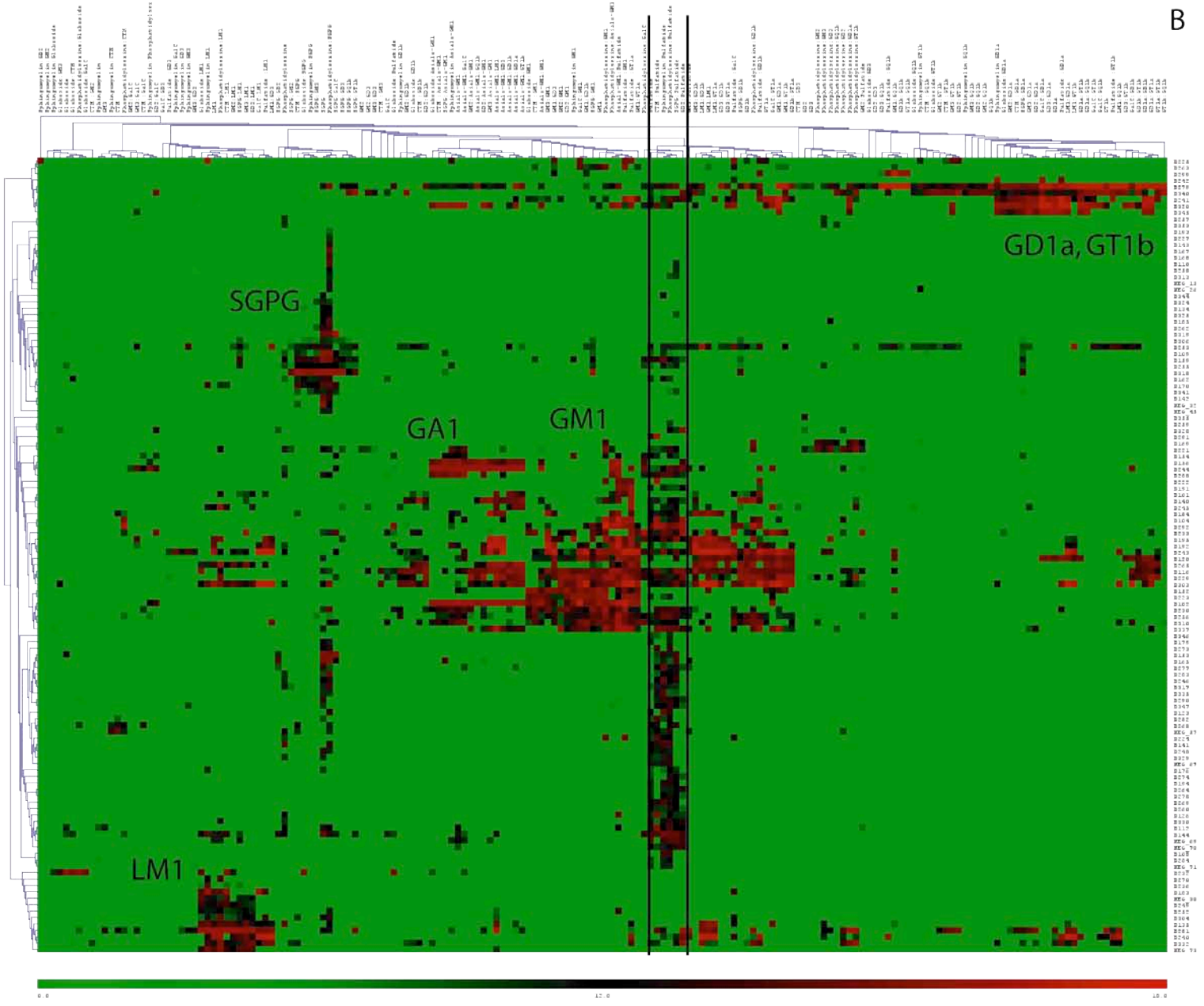
B
GD1a, GT1b
SGPG
GA1
GM1
LM1

Figure 5.9 - Heatmap analysis of glycoarray intensity data

(**A**) Heatmap of GBS versus control sera probed arrays. This array was produced prior to any clustering, and shows all of the 255 sera analysed. On this heatmap, individual sera are listed on the x-axis, and the 181 different antigens probed run along the y-axis. The presence of a spot above the light green background indicates detectable binding, with the intensity given by the colour, as shown below the heatmap, bright red being the most intense. GBS samples are shown to the left of the vertical line, controls to the right. (**B**) Heatmap following removal of negative sera and covariance clustering. Both GBS and control sera are included. On this heatmap, the x and y axis are inverted as compared to (**A**), and the order of samples and antigens has been systematically altered to reveal patterns of binding.

5.2.6 Disease associations

The array intensity data was subsequently compared with the clinical database to identify any associations between the presence of specific antibodies and disease subtype (by electrophysiological criteria), disease severity, preceding infection, cranial nerve and/or bulbar involvement, the presence of sensory signs on examination, and the requirement for mechanical ventilation. Analysis of Variance (ANOVA) was used to statistically assess the significance of any clinical-serological associations, and Mann-Whitney and t-tests were additionally used if large numbers of zero results were present, to ensure ANOVA was robust against violations of model assumptions (non-normality). Both Bonferroni (more stringent) and step up (less stringent) techniques were used to correct for multiple comparisons.

5.2.6.1 Disease subtype

The analysis of antibody associations with AIDP as compared with AMAN was confounded by the small number of electrically conformed AMAN cases (4) and the large number of equivocal cases. Even so, in confirmed AIDP as compared to AMAN cases, 14 antigen spot intensities (GM1 and 13 GM1 containing complexes) were significantly decreased in AIDP following Bonferroni correction (Table 5.9).

When equivocal cases were combined with the AIDP group, all but one (sulfatide:GM1) of these associations remained statistically significant.

Antigen	p-value (AIDP vs. AMAN)	Bonferroni (AIDP vs. AMAN)	Stepup (AIDP vs. AMAN)	Fold-Change(AIDP vs. AMAN)
Globoside:GM1	$2.54x10^{-12}$	$5.16x10^{-10}$	$5.16x10^{-10}$	-871.59
CTH :GM1	$1.54x10^{-11}$	$3.13x10^{-09}$	$1.57x10^{-09}$	-1784.65
GD2:GM1	$6.21x10^{-09}$	$1.26x10^{-06}$	$4.20x10^{-07}$	-1045.65
Asialo-GM1:GM1	$2.57x10^{-08}$	$5.22x10^{-06}$	$1.31x10^{-06}$	-1200.98
Sphingomyelin:GM1	$8.47x10^{-08}$	$1.72x10^{-05}$	$3.44x10^{-06}$	-1210.83
GalC:GM1	$1.23x10^{-07}$	$2.50x10^{-05}$	$3.91x10^{-06}$	-1882.68
GM1	$1.35x10^{-07}$	$2.73x10^{-05}$	$3.91x10^{-06}$	-2279.72
GM1:GD1b	$2.42x10^{-07}$	$4.91x10^{-05}$	$6.14x10^{-06}$	-1669.89
GM1:GT1a	$8.71x10^{-07}$	$1.77x10^{-04}$	$1.97x10^{-05}$	-1505.36
GM2:GM1	$4.48x10^{-06}$	$9.10x10^{-04}$	$9.10x10^{-05}$	-283.45
GM1:GD3	$9.23x10^{-06}$	$1.87x10^{-03}$	$1.70x10^{-04}$	-481.57
Phosphatidylserine:GM1	$1.30x10^{-05}$	$2.63x10^{-03}$	$2.19x10^{-04}$	-2225.63
SGPG:GM1	$2.79x10^{-05}$	$5.66x10^{-03}$	$4.35x10^{-04}$	-706.20
Sulfatide :GM1	$1.37x10^{-04}$	$2.78x10^{-02}$	$1.98x10^{-03}$	-1201.88

Table 5.9 - Disease subtype antigen associations

14 antigens (GM1 and 13 GM1 containing complexes) were significantly associated with the AMAN variant of GBS, as compared with electrically confirmed AIDP. The negative values in the fold change column indicate that binding to these antigens was down-regulated in AIDP as compared with AMAN.

5.2.6.2 Disease severity and requirement for mechanical ventilation

Nine antigen spot intensities (Table 5.10) were found to be significantly associated with more severe disease (GBS disability score >3), but only at the time of randomisation, including GA1 and three GA1 containing complexes. Likewise, three GA1 complex antigens (CTH :GA1, Globoside:GA1 and SGPG:GA1) were statistically significantly associated with the requirement for mechanical ventilation at any time, but only following the less stringent stepup correction for multiple comparisons.

Antigen	p-value (Day 0)	Bonferroni (Day 0)	Bonferroni (Day 6)	Bonferroni (Week 4)	Bonferroni (Week 8)	Bonferroni (Week 26)
CTH :GA1*	$1.16x10^{-05}$	$2.36x10^{-03}$	1	1	1	1
Globoside:GA1*	$1.70x10^{-05}$	$3.45x10^{-03}$	1	1	1	1
PS:GalC	$3.12x10^{-05}$	$6.34x10^{-03}$	1	1	1	1
GA1:GalC	$1.26x10^{-04}$	$2.56x10^{-02}$	1	1	1	1
Globoside:GD3	$1.31x10^{-04}$	$2.66x10^{-02}$	1	1	1	1
GD2:GD3	$1.31x10^{-04}$	$2.66x10^{-02}$	1	1	1	1
GA1	$1.74x10^{-04}$	$3.52x10^{-02}$	1	1	1	1
GD3:GT1b	$1.79x10^{-04}$	$3.64x10^{-02}$	1	1	1	1
GalC:GQ1b	$2.18x10^{-04}$	$4.43x10^{-02}$	1	1	1	1

Table 5.10 - Antigens associated with disease severity
The nine antigens listed are statistically significantly associated with severe disease (GBS disability score >3), but only at the point of randomisation (day 0). At other assessed time points, this association is not seen.

* Antigen also significantly associated with the requirement for mechanical ventilation.

5.2.6.3 Preceding infection

GM1, four GM1 containing complexes, and GT1a:sulfatide complex all returned significantly higher spot intensities when a preceding diarrhoeal illness, as opposed to no preceding illness, was reported (Table 5.11). When campylobacter serology was positive (Table 5.12), nine GD1a containing spots returned significantly higher intensities, and three GM1 containing complexes are also represented if the less stringent correction is applied.

Antigen	p-value(diarrhoea vs. neither)	Bonferroni	Stepup	Fold-Change (diarrhoea vs. neither)
Sulfatide :GM1	$2.58x10^{-05}$	$5.23x10^{-03}$	$4.26x10^{-03}$	19.72
Sulfatide :GT1a	$4.91x10^{-05}$	$9.97x10^{-03}$	$4.26x10^{-03}$	22.81
GalC:GM1	$6.43x10^{-05}$	$1.31x10^{-02}$	$4.26x10^{-03}$	9.15
Asialo-GM1:GM1	$8.66x10^{-05}$	$1.76x10^{-02}$	$4.26x10^{-03}$	7.02
CTH :GM1	$1.05x10^{-04}$	$2.13x10^{-02}$	$4.26x10^{-03}$	5.56

Table 5.11 - Antigens significantly associated with preceding diarrhoea

Antigen	p-value (*C.jejuni* vs. none)	Bonferroni	Stepup	Fold-Change (*C.jejuni* vs. none)
GD1a:GT1b	$1.62x10^{-06}$	$3.29x10^{-04}$	$3.29x10^{-04}$	6.42
GD3:GD1a	$1.30x10^{-05}$	$2.64x10^{-03}$	$1.32x10^{-03}$	4.86
Sulfatide :GD1a	$3.16x10^{-05}$	$6.41x10^{-03}$	$1.99x10^{-03}$	7.41
GalC:GD1a	$4.34x10^{-05}$	$8.80x10^{-03}$	$1.99x10^{-03}$	5.30
GM2:GD1a	$5.79x10^{-05}$	$1.18x10^{-02}$	$1.99x10^{-03}$	3.53
GD1a	$5.88x10^{-05}$	$1.19x10^{-02}$	$1.99x10^{-03}$	5.08
GD1a:GQ1b	$7.62x10^{-05}$	$1.55x10^{-02}$	$2.21x10^{-03}$	3.76
GD2:GD1a	$2.00x10^{-04}$	$4.07x10^{-02}$	$5.09x10^{-03}$	4.09
CTH :GD1a	$2.32x10^{-04}$	$4.71x10^{-02}$	$5.24x10^{-03}$	3.52

Table 5.12 - Identified infection and antigens detected

The only significant differences found were between cases where *Campylobacter jejuni* infection was detected as compared with no detected infection. In the former cases, antibodies directed against the nine antigens listed above were more prevalent. The presence of GD1a, GD3, and GQ1b in this list is in keeping with the fact that *C.jejuni* with α2,3 monofunctional-sialyltransferase activity display GM1 and GD1a like surface lipooligosaccharide, and those strains with α2,3 and α2,8 bifunctional-sialyltransferase activity display mimics of GD3, GT1a and GQ1b ganglioside.

5.2.6.4 Presence of cranial nerve deficits, bulbar impairment or sensory involvement

Sulfatide:GM1 and sulfatide:GT1a complex responses alone were significantly negatively associated with cranial nerve deficits at any time during follow up (Table 5.13). A number of complexes all containing one or more of GM1, GA1 and GT1a were negatively associated with sensory deficit at both randomisation and week 4 (Table 5.14). No antigens were significantly associated with bulbar impairment.

Antigen	p-value (cranial nerve deficit present v. absent)	Bonferroni	Stepup	Fold-Change (present vs. absent)
Sulfatide :GM1	$5.97x10^{-05}$	$1.21x10^{-02}$	$3.03x10^{-03}$	-8.49
Sulfatide :GT1a	$2.06x10^{-04}$	$4.17x10^{-02}$	$8.35x10^{-03}$	-8.68

Table 5.13 - Association with cranial nerve deficit

Only two antigens, sulfatide:GM1 and sulfatide:GT1a complexes, were significantly associated with cranial nerve deficits at any time during follow up. The correlation in this case was negative.

Antigen	p-value (sensory deficit present vs. absent)	Bonferroni	Stepup	Fold-Change(present vs. absent)
GM3:GM1	$2.84x10^{-05}$	$5.77x10^{-03}$	$5.77x10^{-03}$	-5.66
GD2:GM1	$6.05x10^{-05}$	0.01	$6.14x10^{-03}$	-4.18
GalC:GM1	$1.45x10^{-04}$	0.03	$9.11x10^{-03}$	-4.99
GM1:GD1b	$2.52x10^{-04}$	0.05	$9.11x10^{-03}$	-4.76
GA1:Sulfatide	$2.85x10^{-04}$	0.06	$9.11x10^{-03}$	-8.41
GM1	$2.96x10^{-04}$	0.06	$9.11x10^{-03}$	-4.85
Sulfatide :GM1	$3.14x10^{-04}$	0.06	$9.11x10^{-03}$	-7.09
Phosphatidylserine:GM1	$4.94x10^{-04}$	0.10	0.01	-6.23
GM2:GM1	$8.69x10^{-04}$	0.18	0.02	-3.35
Sulfatide :GT1a	$1.02x10^{-03}$	0.21	0.02	-7.03
GM1:GD1a	$1.25x10^{-03}$	0.25	0.02	-4.28
Phosphatidylserine:GA1	$1.25x10^{-03}$	0.25	0.02	-5.11
GM1:GT1a	$1.39x10^{-03}$	0.28	0.02	-4.11
GM2:Asialo-GM1	$1.73x10^{-03}$	0.35	0.03	-2.83
Sphingomyelin:GM1	$2.00x10^{-03}$	0.41	0.03	-3.40
GalC:GT1a	$2.81x10^{-03}$	0.57	0.04	-3.79

Table 5.14 - Antigens negatively correlated with sensory disturbance

The above antigens were negatively correlated with the presence of sensory deficit. As might be expected, there is a degree of overlap with the antigens associated with the pure motor, axonal GBS variant AMAN (Table 5.9).

5.2.7 Low frequency antibodies

Of the 181 antigens screened, 78 were bound by IgG antibodies found in less than 10 of the GBS sera, 38 of these were bound by 4 or fewer, and 22 antigens were recognised by only 1 or 2 sera (Figure 5.10). None of these 78 antigens were additionally bound by IgG antibodies in any of the 74 control sera. Individually, despite uniquely being found in GBS sera, none of these antibody-antigen associations reached statistical significance as compared with control sera, given their low frequency. By way of comparison, the complex with the highest p value still reaching significance in the ANOVA intensity analysis (GA1:sulfatide) was bound by 32 GBS and no control sera. From the alternative perspective, certain GBS sera display very specifically targeted binding patterns - 13 sera showed binding against 1 or 2 complexes only (as demonstrated in

Figure 5.11). Increasing the intensity threshold to define a positive spot to 1000 or 8000 arbitrary units likewise increases the number of sera showing this degree of targeted binding to 24 and 31, respectively. By way of comparison, (Figure 5.12) shows examples of GBS sera displaying more promiscuous binding to multiple different antigens.

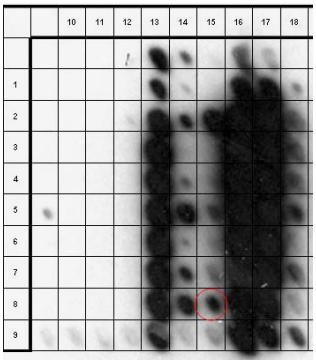

Figure 5.10 - Example of complex antigen bound by only one serum tested
The red circle indicates GD2:GD3 complex, bound only by this serum of the 181 tested.

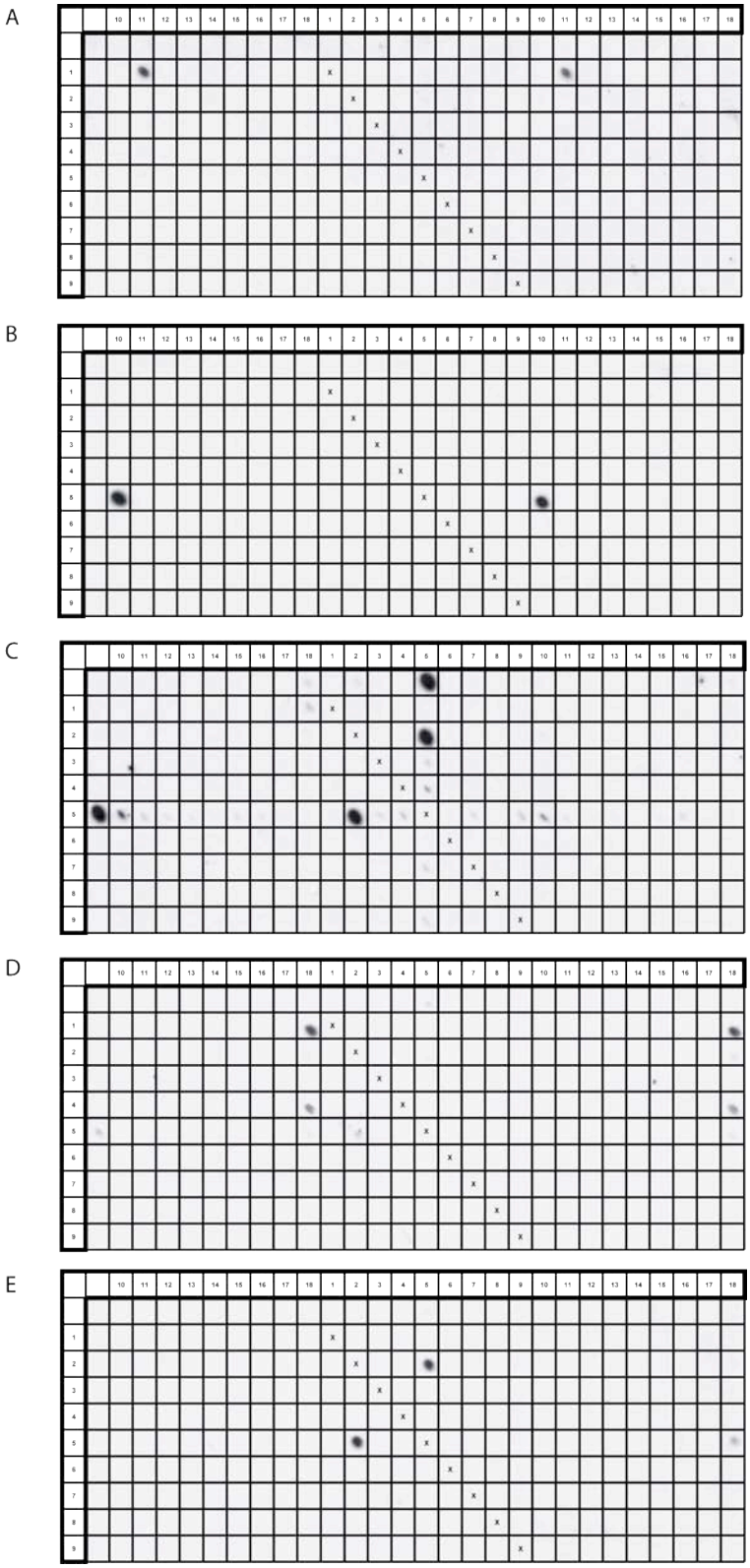

Figure 5.11 - GBS sera with highly specific binding patterns

Each membrane (A-E) represents the IgG binding pattern of one GBS serum.
Key: (1)Sphingomyelin, (2)Phosphatidylserine, (3)Globoside, (4)CTH, (5)SGPG, (6)GM2, (7)GM3, (8)GD2, (9)Asialo-GM1, (10)GalC, (11)LM1, (12)GM1, (13)GD1a, (14)GD1b, (15)GD3, (16)GQ1b, (17)GT1b, (18)Sulfatide.

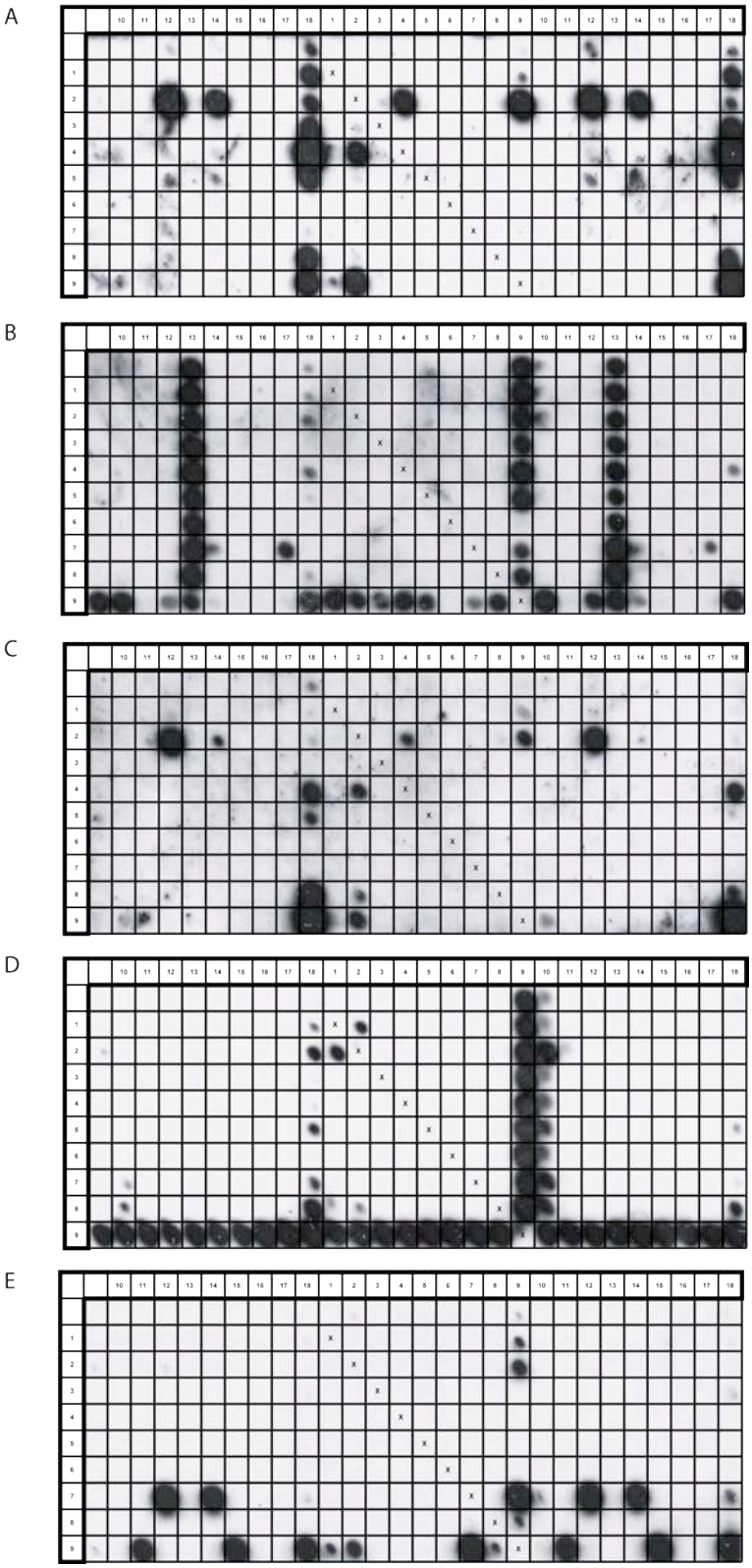

Figure 5.12 - GBS sera with more promiscuous binding patterns

Each membrane (A-E) represents the IgG binding pattern of one GBS serum.
Key: (1)Sphingomyelin, (2)Phosphatidylserine, (3)Globoside, (4)CTH, (5)SGPG, (6)GM2, (7)GM3, (8)GD2, (9)Asialo-GM1, (10)GalC, (11)LM1, (12)GM1, (13)GD1a, (14)GD1b, (15)GD3, (16)GQ1b, (17)GT1b, (18)Sulfatide.

5.3 Discussion

The combinatorial glycoarray technique and the experimental results described in this chapter have substantially increased the number of glycolipid antibody specificities significantly associated with GBS, particularly with respect to AIDP. Use of the array increases the glycolipid antibody detection rate as compared to ELISA, and the inclusion of glycolipid complexes increases this yet further. Rather than identifying a single specificity, however, 176 different targets were bound by IgG present in the 113 disease associated sera with detectable anti-glycolipid and glycolipid complex antibodies. Some complexes were bound by only a few sera, with 8 complexes being recognised by IgG antibodies in one serum each (Figure 5.10). Given their very low frequency these associations do not reach statistical significance. Of course, this does not mean that these antibodies do not have clinical and pathological significance in the individual in which they are found, which could be demonstrated by *in vivo* binding assays or functional readouts. However, to show statistically significant associations for an antibody with a frequency of 1/181 in disease, 3440 control sera would need to be analysed and found to be negative (Table 5.15), even when the effects of multiple comparisons are discounted. This is clearly not practical even using the PVDF glycoarray technique.

	Disease	Control	Total
Positive	1	0	1
Negative	180	3440	3620
Total	181	3440	3621

Table 5.15 - Contingency table required for significance with disease frequency of 1 in 181

To meet statistical significance for antibodies detected with a frequency of 1 in 181 in disease, 3440 control samples would need to be analysed and found negative for the antibody in question. The above contingency table generates a p value of 0.049986 using Fisher's Exact test, without any correction for multiple comparisons.

These observations notwithstanding, the controls used in this part of the study remain its weakest link. Aside from the fact that lesser numbers of controls were able to be obtained compared with disease samples, an argument can be made that control samples should be taken from post-infectious patients who do not go on to develop GBS. Ideally, the samples should be taken at the same time point following infection as the disease sera. Again, this is practically difficult (and not attempted in previous serological studies of GBS) in a large part because patients with uncomplicated gastroenteritis or upper respiratory tract infections rarely seek medical attention and virtually never have blood samples taken 10 to 14 days later. In order to obtain these samples, therefore, a specific targeting and recruitment of such patients would be necessary. Nevertheless, this is likely to prove important in future to ensure that a non-specific, post infectious, antibody response is not being inadvertently and unnecessarily further investigated. Similarly, these antibodies may simply arise as epiphenomena during nerve damage, or be non-specifically elevated in states of inflammation. Therefore, it would also be rewarding to investigate control sera from patients with non-inflammatory neuropathies and from

inflammatory/autoimmune conditions not involving the peripheral nervous system.

Also, disconcertingly, it may be that there is no single antibody specificity in AIDP, and rather that the response has a highly variable fine specificity towards many different glycolipids and complexes. Alternatively, it may simply be that the correct panel of target antigens and complexes is yet to be selected for analysis, and in addition to the vast range of fine specificities, one as yet undiscovered dominant antibody specificity exists in AIDP. It may even be that multimeric antigen structures, containing three or more glycolipids, and even including proteins, are important targets. The inconsistency of the antibody binding pattern seen may reflect the variability of the presentation of GBS, and in this regard the association of certain clinical features with particular antibody specificities is interesting. The fact that there are only significant associations for severity early in the disease course may mean that the antibodies detected have influence on the initial injurious process but are less relevant to the subsequent recovery phase.

Even so, experiments such as this do not prove a pathological role for the large number of different antibodies detected. Nonetheless, evidence is beginning to accumulate of the pathogenic potential of anti-ganglioside complex antibodies. Work using serum samples with anti-GM1:GD1a reactivity shows that a proportion of these sera have the potential to induce neuromuscular blockade, as assessed by electrophysiological measurements in *ex vivo* murine muscle preparations (J. Plomp, unpublished observations). Dissecting out the effect of the presumed critical pathological monoclonal component from polyclonal sera is problematic, yet the future development of monoclonal antibodies for further

study of AIDP pathogenesis must pay attention to the myriad of fine specificities demonstrated by this study. It is clearly possible, as has already demonstrated for GM1 antibodies attenuated or enhanced by GD1a (Greenshields *et al.*, 2009), that the complex enhanced GA1:sulfatide antibodies found in GBS sera will behave entirely differently *in vivo* as compared with the complex attenuated GA1:sulfatide antibodies that were occasionally also found in control sera.

The Node of Ranvier has recently been demonstrated as a site for anti-ganglioside and complement mediated damage (McGonigal *et al.*, 2010). In this context, the fact that the majority of antibodies significantly associated with GBS in this study bind sulfatide containing glycolipid complexes (such as GA1:sulfatide) is intriguing. This myelin associated sulfated glycolipid is enriched at the paranodal loops, where it is responsible for the proper localisation and clustering of K^+- and Na^+ -channels, and of the axonal adhesion molecule Caspr. Mice lacking galactocerebroside and sulfatide (UDP-galactose:ceramide galactosyltransferase-knockout - $CGT^{-/-}$), or sulfatide alone (cerebroside sulfotransferase-knockout - $CST^{-/-}$), exhibit a decrease in Na^+ and K^+ channel clustering, altered nodal length, and abnormal localization of K^+ channels, with contactin widely and abnormally distributed along the internode (Ishibashi *et al.*, 2002). Furthermore, sulfatide is required for the stabilisation of axon-myelin interactions, where it promotes the formation of neurofascin-155 containing lipid rafts (Schafer *et al.*, 2004). As such, anti-sulfatide complex antibody mediated injury at this location could be envisaged to result in a process of demyelination, the pathological hallmark of AIDP. The next step will therefore be to reproducibly generate monoclonal antibodies with the same sulfatide complex activity as those found in human AIDP sera, and investigate their pathogenic effects *in vivo*.

6 The immune response to GSC containing liposomes

6.1 Introduction

Ganglioside complex immunisation experiments were envisaged and designed to address two main areas. Firstly, the ability or otherwise to generate serum responses to ganglioside complexes in different mice could provide further indirect evidence of the presence of ganglioside complexes within the membranes of these experimental animals. It is already known that normal mice littermates (subsequently referred to as GM2 WT mice) are tolerant following immunisation with single ganglioside containing liposomes or *Campylobacter jejuni* derived lipooligosaccharide, but that robust IgG responses are seen in GM2 KO animals lacking longer chain gangliosides (Goodyear *et al.*, 1999;Bowes *et al.*, 2002). If GM2 WT mice proved tolerant of GSC injections also, this would suggest that the tolerogenic effect was due to the presence of similar GSC structures within the animal, whereas a serum response being observed when none is seen with single ganglioside injections would suggest the opposite. Likewise, the ability to investigate GD3s$^{-/-}$ mice, which lack b-series but have a full complement of a-series gangliosides, allows investigation of the antibody response when only one member of the GSC heterodimer is systemically expressed in the immunised animal via the use of a-series:b-series complexes as immunogens.

The experiments described in this chapter also address some of the questions regarding the potential antigens which may drive a GSC antibody response. It has

already been shown, both in experiments performed as earlier components of this study (using mAbs generated from animals injected with single ganglioside containing liposomes, 3.2.4) and from small clinical series (Kuijf *et al.*, 2007), that GSC responses can arise in response to injection with single ganglioside containing liposomes or infection with bacteria displaying only one type of ganglioside mimic on their cell surface. Whether the converse is true (that immunisation with GSCs can induce antibodies against single gangliosides) remains to be seen. These single time point assessments also provide only limited information, whereas investigating serum responses at multiple time points allows greater insight into the dynamics and maturation of the anti-ganglioside immune response.

In addition to developing a greater understanding of the 'mechanics' of the GSC antibody response, the other aim was to generate a predictable and reproducible immune response which could be subsequently exploited to generate αGSC monoclonal antibody producing hybridoma cell lines. This is discussed further in the next chapter (7 - Cloning and characterisation of anti-GSC antibodies, page 201).

6.2 Results

These experiments were commenced before the results of the PVDF glycoarray analysis of Western European AIDP sera were available, and as such immunisations concentrated on complexes of GM1:GD1a and GD1a:GD1b, 2 of the 3 most common targets for GSC antibodies in the largest Japanese series yet published (Kaida *et al.*, 2007). Furthermore, these gangliosides are widely, and relatively cheaply, available. The GD1a:GD1a antigen is also suitable for use in the GD3s$^{-/-}$ immunisation experiments described above, as these mice over-express GD1a but do not produce GD1b.

6.2.1 GM1:GD1a liposomes

Initial experiments were performed using GM1:GD1a ganglioside complex containing liposomes without ova, and without a priming stage or any alum adjuvant. Instead, 3 intravenous (iv) injections 7 days apart were performed using both GM2 WT and GM2 KO animals. In two separate experiments of 3 animals per group each, no αGM1:GD1a IgM or IgG response was seen using ganglioside ELISA up to and including day 35. Follow up experiments involved changing the injection route to intraperitoneal (ip) but otherwise maintaining the same protocol. Again no response was seen with 2 independent experiments.

In order to assess whether it was simply the protocol that was failing to drive antibody production, rather than of the use of GSC antigens themselves, a previously successful protocol (Bowes *et al.*, 2002) was employed. This is the same as described in section 2.2.7, apart from the fact the booster iv injections on days 25, 26 and 27 were initially not performed, and used a priming injection

of ova in alum adjuvant at day 0, followed by 3 injections of IP ganglioside liposomes containing ova (see 2.2.6).

6.2.1.1 ELISA analysis

As can be seen (Figure 6.1), using this protocol both IgM and IgG responses can be seen, as detected by ganglioside complex ELISA performed as previously described (2.2.2). In GM2 WT and GM2 KO animals, anti-GM1:GD1a IgM antibodies can be first detected at day 14. In the GM2 WT animals the OD reading plateaus and subsequently declines slightly at days 21 and 28, whereas it continues to rise in the GM2 KO group (Figure 6.1A). This analysis is once again complicated by the very high, non-specific background ODs seen in methanol only coated negative control wells with IgM antibodies.

The differences between the groups in terms of IgG response was much more clear cut, and binding to the control wells was not seen with these secondary antibodies. GM2 WT animals essentially failed to mount any IgG GSC whatsoever by day 28, whereas long chain ganglioside null GM2 KO mice had detectable αGSC IgG at day 21 and a rising titre at reassessment 7 days later. As the large standard deviation error bars suggest, even the antibody response seen with different mice of the same genotype (and indeed same sex and litter) showed a marked degree of variability, with some GM2 KO mice developing high titres of, and others barely detectable, αGSC antibodies.

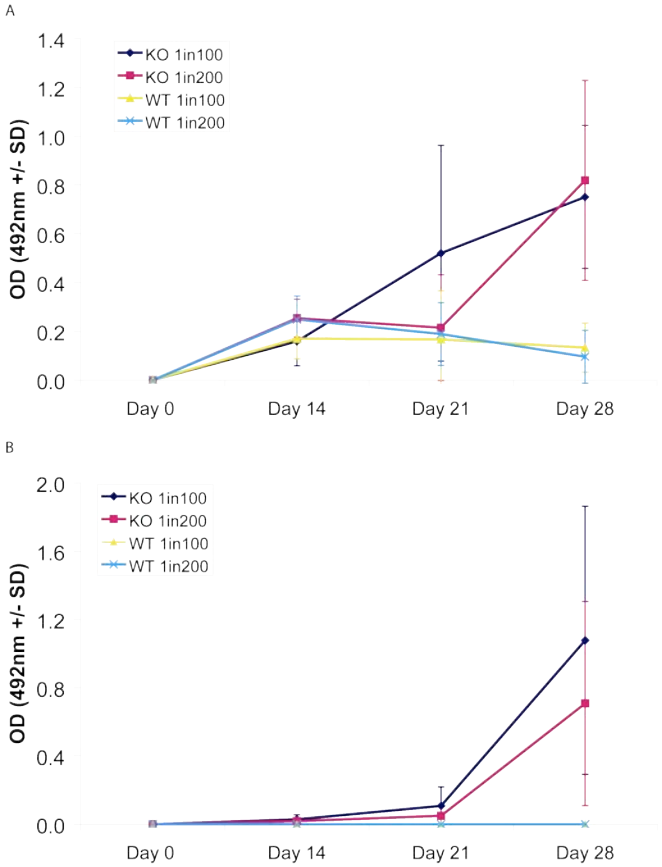

Figure 6.1 - Anti-GSC antibody response following GM1:GD1a immunisation

An IgM response was detected using anti-ganglioside ELISA at day 14 in both GM2 KO and WT animals (**A**). The OD continued to rise through days 21 and 28 in GM2 KO, but not GM2 WT mice. IgG responses (**B**) lagged behind IgM by 7 to 14 days in GM2 KO mice, and no detectable αGSC activity whatsoever was seen in GM2 WT animals. The graph depicts results from one independent experiment with n=5 per group, and is representative of results obtained in two further independent experiments.

6.2.1.2 PVDF glycoarray analysis

As only very small volumes of sera could be collected from mice at each time point, ELISA analysis was only able to be performed against a limited panel of antigens and negative controls, even when half-area ELISA plates were used. This means that although GM1:GD1a antibodies were detected, it is not possible to establish from the ELISA studies the finer specificity of the induced antibody response, particularly in terms of its complex dependent or independent nature. Given that a 10x10 PVDF array could be probed with the same amount of serum

required for a pair of ELISA wells, this technique provided a practical method of assessing the complex dependent nature of this response. A standard PVDF array layout of gangliosides and 1:1 complexes, as shown previously in Figure 3.6, was used.

None of the sera from GM2 WT animals had detectable anti-ganglioside antibodies as assessed by this method, even when using HRP conjugated IgM specific secondary antibodies, and conflicting with the ELISA analysis discussed in 6.2.1.1 above. In contrast, all of the GM2 KO mouse sera with detectable IgG or IgM GM1:GD1a reactivity on ELISA also displayed αGSC binding on PVDF array. However, the finer specificity of this response was again variable, particularly for IgG antibodies (Figure 6.2).The IgG subclass was not assessed.

In general, the GM2 KO IgM response was more consistently complex independent than the IgG response, the latter showing a spectrum of complex independent to strikingly complex dependent binding. Intriguingly, in those animals showing the most complex specific IgG binding pattern (Figure 6.2, 1+2), the antigen bound with the highest intensity was GM2:GD1a, rather than the GM1:GD1a complex used as the immunogen. This was the case in several animals across three separate experiments using freshly prepared GM1:GD1a liposomes and contemporaneously prepared and printed PDVF arrays. In any case, predominant GM1:GD1a complex binding was not seen, although all of the sera binding GM2:GD1a bound GM1:GD1a at a lower signal intensity.

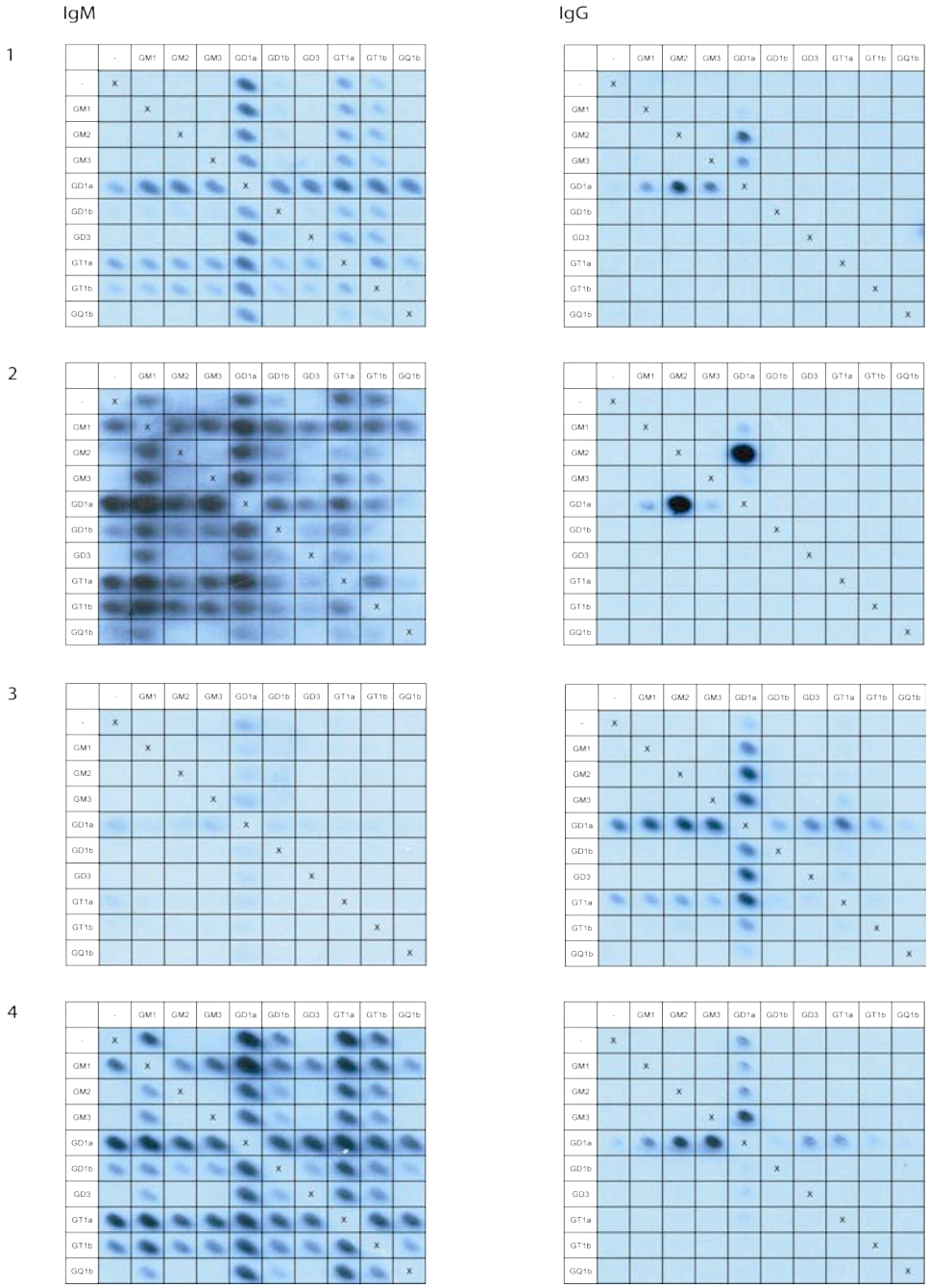

Figure 6.2 - PVDF array analysis of sera from GM1:GD1a immunised GM2 KO mice

The above figure shows examples of paired testing of day 28 serum samples from GM2 KO mice over 3 independent experiments, illustrative of the different antibody responses seen. The IgM response (left hand panels) is broad and complex independent in most GM2 KO animals, showing binding to a range of different gangliosides (including GM1, GD1a, GT1a, GT1b and to a lesser extent GD1b) in a largely complex independent fashion. This is not stereotyped, with distinct differences in the IgM antibodies detected in different animals which have undergone the same immunisation schedule. Above, mouse 3 has faint IgM binding to GD1a and GD1a-series complexes only, mouse 1 demonstrates a greater GD1a and series signal, in addition to complex independent GT1a and GT1b binding. Sera from mice 2 and 4 bind even more promiscuously to include GM1 and GD1b-series complexes to a greater and lesser extent. The right hand panels show the associated IgG responses from the same animals at the same time point. As can be seen, the IgG antibodies present have a narrower specificity, largely being confined to GD1a-series binding except for (**3**) which also demonstrates faint GT1a-series reactivity. As can be seen in (**1**) and especially (**2**), the complex specific nature of the binding was occasionally striking, but intriguingly largely directed against GM2:GD1a complexes.

6.2.2 GD1a : GD1b liposomes

Subsequent experiments were carried out using GD1a:GD1b complex containing liposomes as immunogens. The refined protocol described above was used, with 3 ip injections followed by 3 iv injections of ova containing liposomes following an initial ip priming injection of ova-alum. In these experiments, 3 different genotypes of mouse were used – GM2 WT, GM2 KO, and GD3s$^{-/-}$, the latter of which lack b-series gangliosides but have increased concentrations of a-series gangliosides.

6.2.2.1 ELISA analysis

Similarly to the result seen with GM1:GD1a liposomes, the injection of GD1a:GD1b containing liposomes in GM2 WT failed to result in a detectable IgG response, even when sera from day 35 was analysed. In contrast to the ELISA result in the prior experiment, however, no IgM response was seen either. In both GM2 KO and GD3s$^{-/-}$ groups IgM and IgG responses were seen, although the rise in titre lagged about 7 days behind that seen with the previous antigen (Figure 6.3).

In both the GM2 KO and GD3s$^{-/-}$ groups, anti-GD1a:GD1b IgM and IgG antibodies were first detected on day 21. The OD for IgM continued to rise over the next 14 days, and there was much less non-specific background staining seen with the GD1a:GD1a antigen as compared with GM1:GD1a. As the IgG titre appeared to have plateau'd between days 21 and 28, the mice were rebled 7 days later. At this point there had been a significant further increase in the IgG OD, despite the last IV boost being given on day 27. No statistically significant difference

between GD3s$^{-/-}$ and GM2 KO titres was found at any time point, as assessed by multiple, 2 sample, 2 tailed, T-tests.

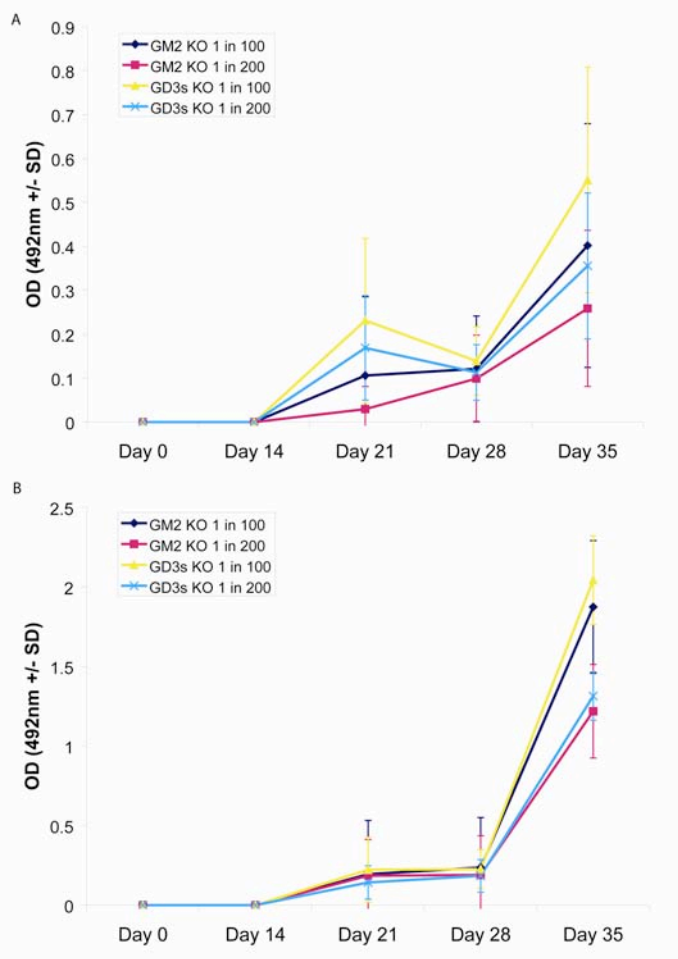

Figure 6.3 - Anti-GSC antibody response following GD1a:GD1b immunisation

The IgM (**A**) and IgG (**B**) response following GD1a:GD1ab immunisation, as assessed by ganglioside ELISA, is shown. No significant difference between GM2 KO and GD3s$^{-/-}$ is seen using this method. The above results come from one experiment with n=4 per group. These patterns are representative of three further experiments, although the absolute ODs varied significantly. Likewise, the variation in response between mice of the same genotype within the same experiment was again large, as illustrated by the large error bars shown above. Results for the GM2 KO group are not shown, as these animals failed to produce a detectable IgM or IgG response even at day 35.

6.2.2.2 PVDF glycoarray analysis

Once again, the PDVF array was required to investigate the finer specificity of the immune response. In essence, GM2 KO mice generated a complex independent response towards both GD1a and GD1b series antigens, whereas

GD3s KO mice produced a similar GD1b response but a highly discrepant GD1a response (Figure 6.4). All membranes shown below are examples of the IgG response.

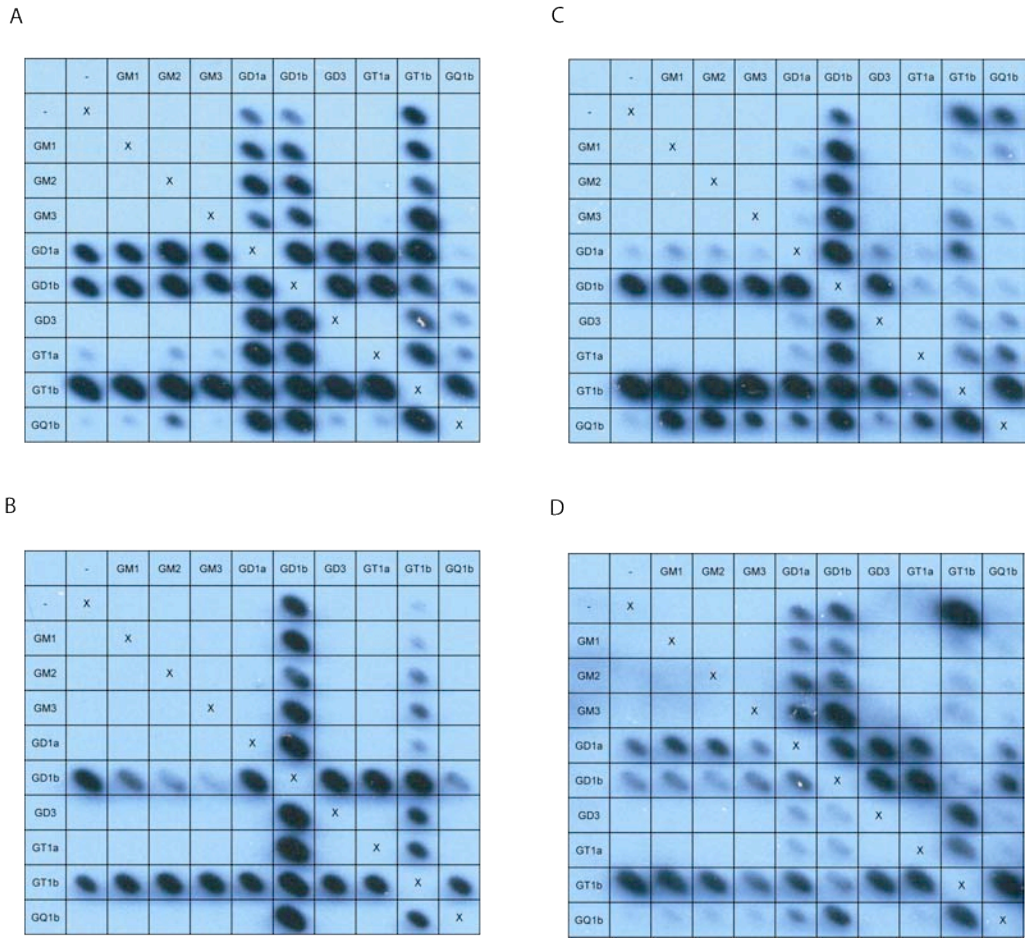

Figure 6.4 – The different complex response of GD1a:GD1b immunisation between GM2 KO and GD2s KO mice

(**A**) shows the typical response seen in GM2 KO animals which was largely stereotyped, generating antibodies against both GD1a and GD1b antigens in a complex independent manner. Additionally some GT1b and patchy GQ1b series binding was occasionally observed. In GD3s KO animals the response was somewhat more diverse (**B-D**). Here, when an antibody response was generated GD1b binding was invariable seen, but GD1a binding was variable, either being completely absent (**B**), much reduced compared with GD1b (**C**) or equivalent (**D**). Again these discrepancies were seen even with age and sex matched mice from the same litter injected with liposomes from the same batches at the same time and intervals.

The differences in GD1a series response between the two genotypes is quantified in (Figure 6.5), where the GD1a series average intensity level is reported as a percentage of the GD1b series average signal intensity reading.

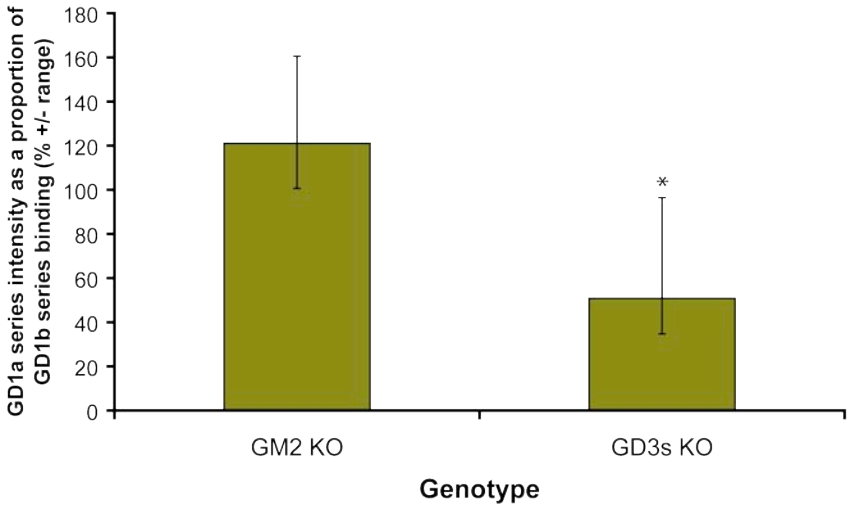

Figure 6.5 - Differing responses of GM2 KO and GD3s KO mice to immunisation with GD1a:GD1b liposomes

By comparing the average signal intensity of the GD1a responses as a proportion of the GD1b response between the different genotypes it can be seen that the GD1a series reactivity of GD3s KO mice is reduced (n=4, *p=0.023, two tailed, two sided T-test). On average, the GD1a signal is 50.9% of the GD1b signal in these mice. However, as shown by the error bar, there is a considerable variation, with some animals demonstrating nearly equivalent GD1a and GD1b reactivity. This is the norm in GM2 KO mice, where additionally some animals show increased GD1a versus GD1b binding.

6.2.3 Sphingomyelin complex response

As the cohort of Dutch GBS associated disease sera were assayed for anti-GSC complex activity and the results analysed it became increasingly clear that a proportion of human cases contained antibodies directed towards sphingomyelin containing complexes. In fact, 88 of 181 sera tested contained sphingomyelin complex binding antibodies (Chapter 5 above). This raised the possibility that, instead of the sphingomyelin simply being an inert carrier lipid for the gangliosides in the liposomes, there may have been additional ganglioside-sphingomyelin complexes present in these liposomes. If this was the case then there would also be the potential for these complexes to act as distinct antigens stimulating a different sphingomyelin-ganglioside complex specific immune response, separate from the heterodimeric ganglioside response initially sought.

Sera from 36 mice previously immunised under previously described conditions with both GM1:GD1a and GD1a:GD1b liposomes were available in sufficient quantities to allow further analysis. These were drawn from all three mouse strains studied. A new, 7x7 grid was devised for these experiments. This contained all of the different lipids and gangliosides used to create the liposomes, as shown (Figure 6.6).

	-	SM	Cho	DCP	GM1	GD1a	GD1b
-	X						
SM		X					
Chol			X				
DCP				X			
GM1					X		
GD1a						X	
GD1b							X

Figure 6.6 - Layout for 7x7 grid

The limited panel above was used to look for additional complex in the sera of mice immunised with ganglioside complex liposomes additionally containing sphingomyelin (SM), cholesterol (chol), and dicetylphosphate (DCP). As previously, the single lipids are spotted in the leftmost column and uppermost row, with the complexes in the squares to the right and below derived by combining the row and column headings.

Serum samples from 13 GM2 KO and 5 WT mice immunised with GM1:GD1a, plus 7 GD3s KO, 6 GM2 KO and 4 WT immunised with GD1a:GD1b, were analysed. All sera were prepared at 1 in 100 dilution and binding detected with HRP conjugated anti-mouse IgG at 1 in 30000 using the standard PVDF array protocol.

6.2.3.1 GM1:GD1a immunisations

Of the 13 GM2 KO sera analysed, IgG in 7/13 (53.8%) bound to sphingomyelin complexes on the array, compared with 0/5 from WT animals (Figure 6.7E). Most

commonly this was GD1a:sphingomyelin (GD1a:SM, seen in all 7 positives), but 3 additionally bound GM1:SM and 1 GD1b:SM. Five of these 7 bound the complex in the context of more general GD1a series binding (Figure 6.7 A+B), with various minor degrees of complex modulation, whereas in 2 sera more dramatic sphingomyelin-complex enhanced binding was seen (Figure 6.7 C+D) .

Quantification of the difference between the sum of binding intensities for GD1a and sphingomyelin in isolation compared with the intensity of GD1a:SM complex binding shows the majority of the sera (5 of the 7 positives) had antibodies with complex enhanced binding patterns. Of the remaining two, one showed a small complex attenuation (serum B) and one showed no change ('complex independent', serum F). This is graphically represented in Figure 6.7F.

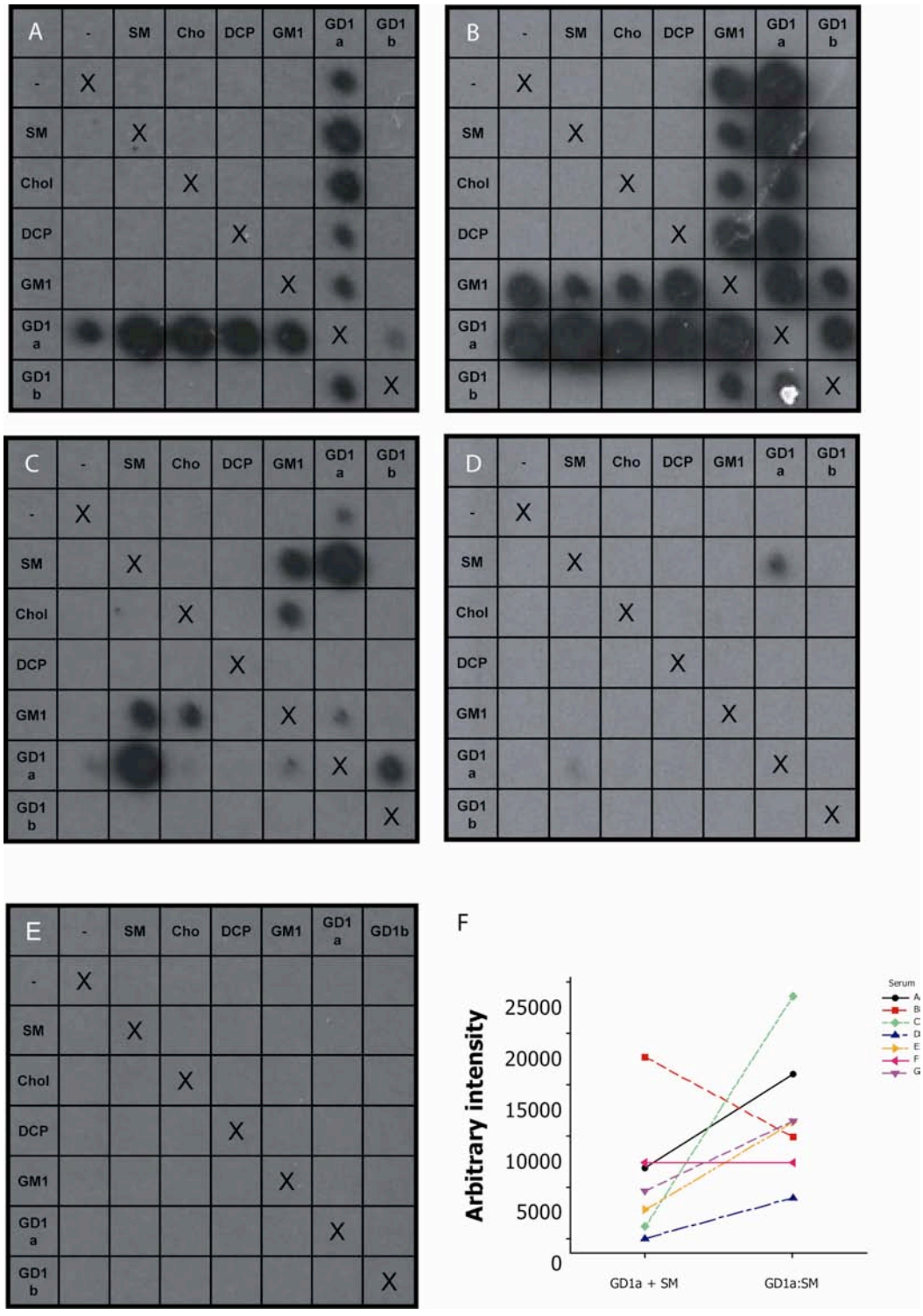

Figure 6.7 - Sphingomyelin complex IgG reactivity following GM1:GD1a immunisation

In the majority of GM2 KO mice showing sphingomyelin complex reactivity following GM1:GD1a liposome immunisation, this occurred in the context of more generalised GD1a-series (**A**) or GD1a and GM1-series (**B**) binding. In two mice, however, GD1a:SM complex reactivity was observed in the absence of anything but very low level binding to the component lipid structures in isolation (**C+D**). (**E**) shows the absence of binding following immunisation of a GM2 WT / littermate control. The value plot (**F**) shows the difference between the sum of binding intensities for GD1a and sphingomyelin in isolation (GD1a+SM) compared with the intensity seen for GD1a:SM complex, confirming that complex enhanced binding is seen with serum C in particular. Sera A to D in the graph correspond to the arrays above. Arrays for E to G are not shown.

6.2.3.2 GD1a:GD1b immunisations

Proportionally more of the GD1a:GD1b immunised animals had IgG antibodies binding Sphingomyelin-complexes, as compared with GM1:GD1a immunised mice. Five of the 7 GD3s KO mice displayed such binding, as did all 6 of the GM2 KOs. Once again, none of the four WT animals raised anti-sphingomyelin complex responses (identical membrane appearances to that already shown in Figure 6.7E).

Likewise, the complex specific nature of the GM2 KO response was again variable. This ranged from generalised GD1b-series binding, sometimes with additional GD1a-series binding, to very complex specific patterns, including exclusive GD1b:SM complex binding. Similarly, GD3s KO mice also showed a variable response, but in contrast never had detectable SM:GD1a complex binding antibodies. The range of responses seen is depicted in Figure 6.8. Here the sphingomyelin complex responses are compared between GM2 KO and GD3s KO mice, following immunisation with GD1a:GD1b liposomes. Both groups show a spectrum of binding patterns, which have a degree of overlap. Some GM2 KO animals generated antibodies with GD1b series binding which was markedly enhanced in the presence of certain additional lipids, such as cholesterol, dicetylphosphate (DCP) and particularly sphingomyelin (SM) (Figure 6.8A). This was sometimes critically dependent on the exact partnering lipid, with sphingomyelin containing ganglioside complexes alone being bound (Figure 6.8B) by some sera. In other examples both GD1a:SM and GD1b:SM complexes were recognised (Figure 6.8C,D), again without detectable binding to any of the component lipids in isolation. In further animals a more complex independent pattern of binding was seen, with either predominant, generalised GD1b series

(Figure 6.8E) or both GD1a and GD1b series (Figure 6.8F) reactivity. In both of these cases greater and lesser degrees of cholesterol:SM complex binding is additionally detected.

Similar patterns were seen in a number of GD3s KO mice, although in contrast to the GM2 KO group, no GD1a:SM complex binding was ever observed. Some antibodies (Figure 6.8G) bound almost exclusively to GD1b:sphingomyelin complexes. Others (Figure 6.8H, I, J, K) additionally displayed GD1b:DCP complex binding, sometimes with an additional, weaker GD1b:cholesterol signal. Most intriguingly, only two sera from GD3s KO mice did not have GD1b:SM binding antibodies and one of these instead had complex specific αGD1a:GD1b IgG reactivity (Figure 6.8L). This serum had not previously been tested on PVDF array as it had proved negative for GD1a:GD1b binding on ELISA.

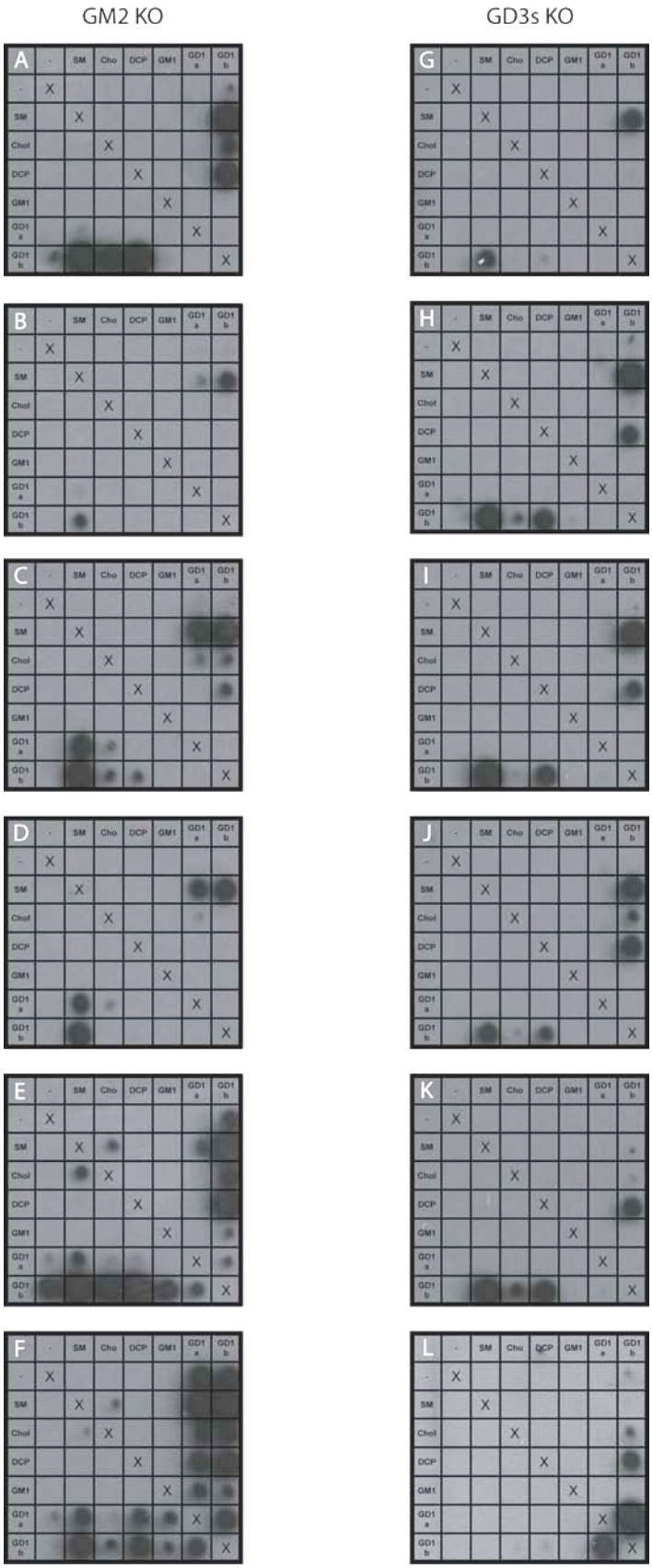

Figure 6.8 - Sphingomyelin complex reactivity following GD1a:GD1b immunisation

The sphingomyelin complex responses are compared between GM2 KO (left column) and GD3s KO mice (right column), following immunisation with GD1a:GD1b liposomes. Each membrane represents a the total IgG response in serum from a single animal.

6.3 Discussion

The most consistently observed result described in the preceding section is the lack of an IgG response directed towards either gangliosides or ganglioside complexes in wild type mice. Neither the complex independent or complex enhanced responses seen in both GM2 KO and GD3s KO animals were ever observed in wild types, using identical immunisation protocols and liposome preparations. Particularly given the relatively frequent detection of complex specific antibodies following GM1:GD1a injections in GM2 KO mice, the absence of this response in the WT implies tolerance to the GM1:GD1a antigen, suggesting it is recognised as self. It is possible, however, that the lack of a response in WT animals is simply a reflection of tolerance towards the individual gangliosides in isolation. This would require that the complex response in GM2 KO was induced by non-complexed single gangliosides present in the injected liposomes. It is difficult to be sure based on the experiments performed whether this is the case, but logically it seems less likely. Furthermore, previous ELISA experiments using GM1:GD1a liposomes and the GM1 complex attenuated mAb DG1 (Figure 3.12) confirm that at least a proportion of the GM1 in GM1:GD1a is complexed, given the markedly reduced binding seen with these liposomes compared to GM1 only liposomes. This alternative explanation would therefore require the complexes known to be present not to have an immunogenic effect. This does not seem to be the case given the complex specific IgG response seen in at least a proportion of the GSC immunised GM2 KO mice.

That the predominant complex response seen in a number of GM1:GD1a immunised GM2 KO mice is directed against GM2:GD1a is puzzling. GM1 and GM2 differ only in that the latter lacks the terminal galactose (Figure 1.5). There are

a number of possibilities. It might be that the GM1 used was contaminated by GM2, but this was not apparent when the GM1 preparation was run on TLC. Although this would not detect minor degrees of contamination it does confirm that the vast majority of the ganglioside present was indeed GM1, and therefore this could not be the sole reason for the observed response. It could additionally be that GM2:GD1a is for some reason more immunogenic that GM1:GD1a, and hence even minor contamination would result in the enhanced GM2:GD1a binding pattern seen. There is, however, no reason to suspect this based on previous single ganglioside work. Alternatively, GM1 could have been enzymatically converted to GM2 either *in vitro* prior to injection or *in vivo* following injection. This is the function of beta-galactosidase, present in lysosomes. However, when reserved portions of several batches of prepared GM1:GD1a liposomes were tested on liposome ELISA following injection they were still bound by the αGM1 positive control antibody DG2, suggesting that GM1 remained, although not every batch was tested in this way, and this again does not rule out more minor degrees of enzymatic degradation *in vitro*. It was not possible to test for *in vivo* degradation. Another possibility is that the structure of GM1:GD1a complex present in the liposomes somehow differs from that on the PVDF array. For example, if the GM1:GD1a complex in the liposome forms with a different angle between to two component gangliosides as compared to that presented on PVDF, access of the antibody to its binding site may be impeded in the latter situation. Conversely, given the shorter chain length of GM2, this might provide better access to the GSC binding site on PVDF than GM1 (Figure 6.9).

In several sera collected following immunisation, a complex independent response was seen. This was an especially common pattern in GD1a:GD1b

immunised animals. Whether there is a complex specific component within the complex independent response has not been addressed by the above experiments. It was hoped that cloning individual B cells from these animals might further address this question, as detailed in the next chapter (7, Cloning and Characterisation of Anti-GSC Antibodies).

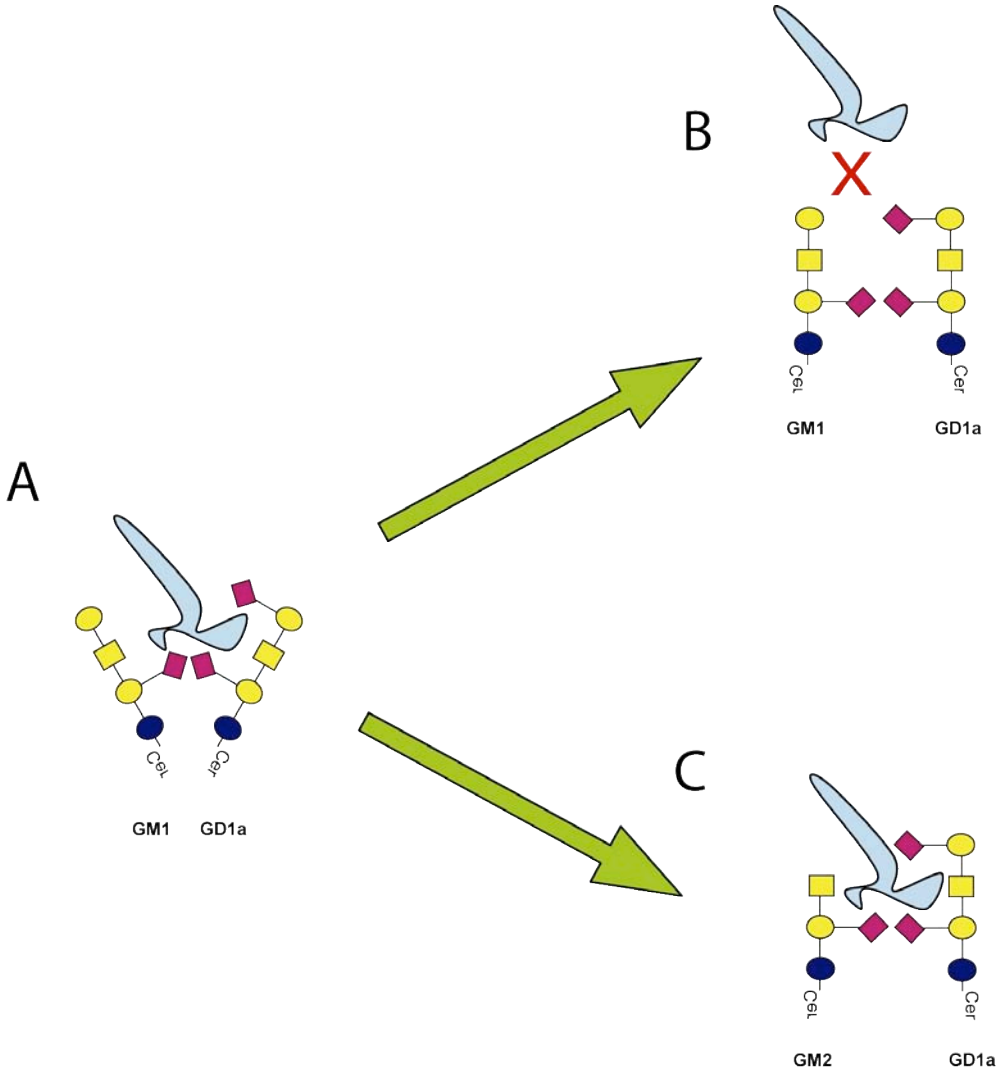

Figure 6.9 - A hypothetical reason for enhanced binding to GM2:GD1a on PVDF despite immunisation with GM1:GD1a

In the above example, the antibody is directed against a structure comprising of the internal sialic acids from both gangliosides and the N-acetylgalactosamine of GD1a. In the liposome (**A**), the paired gangliosides may be splayed apart, exposing the binding site. If the GM1:GD1a formed on the PVDF with a different angle between the two oligosaccharide chains, the terminal galactose of GM1 might sterically hinder and block the interaction. Instead, as the GM2 molecule in a GM2:GD1a complex (C) lacks this terminal galactose (which does not form part of the binding site), binding is improved as the antibody is able to better access this binding site.

At a superficial level it is therefore apparent that immunisation with GSCs can additionally produce a response directed towards single gangliosides presented on PVDF. Of course, it is difficult to discount the possibility that this response is induced by non-complexed single gangliosides present within the injected liposomes. The fact that low level DG1 binding is seen towards GM1:GD1a liposomes in the previously described ganglioside ELISA experiments (Figure 3.12) suggests that at least some GM1 remains non-complexed to GD1a in such liposomes. Another possibility is that the GSCs that are formed within the liposome membrane are broken apart before presentation to B cells. Interestingly in this regard, some GD3s$^{-/-}$ animals injected with GD1a:GD1b containing liposomes generated a response against single GD1a (and GD1a series complexes) despite this ganglioside being present in increased quantities as compared with GD3s$^{+/+}$ mice. These mice are, however, tolerant of injection with GD1a-only liposomes, demonstrating that the response to GD1a in GD1a:GD1b liposomes differs from that to GD1a alone.

The mechanisms involved in the immune response to glycolipid antigens are incompletely understood. Whether T-cell help and CD1 presentation is required is uncertain. Although the above described experiments were not designed to dissect out the finer mechanics of the glycolipid and glycolipid complex response, a number of comments can be made. When animals were injected with non-ova containing ganglioside complex liposomes, either iv or ip, no immune response was seen. Conversely, injections of ova-containing liposomes did result in a response. This has previously been seen as evidence of the requirement for T-cell help, although this evidence is indirect at best. It may alternatively be that the presence of the ova protein results in a generally more inflammatory state which favours the generation of anti-glycolipid antibody via

non T-cell mediated pathways. CD1 molecules are involved in glycolipid presentation to T-cells (Porcelli & Modlin, 1999;Shamshiev *et al.*, 2000;De Libero *et al.*, 2002) and as previously discussed CD1a and CD1e polymorphisms were shown to be associated with modified risks of developing GBS in one study (Caporale *et al.*, 2006). However, more recently, antibody responses to glycolipids in model carbohydrate systems have been shown to require $CD4^+$ T cells but not CD1 molecules or natural killer T (NKT) cells, IgG ganglioside responses have been generated in mice lacking CD1d, and a further study has not confirmed the association between GBS and CD1 polymorphisms (Kuijf *et al.*, 2008;Matsumoto *et al.*, 2008). Likewise, although CD1 molecules are traditionally thought of presenting only one glycolipid molecule at a time, casting doubt on their ability to present glycolipid complex antigens, the binding pocket of CD1d in particular is large enough to potentially be able to accommodate two lipid tail chains concurrently. In fact, when glycolipids with shorter tails are bound by CD1 the remainder of the binding pocket has been shown to contain other 'packing lipids' (Cohen *et al.*, 2009). Natural antibodies have also previously been linked with tolerance, autoimmune disease and transplant rejection (Holers, 2005;Shimizu *et al.*, 2007). The presence of natural antibodies to self-glycolipids might either allow these antigens to be 'mopped up' before the adaptive immune response is activated (and thus maintain tolerance) or alternatively be a sign of intolerance to that particular target. None of the animals studied here ever had detectable anti-ganglioside complex antibodies prior to immunisation. Whether the initial rise and subsequent fall in IgM reactivity in wild-type mice following GM1:GD1a immunisation represents a 'spike' in natural antibody production to detectable levels followed by a re-establishment of tolerance is uncertain. These results are once again

confounded by the very high levels of non-specific IgM binding seen in all animals following immunisation.

Overall, the immunisation protocol resulted in a frequent, if inconsistent, antibody response, which could subsequently be utilised for the production of αGSC antibody producing hybridomas. Clearly, the animals used in this subsequent step would have to be carefully selected to ensure they had generated a robust antibody response, which had the potential to contain an αGSC monospecific component.

7 Cloning and characterisation of anti-GSC antibodies

7.1 Introduction

The generation of a ganglioside complex specific monoclonal antibody was felt to be critical to further understand the pathogenic potential of this subtype of antibodies, their binding characteristics, and to allow an investigation of the tissue distribution of ganglioside complexes. Such antibodies could be used in surface plasmon resonance work, immunofluorescence binding studies, and *ex vivo* and *in vivo* pathological studies.

The technique for creating monoclonal antibodies of defined specificities was developed in the 1970s (Kohler & Milstein, 1975). In essence, B cells are extracted from the spleens (and occasionally other sites) of immunised mice. These cells are then fused with myeloma cells using polyethylene glycol to render them immortal. The myeloma cells lack hypoxanthine-guanine-phosphoribosyl transferase (HGPRT), a critical enzyme in the purine salvage pathway. When *de novo* purine synthesis is also blocked using media containing aminopterin, the unfused cells die. In contrast, fused cells will have regained the HGPRT enzyme from the splenocytes, and can use this salvage pathway to synthesise purines. This media therefore selects out only the successfully fused cells for survival. In traditional liquid-media based techniques, the cells are plated out in multiple wells and the supernatants tested at intervals. Only those containing antibody of the required specificity are expanded and grown further. To ensure monoclonality, serial dilutions are performed, again selecting for

positive wells and discarding negatives, until a pure growth which has originated from one cell is obtained.

Modern techniques using semi-solid media rely on many of the same principles, but following fusion the cells are suspended in a semi-solid, aminopterin containing media. The resulting colonies should already be monoclonal, and can be picked individually and subsequently screened for antibody production. Further details of these techniques are given in chapter 2.

7.2 Results

Both liquid and semi-solid medium techniques were used in the selection and purification of monoclonal lines.

7.2.1 Liquid medium selection

Initial attempts were made using GM1:GD1a immunised animals and traditional liquid based selection media. Variations in the ratios of splenocytes to 653-myeloma cells, the area of wells used for initial and subsequent cell growth (96 well versus 24 well plates), and whether whole blood from other mice was used to feed the fusions, were tested in an attempt to optimise the protocol. A summary of the different experiments is given (Table 7.1). Although the methodology was refined and the number of first screen positive wells increased, this signal was lost when the wells were subsequently split and/or expanded. If this step could be omitted, and monoclonal wells produced from the outset, it was hoped that the cultures would have a better chance of continuing to produce the antibody required.

7.2.2 Semi-solid medium selection

The above was the rationale for moving to a semi-solid medium. Using this method, single colonies could be picked and once positives were indentified it would only be necessary to keep these cells growing, rather than moving to a cloning process involving limiting dilutions.

In this protocol, following exposure to polyethylene glycol (PEG) to fuse the cells, they are returned to a recovery medium in a tissue culture flask for 24hrs

prior to mixing with the semi-solid selection medium and plating out. Unfortunately, in the initial experiment when the cells were resuspended after 24hrs, copious, stringy clumps of cells were noted, suggesting substantial cell death. After 14 days of growth in the semi-solid medium, only a handful of very small, white colonies were visible to the naked eye, rather than to hundreds suggested in the literature accompanying the kit. After taking advice for the kit manufacturer's technical department, it was decided to perform 3 further fusions, varying the recovery time post fusion. Zero, 24 and 48h periods were chosen. The results of these experiments are summarised in Table 7.2.

Immunogen	Mouse Strain	Terminal OD (1 in 100)	Splenocytes ($x10^7$)	Myeloma Cells ($x10^7$)	Ratio (Spleen:Myeloma)	Plates	Fed	Cells / well ($x10^5$)	Positive Wells (1^{st} Screen)	Positive Wells (2^{nd} Screen)
GM1:GD1a	GM2 KO	0.522	2.7	0.27	10:1	6x96	Y	1.2	27	0
GM1:GD1a	GM2 KO	0.158	11.5	0.945	≈10:1	6x96	Y	5.0	3	0
GM1:GD1a	GM2 KO	0.718	5.4	0.68	≈10:1	6x96	Y	2.4	0 (infected)	-
GM1:GD1a	GM2 KO	0.839	6.5	0.65	10:1	12x24	Y	2.5	0	-
GM1:GD1a	GM2 KO	0.552	10.0	20.0	1:2	12x24	Y	10.5	0	-
GM1:GD1a	GM2 KO	1.388	1.8	0.4	≈5:1	6x96	N	0.3	0	0
GM1:GD1a	GM2 KO	0.542	4.3	0.9	≈5:1	6x96	N	0.8	2	0
GM1:GD1a	GM2 KO	1.467 / 1.978 (Pooled)	10 + 8.5	25	1:1.35	6x96	N	2.0	3	0
GD1a:GD1b	GD3s KO	2.34	11.9	2.4	5:1	6x96	N	2.9	4	0
GM1:GD1a	GM2 KO	0.601	3.8	1.1	≈4:1	3x96	N	2.0	3	0
GM1:GD1a	GM2 KO	0.954	7.8	2.1	≈4:1	8x96	N	1.7	7	0
GM1:GD1a	GM2 KO	1.266	8.4	2.1	≈4:1	8x96	N	1.8	10	0
GD1a:GD1b	GD3s KO	1.878	11.4 (+ bone marrow)	2.5	4.5:1	6x96	N	2.8	26	0

Table 7.1 - Summary of fusion experiments using liquid selection media

Table 7.2 - Summary of experiments using semi-solid selection media

Immunogen	Mouse Strain	Terminal OD (1 in 100)	Splenocytes ($x10^7$)	Myeloma Cells ($x10^7$)	Recovery time (h)	Colonies (14 days)	Growing wells (Day 21)	Positive Wells (1^{st} Screen)	Positive Wells (2^{nd} Screen)
					24	not recorded	0		
GD1a:GD1b	GM2 KO	2.04	8.0	1.0	0	36	4	0	
GD1a:GD1b	GM2 KO	1.28	10.6 (+BM)	0.95	24	82	13	1	0
GD1a:GD1b	GD3 KO / GM2 KO	1.40 / 0.61 (pooled)	19.6 (+BM) (pooled)	1.8	48	67	29	3	0

7.3 Discussion

The failure to generate a stable clone of myeloma cells producing anti-ganglioside complex antibodies is a frustrating limitation to the further study of the potential pathogenic effects of such antibodies. The reasons for this failure have not been fully elucidated in the above experiments. A certain chance effect is at play, requiring that some of the limited proportion of splenocytes of the required antibody specificity fuse successfully with the immortal myeloma cells. The increasingly consistent observation of positive wells on the 1st post fusion ELISA screen suggests that this is not the sole problem. With this in mind, it had been initially postulated that non-antibody secreting clones in the wells were outgrowing the antibody secreting clones, resulting in a loss of antibody production. Furthermore, it was also speculated that attempts to clonally dilute the cells were stressing them and causing excessive cell death. The observation that initial positive wells obtained from plucked colonies in the semi-solid selection medium also lost their antibody secretion is counter to these hypotheses. It remains possible that the cells were overly sensitive to attempts to further expand them beyond the single tissue culture plate well stage, for reasons not established.

653 myeloma cell lines were obtained from 2 further sources in case there had been a problem with the viability of the initially used line, but this made no dramatic difference to the outcome of the fusions. After the first two unsuccessful fusions, the viability and growth rate of the 653s pre-fusion was assiduously checked, and repeatedly found to be satisfactory. It may have been that exposure to PEG during the fusion was particularly toxic to the cells, but one might expect this to result in early, rather than delayed, cell death. Never

the less, this was not systematically optimised, and attempts were simply made to follow the previously successful fusion protocol as closely as possible with respect to timings.

Another possibility is that the products of the successful fusions (anti-GSC antibodies) are toxic to the cells producing them. This again seems unlikely as single ganglioside antibodies have previously been produced in this way. These antibodies are only structurally injurious in the nervous system *in vivo*, where their target antigen is much more highly expressed than compared with the haemopoietic system, and then only when also administered with a source of complement. However, GBS is (most usually) a monophasic disease and when ganglioside antibodies are detected in clinical cases their titre declines as the active disease process resolves, indicating that tolerance is re-established. This is generally felt to be due to immuno-regulatory mechanisms involving changes in the balance between pro- and anti-inflammatory cytokines and cells. Based on the speculation at the start of this paragraph, the possibility of self-toxicity of the anti-ganglioside antibodies to the cells producing them could be proposed as another potential mechanism for the re-establishment of tolerance.

Future attempts to produce anti-GSC antibody secreting clones might then best begin with an optimisation of the PEG exposure time, and other components of the fusion process, in the first instance simply looking at the subsequent viability of the fused cells. Once this is completed, comparison could be made between the viability of cells in anti-GSC antibody producing and non-producing wells to look for any toxic effect of the antibodies themselves. Time and resource constraints precluded such assessments being undertaken and included herein.

8 An active immunisation model of GBS

8.1 Introduction

As already discussed, although immune responses were successfully generated against ganglioside complexes (GSCs) expressed in liposomes, a stable clone of myeloma cells producing complex specific monoclonal antibodies was not produced in time to perform further studies assessing the nature and pathogenicity of αGSC antibodies and include the results in this thesis. Some limited studies involving assessment of the binding of neuropathy associated sera with apparent GSC specific binding patterns were undertaken, looking at immunoglobulin deposition in frozen sections of mouse diaphragm neuromuscular tissue (3.2.13). However, as reviewed in the above discussion section (3.3), such studies are restricted not only directly by the small amounts of sera available, limiting optimisation and repetition of the assay, but also by the knock on effect that with these limited resources only small frozen sections can be examined at all. As earlier investigation of the binding of the paired anti-GM1 monoclonal antibodies revealed there is (albeit indirect) evidence to suggest that GSC complexes may be disrupted in frozen, dead tissue. A potential alternative approach to investigate the *in vivo* effects of αGSC antibodies was made possible by the recent development of a new, transgenic, mouse line, created in house by Dr Denggao Yao.

8.1.1 Background

Although animal models of axonal neuropathy mediated by anti-ganglioside antibodies have been created in rabbits following repeated bovine brain

ganglioside injections over long periods (Yuki *et al.*, 2001), such models in mice are limited by the tolerance of wild type animals to ganglioside injections. These animals, which express a full range of gangliosides, fail to produce a robust immune (and in particular, IgG) response when repeatedly injected with gangliosides plus adjuvant administered in liposome form (Figure 8.1A), and as again demonstrated by experiments detailed in chapter 6 above. This hurdle can be overcome by using GalNAcT$^{-/-}$ (also known as "GM2 KO") mice. These mice produce no ganglioside beyond the block in the synthetic pathway resulting from the absence of the GalNAcT enzyme, and instead accumulate the shorter chain gangliosides GM3 and GD3. As they lack gangliosides of greater complexity, such as GQ1b for example, they are intolerant of immunisation with such antigens, and produce robust immune responses including high titres of anti-ganglioside IgG antibodies (Figure 8.1B)(Bowes *et al.*, 2002). However, as these animals do not express the target molecule for this immune response, they do not develop neuronal injury and hence do not display a disease phenotype. As such, current mouse models of anti-ganglioside antibody mediated neuropathies rely on passive transfer of antibody produced in GM2 KO animals into GM2 WT animals, most usually (and reliably) via the intermediate step of creating a clone of myeloma cells producing a ganglioside antibody of defined specificity (Figure 8.1C).

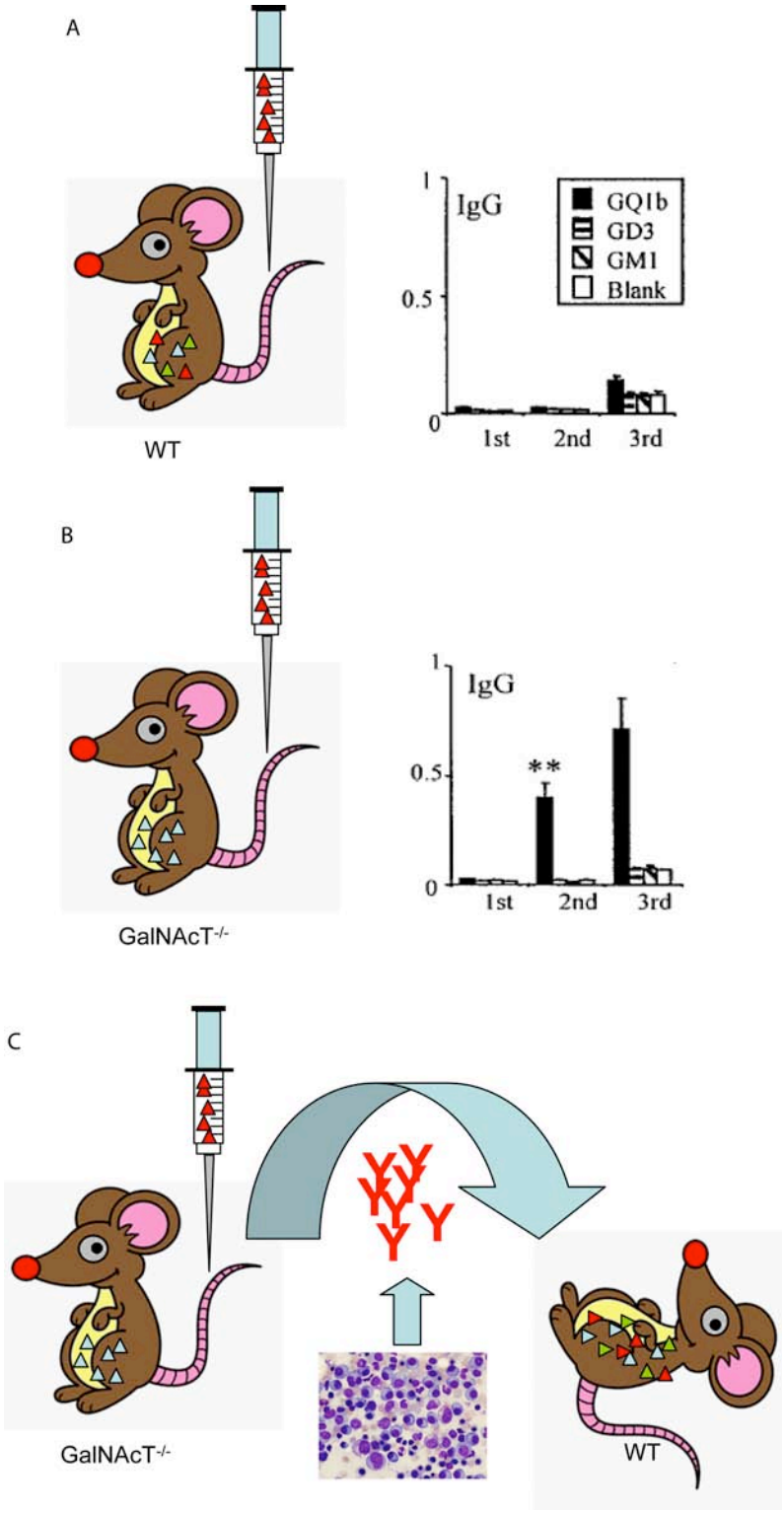

Figure 8.1 – The current passive transfer model of anti-ganglioside mediated neuropathy in mice

Wild type mice (**A**) are tolerant of immunisation with gangliosides, such as GQ1b (red triangles), failing to mount a robust IgG response despite repeated immunisations, as shown in the accompanying graph, taken from (Bowes *et al.*, 2002). This can be overcome by using GalNAcT$^{-/-}$ (GM2 KO) mice (**B**). These mice lack longer chain gangliosides, and produce a strong IgG response on repeat administration of such immunogens (IP GQ1b-liposomes on 3 occasions 2 weeks apart in the example graph). However, given that they do not express the antigen, no disease phenotype ensues. Instead, a passive transfer of antibody from GM2 KO to GM2 WT animals is necessary, usually via the intermediate of antibody producing myeloma clone (**C**).

8.1.2 Development of a transgenic neurofilament promoter GalNAcT / GalNAcT$^{-/-}$ mouse

In an attempt to overcome this double step, and to assess the effect of gangliosides expressed solely within the nervous system, a transgenic mouse was created by Dr Denggao Yao. The approach taken was a tissue specific, axonal rescue of GalNAcT function in GM2 KO mouse, using the neurofilament light (NFL) promoter to drive axonal expression. In brief, the DNA for the GalNAcT gene was purified, fused to a Flag tag for detection of expression, and amplified. Activity of the enzyme was confirmed by insertion into a CMV promoter vector and transfection of GM3 only expressing melanoma cells, in which GM2 expression was subsequently detected by immunofluorescence microscopy using an anti-GM2 antibody (Figure 8.2A). Activity of the NFL promoter was confirmed by insertion of the transgene into a NFL promoter vector, and transfection of an NG108 neuroblastoma cell line. Detection of flag expression confirmed activity of the promoter (Figure 8.2B). The now verified vector was then microinjected into fertilised mouse ova, and by this technique 6 transgenic germline transmitters were generated. However, as the transfection relied on GalNAcT$^{+/+}$ mice for success, these lines had to be crossed onto a GM2 KO line such that systemic ganglioside expression was lost, leaving only that driven by the transgene under NFL control (Figure 8.2C). The resulting genotype is designated Tg(Nfl-GalNAcT)GalNAcT$^{-/-}$, subsequently referred to as NFL Tg.

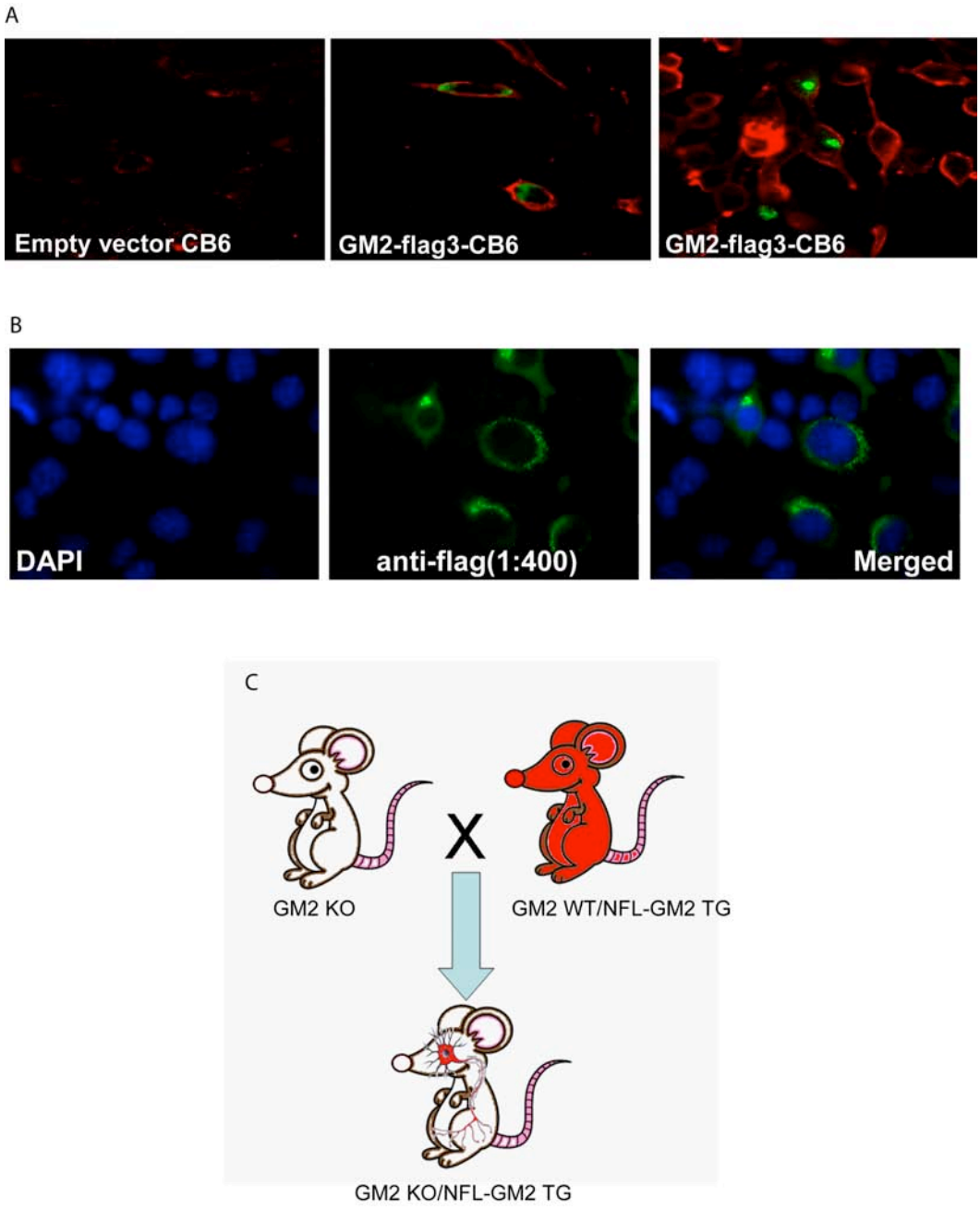

Figure 8.2 - Development of the GM2-neurofilament light transgenic / GM2 KO mouse

(**A**) Transfection of GM3 only expressing melanoma cells, with a strong CMV promoter, results in GM2 expression, as detected by immunofluorescence using a GM2 antibody (green = anti-GM2, red = anti-flag). This demonstrates that the inserted DNA results in the production of an active enzyme. (**B**) Using a different vector, transfection of neuroblastoma cells confirms that the neurofilament light (NFL) promoter is active, as evidenced by detectable flag expression, again using immunofluorescence (green = anti-flag, blue = DAPI). These experiments were performed and pictures kindly supplied by Dr Denggao Yao. (**C**) Following successful microinjection into the fertilised ova of wild type mice, the germline transmitting founders needed to be crossed onto the GM2 KO genotype to give an axon specific rescue. In the above diagram, the red shading represents gangliosides more complex (i.e. of longer chain length) than GM3 and GD3. GM2 KO mice contain no complex gangliosides, whereas WT mice express such gangliosides systemically. In the transgenic WT, the effect of the 'native' GalNAcT gene and enzyme would be expected to dwarf that of the transgene. By crossing the GM2 WT/NFL-GM2-Tg with a GM2 KO, the native gene can be removed, resulting in complex ganglioside expression confined solely to the axons, under the control of the NFL promoter. The resulting genotype is designated Tg(Nfl-GalNAcT)GalNAcT$^{-/-}$, subsequently referred to as NFL Tg.

The transgenic animals were initially tested for axonal ganglioside expression using fluorescently labelled cholera toxin B-subunit and anti-GM1 mAb (DG2), but no binding was detected. However, when a different mAb with a different ganglioside binding profile was used, binding was detected in the neuromuscular tissue of these mice. The antibody used was MOG12, binding primarily to GT1b, but also to GD1a and GD1b (Figure 8.3).This immunofluorescent tissue analysis was carried out by Dr Kay Greenshields. As such, initial experiments to work up an active immunisation model of GBS in NFL Tg mice concentrated on anti-GT1b antibodies and GT1b as an immunogen (sections 8.2.1 to 8.2.3). When high performance thin layer chromatography (HP-TLC, Figure 8.4) (performed by Professor Koichi Furukawa at the Nagoya University School of Medicine, Nagoya, Japan) subsequently demonstrated that GM1 and GD1a expression had also been reconstituted, at least in the Ed2 line (one of the six transgenic lines resulting from the implantation and breeding programmes), a subsequent active immunisation protocol involving GM1:GD1a complex antigens was justified (section 8.2.4).

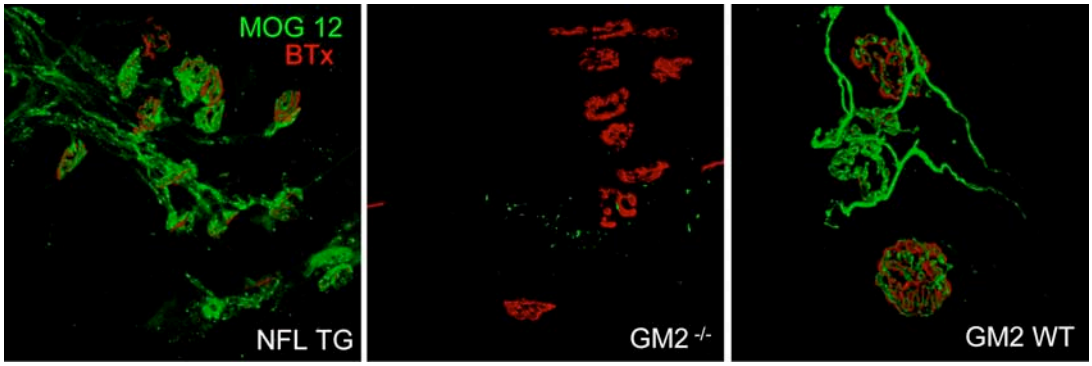

Figure 8.3 - Immunofluorescent staining of neuromuscular tissue from the lumbricals of transgenic, knockout and wild type mice

The MOG12 mAb (green) binds GT1b, GD1b and GD1a, whereas TRITC labelled alpha bungarotoxin (BTx, red) locates the post synaptic apparatus of the neuromuscular junction. As can be seen above (left panel), the presence of the transgene has restored binding by MOG12, as compared with the KO animal (centre panel, where only minor, presumably non-specific, background staining is seen), and to levels equivalent to that seen in wild types (right panel). This implies that the transgene has successfully rescued complex ganglioside synthesis in the axons. These experiments were performed and images kindly supplied by Dr Kay Greenshields.

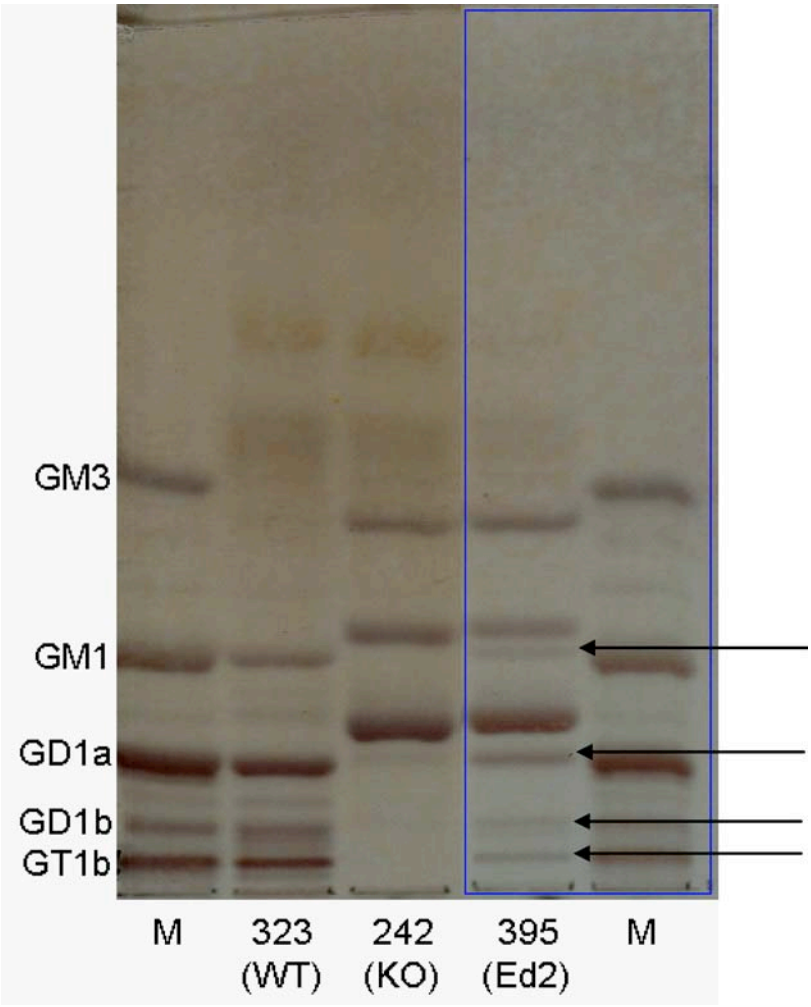

Figure 8.4 - HP-TLC using acidic glycolipid fractions extracted from transgenic, KO and WT mice brain

The WT mouse (323) has strong bands corresponding to the gangliosides GD1a and GT1b, as well as slightly fainter bands representing GM1, GD1b, and other unidentified structures. In contrast, the KO mouse (242) has three strong bands only, corresponding to gangliosides accumulating behind the enzyme block – namely (from top to bottom); GM3, 9-O-acetyl GD3 and GD3. The identity of this central band has only recently been confirmed (Furukawa *et al.*, 2008). Somewhat surprisingly, there appears to be a faint band at the level of GD1a in the KO lane. As can be seen, synthesis of more complex gangliosides has been rescued in the transgenic line Ed2 (mouse 395), indicated by the arrows above, from top to bottom representing GM1, GD1a, GD1b and GT1b. This analysis was performed and the image kindly provided by Professor Koichi Furukawa at the Nagoya University School of Medicine, Nagoya, Japan.

8.2 Results

In the development of the active immunisation model using the NFL Tg mouse and ganglioside antigens, an attempt was made to build up the level of complexity and test the validity of each component in the protocol individually before combining these together in the final protocol. In this way, initial experiments using the transgenics were performed using *ex vivo* preparations of neuromuscular tissue exposed to anti-ganglioside antibodies and complement, before passive transfer of the same antibodies was trialled *in vivo*. Subsequently immunisation experiments were performed, ultimately leading to disease induction, as discussed below.

8.2.1 Ex vivo Model

In these preliminary experiments, whole diaphragms along with a surrounding rim of costal tissue were quickly harvested from NFL Tg, WT and KO mice killed by a rising concentration of CO_2, as per Home Office guidelines. This tissue was then kept alive by bathing in oxygenated, warmer Ringer's solution (Figure 8.5, and see appendix), prior to application of MOG12 (or MOG16, a mAb obtained from the same fusion with a very similar ganglioside binding protocol), followed by normal human serum (NHS) as a source of complement.

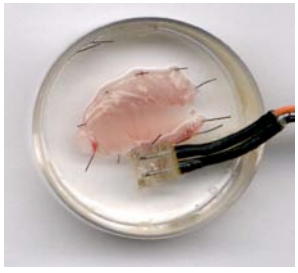

Figure 8.5 - Organ bath containing mouse diaphragm in Ringer's

If the transgene had successfully sensitised the NMJs of the NFL Tg mouse to ganglioside mediated injury, one would expect to be able to detect immunoglobulin deposition, complement activation and neurofilament loss (as a marker of cytoskeletal degradation and neuronal injury), and this was indeed the case. Images from these experiments are shown in Figure 8.6. Panel A shows that IgG is deposited over the NMJs of neuromuscular tissue from NFL Tg animals exposed to anti-ganglioside antibody, and that these antibodies activate complement leading to MAC pore formation when NHS is provided. These appearances are similar to those seen with GM2 WT mice (Figure 8.6B), and in contrast to GM2 KO animals (Figure 8.6C) where no binding is seen. Likewise when Ringer's medium is applied instead of the anti-ganglioside antibody, no binding is seen (Figure 8.6D-F).

Quantification and statistical analysis of the above data confirms that all of IgG binding (Figure 8.7A), C3c (Figure 8.7B), and MAC pore deposition (Figure 8.7C) are significantly increased in NFL Tg and WT mice over controls (non parametric Mann-Whitney test for non normalised data, $p<0.0001$ for all comparisons). There is no statistically significant difference in IgG or C3c staining between WT and NFL Tg tissue, but MAC pore deposition is significantly increased in NFL Tg mice versus WT ($p<0.0001$). Intensity measurements are all given in arbitrary units.

Neurofilament loss over the NMJ was additionally used as an indication of axonal injury, with comparison made between control and antibody treated. The neurofilament signal for GM2 KO tissue was unchanged regardless of whether Ringer's alone (Con) or MOG16 (Ab) was applied (Figure 8.8A, Mann-Whitney, $p=0.295$). In contrast, in both GM2 WT (B) and NFL Tg tissue (C), the level of

neurofilament staining was significantly decreased ($p<0.0001$) in tissue exposed to the antibody. There was no statistically significant difference in neurofilament staining between NFL Tg and GM2 WT either with ($p=0.998$), or without ($p=0.276$), antibody application.

Similar results were seen with two different antibodies (MOG12 and MOG16) and two different transgenic lines (line 30 and Ed2).

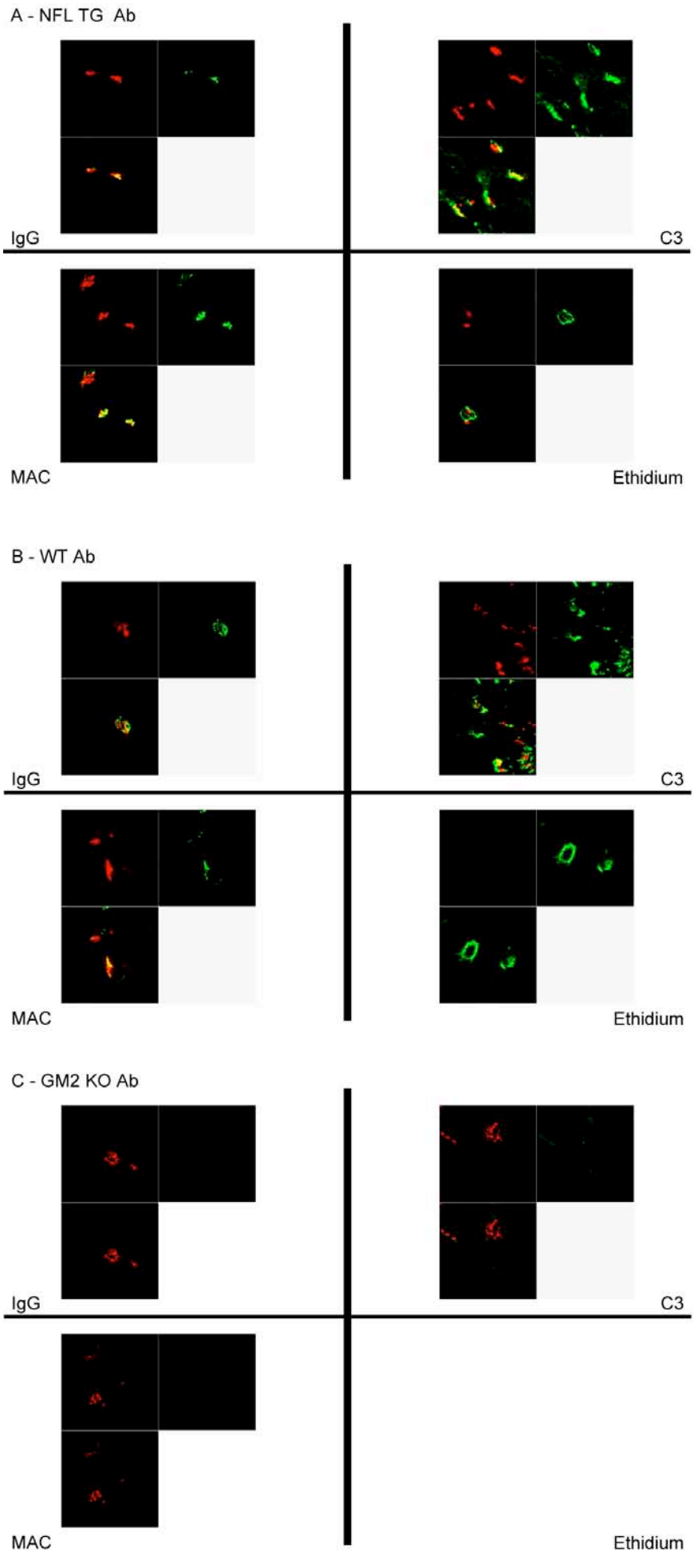
A - NFL TG Ab
IgG
C3
MAC
Ethidium
B - WT Ab
IgG
C3
MAC
Ethidium
C - GM2 KO Ab
IgG
C3
MAC
Ethidium

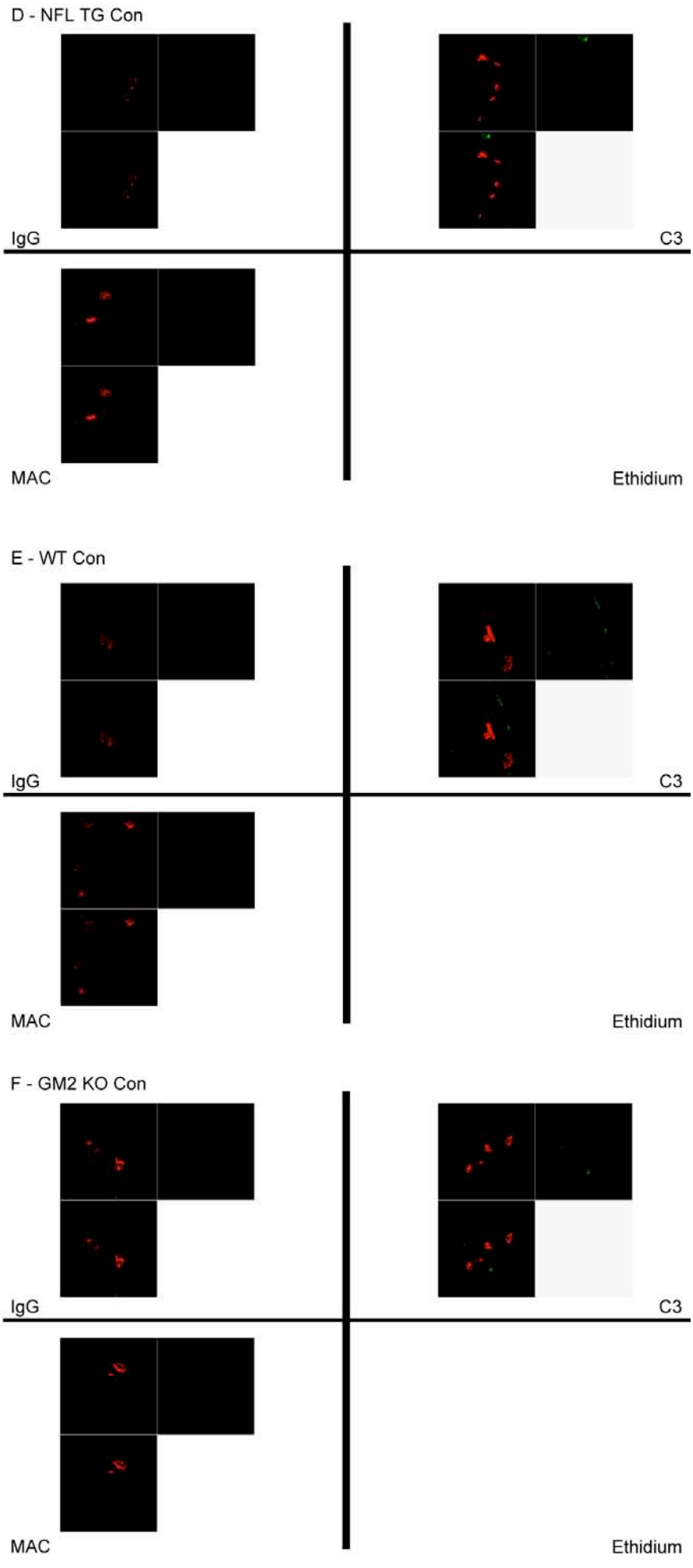
D - NFL TG Con
IgG
C3
MAC
Ethidium
E - WT Con
IgG
C3
MAC
Ethidium
F - GM2 KO Con
IgG
C3
MAC
Ethidium

Figure 8.6 - Ex vivo application demonstrates the sensitivity of transgenic NMJs to anti-ganglioside antibodies

NFL Tg (**A**), GM2 WT (**B**), and GM2 KO (**C**) diaphragm exposed to MOG12 antibody followed by NHS as a source of complement. IgG, C3c, and MAC appear green in their respective panels and the neuromuscular junctions (NMJs) are labelled red with α-bungaratoxin. In the ethidium panels the NMJs are now green and the ethidium stain is red. One representative example of positive ethidium staining over an NMJ (**A**, two ethidium stained nuclei) and one example of negative ethidium staining (**B**, two NMJs with no associated ethidium staining) are shown. This latter appearance was typical of the ethidium pattern seen in all other experimental conditions, for which no additional representative images are shown.

(**D-F**) are control diaphragm preparations exposed to Ringer's medium alone rather than anti-ganglioside antibody, but otherwise identically processed..

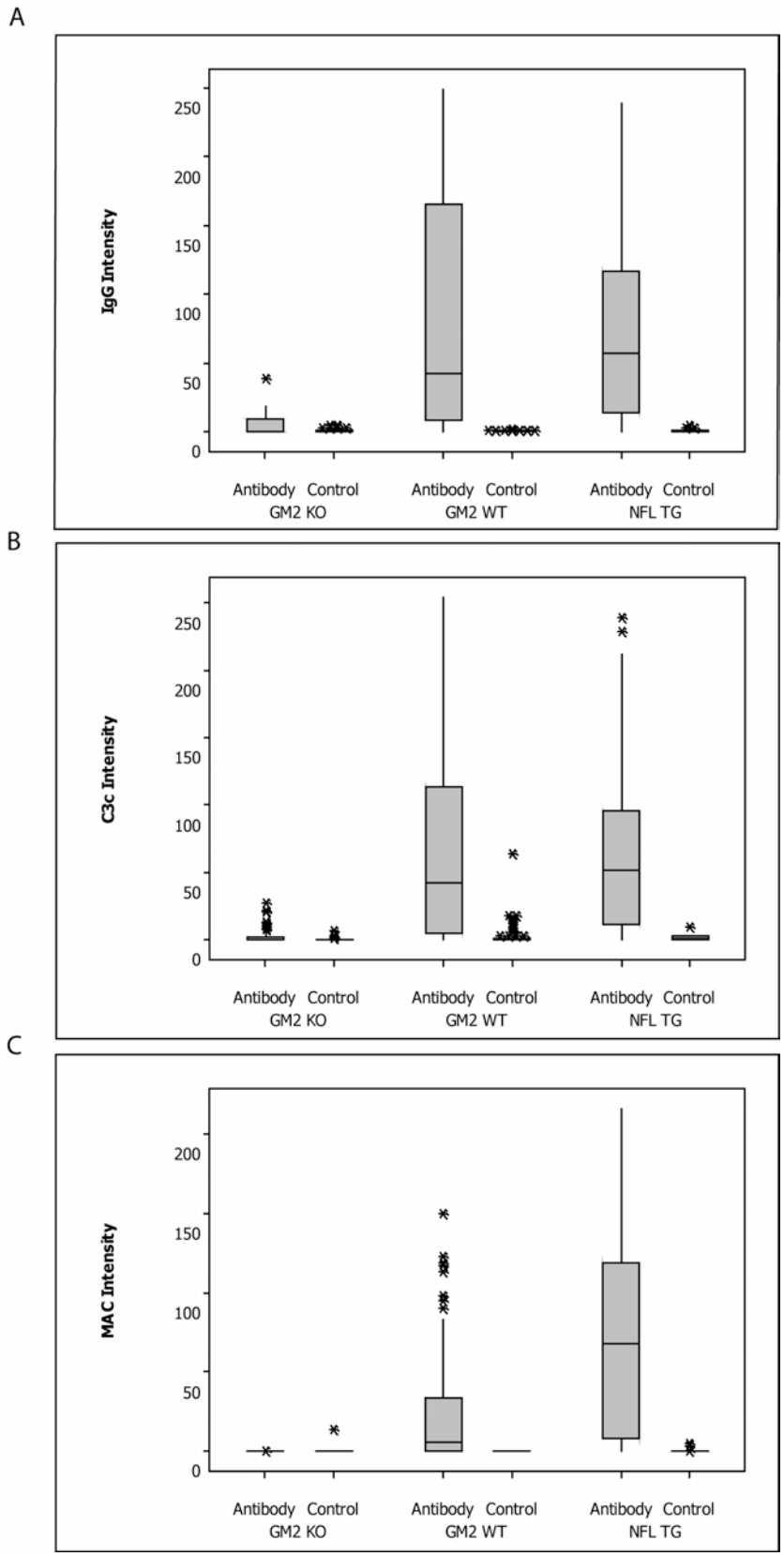

Figure 8.7 - Quantification of *ex vivo* staining data

Box plot showing the quantification of the above *ex-vivo* immunofluorescence experiments. IgG binding (**A**), C3c (**B**), and MAC pore deposition (**C**) levels are shown for all three different mouse strains used. Intensity measurements are all given in arbitrary units.* = outlying value

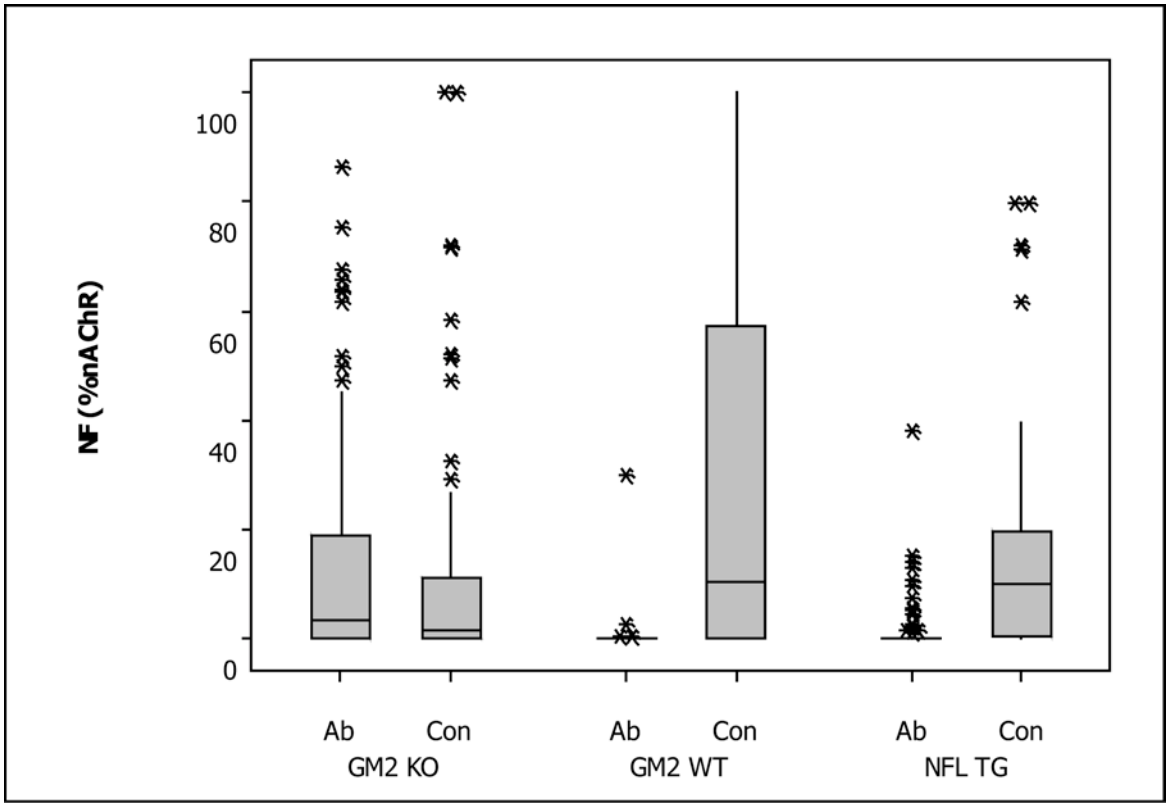

Figure 8.8 - Neurofilament loss over the NMJ following ganglioside antibody and complement administration *ex vivo*

Boxplot showing the staining intensity of neurofilament over the neuromuscular junction either with (Ab) or without (Con) the application of anti-GT1b antibody. A reduced intensity in the antibody treated tissue demonstrates neurofilament loss as a result of axonal damage.

8.2.1.1 Perisynaptic Schwann cell injury

In addition to assessing axonal injury by looking for loss of neurofilament staining as above, the *ex vivo* protocol also involved an assay of perisynaptic Schwann cell (pSc) injury, using an ethidium homodimer stain. It was assumed that, in NFL Tg tissue, such cells, lacking NFL expression, would also lack longer chain gangliosides and hence be resistant to ganglioside antibody and complement mediated damage. However, this was not the case. Counts of the number of dead pSCs per end plate (i.e. those whose nuclei stained with ethidium) revealed the opposite. WT tissue demonstrated levels of pSC death not elevated above KO and controls, whereas in NFL Tg tissue exposed to antibody and complement, dead pSC counts were significantly elevated ($p<0.001$, Table 8.1).

	Number of Ethidium+ Cells / End Plate				
	0	1	2	3	4
NFL TG Ab	144	34	24	3	1
NFL TG Con	214	4	3	0	0
WT Ab	103	1	0	0	0
WT Con	202	3	1	1	0
KO Ab	291	4	0	0	0
KO Con	160	4	2	0	0

Table 8.1 - Counts of ethidium positive cell nuclei per end plate by tissue type

As can be seen, the counts of ethidium positive nuclei overlying the NMJs in NFL Tg mouse hemidiaphragm are substantially elevated above those in other tissues, and in controls. By consolidating these observations into two states (either ethidium positive cells present or absent for each end plate observed), chi squared analysis could be performed to show that these counts were statistically significantly elevated in NFL Tg tissue treated with MOG12 (or indeed MOG 16 in a separate experiment), as compared with all others ($p<0.001$ on both occasions).

8.2.2 Passive transfer (αGT1b)

8.2.2.1 Plethysmography

Having demonstrated the restored sensitivity of NFL Tg mice (over GM2 KOs lacking the transgene) to ganglioside antibody mediated injury in an *ex vivo* setting, the next step was to confirm this *in vivo*. A passive transfer approach was used, involving the intra-peritoneal (ip) injection of MOG16 mAb, followed 16h later by NHS as a source of complement. The functional consequence of axonal injury (muscle paralysis) can be assessed *in vivo* under these conditions by the use of whole body plethysmography. This assesses the function of the respiratory musculature, and in particular, the diaphragm, which is directly bathed in antibody (and NHS) following ip injection, and is therefore primarily affected in such a protocol. On contraction, this muscle reduces the intrathoracic pressure (by increasing the volume), resulting in a movement of air into the lungs. The volume of air moved in and out of the lungs with each breath is known as the tidal volume (TV), and is largely dependent on diaphragmatic function (not withstanding the effects of other accessory and abdominal muscles on respiration). In contrast, other measures of respiratory function, such as

respiratory rate, may at first increase as an attempted compensation for reduced ventilation (i.e. reduced tidal volume) before falling again as exhaustion supervenes. As such, TV was chosen as the best indicator of diaphragmatic paralysis. Baseline TVs in humans, and other measures of respiratory function such as forced vital capacity (FVC), vary with such factors as height (primarily) and age, and are often measured as a "percentage of predicted" in disease processes. In mice, assessment of expected baseline respiratory function by similar methods is to my knowledge, and following an Pubmed search, not available, save for observed median values and ranges in different mouse strains (Reinhard *et al.*, 2002;Schulz *et al.*, 2002). In view of this, baseline TVs in each animal were normalised to 100%, and subsequent changes in TV related to this individually derived baseline. It was first checked that at baseline there were no differences in absolute tidal volume between the different strains by statistical analysis using General Linear Model (GLM) analysis of variance (ANOVA). No statistically significant differences were observed between any of the groups (KO v WT, p=1.000, KO v NFL Tg, p=0.518, WT v NFL Tg, p=1.000) after assessment of 14 GM2 KO, 13 NFL Tg and 8 GM2 WT mice, although the variability in TV appears less in WT as compared to other groups (Figure 8.9).

However, after ip injection of antibody followed by NHS, the tidal volume (TV) in NFL Tg animals begins to fall at 30 minutes, becoming statistically lower than GM2 KO controls at t=60 and beyond, as assessed by multiple paired T-tests performed at each time point (Figure 8.10). An additional 2-way ANOVA with repeated measurements confirmed that both the time post complement injection and the mouse strain had significant influence on TV ($p<0.0001$ for both factors). In control animals (green trace, Figure 8.10), there is an initial

increase in TV, followed by a slower fall back to baseline and below, although never dropping to the levels seen in the NFL Tg. Example plethysmography traces from control GM2 KO mice (Figure 8.10B) and NFL Tg mice (Figure 8.10C) 90 minutes after complement injection show the deflections in the tracing, corresponding to pressure changes and hence air flow, are much more prominent in KO animals, and the fact that they are coloured indicates that the machine is recognising these as breathes. In the NFL Tg traces, a near flat line state is observed, and the absence of colour indicates these breaths are too small (or asymmetrical, or both) to be counted as true breathes by the software.

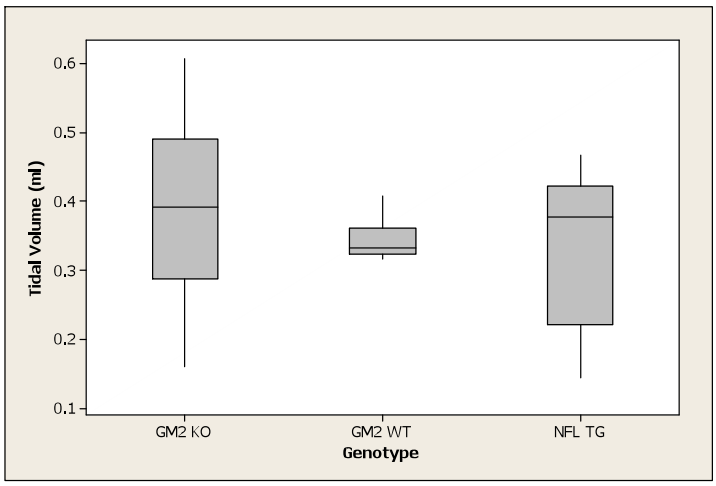

Figure 8.9 - Baseline tidal volume

No significant difference in baseline tidal volume was observed for any of the genotypes studied.

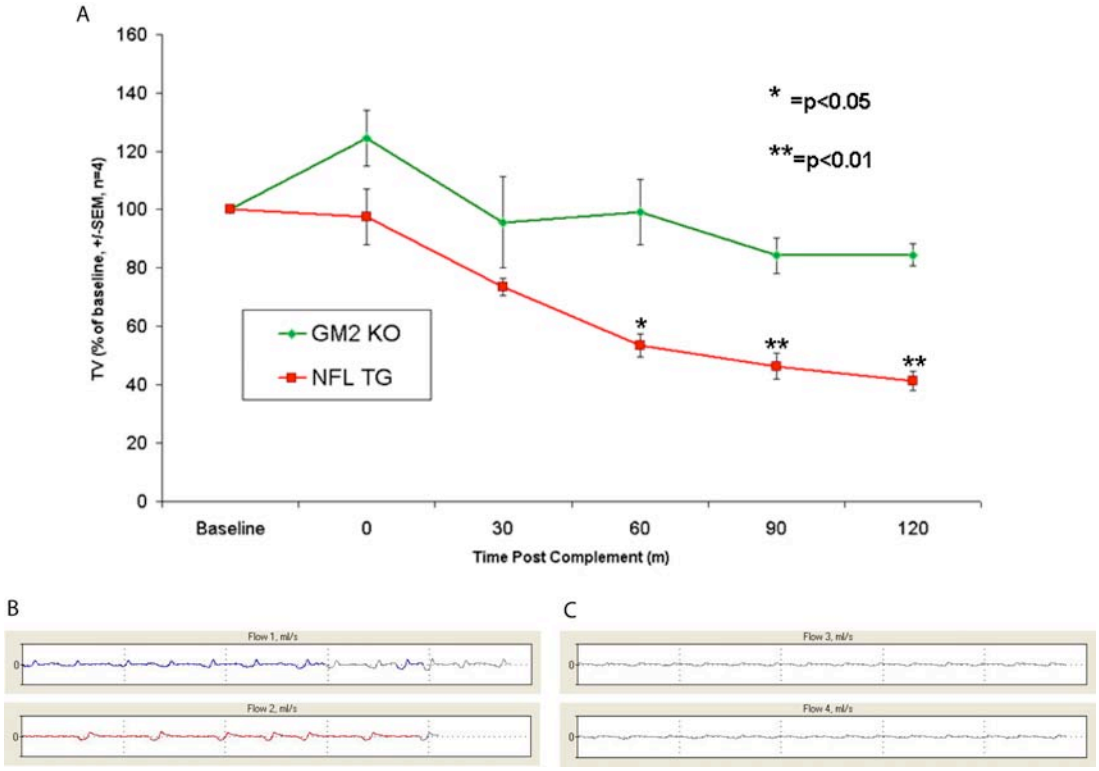

Figure 8.10 - Whole body plethysmography following passive transfer of MOG16 anti-ganglioside antibody

(**A**) Change in tidal volume over time following passive transfer of MOG16 and NHS for NFL Tg (red) and GM2 KO (green) mice. **B**+**C** show example plethysmography traces from control GM2 KO mice (**B**) and NFL Tg mice (**C**) 90 minutes after complement injection.

8.2.2.2 Tissue analysis

Following completion of the plethysmography, mice were culled, and their diaphragm muscles quickly harvested and snap frozen on dry ice. These were then analysed for immunoglobulin and complement deposition as before. This confirmed significantly increased IgG, C3c and MAC deposition over the NMJs of NFL Tg compared with GM2 KO animals, as expected (Figure 8.11, $p<0.0001$ versus GM2 KO by Mann-Whitney, n=6 per group). Despite similar, or even increased, levels of IgG and C3c staining as compared with the *ex vivo* tissue (Figure 8.7), MAC intensity was reduced.

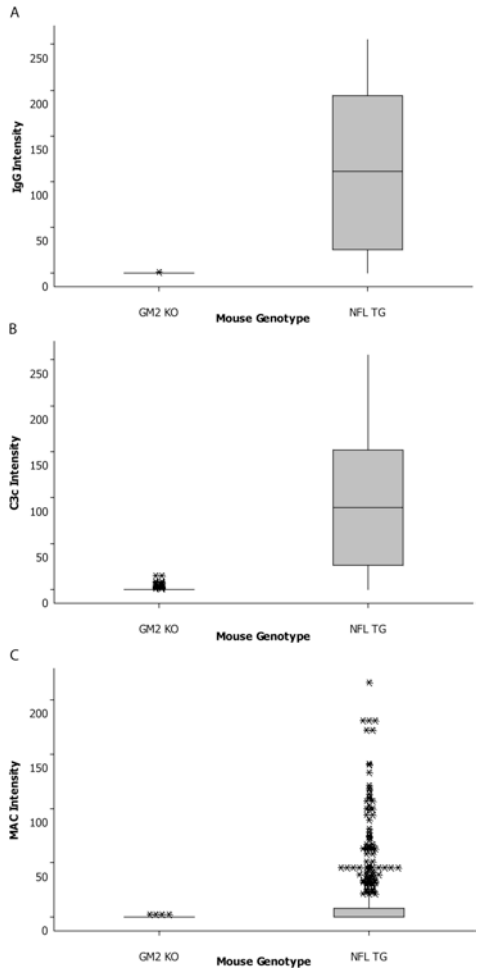

Figure 8.11 - Immunoglobulin and complement deposition following passive transfer

Boxplot quantification of IgG (**A**), C3 (**B**), and MAC (**C**) detected over the neuromuscular junctions of NFL Tg and GM2 KO diaphragms. Significantly increased levels of all three are seen in the NFL Tg strain (all $p<0.0001$ versus GM2 KO by Mann-Whitney, n=6 per group) (*=outlier).

8.2.3 Active immunisation (GT1b)

Having established that the transgenic mice expressed long chain gangliosides (including GT1b) and that their neuromuscular tissue was sensitive to anti-GT1b ganglioside antibody mediated damage, the next step was to investigate their immune response to the same antigen, as a prelude to pursuing an active immunisation model.

8.2.3.1 Immune response

An immunisation protocol was used similar to that previously described for the assessment of the immune response towards GM1:GD1a and GD1a:GD1b complexes. GT1b containing liposomes were produced, and after priming with ova-alum ip (day 0), three ip injections of these ova-containing liposomes were administered on days 7, 14 and 21, followed by three intravenous (iv) injections on days 25, 26 and 27. Blood samples were initially taken on days 0, 14, 21, 28 and 35. This first round of immunisations involved 4 animals in each genotype group, and revealed that a detectable IgG response was not seen until day 21. As such bleeds at earlier time points were subsequently omitted.

Analysis of the anti-GT1b IgG response at these different time points shows that both GM2 KO and NFL Tg genotypes have detectable antibody from day 21, and that the OD measurement continues to rise through day 28 to day 35. There is no statistically significant difference in the levels between these two groups, although the average OD in the NFL Tg is slightly lower at day 21 and beyond. In contrast, the GM2 WT group has a response which does not significantly increase above baseline (Figure 8.12). The IgM response is less clear cut, with all three genotypes showing a progressive, but slight, increase in the corrected OD reading as time progresses (Figure 8.13). This is confounded by the fact that IgM binding to negative control wells also increases substantially over the same period, from 0.04 to 0.74 for some animals

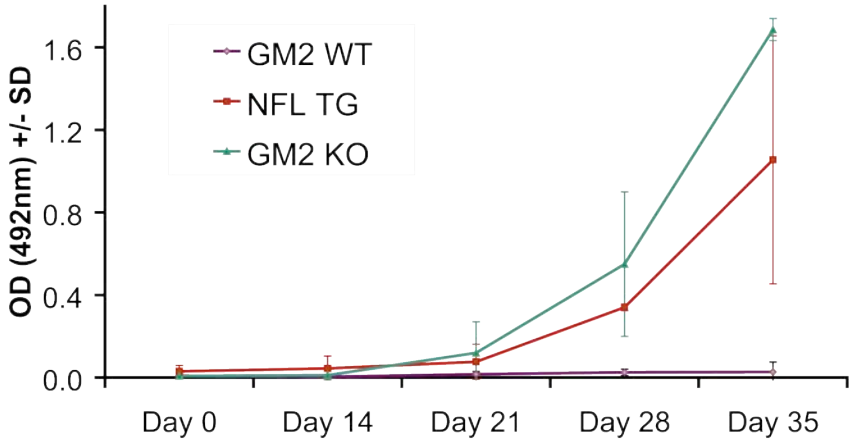

Figure 8.12 - The IgG response to GT1b immunisation in WT, KO and NFL Tg mice

At 1 in 50 dilution in 1%BSA/PBS, a detectable antibody response in WT and NFL Tg mice towards the GT1b immunogen is first detected at day 21, and continues to rise beyond this point. In contrast, the antibody levels in GM2 WT mice does not rise significantly above baseline over the same period. (n=3 per group, statistical analysis by multiple two-tailed T-tests)

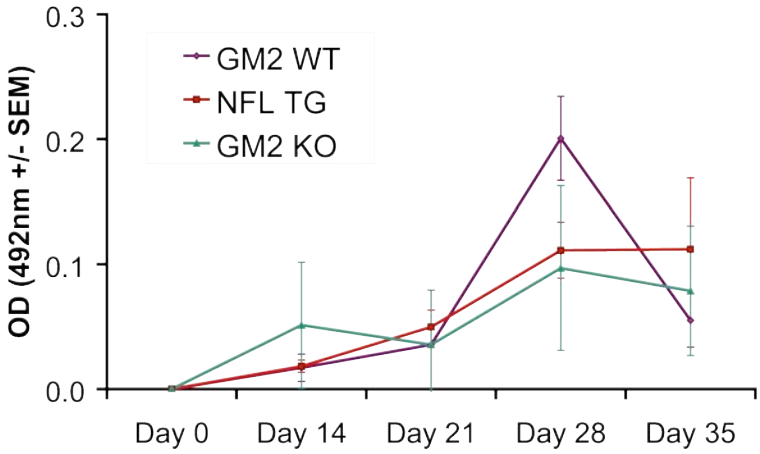

Figure 8.13 - The IgM response to GT1b immunisation in WT, KO and NFL Tg mice

The IgM response in the same animals is less clear cut, and potentially confounded by much higher signal generated in the negative control wells. When this is corrected for, all three genotypes show a trend to higher ODs as time progresses. Unlike the IgG response, this is also seen for the wild type mice, and except for the NFL Tg group, does not increase consistently from week to week.

8.2.3.2 Plethysmography

Following the establishment of the pattern of immune response in the three groups, subsequent experiments were planned to assess the presence of a disease phenotype, pre- and post-complement injection, on day 35 of the protocol (7 days following the final iv boost). As shown above, there was no difference between any of the three mouse strain groups at baseline in terms of tidal volume (TV). There was also no statistical difference in absolute TV between the groups following immunisation, but before complement injection (as assessed by GLM ANOVA with Tukey correction, KO v WT, p=0.605, KO v NFL Tg, p=0.753, WT v NFL Tg, p=0.923). However, following an injection of 1ml of normal human serum ip as a source of complement, the TV fell more in the NFL Tg group, becoming statistically significant with respect to the KO control group 30 minutes after injection, and with respect to the WT control group 60 minutes after injection (as assessed by multiple paired T-tests – again 2 way ANOVA with repeated measures was used to confirm that both the mouse strain and time point had a significant influence on TV). Slight falls in the measured TV in both the GM2 KO and GM2 WT groups were also observed, although there was no statistically significant difference between these two control groups (Figure 8.14).

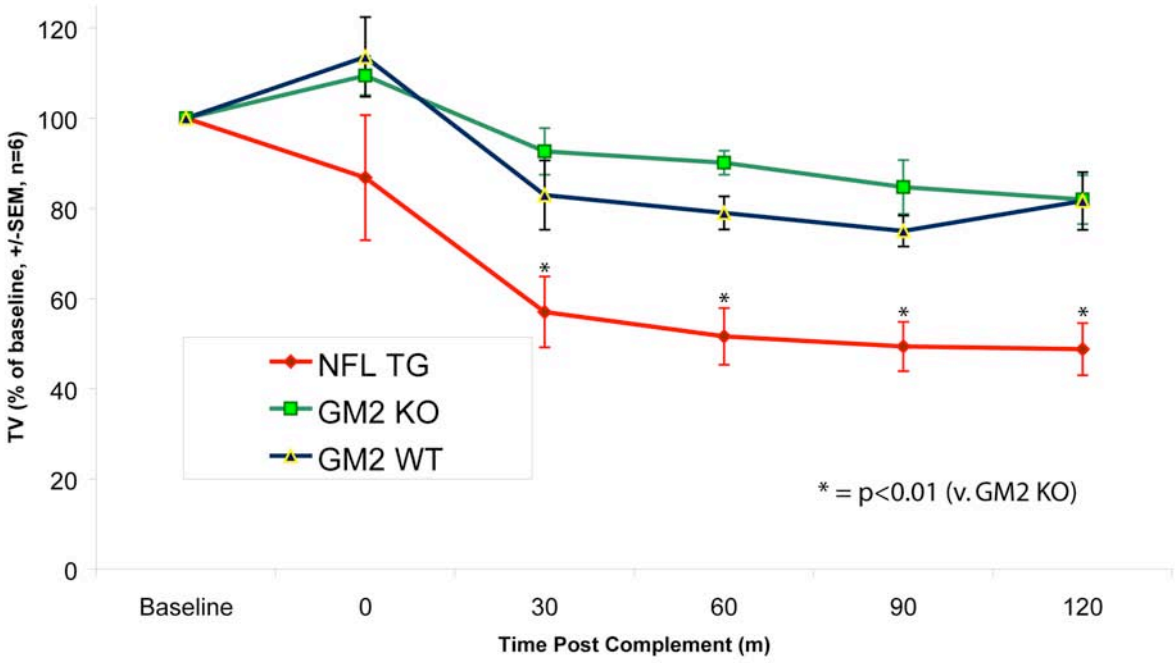

Figure 8.14 - Plethysmography following active immunisation

Although there was no significant difference in absolute tidal volume measurement between the three groups at baseline, or following the immunisation protocol, this measurement fell much more in the NFL Tg genotype following subsequent complement injection than in the two control groups (GM2 KO and GM2 WT). This difference became statistically significant (using multiple paired T-tests) as compared with GM2 KO at 30 minutes and as compared to GM2 WT at 60 minutes. Following an initial rise in TV immediately after complement injection, this measurement also fell in the control groups over the next two hours, with no statistically significant difference in the magnitude of the fall between the two groups.

8.2.3.3 Behavioural testing

Groups of mice from each of the three strains were initially tested at baseline, and no statistically significant differences were seen in any of the parameters measured (as assessed by GLM-ANOVA with Tukey correction). For the balance bar, rotarod at fixed speed, and hindlimb reflex extension tests, all animals in each group achieved the maximum score, and these results are not shown further. Rotarod and grip strength tests were chosen for further analysis at later time points in the protocol, given the variable baseline of and time required to perform platform and open field tests (Figure 8.16 and Figure 8.17).

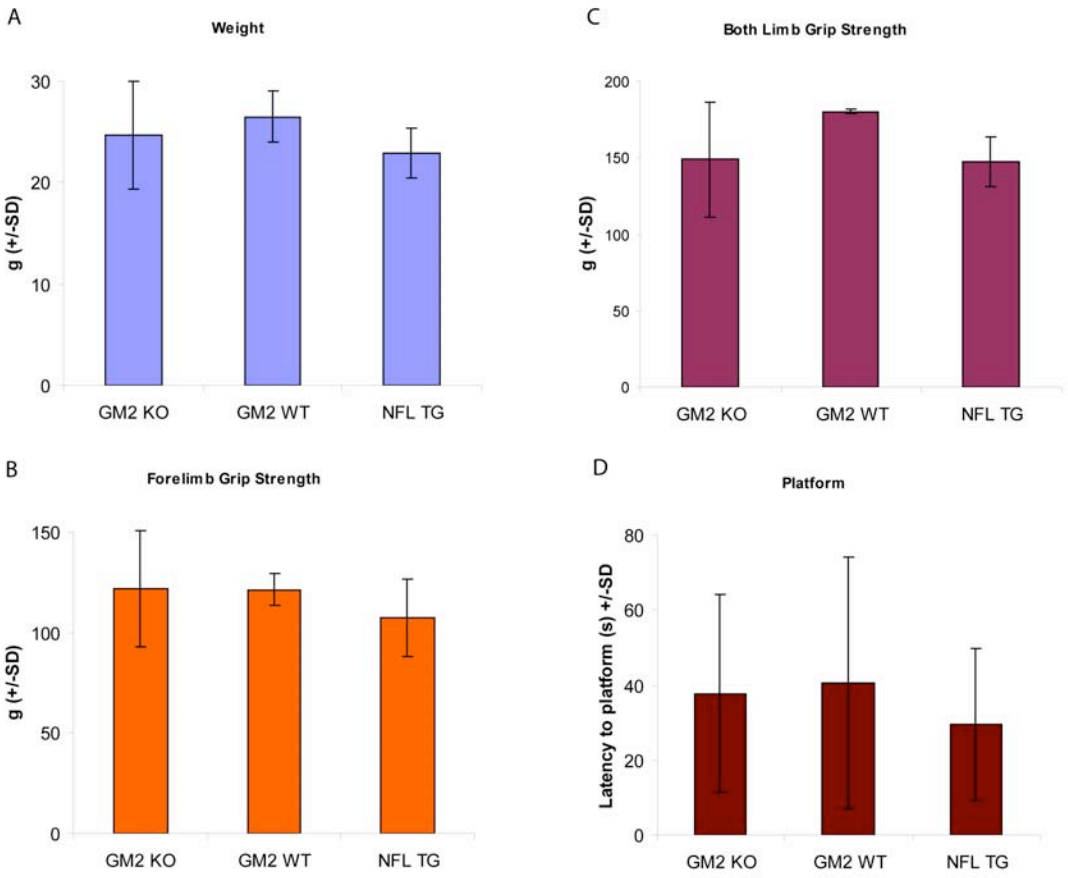

Figure 8.15 - Baseline behavioural and strength testing

On testing of six animals in each genotype group at baseline, when aged 6 to 10 weeks, no significant differences were observed for weight (**A**), forelimb grip strength (**B**), all limb grip strength (**C**), latency to platform (**D**), as well as hindlimb reflex extension pattern and balance bar time (results not shown). Large variability was seen in latency to platform time, and animals which performed similarly in other tests sometimes had very discrepant performances in this area.

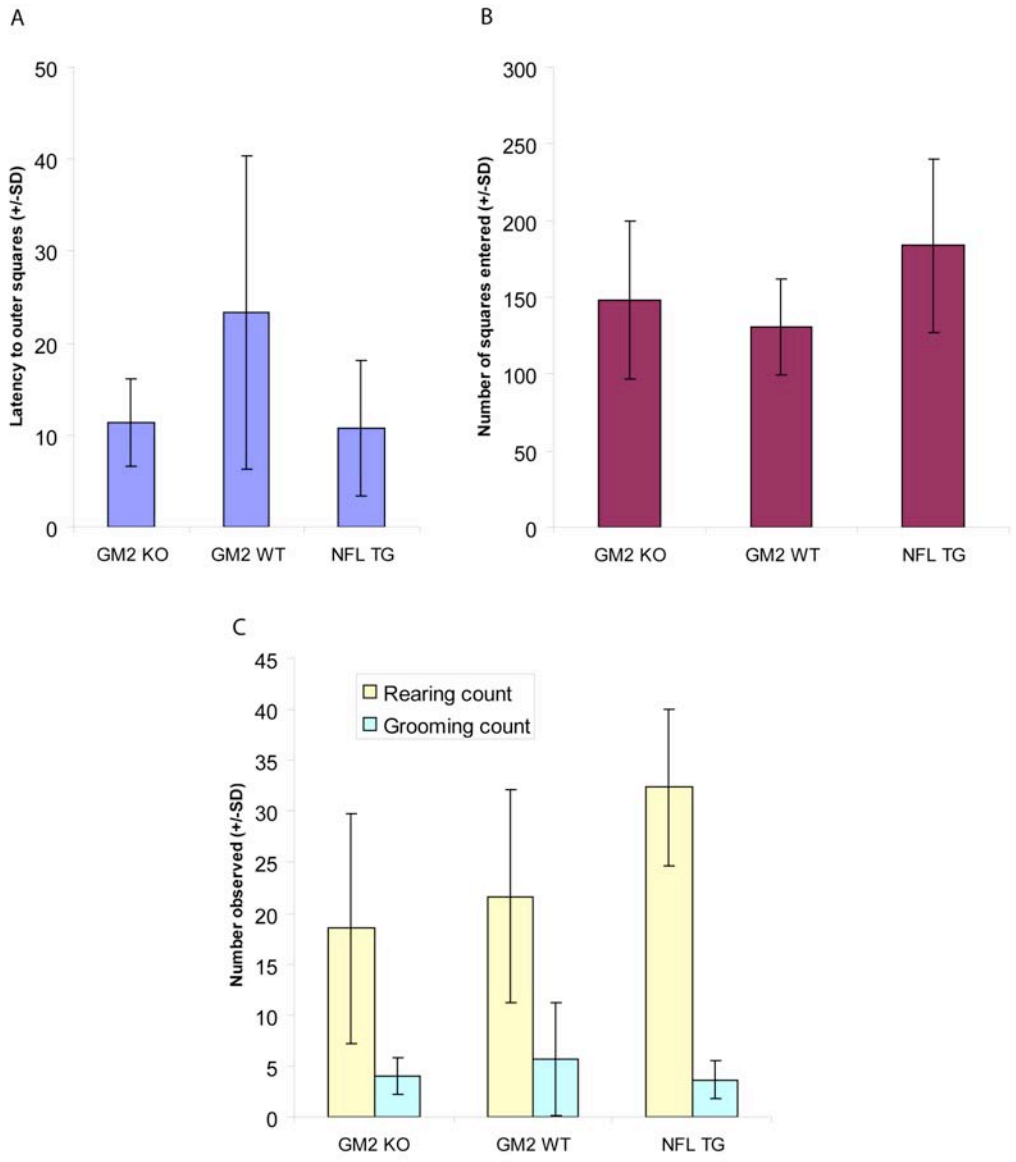

Figure 8.16 - Open field behaviour at baseline

The same mice as in Figure 8.15 were investigated in a 1m^2, walled, open field area for 5 minutes each. Again, no significant differences were observed between any of the genotype groups prior to immunisation and complement injection. Latency to reach the outer squares (**A**), total number of squares entered (**B**), and rearing and grooming counts (**C**), were recorded.

Following the immunisation protocol, but before complement injection, no significant differences in rotarod performance or limb grip strength measurements were seen. Following the immunisation protocol and complement injection, there was a small but non-significant fall in latency to fall on the rotarod at static speed for NFL Tg mice (n=9) versus GM2 KO (n=10, p= 0.0587) and GM2 WT (n=8, p= 0.1340)(Figure 8.17A). There was a greater reduction in

latency to fall from the accelerating rotarod, which was significantly different in the NFL Tg compared to GM2 WT control group (p= 0.0386) but not compared to the GM2 KO group (p= 0.1425,Figure 8.17B). No differences were seen in front limb or all limb grip strength before or after complement injection (data not shown). Statistical assessment was performed using GLM ANOVA with Tukey correction for multiple comparisons.

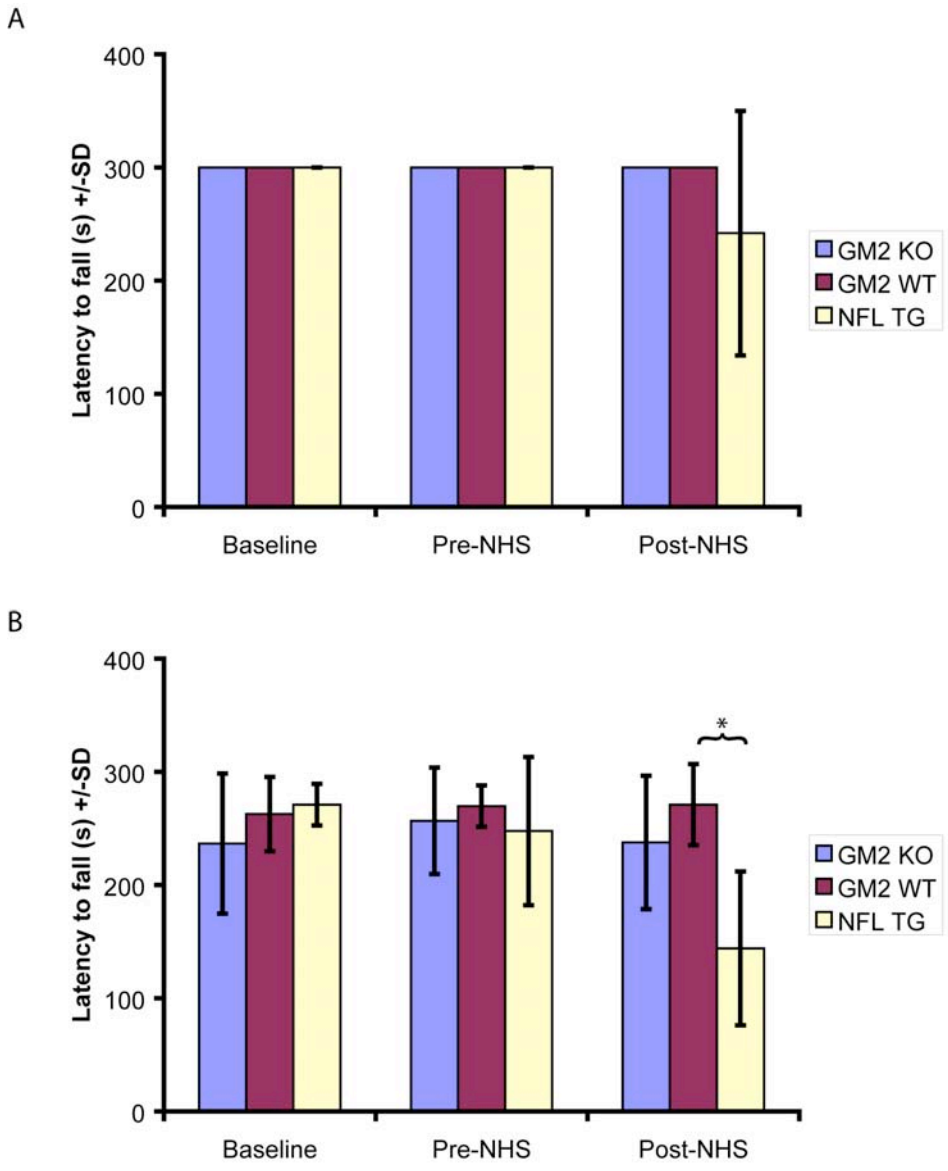

Figure 8.17 - Rotarod testing

At baseline and prior to NHS injection, all mice achieved maximum latency to fall with a static speed rotarod (**A**), and there were no significant differences between scores with the accelerating rotarod (**B**). Following NHS injection, NFL Tg mice fell from the rod after a shorter interval. The change was most pronounced with the accelerating rod, reaching statistical significance as compared with the GM2 WT group under this protocol only (*=p<0.05).

8.2.3.4 Tissue analysis

Following plethysmography and behavioural testing, diaphragm muscles were harvested and processed as for the passive transfer experiments. Although the intensity levels were much lower than seen with the *ex vivo* and passive transfer tissue (Figure 8.7 and Figure 8.11), there was still a significant increase in IgG staining in the NFL Tg tissue as compared with controls (both $p<0.0001$). C3 complement component staining was even weaker and patchier, and the median signal intensity for all three strains was zero. However, MAC intensity in the NFL Tg tissue was significantly increased as compared to the GM2 KO and GM2 WT genotypes ($P<0.0001$). All statistical comparisons used the Mood Median test (given the non-parametric distribution of the data) with $n=6$ per group.

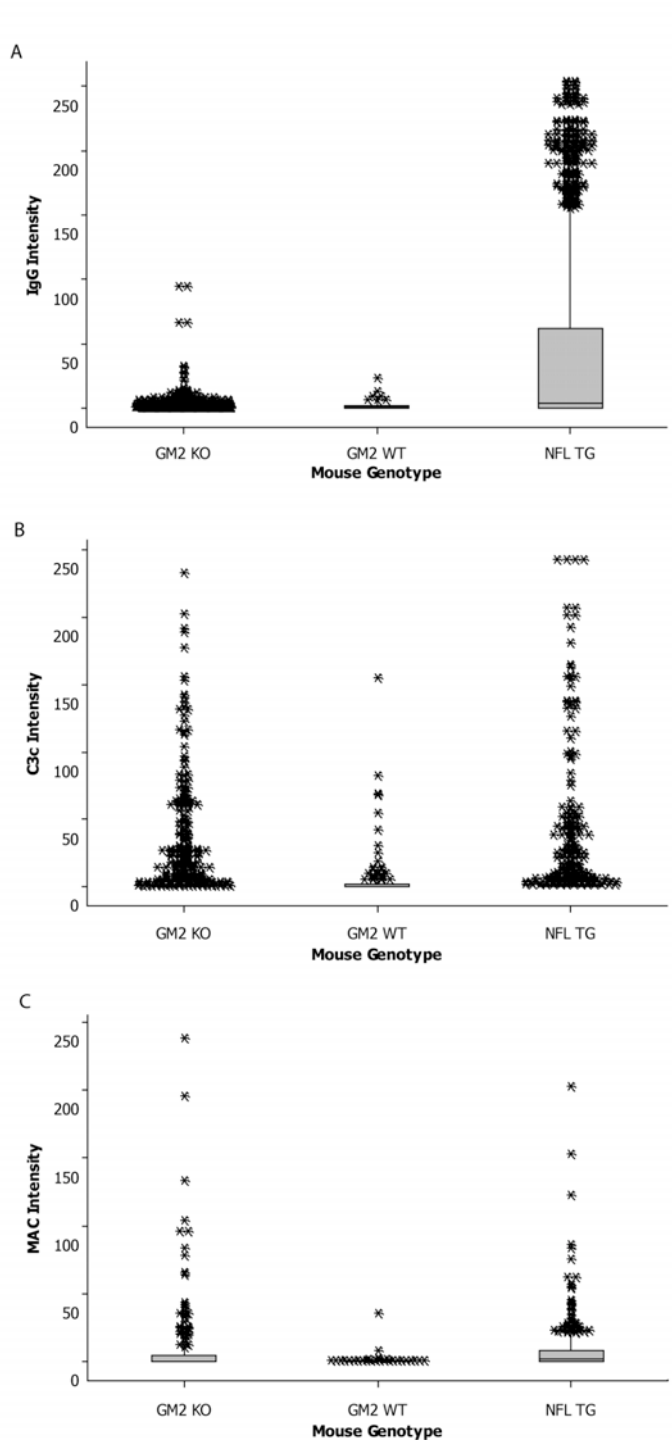

Figure 8.18 - Immunoglobulin and complement deposition following active immunisation with GT1b-liposomes

Although all fluorescent staining was considerably weaker following active immunisation, IgG (**A**) and MAC (**B**) intensities remained significantly elevated in the diaphragms of NFL Tg animals as compared with GM2 KO and GM2 WT controls. C3c levels were not significantly different between any of the groups. Intensity levels are given in arbitrary units, and statistical comparisons performed by the Mood Median test (n=6 per group).

8.2.4 Active immunisation (GM1:GD1a complex)

Having demonstrated the principle for a single ganglioside antigen in the form of GT1b above the next step taken was to attempt to apply a similar protocol to investigate the anti-ganglioside complex response in an active immunisation disease model. Although immunofluorescence staining using the initially generated neurofilament transgenic mouse line had failed to demonstrate GM1 binding, subsequent HP-TLC analysis of brain tissue from the later produced 'Ed2' line showed bands corresponding to both GM1 and GD1a. As GM1:GD1a complex antibodies were also the most frequently observed in series of GBS patients (Kaida *et al.*, 2007) prior to the investigation of the Dutch cohort detailed above (p142, Ch5) this complex was chosen to be the immunogen for this experiment.

8.2.4.1 Immune response

For unexplained reasons, the first round of GM1:GD1a immunisations, in a group of 4 NFL Tg mice, failed to induce any detectable immune response in the form of either an anti-GM1:GD1a IgM or IgG titre. The initial suspicion was that these mice might be tolerant to such a challenge, in keeping with the response seen previously in GM2 WT mice. However, when this experiment was repeated with a further batch of 4 mice, detectable anti-GM1:GD1a IgG titres were observed at day 28 and beyond in all mice.

Unfortunately, these mice were lost in an animal house mix up. Three mice in a subsequent batch died shortly after an iv boost injection and as such further analysis was not possible. My time in the laboratory came to an end before these experiments could be repeated.

8.3 Discussion

The successful transgenic, axonal specific rescue of ganglioside synthesis in GM2 KO ganglioside deficient mice has allowed the development the first single animal active immunisation model of acute motor axonal neuropathy in mice, as described above. This model not only provides a useful tool to further investigate the pathogenesis of this condition and to assess potential therapeutic strategies, but also raises a number of questions of more general relevance. In particular, the observation that confirmed axon specific expression of long chain gangliosides fails to induce systemic tolerance is intriguing. Is it, as initially hypothesised, that absence of ganglioside expression in those immune system organs involved in tolerance is responsible for this finding? Alternatively, could the reduced level of nervous system ganglioside expression in the NFL Tg simply be below a critical threshold required to induce tolerance? Ganglioside composition and immunohistochemical analysis of various immune and non-immune organs from NFL Tg and GM2 WT animals is planned to further investigate this. Instead, might the increased levels of GM3, 9-O-acetyl GD3 and GD3 present in NFL Tg mice be forming complexes with the reduced levels of longer chain gangliosides, which shield them from tolerogenic immune recognition but not from antibody attack in states of inflammation?

Likewise, the observation that perisynaptic Schwann cells are sensitised to antibody attack in the transgenic animals *ex vivo* warrants further consideration. As these cells do not themselves synthesise neurofilament, they would be expected to remain ganglioside deficient in the NFL Tg mouse, and hence resistant to antibody and complement mediated cytotoxicity. It may simply be that the cells are subject to bystander injury resulting from the disruption of the

juxtaposed neuromuscular junction (NMJ). The fact that similar injury is not seen in wild type controls which also sustain NMJ injury argues against this possibility. Similarly, the possibility that the antibodies are binding to the increased levels of GM3, 9-O-acetyl GD3 and GD3 present in the transgenic animals is discounted by the absence of pSc injury in the GM2 KO. Ganglioside transfer between nearby cell membranes has previously been observed, at least under experimental conditions (Heffer-Lauc *et al.*, 2005). This seems the most likely explanation, especially given the occasional immunofluorescent evidence of IgG binding to the pSc membranes. This suggests, however, that some difference in the way transferred gangliosides sit in the cell membrane renders them susceptible to antibody mediated attack, while endogenously produced membrane gangliosides are shielded from such recognition in WT animals. Different accessibility of endogenous and exogenously administered ganglioside has recently been demonstrated for tetanus toxin (TeNT H_C). (Chen *et al.*, 2009)

That the axonal rescue of complex ganglioside expression sensitises the diaphragm to anti-ganglioside mediated injury and results in significant paralysis in NFL Tg mice following immunisation and complement administration is clear. In the absence of such gangliosides in GM2 KO mice, despite higher titres of anti-ganglioside antibodies, only a small fall in tidal volume is seen. In GM2 WT mice without detectable antibody titres but with the target gangliosides normally expressed, again only a small fall in tidal volume is seen. The fact that a small fall in TV is seen in these mice is consistent with previous observations (Halstead S.K. *et al.*, 2008) and can be attributed to a splinting effect from the 1-2ml of fluid injected into the abdominal cavity, as well as a settling and acclimatisation of the animals to the plethysmography chamber over time. These changes are not suggestive of a neuromuscular injury.

Also in line with previous passive transfer experiments, however, an exogenous source of complement is required before the disease phenotype will develop. Even in the presence of sustained circulating antibody titres over days to weeks, diaphragmatic paralysis only develops when a complement source is injected ip. The restricted, local effect of the injected complement source may also explain why the wider neurological function of the mice is only mildly disturbed. Why such a source is required is not clear, and is an area for future study. It has been hypothesised that mouse complement has only a limited potency, and that complement regulators such as decay accelerating factor (DAF) and CD59 (Halstead *et al.*, 2004a) are protective, but this does not seem to be the full story. Other scientists in the group have recently observed that some ganglioside antibodies are rapidly removed from the cell membrane by an internalisation process (Fewou, unpublished observations), and if a similar process operates *in vivo* this may result in a further tier of protection against complement induced damage. It may therefore be that a second insult is required to initiate complement mediated nerve injury – along the lines of a two-hit hypothesis – and this second hit could potentially be one or more of the systemic inflammatory response to a septic state, a disruption of the blood nerve barrier, or interference with the antibody internalisation process.

Even though performance on the rotarod was impaired in NFL Tg compared to GM2 WT following NHS injection, this is likely to be an indirect measure of respiratory embarrassment rather than a sign of more generalised neurological dysfunction in most cases, especially as no differences in grip strength were observed. Nevertheless, a small subset of animals did seem to develop more generalised paralysis following complement injection, although the reason for their apparent enhanced sensitivity is not at present known. Many more animals

did not, and further experiments and modifications to the protocol will therefore involve an exploration of the mechanisms by which most neuromuscular tissue remains resistant to damage even in the presence of systemically produced, circulating antibodies which are apparently auto-reactive.

The effect of actively induced anti-ganglioside complex antibodies in the same model remains to be elucidated. Investigation of this aspect was unfortunately confounded by technical problems and time constraints.

9 Conclusion

9.1 Summary

The work described in this thesis has advanced knowledge in the field of glycolipid complexes, particularly with respect to anti-glycolipid complex antibodies and their association with inflammatory neuropathies such as Guillain-Barré syndrome. Far from being an obscure quirk in the immunobiology of these diseases, ganglioside complexes have been shown to be of potentially much wider relevance, as evidenced by the observation of their influence on the interaction of other lectins (such as bacterial toxins and siglecs) with their carbohydrate targets. In the PVDF glycoarray, a methodology for efficiently assessing these interactions *in vitro* has been developed with substantial advantages over traditional ELISA and TLC techniques. When this technology was applied to a cohort of Western European GBS patients, a spectrum of previously undiscovered antibody specificities was found to be associated with the disease. Most impressively, the antibody detection rate in the AIDP variant was increased from 14.3% by ELISA to 62.5% using the glycoarray. Furthermore, a number of different antibody specificities correlated with particular clinical features, such as the presence or otherwise of sensory deficits, the disease severity and the requirement for mechanical ventilation. The single animal active immunisation disease model enabled by the neurofilament-light GalNAcT transgenic mouse shows that gangliosides expressed solely within the nervous system are not sufficient to engender immune tolerance. Immune tolerance, the process whereby the immune system does not respond to a particular (usually self or self-related) antigen can be central, peripheral or acquired. In the former,

developing lymphocytes which display a too great self-reactivity are deleted prior to their final maturation. Peripheral tolerance can occur if antigen presentation does not include the appropriate co-stimulatory molecules or by the action of regulatory components of the immune system, such as T reg cells, amongst other mechanisms. Acquired tolerance can occur if specific doses of antigen (usually very large or very small) are repeatedly administered, most notably via the oral route. Whatever the mechanism at play in GBS, the above observations support the hypothesis that differential expression of GSCs between the immune and nervous systems might allow escape of tolerance in the clinical disease.

Given that only a fraction of people exposed to self-mimicking antigens on bacteria such as *Campylobacter jejuni* go on to generate a self-reactive immune response and GBS, and given that around 5% of GBS patients have a recurrence of their disease (at least 20 times more often than would be expected by chance alone), it seems that there must be some host factor at play which predisposes to a breakdown in tolerance. As previously discussed, this host factor has so far escaped detection. It is exciting to speculate, based on the observations in NFL Tg mice described above, that differences in ganglioside/glycolipid expression between the immune and nervous system compartments might allow tolerance to be evaded. There may even be disparity in ganglioside complex formation between sites were immune tolerance is regulated and the peripheral nerves. Alternatively, it could be that antibodies are generated which are not self reactive until existing nerve GSCs are disrupted and their target antigen is exposed.

9.2 Weaknesses

The are, of course, a number of weaknesses in the work here presented. The nature of the complex binding site and of the glycolipid-glycolipid interaction producing it have not been directly demonstrated, and as such the concepts shown in Figure 3.16 remain speculative. The discrepancy between ELISA, PVDF, TLC and indeed *ex vivo* binding patterns was consistently noted but not systematically investigated. The effects of changes in antigen density, the solvents used, pH, temperature and the presence of cations such as Ca^{2+} were not assessed and could potentially explain these differences. GSC specific neuropathy associated sera were only occasionally available for *ex vivo* tissue binding studies, and then only in sufficient quantities to use in frozen section preparations. In this setting there is concern that any ganglioside complexes present might be disrupted as the tissue dies / is frozen.

The uses of normalised intensity data in early mAb / PVDF studies might also be criticised. This was used only to try and minimise differences in the activity of the ECL+ and exposure time between assays performed on different days. This was felt acceptable when generating replicates to inform comparisons on the magnitude and direction of complex modulated binding. When comparisons between binding of different lectins to different arrays on different days were required this was abandoned and only absolute intensity values were used. Initial problems with measuring spot intensity accurately were noted, and on some occasions spots clearly more intense by eye would return lower values whereas low intensity spots with high background would be overestimated. This was largely addressed by appropriately applying the local background correction functionality of the ImageQuant/TotalLab software, however some difficulties

remained when there was significant overlap of neighbouring spots. In such circumstances automated background correction would take into account the neighbouring spot, leading to an erroneous reduction of reported intensity. This meant that a selective disabling of such correction, along with assiduous spot definition, was required. This not only made the process much less automated and efficient that it would otherwise have been, but additionally introduced a degree of subjectivity into spot / background assignment. To reduce the chance of bias being introduced into such assessments, digitised PVDF images were coded and the analyst blinded to the serum / lectin applied.

Although inter- and intra- assay coefficient of variation measurements performed using the 10x10 array and mAbs were favourable, the performance of the larger 28x10 array was less impressive. This was only appreciated when the variation in the intensity of certain spots on the positive control sera array were compared over the 3 month period taken to process all 181 GBS sera and 74 controls. In retrospect, optimisation of the larger array should have been undertaken prior to proceeding with the above analysis. Additionally, although an estimate of the sensitivity, specificity and likelihood ratio statistics of the test were calculated, this should ideally be confirmed on a second cohort of GBS serum samples. The inadequacy of the control samples in this component of the study has previously been discussed in 5.3 above.

The immunisation data is arguably the weakest component of this study. Production of a GSC specific mAb was prioritised over further investigation of the nature of the GSC immune response. When major difficulties were encountered with the former, the latter aim did not really proceed. Although single ganglioside immunisations had been performed previously, and

observations in these studies could be drawn upon, the lack of a direct comparison between parallel immunisation with ganglioside A, ganglioside B and ganglioside complex A:B significantly limits the conclusions which can be drawn from this work. Likewise, reasons for the huge variability in response between different animals of the same genotype, age and sex to the same ganglioside complex liposome preparation were not investigated.

9.3 Parallel developments

Nevertheless, whilst this work was in progress a handful of other investigators have advanced understanding of the functional importance of glycolipid complexes using a variety of different approaches. These have proved both complimentary to and supportive of observations made in the course of this thesis. Researchers in Seattle have shown that GM2:GM3 complexes interact with CD82 and inhibit the growth and mobility of HCV29 cancer cells. This effect is much enhanced as compared to the effect of either ganglioside in combination, and rather than simply being a summative or multiplicative effect of the two separate gangliosides, the complex itself appears to be critically important. This was demonstrated by creating nanospheres in the presence of Ca^{2+}, whereby the effect of the complex was magnified as compared to aqueous solutions of the gangliosides. The authors also demonstrated the heterodimeric complexes form in solution in the presence of Ca^{2+} using ion-spray mass spectrometry. Furthermore, they were able to generate a complex specific GM2:GM3 complex monoclonal antibody. The specificity of this was confirmed in all of TLC, ELISA and cell based systems (the latter involving exogenous gangliosides reinserted into ganglioside null cells). This antibody alone was effective in blocking the effect of GM2:GM3 complex on cell motility, whereas antibodies against GM2 and

GM3 alone where not, although a mixture of the two single-ganglioside specific antibodies was not tested in this regard. (Todeschini *et al.*, 2008)

Confirming the hypothesis stated in the discussion section of chapter 3 (and in particular, illustrated in figure 3.16A), Chen and colleagues have now demonstrated that the two binding sites of tetanus toxin can bind components of two different gangliosides. Furthermore, the observation of the complex enhanced effect of GM1:GD3 complexes on tetanus toxin is further supported by the demonstration that GM1 binds the 'W' pocket and GD3 the 'R' pocket of the toxin. This was shown initially in solid phase assays using mutated tetanus toxin lacking one or both of the binding domains. Interestingly, in cell-based systems using PC12 cells displaying endogenous GD1b, GT1b and GQ1b, no binding was seen with untreated cells. When these cells were depleted of endogenous ganglioside and then reloaded with either GT1b, GM1, GD3, or GM1 and GD3, binding was only seen with GT1b and GM1 plus GD3 together. Additionally, both binding sites of tetanus toxin were required for high affinity binding in all assays. (Chen *et al.*, 2009) Although the gangliosides themselves do not necessarily have to form chemical bonds in such a system, these observations are clear evidence that components of two different glycolipids can form a functional receptor for one lectin molecule.

In the field of GBS and anti-ganglioside antibodies, it has been previously recognised that anti-GD1b antibodies are associated with ataxia, but around 50% of those with GD1b-antibodes do not develop ataxia. Kusunoki and co-workers were able to show that this apparent inconsistency is explained by the ability or otherwise of GD1b antibodies to bind GD1b complexes. In the ataxia group, the addition of GD1a or GT1b to GD1b reduced binding significantly more than in the

non-ataxia group. Furthermore, all 8 of the non-ataxic sera additionally contained antibodies binding to other ganglioside complexes not containing GD1b, whereas only 2 of 9 ataxic sera had such antibodies. (Kaida *et al.*, 2008) Once again, this is further evidence to support the assertion that the fine specificity of antibodies with respect to their complex enhanced or attenuated qualities has important pathogenic implications.

Nevertheless, significant questions in this field remain unanswered. Although some lectins display consistent patterns of binding to GSCs throughout the range of immunoassays performed, many others do not. By extension, this casts doubt on whether these lectins and others interact with GSCs in the most important system of all, the living membrane. Indeed, evidence for the existence of GSCs *in vivo* remains limited and largely circumstantial, as above. With this in mind, a more detailed understanding of the nature and mechanism of glycolipid *cis* interactions is additionally lacking. The variability in binding of the same antibody in different solid phase systems highlights the potential pitfalls in concluding if an antibody binds exclusively to a GSC in an *in vitro* system, and also binds to tissue, that the tissue likewise contains the GSC (and *vice versa*).

Whether even more complex multimers of glycolipids, with or without proteins and glycoproteins, can also influence lectin interactions and act as distinct antigenic targets themselves is also not known. As previously discussed, examining these increasingly complex structures multiplies the difficulty of the necessary experimentation and will require targeted rather than wide ranging screening type approaches.

9.4 Future work

The work described in this thesis thus contributes to the existing body of knowledge but also suggests further investigations, which may be usefully pursued in future. These form two distinct but complementary lines of enquiry. The first would address the intrinsic nature of glycolipids and glycolipid complexes *in vivo* and investigate their behaviour, location and turnover in the living membrane. It is clearly important for further understanding of lectin-carbohydrate interactions in their many forms that this is understood in greater detail. As has been stated, relying on even apparently highly specific monoclonal antibodies for these studies is potentially flawed. Other methods might be more usefully utilised. Clearly, light microscopy lacks the resolution to delineate individual gangliosides or complexes thereof. Fluorescence related energy transfer (FRET) approaches are one possibility. In these techniques, energy omitted from one fluorophore excites another in close proximity (within ≈10nm) producing a signal. (Stryer & Haugland, 1967) Although such approaches require labelling of the molecules under study, potentially modifying their interactions, these studies can be performed in membranes, and do not involve antibodies. (Silvius & Nabi, 2006) However, this technology would rely on assessing either artificial bilayers or cells into which exogenously labelled gangliosides had been reintroduced. From the earlier discussion, it is apparent that endogenous and exogenous ganglioside in the cell membrane do not necessarily interact in the same way, potentially confounding such an approach. Another possibility would be to use a scanning probe microscopy method like atomic force microscopy (AFM) to map out the distribution of glycolipids in membrane systems. This technique employs a nanometre scale probe to map out the topography of cell

surfaces and lipid bilayers, and has previously been used to demonstrate the existence of lipid microdomains. (Connell & Smith, 2006)

Aside from this, future work might also further investigate the generation and pathological importance of anti-glycolipid complexes in the inflammatory neuropathies. A major limitation in the work just described was the failure to generate a complex specific monoclonal antibody. Armed with such a reagent, and appropriate controls, multiple further experiments would be possible. Most simply, one could look for pathological readout in systems similar to those previously used – namely *ex vivo* neuromuscular tissue assessed by electrophysiology, fluorescent microscopy looking for cytoskeletal degradation, and by passive transfer into animals. Attempts to model anti-complex antibody mediated neuropathy by active immunisation were precluded by time constraints but could easily be revisited. It would also be informative to assess the binding pattern of complex antibodies in neuromuscular tissue. This might directly address the hypothesis that motor and sensory nerves have different sensitivity to differing antibodies because of their different ganglioside complex profiles, and might provide further insight into the mechanism by which self tolerance is overcome if immune tissue was additionally examined for the presence of binding to the same complexes. The caveats regarding the conclusion that binding of an apparent complex specific antibody *in vivo* equates to the presence of the complex in the living membrane of course remain.

The mechanisms by which these antibodies are generated and the cells involved in this process have also not been investigated. B1 cells are present in the peritoneal cavity and associated with the production of natural antibody of the IgM subclass. Although it would not be expected that these cells themselves

produce pathogenic IgG GSC antibodies, they may be involved with the early immune response and have the potential to modify the future reactivity. Both B cells, notably in the marginal zone, and also dendritic cells, express CD1 molecules and seem likely to be involved in the presentation of processed glycolipid antigens to T cells. The various contributions of these cell types to the glycolipid immune response remain to be conclusively demonstrated, as do the particular aberrations which must occur to lead to the dysimmune pathology in GBS.

The majority of previous work in this field has focussed on ganglioside antibodies, yet the glycoarray analysis of a cohort of largely AIDP cases demonstrated the frequent presence of antibodies towards complexes of sulfatide and SGPG. Further investigation of these will likely require a modification of existing approaches. It seems likely that wild type mice will prove tolerant to sulfatide and sulfatide complex immunisations (although this remains to be demonstrated). Future studies may therefore need to utilise sulfatide deficient animals. (Fewou *et al.*, 2010) Conversely, mice lack SGPG and previous studies of anti-SGPG neuropathies have used other animals, including cats. (Ilyas *et al.*, 2008)

Area for further investigation	Potential studies / Methods
1. Biophysical properties of GSCs in membranes	FRET, AFM *Ex vivo* studies with GSC specific mAbs
2. Distribution of GSCs *in vivo*	FRET, AFM *Ex vivo* studies with GSC specific mAbs Obtain GSC specific disease associated sera in greater quantities than routinely available for pathogenic studies
3. Interaction of GSCs with the immune system	Cloning of GSC specific mAbs (including sulfatide complex antibodies)
4. Pathological potential of αGSC antibodies	*Ex vivo* studies with GSC specific mAbs Cloning of GSC specific mAbs (including sulfatide complex antibodies) Obtain GSC specific disease associated sera in greater quantities than routinely available for pathogenic studies
5. Clinical serological associations	Confirm association and define test characteristics of the glycoarray using a second cohort of GBS patients Include larger numbers of controls, ideally post-infectious, non-neuropathy inflammatory, and non-inflammatory neuropathy

Table 9.1 - Summary of proposed future work

It therefore seems likely that a combination of approaches will be required to identify and evaluate putative pathogenic antibodies in GBS, and in AIDP in particular (Table 9.1). However, a greater understanding of this pathological process would seem be one of the first crucial steps in advancing disease modifying treatment for these conditions. As yet, this has not changed significantly in over 20 years.

Appendices

1 Commonly used solutions

PBS

NaCl	80g
KH_2PO_4	2g
$Na_2HPO_4.12H_2O$	29g
KCl	2g

Make up to 1000ml with dH_2O.

Dilute 1 in 10 to use.

pH to 7.4.

2%/1% BSA

2g/1g bovine serum albumin
100ml PBS

OPD detection buffer

14ml 0.1M Citrate (10.507g to 500ml dH_2O)
16ml 0.2M Na_2HPO_4 (14.196g to 500ml dH_2O)
30ml dH_2O
1x OPD tablet (Sigma)
20µl H_2O_2

OPD stop solution

4M H_2SO_4 (54ml to 500ml dH_2O, perform in hood, add acid slowly to water)

Orcinol

0.1g orcinol
97ml dH_2O
3ml H_2SO_4 (add last, slowly)

Resorcinol

2.5ml 2% resorcinol
62.5µl 0.1M $CuSO_4$
2.427ml dH_2O
20ml HCl (add last)

0.4% PIBM

0.1g polyisobutlymethacrylate
Dissolve in 1ml of chloroform
Make up to 25ml with n-hexane

Ringer's medium

NaCl	67.79g	
KCl	3.35g	
$NaHCO_3$	19.32g	
NaH_2PO_4	1.19g	(or $NaH_2PO_4.2H_2O$, 1.56g)
Glucose	19.82g	
1M $MgCl_2$	10ml	

Make up to 1000ml with dH_2O.

Dilute 1 in 10 to use, bubble with O_2 and add 2ml 1M $CaCl_2$ per 1000ml.

pH to 7.4.

20% / 10% complete medium

500ml RPMI with L-glutamine
100ml / 50ml foetal bovine serum
10ml penicillin / streptomycin solution

2 Example array programme

Layout for 10x10 grid

	34	36	38	40	42	44	46	48	50	52	54
15	+	GM1	GM2	GM3	GD1a	GD1b	GD3	GT1a	GT1b	GQ1b	+
17	GM1	-	1	2	3	4	5	6	7	8	
19	GM2	1	-	9	10	11	12	13	14	15	
21	GM3	2	9	-	16	17	18	19	20	21	
23	GD1a	3	10	16	-	22	23	24	25	26	
25	GD1b	4	11	17	22	-	27	28	29	30	
27	GD3	5	12	18	23	27	-	31	32	33	
29	GT1a	6	13	19	24	28	31	-	34	35	
31	GT1b	7	14	20	25	29	32	34	-	36	
33	GQ1b	8	15	21	26	30	33	35	36	-	
35	+										+

Programme for first slide

	Position x	Position y	Type	Width (x)	Height (y)	Volume	Vial
1	15	34	Band	0.4	0.4	0.1	e3 : 47
2	17	34	Band	0.4	0.4	0.1	a2 : 2
3	19	34	Band	0.4	0.4	0.1	a3 : 3
4	21	34	Band	0.4	0.4	0.1	a4 : 4
5	23	34	Band	0.4	0.4	0.1	a5 : 5
6	25	34	Band	0.4	0.4	0.1	a6 : 6
7	27	34	Band	0.4	0.4	0.1	a7 : 7
8	29	34	Band	0.4	0.4	0.1	a8 : 8
9	31	34	Band	0.4	0.4	0.1	a9 : 9
10	33	34	Band	0.4	0.4	0.1	a10 : 10
11	35	34	Band	0.4	0.4	0.1	e3 : 47
12	15	36	Band	0.4	0.4	0.1	a2 : 2
13	17	36	Band	0.4	0.4	0.1	A1 : 1
14	19	36	Band	0.4	0.4	0.1	a11 : 11
15	21	36	Band	0.4	0.4	0.1	b1 : 12
16	23	36	Band	0.4	0.4	0.1	b2 : 13
17	25	36	Band	0.4	0.4	0.1	b3 : 14
18	27	36	Band	0.4	0.4	0.1	b4 : 15
19	29	36	Band	0.4	0.4	0.1	b5 : 16
20	31	36	Band	0.4	0.4	0.1	b6 : 17
21	33	36	Band	0.4	0.4	0.1	b7 : 18
22	15	38	Band	0.4	0.4	0.1	a3 : 3
23	17	38	Band	0.4	0.4	0.1	a11 : 11
24	19	38	Band	0.4	0.4	0.1	A1 : 1
25	21	38	Band	0.4	0.4	0.1	b8 : 19
26	23	38	Band	0.4	0.4	0.1	b9 : 20
27	25	38	Band	0.4	0.4	0.1	b10 : 21
28	27	38	Band	0.4	0.4	0.1	b11 : 22
29	29	38	Band	0.4	0.4	0.1	c1 : 23
30	31	38	Band	0.4	0.4	0.1	c2 : 24
31	33	38	Band	0.4	0.4	0.1	c3 : 25
32	15	40	Band	0.4	0.4	0.1	a4 : 4
33	17	40	Band	0.4	0.4	0.1	b1 : 12
34	19	40	Band	0.4	0.4	0.1	b8 : 19
35	21	40	Band	0.4	0.4	0.1	A1 : 1
36	23	40	Band	0.4	0.4	0.1	c4 : 26
37	25	40	Band	0.4	0.4	0.1	c5 : 27
38	27	40	Band	0.4	0.4	0.1	c6 : 28
39	29	40	Band	0.4	0.4	0.1	c7 : 29
40	31	40	Band	0.4	0.4	0.1	c8 : 30
41	33	40	Band	0.4	0.4	0.1	c9 : 31
42	15	42	Band	0.4	0.4	0.1	a5 : 5
43	17	42	Band	0.4	0.4	0.1	b2 : 13
44	19	42	Band	0.4	0.4	0.1	b9 : 20
45	21	42	Band	0.4	0.4	0.1	c4 : 26
46	23	42	Band	0.4	0.4	0.1	A1 : 1
47	25	42	Band	0.4	0.4	0.1	c10 : 32
48	27	42	Band	0.4	0.4	0.1	c11 : 33
49	29	42	Band	0.4	0.4	0.1	d1 : 34
50	31	42	Band	0.4	0.4	0.1	d2 : 35
51	33	42	Band	0.4	0.4	0.1	d3 : 36
52	15	44	Band	0.4	0.4	0.1	a6 : 6

53	17	44	Band	0.4	0.4	0.1	b3 : 14
54	19	44	Band	0.4	0.4	0.1	b10 : 21
55	21	44	Band	0.4	0.4	0.1	c5 : 27
56	23	44	Band	0.4	0.4	0.1	c10 : 32
57	25	44	Band	0.4	0.4	0.1	A1 : 1
58	27	44	Band	0.4	0.4	0.1	d4 : 37
59	29	44	Band	0.4	0.4	0.1	d5 : 38
60	31	44	Band	0.4	0.4	0.1	d6 : 39
61	33	44	Band	0.4	0.4	0.1	d7 : 40
62	15	46	Band	0.4	0.4	0.1	a7 : 7
63	17	46	Band	0.4	0.4	0.1	b4 : 15
64	19	46	Band	0.4	0.4	0.1	b11 : 22
65	21	46	Band	0.4	0.4	0.1	c6 : 28
66	23	46	Band	0.4	0.4	0.1	c11 : 33
67	25	46	Band	0.4	0.4	0.1	d4 : 37
68	27	46	Band	0.4	0.4	0.1	A1 : 1
69	29	46	Band	0.4	0.4	0.1	d8 : 41
70	31	46	Band	0.4	0.4	0.1	d9 : 42
71	33	46	Band	0.4	0.4	0.1	d10 : 43
72	15	48	Band	0.4	0.4	0.1	a8 : 8
73	17	48	Band	0.4	0.4	0.1	b5 : 16
74	19	48	Band	0.4	0.4	0.1	c1 : 23
75	21	48	Band	0.4	0.4	0.1	c7 : 29
76	23	48	Band	0.4	0.4	0.1	d1 : 34
77	25	48	Band	0.4	0.4	0.1	d5 : 38
78	27	48	Band	0.4	0.4	0.1	d8 : 41
79	29	48	Band	0.4	0.4	0.1	A1 : 1
80	31	48	Band	0.4	0.4	0.1	d11 : 44
81	33	48	Band	0.4	0.4	0.1	e1 : 45
82	15	50	Band	0.4	0.4	0.1	a9 : 9
83	17	50	Band	0.4	0.4	0.1	b6 : 17
84	19	50	Band	0.4	0.4	0.1	c2 : 24
85	21	50	Band	0.4	0.4	0.1	c8 : 30
86	23	50	Band	0.4	0.4	0.1	d2 : 35
87	25	50	Band	0.4	0.4	0.1	d6 : 39
88	27	50	Band	0.4	0.4	0.1	d9 : 42
89	29	50	Band	0.4	0.4	0.1	d11 : 44
90	31	50	Band	0.4	0.4	0.1	A1 : 1
91	33	50	Band	0.4	0.4	0.1	e2 : 46
92	15	52	Band	0.4	0.4	0.1	a10 : 10
93	17	52	Band	0.4	0.4	0.1	b7 : 18
94	19	52	Band	0.4	0.4	0.1	c3 : 25
95	21	52	Band	0.4	0.4	0.1	c9 : 31
96	23	52	Band	0.4	0.4	0.1	d3 : 36
97	25	52	Band	0.4	0.4	0.1	d7 : 40
98	27	52	Band	0.4	0.4	0.1	d10 : 43
99	29	52	Band	0.4	0.4	0.1	e1 : 45
100	31	52	Band	0.4	0.4	0.1	e2 : 46
101	33	52	Band	0.4	0.4	0.1	A1 : 1
102	15	54	Band	0.4	0.4	0.1	e3 : 47
103	35	54	Band	0.4	0.4	0.1	e3 : 47

Subsequent slides produced by sequentially adding 31.4mm to x co-ordinates 5 times. Second column of six slides produced by adding 92mm to y co-ordinates of first six.

Vial assignment

A1 : 1	-	- (Methanol)	
A2 : 2		GM1	100μg/ml
A3 : 3		GM2	100μg/ml
A4 : 4		GM3	100μg/ml
A5 : 5		GD1a	100μg/ml
A6 : 6		GD1b	100μg/ml
A7 : 7		GD3	100μg/ml
A8 : 8		GT1a	100μg/ml
A9 : 9		GT1b	100μg/ml
A10 : 10		GQ1b	100μg/ml
A11 : 11	1	GM1/GM2	100μg/ml
B1 : 12	2	GM1/GM3	100μg/ml
B2 : 13	3	GM1/GD1a	100μg/ml
B3 : 14	4	GM1/GD1b	100μg/ml
B4 : 15	5	GM1/GD3	100μg/ml
B5 : 16	6	GM1/GT1a	100μg/ml
B6 : 17	7	GM1/GT1b	100μg/ml
B7 : 18	8	GM1/GQ1b	100μg/ml
B8 : 19	9	GM2/GM3	100μg/ml
B9 : 20	10	GM2/GD1a	100μg/ml
B10 : 21	11	GM2/GD1b	100μg/ml
B11 : 22	12	GM2/GD3	100μg/ml
C1 : 23	13	GM2/GT1a	100μg/ml
C2 : 24	14	GM2/GT1b	100μg/ml
C3 : 25	15	GM2/GQ1b	100μg/ml
C4 : 26	16	GM3/GD1a	100μg/ml
C5 : 27	17	GM3/GD1b	100μg/ml
C6 : 28	18	GM3/GD3	100μg/ml
C7 : 29	19	GM3/GT1a	100μg/ml
C8 : 30	20	GM3/GT1b	100μg/ml
C9 : 31	21	GM3/GQ1b	100μg/ml
C10 : 32	22	GD1a/GD1b	100μg/ml
C11 : 33	23	GD1a/GD3	100μg/ml
D1 : 34	24	GD1a/GT1a	100μg/ml
D2 : 35	25	GD1a/GT1b	100μg/ml
D3 : 36	26	GD1a/GQ1b	100μg/ml
D4 : 37	27	GD1b/GD3	100μg/ml
D5 : 38	28	GD1b/GT1a	100μg/ml
D6 : 39	29	GD1b/GT1b	100μg/ml
D7 : 40	30	GD1b/GQ1b	100μg/ml
D8 : 41	31	GD3/GT1a	100μg/ml
D9 : 42	32	GD3/GT1b	100μg/ml
D10 : 43	33	GD3/GQ1b	100μg/ml
D11 : 44	34	GT1a/GT1b	100μg/ml
E1 : 45	35	GT1a/GQ1b	100μg/ml
E2 : 46	36	GT1b/GQ1b	100μg/ml
E3 : 47	+	+ (Blue)	

3 Antigens significantly associated with GBS using stepup correction

Antigen	Bonferroni (p-value)	Stepup (p-value)	Disease Mean	Control Mean
Sulfatide :GalC	0.11	0.01	1.90	0
Phosphatidylserine:GM1	0.11	0.01	2.06	0
Sulfatide :GD1b	0.12	0.01	1.99	0
Sulfatide :GM1	0.14	0.01	2.08	0
Phosphatidylserine:Asialo-GM1	0.16	0.01	1.90	0
GD2:Sulfatide	0.17	0.01	2.38	0.36
SGPG:GM1	0.21	0.01	1.70	0
Phosphatidylserine:GD1b	0.22	0.01	1.78	0
GM1:LM1	0.60	0.03	1.57	0
GM1	0.61	0.03	1.45	0
GM1:GT1a	0.74	0.04	1.43	0
SGPG:GD1b	0.93	0.04	1.22	0
LM1:GD1b	1	0.04	1.41	0
GM1:GD1b	1	0.04	1.34	0
GM3:GD1b	1	0.04	1.29	0
GD2:Asialo-GM1	1	0.04	1.29	0
Phosphatidylserine	1	0.04	1.37	0.16
Asialo-GM1:LM1	1	0.04	1.67	0.14
Asialo-GM1:GM1	1	0.04	1.19	0
GM1:GD1a	1	0.04	1.39	0
GalC:GT1a	1	0.04	1.36	0
Asialo-GM1:GD3	1	0.04	1.34	0
GM1:GD3	1	0.04	1.25	0
SGPG:GalC	1	0.04	1.16	0
GM3:GM1	1	0.04	1.27	0
Sphingomyelin:GM1	1	0.04	1.23	0
Asialo-GM1:GD1a	1	0.04	1.27	0
GD1b	1	0.04	1.20	0
Phosphatidylserine:GalC	1	0.04	1.12	0
LM1:GT1a	1	0.05	1.21	0
GalC:GM1	1	0.05	1.22	0

4 Publications arising

Combinatorial glycoarray.

Rinaldi S, Brennan KM, Willison HJ.
Methods in Molecular Biology. 2012 Jan 808:413-423.

Lipid arrays identify myelin-derived lipids and lipid complexes as prominent targets for oligoclonal band antibodies in multiple sclerosis.

Brennan KM, Galban-Horcajo F, Rinaldi S, O'Leary CP, Goodyear CS, Kalna G, Arthur A, Elliot C, Barnett S, Linington C, Bennett JL, Owens GP, Willison HJ.

Journal of Neuroimmonology. 2011 Sep 15;238(1-2):87-95

The GD1a glycan is a cellular receptor for adenoviruses causing epidemic keratoconjunctivitis.

Nilsson EC, Storm RJ, Bauer J, Johansson SM, Lookene A, Ångström J, Hedenström M, Eriksson TL, Frängsmyr L, Rinaldi S, Willison HJ, Pedrosa Domellöf F, Stehle T, Arnberg N.
Nature Medicine. 2011 Jan;17(1):105-9

Transgenic rescue of ganglioside expression in the peripheral nervous system of ganglioside-null mice facilitates an active immunisation model of acute motor axonal neuropathy

Yao D, Rinaldi S, Greenshields K, McKinnon A, Fewou S, Furukawa K, Brophy PJ, Willison HJ.
Journal of the Peripheral Nervous System 2010 (Abstract)

Title:
TRANSGENIC RESCUE OF GANGLIOSIDE EXPRESSION IN THE PERIPHERAL NERVOUS SYSTEM OF GANGLIOSIDE-NULL MICE FACILITATES AN ACTIVE IMMUNISATION MODEL OF ACUTE MOTOR AXONAL NEUROPATHY

Authors:
Denggao Yao (1), Simon Rinaldi (1), Kay Greenshields (1), Allan McKinnon (1), Simon Fewou (1), Koichi Furukawa (2), Peter J. Brophy (3), Hugh J. Willison (1)

Institution(s):
(1) Division of Clinical Neurosciences, University of Glasgow, Glasgow, UK
(2) Department of Biochemistry, Nagoya University School of Medicine, Nagoya, Japan
(3) Centre for Neuroregeneration, University of Edinburgh, Edinburgh, UK

Body of Abstract:
In the motor axonal variant of Guillain-Barré syndrome (GBS) antibodies to complex gangliosides are frequently found. Evidence shows that these antibodies have pathogenic effects on the structure and function of the neuromuscular junction (NMJ) and nodes of Ranvier. Mouse models of this disease are confounded by the fact that wild type (WT) mice, expressing the normal complement of gangliosides, are immunologically tolerant when immunised with exogenous gangliosides. Conversely, N-acetylgalactosaminyl-transferase knockout ($GalNAcT^{-/-}$) mice, lacking all complex gangliosides, produce high affinity antibody responses to complex ganglioside immunisation, but do not develop neuropathology as they lack the target antigen. Our current model therefore relies on passive immunisation into WT mice of anti-ganglioside antibody generated in $GalNAcT^{-/-}$ mice. To overcome this double step, and assess the tolerogenic effect of gangliosides solely expressed in axons, we crossed a transgenic mouse expressing GalNAcT driven by an axonal neurofilament-light (NFL) promoter onto a $GalNAcT^{-/-}$ background to create GalNAcT Tg/KO mice. Rescue of neuronal ganglioside expression was demonstrated by thin layer chromatography of brain glycolipid, and by immunofluorescence staining of neuromuscular tissue, using an anti-GT1b ganglioside antibody. The sensitivity of the transgenic NMJ to anti-GT1b antibody and complement mediated injury was first established using *ex vivo* preparations of hemidiaphragm. Antibody bound to the pre-synaptic membrane, fixed complement, and led to membrane attack complex deposition in GalNAcT Tg/KO and WT mice, but not in $GalNAcT^{-/-}$ mice. In i*n vivo* passive transfer studies with intra-peritoneal (IP) anti-GT1b antibody plus complement, GalNAcT Tg/KO mice developed respiratory failure, whereas $GalNAcT^{-/-}$ mice did not. Furthermore, immunisation of transgenic animals with GT1b-liposomes produces a vigorous antibody response indistinguishable from that seen in $GalNAcT^{-/-}$ mice, compared with a blunted response in WT mice. When provided with a source of complement delivered IP, GT1b immunised transgenic mice develop diaphragmatic paralysis. This model demonstrates that local axonal expression of ganglioside does not induce systemic immunological tolerance, and in doing so allows for the production of an active immunisation model of motor axonal GBS in a single mouse line, through the re-sensitisation of axons to antibody mediated injury.

(340 words)

Heteromeric glycolipid complexes as modulators of autoantibody and lectin binding.

Rinaldi S, Brennan KM, Willison HJ.
Progress in Lipid Research. 2010 Jan;49(1):87-95

Analysis of lectin binding to glycolipid complexes using combinatorial glycoarrays.

Rinaldi S, Brennan KM, Goodyear CS, O'Leary C, Schiavo G, Crocker PR, Willison HJ.
Glycobiology. 2009 Jul;19(7):789-96.

Detection of autoantibody and lectin binding to ganglioside complexes using a novel combinatorial glycoarray.

Rinaldi S, Brennan KM, Greenshields KN, Goodyear CS, O'Leary C, Schiavo G, Crocker PR, Willison HJ.
Journal of the Peripheral Nervous System. 2009 Jul;14(21):126 (Abstract).

Detection of Autoantibody and Lectin Binding to Ganglioside Complexes Using a Novel Combinatorial Glycoarray

Simon Rinaldi[1], Kathryn M. Brennan[1], Kay N. Greenshields[1], Carl S. Goodyear[1], Colin O'Leary[1], Giampietro Schiavo[2], Paul R. Crocker[3], and Hugh J. Willison[1].

[1] Division of Clinical Neurosciences, Glasgow Biomedical Research Centre, University of Glasgow, Glasgow G12 8TA, UK.

[2] Molecular NeuroPathobiology Laboratory, Cancer Research UK London Research Institute, 44 Lincoln's Inn Fields, London, WC2A 3PX, UK.

[3] Wellcome Trust Biocentre, University of Dundee, Dow Street, Dundee DD1 5EH, UK.

Ganglioside complexes (GSCs) have been demonstrated as ligands for antibodies and lectins, including those found in the serum of Guillain-Barré syndrome patients. Investigating such reactivity using ELISA is problematic, principally because of the increased quantities of antigen and antisera required to accommodate the combinatorial dimension. To overcome this, we have developed a miniaturised system using a TLC autosampler to create matrices of 100 glycolipids and their 1:1 complexes in 100 nanolitre volumes on 20x20mm polyvinyl-difluoride (PVDF) membranes. These PVDF glycoarrays are then probed with a variety of different lectins, and binding detected by chemiluminescence and autoradiography. Using a prototypic anti-GM1 monoclonal antibody, the inter- and intra-assay coefficients of variation were calculated as 4.1% and 8.6%, comparable with ELISA. We have demonstrated that the binding of neuropathy sera to glycolipids can be enhanced, attenuated, or unaffected by complexes, and that this phenomenon is observed for other carbohydrate binding proteins. Thus, a tetanus neurotoxin binding fragment binds GM1:GD3 ('complex enhanced') whilst failing to react with either component ganglioside alone. The immunomodulatory receptor siglec-7 displays the reverse pattern, binding GD3 in isolation, but not when this ganglioside is complexed with GM1 ('complex attenuated'). Conversely, the anti-disialosyl monoclonal antibody CGM3 reacts equally with all GD3 containing complexes ('complex independent'). This complex independent pattern is also seen for cholera toxin B and GM1. We have shown that the GSC reactivities of a pair of anti-GM1 monoclonal antibodies *in vitro* correlate with their pathological potential *in vivo*. One antibody is prevented from binding GM1 in solid phase assays and live neural tissue by the presence of a *cis* interaction between GM1 and GD1a, and is therefore 'non-pathogenic'. Conversely, a second anti-GM1 antibody is able to bind GM1:GD1a complexes in assays and live tissue, and thereby exert pathogenic effects. Immunising GalNAcT$^{-/-}$ mice (lacking all complex gangliosides) with GSC-containing unilamellar liposomes created by a freeze-thaw-extrusion method can induce a complex independent IgM response which transforms to complex dependency on IgG class switching. These studies are advancing our knowledge of the immunological, pathological and clinical relevance of GSCs in autoimmune peripheral neuropathies and in other paradigms involving protein-carbohydrate interactions.

The neuropathic potential of anti-GM1 autoantibodies is regulated by the local glycolipid environment.

Greenshields KN, Halstead SK, Zitman FMP, Rinaldi S, Brennan KM, O'Leary C, Chamberlain LH, Easton A, Roxburgh J, Pediani J, Furukawa K, Furukawa K, Goodyear CS, Plomp JJ and Willison HJ.
Journal of Clinical Investigation. 2009 Mar;119(3):595-610.

Ganglioside antibodies and neuropathies.

Rinaldi S, Willison HJ.
Current Opinion in Neurology 2008 Oct;21(5):540-546.

List of references

Alshekhlee, A., Hussain, Z., Sultan, B., & Katirji, B. (2008). Guillain-Barre syndrome: incidence and mortality rates in US hospitals. *Neurology* 70, 1608-1613.

Alter, M. (1990). The epidemiology of Guillain-Barre syndrome. *Ann.Neurol.* 27 Suppl, S7-12.

Archelos, J. J., Roggenbuck, K., Schneider-Schaulies, J., Toyka, K. V., & Hartung, H. P. (1993). Detection and quantification of antibodies to the extracellular domain of P0 during experimental allergic neuritis. *J Neurol Sci.* 117, 197-205.

Asbury, A. K. (1978). Criteria for diagnosis of Guillain-Barre syndrome. *Ann.Neurol* 3, 565-566.

Asbury, A. K. (1990). Guillain-Barre syndrome: historical aspects. *Ann.Neurol.* 27 Suppl, S2-S6.

Asbury, A. K. & Cornblath, D. R. (1990). Assessment of current diagnostic criteria for Guillain-Barre syndrome. *Ann.Neurol.* 27 Suppl, S21-S24.

Aspinall, G. O., McDonald, A. G., Pang, H., Kurjanczyk, L. A., & Penner, J. L. (1994). Lipopolysaccharides of Campylobacter jejuni serotype O:19: structures of core oligosaccharide regions from the serostrain and two bacterial isolates from patients with the Guillain-Barre syndrome. *Biochemistry* 33, 241-249.

Beghi, E., Kurland, L. T., Mulder, D. W., & Wiederholt, W. C. (1985). Guillain-Barre syndrome. Clinicoepidemiologic features and effect of influenza vaccine. *Arch Neurol* 42, 1053-1057.

Bernsen, R. A., Jacobs, H. M., de Jager, A. E., & van der Meche, F. G. (1997). Residual health status after Guillain-Barre syndrome. *J.Neurol.Neurosurg.Psychiatry* 62, 637-640.

Bickerstaff, E. R. (1957). Brain-stem encephalitis; further observations on a grave syndrome with benign prognosis. *Br.Med J* 1, 1384-1387.

Bowes, T., Wagner, E. R., Boffey, J., Nicholl, D., Cochrane, L., Benboubetra, M., Conner, J., Furukawa, K., Furukawa, K., & Willison, H. J. (2002). Tolerance to self gangliosides is the major factor restricting the antibody response to lipopolysaccharide core oligosaccharides in Campylobacter jejuni strains associated with Guillain-Barre syndrome. *Infect.Immun.* 70, 5008-5018.

Bradford, J. R., Bashford, E. F., & Wilson, J. A. Acute infective polyneuritis. Quart J Med 12, 88-103. 1919.

Braun, P. E., Frail, D. E., & Latov, N. (1982). Myelin-associated glycoprotein is the antigen for a monoclonal IgM in polyneuropathy. *J Neurochem.* 39, 1261-1265.

Buchwald, B., Zhang, G., Vogt-Eisele, A. K., Zhang, W., Ahangari, R., Griffin, J. W., Hatt, H., Toyka, K. V., & Sheikh, K. A. (2007). Anti-ganglioside antibodies alter presynaptic release and calcium influx. *Neurobiology of Disease.28(1):113-21.*

Caporale, C. M., Papola, F., Fioroni, M. A., Aureli, A., Giovannini, A., Notturno, F., Adorno, D., Caporale, V., & Uncini, A. (2006). Susceptibility to Guillain-Barre syndrome is associated to polymorphisms of CD1 genes. *Journal of Neuroimmunology* 177, 112-118.

Chen, C., Fu, Z., Kim, J. J., Barbieri, J. T., & Baldwin, M. R. (2009). Gangliosides as high affinity receptors for tetanus neurotoxin. *J Biol.Chem* 284, 26569-26577.

Chiba, A., Kusunoki, S., Obata, H., Machinami, R., & Kanazawa, I. (1997). Ganglioside composition of the human cranial nerves, with special reference to pathophysiology of Miller Fisher syndrome. *Brain Res.* 745, 32-36.

Chiba, A., Kusunoki, S., Shimizu, T., & Kanazawa, I. (1992). Serum IgG antibody to ganglioside GQ1b is a possible marker of Miller Fisher syndrome. *Ann.Neurol.* 31, 677-679.

Cohen, N. R., Garg, S., & Brenner, M. B. (2009). Antigen Presentation by CD1 Lipids, T Cells, and NKT Cells in Microbial Immunity. *Adv.Immunol.* 102, 1-94.

Connell, S. D. & Smith, D. A. (2006). The atomic force microscope as a tool for studying phase separation in lipid membranes. *Mol.Membr.Biol.* 23, 17-28.

Considine, P. J., Duggan, P., & Eadie, A. (1986). Enzyme linked immunosorbent assay (ELISA) for the determination of protein-A. *Biosci.Rep.* 6, 933-936.

De Angelis, M. V., Notturno, F., Caporale, C. M., Pace, M., & Uncini, A. (2007). Polymorphisms of CD1 genes in chronic dysimmune neuropathies. *Journal of Neuroimmunology.186(1-2):161-3.*

De Libero, G., Donda, A., Gober, H. J., Manolova, V., Mazorra, Z., Shamshiev, A., & Mori, L. (2002). A new aspect in glycolipid biology: glycosphingolipids as antigens recognized by T lymphocytes. *Neurochem.Res.* 27, 675-685.

Deinhardt, K., Berninghausen, O., Willison, H. J., Hopkins, C. R., & Schiavo, G. (2006). Tetanus toxin is internalized by a sequential clathrin-dependent mechanism initiated within lipid microdomains and independent of epsin1. *J.Cell Biol.* 174, 459-471.

Dornonville, d. l. C. & Jakobsen, J. (2005). Residual neuropathy in long-term population-based follow-up of Guillain-Barre syndrome. *Neurology* 64, 246-253.

Eggens, I., Fenderson, B. A., Toyokuni, T., & Hakomori, S. (1989). A role of carbohydrate-carbohydrate interaction in the process of specific cell recognition during embryogenesis and organogenesis: a preliminary note. *Biochem.Biophys.Res.Commun.* 158, 913-920.

Fenderson, B. A., Zehavi, U., & Hakomori, S. (1984). A multivalent lacto-N-fucopentaose III-lysyllysine conjugate decompacts preimplantation mouse embryos, while the free oligosaccharide is ineffective. *J.Exp.Med.* 160, 1591-1596.

Fewou, S. N., Fernandes, A., Stockdale, K., Francone, V. P., Dupree, J. L., Rosenbluth, J., Pfeiffer, S. E., & Bansal, R. (2010). Myelin protein composition is altered in mice lacking either sulfated or both sulfated and non-sulfated galactolipids. *J Neurochem.* 112, 599-610.

Fisher, M. (1956). An unusual variant of acute idiopathic polyneuritis (syndrome of ophthalmoplegia, ataxia and areflexia). *N.Engl.J.Med.* 255, 57-65.

Furukawa, K., Aixinjueluo, W., Kasama, T., Ohkawa, Y., Yoshihara, M., Ohmi, Y., Tajima, O., Suzumura, A., Kittaka, D., & Furukawa, K. (2008). Disruption of GM2/GD2 synthase gene resulted in overt expression of 9-O-acetyl GD3 irrespective of Tis21. *J.Neurochem.* 105, 1057-1066.

Geleijns, K., Jacobs, B. C., van Rijs, W., Tio-Gillen, A. P., Laman, J. D., & van Doorn, P. A. (2004). Functional polymorphisms in LPS receptors CD14 and TLR4 are not associated with disease susceptibility or Campylobacter jejuni infection in Guillain-Barre patients. *Journal of Neuroimmunology* 150, 132-138.

Ginsberg, L., Malik, O., Kenton, A. R., Sharp, D., Muddle, J. R., Davis, M. B., Winer, J. B., Orrell, R. W., & King, R. H. M. (2004). Coexistent hereditary and inflammatory neuropathy. *Brain* 127, 193-202.

Godschalk, P. C., Kuijf, M. L., Li, J., St Michael, F., Ang, C. W., Jacobs, B. C., Karwaski, M. F., Brochu, D., Moterassed, A., Endtz, H. P., van Belkum, A., & Gilbert, M. (2007a). Structural characterization of Campylobacter jejuni lipooligosaccharide outer cores associated with Guillain-Barre and Miller Fisher syndromes. *Infection & Immunity.75(3):1245-54.*

Godschalk, P. C., van Belkum, A., van den, B. N., van Netten, D., Ang, C. W., Jacobs, B. C., Gilbert, M., & Endtz, H. P. (2007b). PCR-restriction fragment length polymorphism analysis of Campylobacter jejuni genes involved in lipooligosaccharide biosynthesis identifies putative molecular markers for Guillain-Barre syndrome. *Journal of Clinical Microbiology.45(7):2316-20.*

Goodyear, C. S., O'Hanlon, G. M., Plomp, J. J., Wagner, E. R., Morrison, I., Veitch, J., Cochrane, L., Bullens, R. W., Molenaar, P. C., Conner, J., & Willison, H. J. (1999). Monoclonal antibodies raised against Guillain-Barre syndrome-associated Campylobacter jejuni lipopolysaccharides react with neuronal gangliosides and paralyze muscle-nerve preparations. *J.Clin.Invest* 104, 697-708.

Greenshields, K. N., Halstead, S. K., Zitman, F. M., Rinaldi, S., Brennan, K. M., O'Leary, C., Chamberlain, L. H., Easton, A., Roxburgh, J., Pediani, J., Furukawa, K., Furukawa, K., Goodyear, C. S., Plomp, J. J., & Willison, H. J. (2009). The neuropathic potential of anti-GM1 autoantibodies is regulated by the local glycolipid environment in mice. *J.Clin.Invest* 119, 595-610.

Griffin, J. W., Li, C. Y., Ho, T. W., Tian, M., Gao, C. Y., Xue, P., Mishu, B., Cornblath, D. R., Macko, C., McKhann, G. M., & Asbury, A. K. (1996). Pathology of the motor-sensory axonal Guillain-Barre syndrome. *Ann.Neurol.* 39, 17-28.

Gruener, G., Bosch, E. P., Strauss, R. G., Klugman, M., & Kimura, J. (1987). Prediction of early beneficial response to plasma exchange in Guillain-Barre syndrome. *Arch Neurol* 44, 295-298.

Guillain, G., Strohl, A., & Barré, J. (1916). Sur un syndrome de radiculo-névrite avec hyperalbuminose du liquide céphalo-rachidien sans réaction cellulaire. Remarques sur les caractéres cliniques et graphiques des réflexes tendineux. *Bull Soc Méd Hôp Paris* 40, 1462-1470.

Guillain, G. Radiculoneuritis with acellular hyperalbuminosis of the cerebrospinal fluid. Arch Neurol Psychiat , 975-990. 1936.

Hadden, R. D., Karch, H., Hartung, H. P., Zielasek, J., Weissbrich, B., Schubert, J., Weishaupt, A., Cornblath, D. R., Swan, A. V., Hughes, R. A., & Toyka, K. V. (2001). Preceding infections, immune factors, and outcome in Guillain-Barre syndrome. *Neurology* 56, 758-765.

Hahn, A. F., Feasby, T. E., Wilkie, L., & Lovgren, D. (1993). Antigalactocerebroside antibody increases demyelination in adoptive transfer experimental allergic neuritis. *Muscle Nerve* 16, 1174-1180.

Halstead S.K., Zitman F.M., Humphreys P.D., Greenshields K., Verschuuren J.J., Jacobs B.C., Rother R.P., Plomp J.J., & Willison H.J. (2008). Eculizumab prevents anti-ganglioside antibody-mediated neuropathy in a murine model. *Brain* 131, 1197-1208.

Halstead, S. K., Lin, F., O'Hanlon, G. M., Humphreys, P. D., Bullens, R. W. M., Plomp, J. J., Morgan, B. P., Medof, M. E., & Willison, H. J. (2004a). CD59 and DAF protect motor nerve terminals from membrane attack complex mediated injury in murine Guillain-Barre syndrome. *Molecular Immunology* 41, 240.

Halstead, S. K., O'Hanlon, G. M., Humphreys, P. D., Morrison, D. B., Morgan, B. P., Todd, A. J., Plomp, J. J., & Willison, H. J. (2004b). Anti-disialoside antibodies kill perisynaptic Schwann cells and damage motor nerve terminals via membrane attack complex in a murine model of neuropathy. *Brain* 127, 2109-2123.

Haymaker, W. E. & Kernohan, J. W. (1949). The Landry-Guillain-Barre syndrome; a clinicopathologic report of 50 fatal cases and a critique of the literature. *Medicine (Baltimore)* 28, 59-141.

Heffer-Lauc, M., Lauc, G., Nimrichter, L., Fromholt, S. E., & Schnaar, R. L. (2005). Membrane redistribution of gangliosides and glycosylphosphatidylinositol-anchored proteins in brain tissue sections under conditions of lipid raft isolation. *Biochim.Biophys.Acta* 1686 3, 200-208.

Heininger, K., Stoll, G., Linington, C., Toyka, K. V., & Wekerle, H. (1986). Conduction failure and nerve conduction slowing in experimental allergic neuritis induced by P2-specific T-cell lines. *Ann.Neurol* 19, 44-49.

Hiraga, A., Kuwabara, S., Nakamura, A., Yuki, N., Hattori, T., & Matsunaga, T. (2007). Fisher/Gullain-Barre overlap syndrome in advanced AIDS. *Journal of the Neurological Sciences.258(1-2):148-50.*

Holers, V. M. (2005). Complement receptors and the shaping of the natural antibody repertoire. *Springer Semin.Immunopathol.* 26, 405-423.

Houliston, R. S., Koga, M., Li, J., Jarrell, H. C., Richards, J. C., Vitiazeva, V., Schweda, E. K., Yuki, N., & Gilbert, M. (2007a). A Haemophilus influenzae strain associated with Fisher syndrome expresses a novel disialylated ganglioside mimic. *Biochemistry.46(27):8164-71.*

Houliston, R. S., Yuki, N., Hirama, T., Khieu, N. H., Brisson, J. R., Gilbert, M., & Jarrell, H. C. (2007b). Recognition characteristics of monoclonal antibodies that are cross-reactive with gangliosides and lipooligosaccharide from Campylobacter jejuni strains associated with Guillain-Barre and Fisher syndromes. *Biochemistry.46(1):36-44.*

Hughes, R. A. & Cornblath, D. R. (2005). Guillain-Barre syndrome. *Lancet* 366, 1653-1666.

Hughes, R. A., Newsom-Davis, J. M., Perkin, G. D., & Pierce, J. M. (1978). Controlled trial prednisolone in acute polyneuropathy. *Lancet* 2, 750-753.

Hughes, R. A., Raphael, J. C., Swan, A. V., & Doorn, P. A. (2004). Intravenous immunoglobulin for Guillain-Barre syndrome. *Cochrane.Database.Syst.Rev.* CD002063.

Hughes, R. A. & Rees, J. H. (1997). Clinical and epidemiologic features of Guillain-Barre syndrome. *J Infect.Dis.* 176 Suppl 2, S92-S98.

Hughes, R. A., Swan, A. V., Raphael, J. C., Annane, D., van Koningsveld, R., & Van Doorn, P. A. (2007). Immunotherapy for Guillain-Barre syndrome: a systematic review. *Brain* 130, 2245-2257.

Hughes, R. A., Swan, A. V., van Koningsveld, R., & Van Doorn, P. A. (2006). Corticosteroids for Guillain-Barre syndrome. *Cochrane.Database.Syst.Rev.* CD001446.

Hughes, R. A., Wijdicks, E. F., Benson, E., Cornblath, D. R., Hahn, A. F., Meythaler, J. M., Sladky, J. T., Barohn, R. J., & Stevens, J. C. (2005). Supportive care for patients with guillain-barre syndrome. *Arch.Neurol.* 62, 1194-1198.

Ilyas, A. A. & Chen, Z. W. (2007). Lewis rats immunized with GM1 ganglioside do not develop peripheral neuropathy. *Journal of Neuroimmunology.188(1-2):34-8.*

Ilyas, A. A., Gu, Y., Dalakas, M. C., Quarles, R. H., & Bhatt, S. (2008). Induction of experimental ataxic sensory neuronopathy in cats by immunization with purified SGPG. *J Neuroimmunol.* 193, 87-93.

Ilyas, A. A., Willison, H. J., Quarles, R. H., Jungalwala, F. B., Cornblath, D. R., Trapp, B. D., Griffin, D. E., Griffin, J. W., & McKhann, G. M. (1988). Serum antibodies to gangliosides in Guillain-Barre syndrome. *Ann.Neurol.* 23, 440-447.

Ishibashi, T., Dupree, J. L., Ikenaka, K., Hirahara, Y., Honke, K., Peles, E., Popko, B., Suzuki, K., Nishino, H., & Baba, H. (2002). A myelin galactolipid, sulfatide, is essential for maintenance of ion channels on myelinated axon but not essential for initial cluster formation. *J.Neurosci.* 22, 6507-6514.

Ito, M., Kuwabara, S., Odaka, M., Misawa, S., Koga, M., Hirata, K., & Yuki, N. (2008). Bickerstaff's brainstem encephalitis and Fisher syndrome form a continuous spectrum : Clinical analysis of 581 cases. *J.Neurol.*

IUPAC-IUB Commission on Biochemical Nomenclature (1978). The nomenclature of lipids (Recommendations 1976) IUPAC-IUB Commission on Biochemical Nomenclature. *Biochem.J* 171, 21-35.

Kaida, K., Kamakura, K., Ogawa, G., Ueda, M., Motoyoshi, K., Arita, M., & Kusunoki, S. (2008). GD1b-specific antibody induces ataxia in Guillain-Barre syndrome. *Neurology* 71, 196-201.

Kaida, K., Kanzaki, M., Morita, D., Kamakura, K., Motoyoshi, K., Hirakawa, M., & Kusunoki, S. (2006). Anti-ganglioside complex antibodies in Miller Fisher syndrome. *J.Neurol.Neurosurg.Psychiatry* 77, 1043-1046.

Kaida, K., Morita, D., Kanzaki, M., Kamakura, K., Motoyoshi, K., Hirakawa, M., & Kusunoki, S. (2004). Ganglioside complexes as new target antigens in Guillain-Barre syndrome. *Ann.Neurol.* 56, 567-571.

Kaida, K., Morita, D., Kanzaki, M., Kamakura, K., Motoyoshi, K., Hirakawa, M., & Kusunoki, S. (2007). Anti-ganglioside complex antibodies associated with severe disability in GBS. *J.Neuroimmunol.* 182, 212-218.

Kanter, J. L., Narayana, S., Ho, P. P., Catz, I., Warren, K. G., Sobel, R. A., Steinman, L., & Robinson, W. H. (2006). Lipid microarrays identify key mediators of autoimmune brain inflammation. *Nat.Med.* 12, 138-143.

Klenk , E. (1935). Über die natur der phophatide und anderer lipoide des gehirns und der leber bei der niemann-pickschen krankheit. *Z Phys Chem* 235, 24-36.

Koga, M. & Yuki, N. (2007). Campylobacter jejuni CST-II polymorphisms and association with development of Guillain-Barre syndrome [1]. *Neurology.69(17)()(pp 1727), 2007.*

Kohler, G. & Milstein, C. (1975). Continuous cultures of fused cells secreting antibody of predefined specificity. *Nature* 256, 495-497.

Kuijf, M. L., Geleijns, K., Ennaji, N., van Rijs, W., Van Doorn, P. A., & Jacobs, B. C. (2008). Susceptibility to Guillain-Barre syndrome is not associated with CD1A and CD1E gene polymorphisms. *J.Neuroimmunol.* 205, 110-112.

Kuijf, M. L., Godschalk, P. C., Gilbert, M., Endtz, H. P., Tio-Gillen, A. P., Ang, C. W., Van Doorn, P. A., & Jacobs, B. C. (2007). Origin of ganglioside complex antibodies in Guillain-Barre syndrome. *J.Neuroimmunol.* 188, 69-73.

Kuijf, M. L., Van Doorn, P. A., Tio-Gillen, A. P., Geleijns, K., Ang, C. W., Hooijkaas, H., Hop, W. C. J., & Jacobs, B. C. (2005). Diagnostic value of anti-GM1 ganglioside serology and validation of the INCAT-ELISA. *Journal of the Neurological Sciences* 239, 37-44.

Kuwabara, S., Misawa, S., Takahashi, H., Sawai, S., Kanai, K., Nakata, M., Mori, M., Hattori, T., & Yuki, N. (2007). Anti-GQ1b antibody does not affect neuromuscular transmission in human limb muscle. *Journal of Neuroimmunology.189(1-2):158-62.*

Landry, O. Note sur la paralysie ascendante aigue. Gazette Hebdomadaire de Medicin 6, 472-488. 1879.

Lehmann, H. C., Lopez, P. H., Zhang, G., Ngyuen, T., Zhang, J., Kieseier, B. C., Mori, S., & Sheikh, K. A. (2007). Passive immunization with anti-ganglioside antibodies directly inhibits axon regeneration in an animal model. *Journal of Neuroscience.27(1):27-34.*

Lencer, W. I., Hirst, T. R., & Holmes, R. K. (1999). Membrane traffic and the cellular uptake of cholera toxin. *Biochim.Biophys.Acta* 1450, 177-190.

Lloyd, K. O., Gordon, C. M., Thampoe, I. J., & DiBenedetto, C. (1992). Cell surface accessibility of individual gangliosides in malignant melanoma cells to antibodies is influenced by the total ganglioside composition of the cells. *Cancer Res.* 52, 4948-4953.

Ma, J. J., Nishimura, M., Mine, H., Kuroki, S., Nukina, M., Ohta, M., Saji, H., Obayashi, H., Saida, T., Kawakami, H., & Uchiyama, T. (1998). HLA and T-cell receptor gene polymorphisms in Guillain-Barre syndrome. *Neurology* 51, 379-384.

Matsumoto, Y., Yuki, N., Van Kaer, L., Furukawa, K., Hirata, K., & Sugita, M. (2008). Cutting edge: Guillain-barre syndrome-associated IgG responses to gangliosides are generated independently of CD1 function in mice. *Journal of Immunology* 180, 39-43.

McGonigal, R., Rowan, E. G., Greenshields, K. N., Halstead, S. K., Humphreys, P. D., Rother, R. P., Furukawa, K., & Willison, H. J. (2010). Anti-GD1a antibodies activate complement and calpain to injure distal motor nodes of Ranvier in mice. *Brain* 133, 1944-1960.

McKhann, G. M. (1990). Guillain-Barre syndrome: clinical and therapeutic observations. *Ann.Neurol*. 27 Suppl, S13-S16.

McKhann, G. M., Cornblath, D. R., Griffin, J. W., Ho, T. W., Li, C. Y., Jiang, Z., Wu, H. S., Zhaori, G., Liu, Y., Jou, L. P., Liu, T. C., Gao, C. Y., Mao, J. Y., Blaser, M. J., Mishu, B., & Asbury, A. K. (1993). Acute Motor Axonal Neuropathy - A Frequent Cause of Acute Flaccid Paralysis in China. *Annals of Neurology* 33, 333-342.

Munch, C., Epplen, J. T., Meins, M., Meyer, R., Weber, J. R., & Meyer, T. (2008). Severe Guillain-Barre syndrome associated with chromosome 17p11.2-12 duplication. *Muscle & Nerve* 37, 256-258.

Notturno, F., Caporale, C. M., & Uncini, A. (2008). Acute sensory ataxic neuropathy with antibodies to GD1b and GQ1b gangliosides and prompt recovery. *Muscle and Nerve.37(2)()(pp 265-268), 2008.Date of Publication: Feb 2008.* 265-268.

Ogino, M., Orazio, N., & Latov, N. (1995). IgG anti-GM1 antibodies from patients with acute motor neuropathy are predominantly of the IgG1 and IgG3 subclasses. *J Neuroimmunol*. 58, 77-80.

Paterson, G., Wilson, G., Kennedy, P. G., & Willison, H. J. (1995). Analysis of anti-GM1 ganglioside IgM antibodies cloned from motor neuropathy patients demonstrates diverse V region gene usage with extensive somatic mutation. *J Immunol*. 155, 3049-3059.

Perera, V. N., Nachamkin, I., Ung, H., Patterson, J. H., McConville, M. J., Coloe, P. J., & Fry, B. N. (2007). Molecular mimicry in Campylobacter jejuni: role of the lipo-oligosaccharide core oligosaccharide in inducing anti-ganglioside antibodies. *FEMS Immunology & Medical Microbiology.50(1):27-36*.

Plomp, J. J., Molenaar, P. C., O'Hanlon, G. M., Jacobs, B. C., Veitch, J., Daha, M. R., Van Doorn, P. A., van der Meche, F. G., Vincent, A., Morgan, B. P., & Willison, H. J. (1999). Miller Fisher anti-GQ1b antibodies: alpha-latrotoxin-like effects on motor end plates. *Ann.Neurol*. 45, 189-199.

Porcelli, S. A. & Modlin, R. L. (1999). The CD1 system: Antigen-presenting molecules for T cell recognition of lipids and glycolipids. *Annual Review of Immunology* 17, 297-329.

Raphael, J. C., Chevret, S., Hughes, R. A., & Annane, D. (2002). Plasma exchange for Guillain-Barre syndrome. *Cochrane.Database.Syst.Rev*. CD001798.

Rees, J. H., Thompson, R. D., Smeeton, N. C., & Hughes, R. A. (1998). Epidemiological study of Guillain-Barre syndrome in south east England. *J.Neurol.Neurosurg.Psychiatry* 64, 74-77.

Reinhard, C., Eder, G., Fuchs, H., Ziesenis, A., Heyder, J., & Schulz, H. (2002). Inbred strain variation in lung function. *Mamm.Genome* 13, 429-437.

Roberts, M., Willison, H., Vincent, A., & Newsomdavis, J. (1994). Serum Factor in Miller-Fisher Variant of Guillain-Barre-Syndrome and Neurotransmitter Release. *Lancet* 343, 454-455.

Ropper, A. H. (1986). Unusual clinical variants and signs in Guillain-Barre syndrome. *Arch Neurol* 43, 1150-1152.

Rostami, A., Burns, J. B., Brown, M. J., Rosen, J., Zweiman, B., Lisak, R. P., & Pleasure, D. E. (1985). Transfer of experimental allergic neuritis with P2-reactive T-cell lines. *Cell Immunol*. 91, 354-361.

Schafer, D. P., Bansal, R., Hedstrom, K. L., Pfeiffer, S. E., & Rasband, M. N. (2004). Does paranode formation and maintenance require partitioning of neurofascin 155 into lipid rafts? *J.Neurosci*. 24, 3176-3185.

Schulz, H., Johner, C., Eder, G., Ziesenis, A., Reitmeier, P., Heyder, J., & Balling, R. (2002). Respiratory mechanics in mice: strain and sex specific differences. *Acta Physiol Scand*. 174, 367-375.

Shamshiev, A., Donda, A., Prigozy, T. I., Mori, L., Chigorno, V., Benedict, C. A., Kappos, L., Sonnino, S., Kronenberg, M., & De Libero, G. (2000). The alphabeta T cell response to self-glycolipids shows a novel mechanism of CD1b loading and a requirement for complex oligosaccharides. *Immunity* 13, 255-264.

Shimizu, I., Kawahara, T., Haspot, F., Bardwell, P. D., Carroll, M. C., & Sykes, M. (2007). B-cell extrinsic CR1/CR2 promotes natural antibody production and tolerance induction of anti-alphaGAL-producing B-1 cells. *Blood* 109, 1773-1781.

Silvius, J. R. & Nabi, I. R. (2006). Fluorescence-quenching and resonance energy transfer studies of lipid microdomains in model and biological membranes. *Mol.Membr.Biol*. 23, 5-16.

Simons, K. & Ikonen, E. (1997). Functional rafts in cell membranes. *Nature* 387, 569-572.

Singer, S. J. & Nicolson, G. L. (1972). The fluid mosaic model of the structure of cell membranes. *Science* 175, 720-731.

Sinha, S., Prasad, K. N., Jain, D., Pandey, C. M., Jha, S., & Pradhan, S. (2007). Preceding infections and anti-ganglioside antibodies in patients with Guillain-Barresyndrome: A single centre prospective case-control study. *Clinical Microbiology and Infection.13(3)()(pp 334-337), 2007.Date of Publication: Mar 2007*. 334-337.

Slee, M., Selvan, A., & Donaghy, M. (2007). Multifocal motor neuropathy: the diagnostic spectrum and response to treatment. *Neurology.69(17):1680-7*.

Sonnino, S., Mauri, L., Chigorno, V., & Prinetti, A. (2007). Gangliosides as components of lipid membrane domains. *Glycobiology* 17, 1R-13R.

Stryer, L. & Haugland, R. P. (1967). Energy transfer: a spectroscopic ruler. *Proc.Natl.Acad.Sci.U.S.A* 58, 719-726.

Susuki, K., Rasband, M. N., Tohyama, K., Koibuchi, K., Okamoto, S., Funakoshi, K., Hirata, K., Baba, H., & Yuki, N. (2007). Anti-GM1 antibodies cause complement-mediated disruption of sodium channel clusters in peripheral motor nerve fibers. *Journal of Neuroscience.27(15):3956-67.*

Svennerholm, L., Bostrom, K., Fredman, P., Jungbjer, B., Lekman, A., Mansson, J. E., & Rynmark, B. M. (1994). Gangliosides and allied glycosphingolipids in human peripheral nerve and spinal cord. *Biochim.Biophys.Acta* 1214, 115-123.

Taboada, E. N., van Belkum, A., Yuki, N., Acedillo, R. R., Godschalk, P. C. R., Koga, M., Endtz, H. P., Gilbert, M., & Nash, J. H. E. (2007). Comparative genomic analysis of Campylobacter jejuni associated with Guillain-Barre and Miller Fisher syndromes: Neuropathogenic and enteritis-associated isolates can share high levels of genomic similarity. *BMC Genomics.8, 2007.Article Number: 359.Date of Publication: 05 Oct 2007.*

Takada, K., Shimizu, J., & Kusunoki, S. (2008). Apoptosis of primary sensory neurons in GD1b-induced sensory ataxic neuropathy. *Experimental Neurology.209(1)()(pp 279-283), 2008.Date of Publication: Jan 2008.* 279-283.

Tam, C. C., O'Brien, S. J., Petersen, I., Islam, A., Hayward, A., & Rodrigues, L. C. (2007). Guillain-Barre syndrome and preceding infection with campylobacter, influenza and Epstein-Barr virus in the general practice research database. *PLoS.ONE.* 2, e344.

Tamura, N., Kuwabara, S., Misawa, S., Kanai, K., Nakata, M., Sawai, S., Mori, M., & Hattori, T. (2007). Time course of axonal regeneration in acute motor axonal neuropathy. *Muscle Nerve* 35, 793-795.

The Guillain-Barre Syndrome Study Group (1985). Plasmapheresis and Acute Guillain-Barre-Syndrome. *Neurology* 35, 1096-1104.

Todeschini, A. R., Dos Santos, J. N., Handa, K., & Hakomori, S. I. (2008). Ganglioside GM2/GM3 complex affixed on silica nanospheres strongly inhibits cell motility through CD82/cMet-mediated pathway. *Proc.Natl.Acad.Sci.U.S.A* 105, 1925-1930.

Todeschini, A. R. & Hakomori, S. I. (2008). Functional role of glycosphingolipids and gangliosides in control of cell adhesion, motility, and growth, through glycosynaptic microdomains. *Biochim.Biophys.Acta* 1780, 421-433.

Toothaker, T. B. & Brannagan, T. H., III (2007). Chronic inflammatory demyelinating polyneuropathies: current treatment strategies. *Curr.Neurol.Neurosci.Rep.* 7, 63-70.

Townson, K., Boffey, J., Nicholl, D., Veitch, J., Bundle, D., Zhang, P., Samain, E., Antoine, T., Bernardi, A., Arosio, D., Sonnino, S., Isaacs, N., & Willison, H. J. (2007). Solid phase immunoadsorption for therapeutic and analytical studies on neuropathy-associated anti-GM1 antibodies. *Glycobiology* 17, 294-303.

van der Meche, F. G. & Schmitz, P. I. (1992). A randomized trial comparing intravenous immune globulin and plasma exchange in Guillain-Barre syndrome. Dutch Guillain-Barre Study Group. *N.Engl.J Med* 326, 1123-1129.

van der Meche, F. G., Van Doorn, P. A., Meulstee, J., & Jennekens, F. G. (2001). Diagnostic and classification criteria for the Guillain-Barre syndrome. *Eur.Neurol.* 45, 133-139.

van Koningsveld, R., Schmitz, P. I., Meche, F. G., Visser, L. H., Meulstee, J., & Van Doorn, P. A. (2004). Effect of methylprednisolone when added to standard treatment with intravenous immunoglobulin for Guillain-Barre syndrome: randomised trial. *Lancet* 363, 192-196.

van Koningsveld, R., Van Doorn, P. A., Schmitz, P. I., Ang, C. W., & van der Meche, F. G. (2000). Mild forms of Guillain-Barre syndrome in an epidemiologic survey in The Netherlands. *Neurology* 54, 620-625.

van Sorge, N. M., Yuki, N., Jansen, M. D., Nishimoto, Y., Susuki, K., Wokke, J. H., van de Winkel, J. G., van den Berg, L. H., & Van der Pol, W. L. (2007). Leukocyte and complement activation by GM1-specific antibodies is associated with acute motor axonal neuropathy in rabbits. *Journal of Neuroimmunology.182(1-2):116-23.*

Varki, A. (1994). Selectin ligands. *Proc.Natl.Acad.Sci.U.S.A* 91, 7390-7397.

Waksman, B. H. & Adams, R. D. (1955). Allergic neuritis: an experimental disease of rabbits induced by the injection of peripheral nervous tissue and adjuvants. *J Exp.Med* 102, 213-236.

Walgaard, C., Lingsma, H. F., Ruts, L., Drenthen, J., van Koningsveld, R., Garssen, M. J., Van Doorn, P. A., Steyerberg, E. W., & Jacobs, B. C. (2010). Prediction of respiratory insufficiency in Guillain-Barre syndrome. *Ann.Neurol.* 67, 781-787.

Willison, H. J., Paterson, G., Kennedy, P. G., & Veitch, J. (1994). Cloning of human anti-GM1 antibodies from motor neuropathy patients. *Ann.Neurol.* 35, 471-478.

Willison, H. J. & Veitch, J. (1994). Immunoglobulin subclass distribution and binding characteristics of anti-GQ1b antibodies in Miller Fisher syndrome. *J.Neuroimmunol.* 50, 159-165.

Willison, H. J., Veitch, J., Paterson, G., & Kennedy, P. G. E. (1993). Miller Fisher Syndrome Is Associated with Serum Antibodies to Gq1B Ganglioside. *Journal of Neurology Neurosurgery and Psychiatry* 56, 204-206.

Willison, H. J., Veitch, J., Swan, A. V., Baumann, N., Comi, G., Gregson, N. A., Illa, I., Zielasek, J., & Hughes, R. A. (1999). Inter-laboratory validation of an ELISA for the determination of serum anti-ganglioside antibodies. *Eur.J.Neurol.* 6, 71-77.

Willison, H. J. & Yuki, N. (2002). Peripheral neuropathies and anti-glycolipid antibodies. *Brain* 125, 2591-2625.

Winer, J. B., Hughes, R. A., Anderson, M. J., Jones, D. M., Kangro, H., & Watkins, R. P. (1988). A prospective study of acute idiopathic neuropathy. II. Antecedent events. *J.Neurol.Neurosurg.Psychiatry* 51, 613-618.

Yuki, N. (2007a). Campylobacter sialyltransferase gene polymorphism directs clinical features of Guillain-Barre syndrome. *Journal of Neurochemistry.103 Suppl 1:150-8.*

Yuki, N. (2007b). Ganglioside mimicry and peripheral nerve disease. [Review] [153 refs]. *Muscle & Nerve.35(6):691-711.*

Yuki, N. & Kuwabara, S. (2007). Axonal Guillain-Barre syndrome: Carbohydrate mimicry and pathophysiology. *Journal of the Peripheral Nervous System.* 12(4):238-249.

Yuki, N., Sato, S., Tsuji, S., Ohsawa, T., & Miyatake, T. (1993). Frequent Presence of Anti-Gq1B Antibody in Fishers Syndrome. *Neurology* 43, 414-417.

Yuki, N., Yamada, M., Koga, M., Odaka, M., Susuki, K., Tagawa, Y., Ueda, S., Kasama, T., Ohnishi, A., Hayashi, S., Takahashi, H., Kamijo, M., & Hirata, K. (2001). Animal model of axonal Guillain-Barre syndrome induced by sensitization with GM1 ganglioside. *Annals of Neurology* 49, 712-720.

Yuki, N., Yoshino, H., Sato, S., & Miyatake, T. (1990). Acute Axonal Polyneuropathy Associated with Anti-Gm1 Antibodies Following Campylobacter Enteritis. *Neurology* 40, 1900-1902.

Zerbi, D., Celano, I., Forlani, G., Garelli, S., Mosconi, L., & Valbonesi, M. (1981). Plasmapheresis in the treatment of four cases of Guillain-Barre syndrome (acute form). *Ital.J Neurol Sci.* 2, 331-336.

zu Horste, G. M., Hartung, H. P., & Kieseier, B. C. (2007). From bench to bedside--experimental rationale for immune-specific therapies in the inflamed peripheral nerve. *Nat.Clin.Pract.Neurol.* 3, 198-211.